Distribution Agreement

In presenting this thesis or dissertation as a partial fulfillment of the requirements for an advanced degree from Emory University, I hereby grant to Emory University and its agents the non-exclusive license to archive, make accessible, and display my thesis or dissertation in whole or in part in all forms of media, now or hereafter known, including display on the world wide web. I understand that I may select some access restrictions as part of the online submission of this thesis or dissertation. I retain all ownership rights to the copyright of the thesis or dissertation. I also retain the right to use in future works (such as articles or books) all or part of this thesis or dissertation.

Signature:

_____ _____

Kathryn L. Nawrocki Date

Impact of Nutrition on Sporulation and Pathogenesis in *Clostridium difficile*

By

Kathryn L. Nawrocki
Doctor of Philosophy

Graduate Division of Biological and Biomedical Sciences
Microbiology and Molecular Genetics

_____
Shonna M. McBride, Ph.D.
Advisor

_____
Joanna B. Goldberg, Ph.D.
Committee Member

_____
Charles P. Moran, Jr., Ph.D.
Committee Member

_____
Philip N. Rather, Ph.D.
Committee Member

_____
David S. Weiss, Ph.D.
Committee Member

Accepted:

_____
Lisa A. Tedesco, Ph.D.
Dean of the James T. Laney School of Graduate Studies

_____
Date

Impact of Nutrition on Sporulation and Pathogenesis in *Clostridium difficile*

By

Kathryn L. Nawrocki
B.S., Michigan State University, 2011

Advisor: Shonna M. McBride, Ph.D.

An abstract of
a dissertation submitted to the Faculty of the
James T. Laney School of Graduate Studies of Emory University
in partial fulfillment of the requirements for the degree of
Doctor of Philosophy
in Microbiology and Molecular Genetics
2016

ABSTRACT

Impact of Nutrition on Sporulation and Pathogenesis in *Clostridium difficile*
By Kathryn L. Nawrocki

Clostridium difficile is an antibiotic-associated nosocomial pathogen that causes severe gastrointestinal disease. *C. difficile* is a Gram-positive obligate anaerobe and is transmitted via the fecal-oral route as a dormant spore. Spores are ingested and germinate into vegetative cells in the presence of bile salts in the gastrointestinal tract. As vegetative *C. difficile* traverses the large intestine and colon, it begins to undergo sporulation so it can survive in the aerobic environment after exiting the host. The regulation of sporulation in *C. difficile* is poorly understood, but prior work suggested a link between sporulation and the nutritional state of the cell. We decided to investigate the role of CodY in sporulation. CodY is a global transcriptional repressor, but only binds its target sites when guanosine triphosphate and branched chain amino acids are readily available. CodY is a direct link between the metabolite pool and transcription in the cell. We concluded that CodY is a negative regulator of *C. difficile* sporulation. In conjunction with this work, we also examined the role of the readily available gastrointestinal metabolite, ethanolamine. Many pathogenic bacteria utilize ethanolamine to gain an advantage over the microbiota. We verified that *C. difficile* utilizes ethanolamine, but ethanolamine does not appear to have an effect on sporulation *in vitro*. We investigated ethanolamine metabolism in the hamster model of infection. While ethanolamine did not impact sporulation post-mortem, it does influence the progression of disease in infected hamsters. When we infected hamsters with mutants that were unable utilize ethanolamine, they developed symptoms and succumbed to infection at an earlier time than hamsters infected with wild-type. While the inability to utilize ethanolamine causes disease at an earlier time, it does not appear to have any direct effect on virulence factor production. This suggests that ethanolamine utilization may play a role in delaying the onset of disease. This work determined that the initiation of sporulation and nutritional state are linked, but that the metabolite ethanolamine does not appear to modulate sporulation, but instead alters disease progression. Overall, this work has shed light onto sporulation and pathogenesis of *C. difficile*.

Impact of Nutrition on Sporulation and Pathogenesis in *Clostridium difficile*

By

Kathryn L. Nawrocki
B.S., Michigan State University, 2011

Advisor: Shonna M. McBride, Ph.D.

A dissertation submitted to the Faculty of the
James T. Laney School of Graduate Studies of Emory University
in partial fulfillment of the requirements for the degree of
Doctor of Philosophy
in Microbiology and Molecular Genetics
2016

ACKNOWLEDMENTS

To my committee members: Thank for you keeping me grounded, especially in these last few months. Thank you for challenging and guiding me to develop into the scientist I am today. Lastly, thank you for showing me what true mentorship is like.

To the members of the NM Club and my classmates: You were the saving grace of each day, my second family. You are responsible for making graduate school fun. Thank you for always being ready to listen or help in whatever capacity necessary. You are all amazing, and I am a better person for knowing you.

To my family: Thank you for the constant support throughout the years. Thank you for always believing in me and having my back. I don't know if I would have made it this far in life without your kindness, honesty, and love.

TABLE OF CONTENTS

LIST OF FIGURES AND TABLES

Figure 7. The Δ*CD1492* mutant has decreased expression of toxin, motility and sporulation regulators

Table 4. Comparison of gene expression and phenotypes of *rstA* and *CD1492* null mutants.

Chapter 11: Appendix VII - Antimicrobial Peptide Resistance Mechanisms of Gram-Positive Bacteria

Table 1. Summary of Gram-Positive Antimicrobial Peptides (AMP) Resistance Mechanisms

Figure 1. Overview of Antimicrobial Peptide Resistance Mechanisms in Gram-Positive Bacteria

CHAPTER 1

Introduction

Clostridium difficile is an obligately anaerobic, spore-forming, Gram-positive bacillus. *C. difficile* was originally identified in 1935 as *Bacillus difficilis* (1), the name deriving from the difficulty in culturing the organism. *C. difficile* was first isolated from infant fecal samples, and was considered a member of the natural flora of infants aged 10 days to 1 year (1). The infants studied were asymptomatic. During this initial investigation, Hall and O'Toole determined that *C. difficile* produced an exotoxin by injecting *C. difficile* culture filtrates intraperitoneally into guinea pigs. They concluded that *C. difficile* produced a heat-labile exotoxin, but that *C. difficile* did not have any major clinical implications on human health (1). Further characterization of *C. difficile* was performed in 1937. This study came to similar conclusions as Hall and O'Toole; namely, that *C. difficile* toxin was lethal in a variety of animals, but the bacterium posed no real threat to humans (1, 2). *C. difficile* then largely disappeared from the scientific literature by name until 1960, when it was isolated from the large intestine of a Wendell seal (3). By this time, scientists had renamed *Bacillus difficilis* to *Clostridium difficile.* In 1962, a report was issued by Montana State College and the Communicable Disease Center of the U.S. Public Health Service documenting eight incidences from 1943 to 1961, where *C. difficile* was isolated (4). In this report, *C. difficile* was isolated from a variety of infection sites with diverse pathologies. All isolates were characterized by their morphology, culture requirements, and lethality following intramuscular injection into guinea pigs. At this time, the researchers concluded that *C. difficile* was simply a fecal contaminate and not the causative agent in any of the cases (4). It was not until 1977 when *Clostridium* BVA 17 HF1-9 was shown to

be the causative agent of clindamycin-associated colitis in hamsters and guinea pigs that the scientific community began to take notice of *C. difficile* and its potential to be a human pathogen (5-7).

C. difficile infection (CDI) causes a range of clinical manifestations from mild diarrhea and colitis, to the life-threatening conditions of toxic megacolon, pseudomembranous colitis (PMC), and bowel perforation (8). PMC is characterized by severe inflammation of the colon with the formation of yellow plaques on the necrotic mucosal surface. The plaques consist predominately of leukocytes, fibrin, and mucin (9). PMC was first described in 1893, but the causative agent was unknown for many decades (10). Cases of PMC were uncommon for many years following its first description. However, in the 1950s and '60s, doctors began to notice that PMC frequently occurred following surgery and antibiotic treatment (11-14). At this time, it was thought that *Staphylococcus aureus* was the causative agent of PMC because it could be readily cultured from patients' stool (14-17). A large study in 1974 that focused on the adverse outcomes of clindamycin treatment challenged the idea that *S. aureus* was the cause of PMC (18). In the course of this study, the authors were unable to culture *S. aureus* from patient samples. It was then in 1978 that *C. difficile* was identified to be the etiological agent of PMC in humans (19).

C. difficile causes symptoms and disease, such as PMC, through a toxin-dependent manner. The major effectors of *C. difficile* disease are two large toxins, TcdA and TcdB (20-22). TcdA and TcdB glycosylate host Rho and Rac GTPases leading to host cell death. (23-27). Strains of *C. difficile* that do not produce toxin do not cause disease (20, 28).

Since the identification of *C. difficile* as the cause of PMC, cases of CDI have continued to rise (29). It is estimated that 453,000 cases of CDI occur annually in the United States, resulting in an estimated 29,300 deaths (30). Approximately 20% of CDI patients suffer from recurrence following completion of treatment (30). Common risk factors associated with CDI include prior antibiotic use, use of proton pump inhibitors, stays within healthcare-associated settings, and increased age (65 years and older) (31-35). The rise in the number of cases of CDI is associated with better reporting, but is also an indicator of antibiotic overuse.

A physiological characteristic of *C. difficile* that has also lead to its rise as a major nosocomial pathogen is its ability to sporulate. Sporulation is a complex cellular process by which a vegetative cell produces a metabolically dormant spore. In *Bacillus subtilis*, the classically studied spore former, sporulation is initiated in times of nutrient distress (36, 37). The process of sporulation is regulated by the transcription factor, Spo0A (38). Spo0A is highly conserved in other spore-forming bacteria, including *C. difficile* (39). Spo0A activity is regulated by its phosphorylation state (40). While the factors that control the phosphorylation state of Spo0A in *B. subtilis* are well described, many of these factors have no know homologues in *C. difficile* (41). While the process and regulation of sporulation in *C. difficile* is not fully elucidated, spores are still a major issue in the management of CDI in healthcare associated settings and in the host.

The host's natural microbiota protects from *C. difficile* infection. This protection is referred to as colonization resistance (42). The general theory is that colonization resistance is conferred by the metabolic and immunologic interactions between the host and microbial community that limit the expansion of foreign invaders. But what particular metabolic and

immunologic interactions protect against CDI are still under investigation. It is known that a result of antibiotic treatment is a decrease in microbial diversity in the host (43-45), resulting in an altered intestinal metabolome. This altered intestinal metabolome leads to an environment that supports *C. difficile* growth in the host gastrointestinal tract. *C. difficile* is transmitted via the fecal-oral route as a dormant spore (39). Once the spore is ingested, it will pass through the stomach unharmed and become exposed to bile salts in the intestine. Exposure to the primary bile salt taurocholate causes *C. difficile* spores to germinate into vegetative cells in the host gastrointestinal tract (46-48). The presence of taurocholate in the intestine is controlled by the microbiota. Primary bile salts are produced by the host in the liver and then secreted into the intestines (49, 50). In the intestines of a healthy individual, primary bile salts are chemically processed by commensal bacteria into secondary bile salts (51). In the absence of certain commensal bacteria, primary bile salts, including taurocholate, are present in the system at higher concentrations, allowing for spore germination of *C. difficile*. In addition to more primary bile salts being present, there is also a depletion of secondary bile salts following antibiotic treatment (51). Some secondary bile salts have been shown to limit *C. difficile* growth and germination (52). Therefore, the microbial processing of bile salts limits the quantity of a germinant and increases the presence of *C. difficile* inhibitors (51-53).

Disruptions to the intestinal metabolome alter what nutrient sources are present that can support bacterial growth. The colonic epithelium decorates its surface with a variety of glycosylated proteins. Certain commensals can liberate these sugars and release them into the lumen of the intestine (54). Sialic acid is commonly liberated by commensals and rapidly consumed (54, 55). Additionally, the commensal flora can ferment liberated sugars

and other complex carbohydrates into short-chain fatty acids (56). Short-chain fatty acids, alongside sialic acid, support the growth of commensal bacteria. Following antibiotic treatment, commensal diversity decreases, often leaving some metabolites underutilized. It has been shown that *C. difficile* can utilize sialic acid, short-chain fatty acids, and succinate for growth if available (55, 57). It is likely that other metabolites are utilized by *C. difficile* for growth when commensals are absent, but these metabolites have yet to be described. Nutrient source limitation is another aspect of host colonization resistance that can limit the growth of *C. difficile* and prevent infection.

In addition to providing colonization resistance through the control of the intestinal metabolome, commensal bacteria also maintain immune homeostasis in the gut. Upon antibiotic treatment, immune factors such as RegIIIgamma (Reg3g), a secreted lectin, are down regulated (58-60). Reg3g and its human counterpart HIP/PAP are bactericidal lectins that target Gram-positive bacteria through peptidoglycan-dependent interactions (61). The down regulation of Reg3g can be restored by activation of Toll-like receptors (TLR) 4 and 5 through the addition of exogenous lipopolysaccharide and bacterial flagellin, respectively (58, 59). The reactivation of TLR5 by the addition of exogenous flagellin has been shown to reduce *C. difficile* growth and toxin production (59). The commensal flora maintain activation of TLRs. Upon antibiotic perturbation, TLR activation is lost and the host becomes more susceptible to CDI due to the generation of an immunodeficient environment (59). Therefore, immune homeostasis is another aspect of colonization resistance against *C. difficile*.

C. difficile can be considered an opportunistic pathogen. *C. difficile* is estimated to asymptomatically colonize 2-5% of the adult population (62). *C. difficile* has also been

found to temporarily colonize 60 to 70% of healthy infants (63, 64). *C. difficile* is thought to be evicted by the development of the adult colonic flora within the first 12 to 24 months of life (63). Isolates colonizing infants are often toxigenic, leading to a toxin A-specific antibody response can limit the severity of disease during future infection (63). Adult asymptomatic carriers of *C. difficile* also produce toxin A-specific antibody (65). The addition of toxin A-specific antibody in conjugation with traditional antibiotic treatment has been shown to decrease recurrence of CDI (66).

CDI is commonly treated with the oral antibiotics metronidazole and vancomycin. While these antibiotics can effectively treat CDI, they further disrupt to the microflora, promoting growth of vancomycin-resistant enterococci (67). Treating an antibiotic-associated disease with an antibiotic is not an ideal treatment method. Recurrent CDI infections often occur following antibiotic treatment (68). Therefore, there is interest in using non-antibiotic treatments for CDI. Fecal microbiota transplantation (FMT) is the transplantation of a healthy donor's fecal material into an infected patient. FMT is considered a form of bacteriotherapy (69). FMT was described as a potential treatment for PMC long before the cause of PMC was known (70). Unlike antibiotic therapy, FMT does not cause further disruption of the already perturbed flora, but instead re-establishes the microbial balance in the gut (71, 72). At present, there is limited controlled data on FMT's safety profile and efficacy for the treatment of CDI (73). There is concern about how the transplantation of unknown bacteria, viruses, and fungi from the healthy donor may affect patients. Therefore, the Food and Drug Administration (FDA) has restricted the use of FMT to patients suffering from multiple antibiotic treatment failures and recurrent events of CDI (73). In an attempt to work around the restrictions of FMT, many groups have started

investigating the potential of bacterial cocktails for the treatment of CDI. In contrast to FMT, these cocktails are made up of known bacteria and can be produced in a more controlled manner. The first of these cocktails demonstrated that only 10 commensal species were needed to cure patients with recurrent CDI (74). This was a limited study with only 6 patients, but the outcome was very promising. Studies have continued to examine which commensal bacteria are able to limit and treat CDI (71, 75, 76). While bacteriotherapy is likely the future treatment for CDI, the reason why bacteriotherapy is so effective in treating CDI still under investigation.

C. difficile has only been classified as a human pathogen since 1978 (19). Due to the recent elevation of *C. difficile* to pathogen status, many of the interactions between *C. difficile*, the host, and the microbiota remain to be elucidated. Our lab first demonstrated a potential link between sporulation, pathogenesis, and nutritional state during the study of the oligopeptide permeases, Opp and App (77) (See appendix). We continued this line of investigation by examining the role of CodY, a global nutritional regulator, in sporulation. Additionally, we examined the role of ethanolamine metabolism in *C. difficile* pathogenesis. Overall in this work, we continued to investigate the relationship between the nutritional state of the cell and pathogenesis and sporulation in *C. difficile*. Understanding how *C. difficile* responds to the environment may provide key insights into *C. difficile* physiology, and open possibilities for limiting CDI. We utilized a variety of molecular and genetic techniques, in addition to work in the hamster model of CDI. This work contributes to the growing *C. difficile* field and sheds more light on the interactions of *C. difficile* with its environment.

REFERENCES

1. **Hall IC, O'Toole E.** 1935. Intestinal flora in new-born infants: with a description of a new pathogenic anaerobe, *Bacillus difficilis*. American journal of diseases of children **49:**390-402.
2. **Snyder ML.** 1937. Further studies on *Bacillus difficilis* (Hall and O'Toole). The Journal of Infectious Diseases**:**223-231.
3. **McBee R.** 1960. Intestinal flora of some Antarctic birds and mammals. Journal of bacteriology **79:**311.
4. **Smith LD, King EO.** 1962. Occurrence of *Clostridium difficile* in infections of man. J Bacteriol **84:**65-67.
5. **Bartlett JG, Onderdonk AB, Cisneros RL, Kasper DL.** 1977. Clindamycin-associated colitis due to a toxin-producing species of Clostridium in hamsters. J Infect Dis **136:**701-705.
6. **Bartlett JG.** 2004. Commentary: Bartlett JG, Onderdonk AB, Cisneros RL, Kasper DL. Clindamycin-associated colitis due to a toxin-producing species of Clostridium in hamsters. J Infect Dis 1977; 136: 701. Journal of Infectious Diseases **190:**202-209.
7. **George WL, Sutter VL, Finegold SM.** 1977. Antimicrobial agent-induced diarrhea: a bacterial disease. The Journal of Infectious Diseases **136:**822-828.
8. **Dobson G, Hickey C, Trinder J.** 2003. *Clostridium difficile* colitis causing toxic megacolon, severe sepsis and multiple organ dysfunction syndrome. Intensive care medicine **29:**1030-1030.
9. **Goulston SJM, McGovern VJ.** 1965. Pseudo-membranous colitis. Gut **6:**207-212.

10. **Finney JMT.** 1893. Gastroenterostomy for cicatrizing ulcer of the pylorus. Bull Johns Hopkins Hosp **4:**53-55.

11. **Reiner L, Schlesinger M, Miller G.** 1952. Pseudomembranous colitis following aureomycin and chloramphenicol. Arch Pathol **54:**39-67.

12. **Pettet JD, Baggenstoss A, Dearing W, Judd Jr E.** 1954. Postoperative pseudomembranous enterocolitis. Surgery, gynecology & obstetrics **98:**546.

13. **Pearce C, Dineen P.** 1960. A study of pseudomembranous enterocolitis. The American Journal of Surgery **99:**292-300.

14. **Speare GS.** 1954. Staphylococcus pseudomembranous enterocolitis, a complication of antibiotic therapy. The American Journal of Surgery **88:**523-534.

15. **Prohaska Jv.** 1959. Pseudomembranous enterocolitis; the experimental induction of the disease with *Staphylococcus aureus* and its enterotoxin. AMA archives of surgery **79:**197.

16. **Hummel RP, Altemeier WA, Hill EO.** 1964. Iatrogenic Staphylococcal Enterocolitis. Annals of Surgery **160:**551-557.

17. **Khan MY, Hall WH.** 1966. Staphylococcal enterocolitis—treatment with oral vancomycin. Annals of internal medicine **65:**1-8.

18. **Tedesco FJ, Barton RW, ALPERS DH.** 1974. Clindamycin-associated colitis: a prospective study. Annals of Internal Medicine **81:**429-433.

19. **Bartlett JG, Moon N, Chang TW, Taylor N, Onderdonk AB.** 1978. Role of *Clostridium difficile* in antibiotic-associated pseudomembranous colitis. Gastroenterology **75:**778-782.

20. **Kuehne SA, Cartman ST, Heap JT, Kelly ML, Cockayne A, Minton NP.** 2010. The role of toxin A and toxin B in *Clostridium difficile* infection. Nature **467:**711-713.

21. **Lyerly DM, Krivan HC, Wilkins TD.** 1988. *Clostridium difficile*: its disease and toxins. Clin Microbiol Rev **1:**1-18.

22. **Lyerly DM, Saum KE, MAcDONALD DK, Wilkins TD.** 1985. Effects of *Clostridium difficile* toxins given intragastrically to animals. Infection and immunity **47:**349-352.

23. **Just I, Selzer J, Wilm M, von Eichel-Streiber C, Mann M, Aktories K.** 1995. Glucosylation of Rho proteins by *Clostridium difficile* toxin B.

24. **Just I, Wilm M, Selzer J, Rex G, von Eichel-Streiber C, Mann M, Aktories K.** 1995. The enterotoxin from *Clostridium difficile* (ToxA) monoglucosylates the Rho proteins. Journal of Biological Chemistry **270:**13932-13936.

25. **Qa'Dan M, Ramsey M, Daniel J, Spyres LM, Safiejko-Mroczka B, Ortiz-Leduc W, Ballard JD.** 2002. *Clostridium difficile* toxin B activates dual caspase-dependent and caspase-independent apoptosis in intoxicated cells. Cellular microbiology **4:**425-434.

26. **He D, Hagen S, Pothoulakis C, Chen M, Medina N, Warny M, LaMont J.** 2000. *Clostridium difficile* toxin A causes early damage to mitochondria in cultured cells. Gastroenterology **119:**139-150.

27. **Brito GA, Fujji J, Carneiro-Filho BA, Lima AA, Obrig T, Guerrant RL.** 2002. Mechanism of *Clostridium difficile* toxin A–induced apoptosis in T84 cells. Journal of Infectious Diseases **186:**1438-1447.

28. **Kuehne SA, Cartman ST, Minton NP.** 2011. Both, toxin A and toxin B, are important in *Clostridium difficile* infection. Gut Microbes **2:**252-255.

29. **Miller BA, Chen LF, Sexton DJ, Anderson DJ.** 2011. Comparison of the burdens of hospital-onset, healthcare facility-associated *Clostridium difficile* Infection and of healthcare-associated infection due to methicillin-resistant Staphylococcus aureus in community hospitals. Infect Control Hosp Epidemiol **32:**387-390.

30. **Lessa FC, Gould CV, McDonald LC.** 2012. Current status of *Clostridium difficile* infection epidemiology. Clin Infect Dis **55 Suppl 2:**S65-70.

31. **Dubberke ER, Reske KA, Yan Y, Olsen MA, McDonald LC, Fraser VJ.** 2007. *Clostridium difficile*—Associated Disease in a Setting of Endemicity: Identification of Novel Risk Factors. Clinical Infectious Diseases **45:**1543-1549.

32. **Linsky A, Gupta K, Lawler EV, Fonda JR, Hermos JA.** 2010. Proton pump inhibitors and risk for recurrent *Clostridium difficile* infection. Archives of internal medicine **170:**772-778.

33. **Kwok CS, Arthur AK, Anibueze CI, Singh S, Cavallazzi R, Loke YK.** 2012. Risk of *Clostridium difficile* Infection With Acid Suppressing Drugs and Antibiotics: Meta-Analysis. Am J Gastroenterol **107:**1011-1019.

34. **McFarland LV, Mulligan ME, Kwok RY, Stamm WE.** 1989. Nosocomial acquisition of *Clostridium difficile* infection. N Engl J Med **320:**204-210.

35. **Bartlett JG, Gerding DN.** 2008. Clinical recognition and diagnosis of *Clostridium difficile* infection. Clin Infect Dis **46 Suppl 1:**S12-18.

36. **Schaeffer P, Millet J, Aubert JP.** 1965. Catabolic repression of bacterial sporulation. Proc Natl Acad Sci U S A **54:**704-711.

37. **Grelet N.** 1957. Growth limitation and sporulation. J appl Bacteriol **20:**315-324.

38. **Molle V, Fujita M, Jensen ST, Eichenberger P, González-Pastor JE, Liu JS, Losick R.** 2003. The Spo0A regulon of *Bacillus subtilis*. Molecular microbiology **50:**1683-1701.

39. **Deakin LJ, Clare S, Fagan RP, Dawson LF, Pickard DJ, West MR, Wren BW, Fairweather NF, Dougan G, Lawley TD.** 2012. The *Clostridium difficile spo0A* gene is a persistence and transmission factor. Infect Immun **80:**2704-2711.

40. **Baldus JM, Green BD, Youngman P, Moran CP, Jr.** 1994. Phosphorylation of *Bacillus subtilis* transcription factor Spo0A stimulates transcription from the spoIIG promoter by enhancing binding to weak 0A boxes. J Bacteriol **176:**296-306.

41. **Paredes-Sabja D, Shen A, Sorg JA.** 2014. *Clostridium difficile* spore biology: sporulation, germination, and spore structural proteins. Trends Microbiol **22:**406-416.

42. **Vollaard EJ, Clasener HA.** 1994. Colonization resistance. Antimicrobial Agents and Chemotherapy **38:**409-414.

43. **O'Sullivan O, Coakley M, Lakshminarayanan B, Conde S, Claesson MJ, Cusack S, Fitzgerald AP, O'Toole PW, Stanton C, Ross RP.** 2013. Alterations in intestinal microbiota of elderly Irish subjects post-antibiotic therapy. J Antimicrob Chemother **68:**214-221.

44. **Sullivan Å, Edlund C, Nord CE.** 2001. Effect of antimicrobial agents on the ecological balance of human microflora. The Lancet infectious diseases **1:**101-114.

45. **Dethlefsen L, Huse S, Sogin ML, Relman DA.** 2008. The pervasive effects of an antibiotic on the human gut microbiota, as revealed by deep 16S rRNA sequencing. PLoS biol **6:**e280.

46. **Sorg JA, Sonenshein AL.** 2008. Bile salts and glycine as cogerminants for *Clostridium difficile* spores. J Bacteriol **190:**2505-2512.

47. **Wilson KH, Silva J, Fekety FR.** 1981. Suppression of *Clostridium difficile* by normal hamster cecal flora and prevention of antibiotic-associated cecitis. Infect Immun **34:**626-628.

48. **George WL, Sutter VL, Citron D, Finegold SM.** 1979. Selective and differential medium for isolation of *Clostridium difficile*. J Clin Microbiol **9:**214-219.

49. **Russell DW.** 2003. The enzymes, regulation, and genetics of bile acid synthesis. Annu Rev Biochem **72:**137-174.

50. **Chiang JY.** 2009. Bile acids: regulation of synthesis. J Lipid Res **50:**1955-1966.

51. **Giel JL, Sorg JA, Sonenshein AL, Zhu J.** 2010. Metabolism of bile salts in mice influences spore germination in *Clostridium difficile*. PLoS One **5:**e8740.

52. **Theriot CM, Bowman AA, Young VB.** 2016. Antibiotic-Induced Alterations of the Gut Microbiota Alter Secondary Bile Acid Production and Allow for *Clostridium difficile* Spore Germination and Outgrowth in the Large Intestine. mSphere **1**.

53. **Theriot CM, Young VB.** 2015. Interactions Between the Gastrointestinal Microbiome and *Clostridium difficile*. Annu Rev Microbiol **69:**445-461.

54. **Sonnenburg JL, Xu J, Leip DD, Chen C-H, Westover BP, Weatherford J, Buhler JD, Gordon JI.** 2005. Glycan Foraging in Vivo by an Intestine-Adapted Bacterial Symbiont. Science **307:**1955-1959.

55. **Ng KM, Ferreyra JA, Higginbottom SK, Lynch JB, Kashyap PC, Gopinath S, Naidu N, Choudhury B, Weimer BC, Monack DM.** 2013. Microbiota-liberated host sugars facilitate post-antibiotic expansion of enteric pathogens. Nature **502:**96-99.

56. **Wong JM, De Souza R, Kendall CW, Emam A, Jenkins DJ.** 2006. Colonic health: fermentation and short chain fatty acids. Journal of clinical gastroenterology **40:**235-243.

57. **Ferreyra JA, Wu KJ, Hryckowian AJ, Bouley DM, Weimer BC, Sonnenburg JL.** 2014. Gut microbiota-produced succinate promotes *C. difficile* infection after antibiotic treatment or motility disturbance. Cell host & microbe **16:**770-777.

58. **Brandl K, Plitas G, Mihu CN, Ubeda C, Jia T, Fleisher M, Schnabl B, DeMatteo RP, Pamer EG.** 2008. Vancomycin-resistant enterococci exploit antibiotic-induced innate immune deficits. Nature **455:**804-807.

59. **Jarchum I, Liu M, Lipuma L, Pamer EG.** 2011. Toll-Like Receptor 5 Stimulation Protects Mice from Acute *Clostridium difficile* Colitis. Infection and Immunity **79:**1498-1503.

60. **Kinnebrew MA, Ubeda C, Zenewicz LA, Smith N, Flavell RA, Pamer EG.** 2010. Bacterial flagellin stimulates Toll-like receptor 5-dependent defense against vancomycin-resistant Enterococcus infection. J Infect Dis **201:**534-543.

61. **Cash HL, Whitham CV, Behrendt CL, Hooper LV.** 2006. Symbiotic Bacteria Direct Expression of an Intestinal Bactericidal Lectin. Science (New York, NY) **313:**1126-1130.

62. **Rivera EV, Woods S.** 2003. Prevalence of asymptomatic *Clostridium difficile* colonization in a nursing home population: a cross-sectional study. J Gend Specif Med **6:**27-30.

63. **Jangi S, Lamont JT.** 2010. Asymptomatic Colonization by *Clostridium difficile* in Infants: Implications for Disease in Later Life. Journal of Pediatric Gastroenterology and Nutrition **51:**2-7.

64. **Kong LY, Dendukuri N, Schiller I, Bourgault A-M, Brassard P, Poirier L, Lamothe F, Béliveau C, Michaud S, Turgeon N.** 2015. Predictors of asymptomatic *Clostridium difficile* colonization on hospital admission. American journal of infection control **43:**248-253.

65. **Kyne L, Warny M, Qamar A, Kelly CP.** 2000. Asymptomatic carriage of *Clostridium difficile* and serum levels of IgG antibody against toxin A. N Engl J Med **342:**390-397.

66. **Lowy I, Molrine DC, Leav BA, Blair BM, Baxter R, Gerding DN, Nichol G, Thomas WD, Jr., Leney M, Sloan S, Hay CA, Ambrosino DM.** 2010. Treatment with monoclonal antibodies against *Clostridium difficile* toxins. N Engl J Med **362:**197-205.

67. **Al-Nassir WN, Sethi AK, Li Y, Pultz MJ, Riggs MM, Donskey CJ.** 2008. Both Oral Metronidazole and Oral Vancomycin Promote Persistent Overgrowth of

Vancomycin-Resistant Enterococci during Treatment of *Clostridium difficile*-Associated Disease. Antimicrobial Agents and Chemotherapy **52:**2403-2406.

68. **Chang JY, Antonopoulos DA, Kalra A, Tonelli A, Khalife WT, Schmidt TM, Young VB.** 2008. Decreased Diversity of the Fecal Microbiome in Recurrent *Clostridium difficile*—Associated Diarrhea. Journal of Infectious Diseases **197:**435-438.

69. **Borody TJ, Warren EF, Leis SM, Surace R, Ashman O, Siarakas S.** 2004. Bacteriotherapy using fecal flora: toying with human motions. Journal of clinical gastroenterology **38:**475-483.

70. **Eiseman B, Silen W, Bascom GS, Kauvar AJ.** 1958. Fecal enema as an adjunct in the treatment of pseudomembranous enterocolitis. Surgery **44:**854-859.

71. **Weingarden AR, Chen C, Bobr A, Yao D, Lu Y, Nelson VM, Sadowsky MJ, Khoruts A.** 2014. Microbiota transplantation restores normal fecal bile acid composition in recurrent *Clostridium difficile* infection. Am J Physiol Gastrointest Liver Physiol **306:**G310-319.

72. **Seekatz AM, Aas J, Gessert CE, Rubin TA, Saman DM, Bakken JS, Young VB.** 2014. Recovery of the gut microbiome following fecal microbiota transplantation. MBio **5:**e00893-00814.

73. **Adminstration USFaD.** 2013. Guidance for Industry: Enforcement Policy Regarding Investigational New Drug Requirements for Use of Fecal Microbiota for Transplantation to Treat *Clostridium difficile* Infection Not Responsive to Standard Therapies, *on* U.S. Food and Drug Adminstration.

http://www.fda.gov/biologicsbloodvaccines/guidancecomplianceregulatoryinformation/guidances/vaccines/ucm361379.htm. Accessed

74. **Tvede M, Rask-Madsen J.** 1989. Bacteriotherapy for chronic relapsing *Clostridium difficile* diarrhoea in six patients. Lancet **1:**1156-1160.

75. **Lawley TD, Clare S, Walker AW, Stares MD, Connor TR, Raisen C, Goulding D, Rad R, Schreiber F, Brandt C, Deakin LJ, Pickard DJ, Duncan SH, Flint HJ, Clark TG, Parkhill J, Dougan G.** 2012. Targeted restoration of the intestinal microbiota with a simple, defined bacteriotherapy resolves relapsing *Clostridium difficile* disease in mice. PLoS Pathog **8:**e1002995.

76. **Khanna S, Pardi DS, Kelly CR, Kraft CS, Dhere T, Henn MR, Lombardo M-J, Vulic M, Ohsumi T, Winkler J.** 2016. A novel microbiome therapeutic increases gut microbial diversity and prevents recurrent *Clostridium difficile* infection. Journal of Infectious Diseases**:**jiv766.

77. **Edwards AN, Nawrocki KL, McBride SM.** 2014. Conserved oligopeptide permeases modulate sporulation initiation in *Clostridium difficile*. Infect Immun **82:**4276-4291.

CHAPTER 2

CodY-dependent Regulation of Sporulation in *Clostridium difficile*

Kathryn L. Nawrocki, Adrianne N. Edwards, Nadine Daou, Laurent Bouillaut and Shonna M. McBride

This work was published in 2016 in the *Journal of Bacteriology*.

K.L.N. performed experiments as listed: TY media growth curves, growth curves and sporulation assays for the 630Δ*erm* strain set in 70:30 medium, toxin Western blots, all ethanol-resistance assays, all alkaline phosphatase assays, all qRT-PCR studies, and germination studies. K.L.N also generated all figures, and wrote the manuscript.

Article Citation:

Nawrocki, K. L., Edwards, A. N., Daou, N., Bouillaut, L., & McBride, S. M. (2016). CodY-dependent Regulation of Sporulation in *Clostridium difficile*. *Journal of Bacteriology*, JB-00220. 198(15):2113-30 doi: 10.1128/JB.00220-16 PMCID 27246573

ABSTRACT

Clostridium difficile must form a spore to survive outside of the gastrointestinal tract. The factors that trigger sporulation in *C. difficile* remain poorly understood. Previous studies have suggested that a link exists between nutritional status and sporulation initiation in *C. difficile*. In this study, we investigated the impact of the global nutritional regulator, CodY, on sporulation in *C. difficile* strains from the historical 012 ribotype and the current epidemic 027 ribotype. Sporulation frequencies were increased in both backgrounds, demonstrating that CodY represses sporulation in *C. difficile*. The 027 *codY* mutant exhibited a greater increase in spore formation than the 012 *codY* mutant. To determine the role of CodY in the observed sporulation phenotypes, we examined several factors that are known to influence sporulation in *C. difficile*. Using transcriptional reporter fusions and qRT-PCR, we found that two loci associated with the initiation of sporulation, *opp* and *sinR*, are regulated by CodY. The data demonstrate that CodY is a repressor of sporulation in *C. difficile* and that the impact of CodY on sporulation and expression of specific genes is significantly influenced by the strain background. These results suggest that the variability of CodY-dependent regulation is an important contributor to virulence and sporulation in current epidemic isolates. This study provides further evidence that nutritional state, virulence and sporulation are linked in *C. difficile*.

IMPORTANCE

This study sought to examine the relationship between nutrition and sporulation in *C. difficile* by examining the global nutritional regulator, CodY. CodY is a known virulence and nutritional regulator of *C. difficile*, but its role in sporulation was unknown. Herein, we

demonstrate that CodY is a negative regulator of sporulation in two different ribotypes of *C. difficile*. We also demonstrate that CodY regulates the known effectors of sporulation, Opp and SinR. These results support the idea that nutrient limitation is a trigger for sporulation in *C. difficile* and that the response to nutrient limitation is coordinated by CodY. Additionally, we demonstrate that CodY has an altered role in sporulation regulation for some strains.

INTRODUCTION

Clostridium difficile is a Gram-positive, spore forming, anaerobic pathogen. It is found primarily within the mammalian gastrointestinal (GI) tract where it can cause severe, toxin-mediated GI disease (1-4). *C. difficile* is transmitted through the fecal-oral route, primarily in health-care associated settings, where it is a leading cause of nosocomial infections (5-7). But, for *C. difficile* to survive outside of the host, it must form a spore. Spores are an easily transmissible form of *C. difficile* because they are metabolically dormant and highly resistant to a variety of disinfectants and antibiotics, allowing them to persist on surfaces outside of the host (8). *C. difficile* spores serve as both a survival mechanism in the environment and as the infectious vehicle for transmission (8).

Akin to other studied spore-formers, *C. difficile* sporulation is controlled through the master sporulation regulator, Spo0A, which is active when phosphorylated and is essential for sporulation (8, 9). The regulatory components and signals that feed into Spo0A activation in *C. difficile* are not thoroughly elucidated, as many factors that activate or inactivate Spo0A in other spore formers are not present in sequenced *C. difficile* genomes (10-12). In *Bacillus* species, Spo0A activation is controlled through a phosphorelay. The

sporulation phosphorelays of *Bacillus* spp. are tightly regulated, and the flow of phosphate through the relay is managed in response to nutrient availability, stress, and other environmental signals (13-16). There is no known phosphorelay in *C. difficile*, and the factors that lead to Spo0A activation in this bacterium are poorly understood (10-12, 17, 18).

One hypothesized trigger of sporulation in *C. difficile* is nutrient deprivation, for which CodY plays a regulatory role. In previous work, we found that the two oligopeptide transporters, Opp and App, inhibit the initiation of sporulation in *C. difficile* (19). It was proposed that Opp and App inhibit sporulation by importing peptides into the cell. Imported peptides are thought to act as indirect inhibitors of sporulation by enhancing the nutritional state of the cell. But, the mechanisms through which imported peptides and other nutrients affect sporulation are unclear. To further probe how the nutritional state may trigger sporulation in *C. difficile*, we investigated the effects of the transcriptional regulator, CodY, on sporulation.

CodY is a global nutritional regulator found in many Gram-positive organisms (20-24). CodY was first discovered in *B. subtilis* and has the role of maintaining active growth, in part by regulating genes involved in nutrient acquisition and amino acid synthesis (25-27). CodY is a transcriptional regulator and sensor of the metabolic state of the cell. When nutrients are abundant, such as during exponential growth, CodY is bound by branched chain amino acids (BCAAs) and GTP, and acts primarily as a transcriptional repressor of alternative metabolic pathways (28-30). The availability of BCAAs and GTP impacts the DNA-binding capacity of CodY, allowing it to respond to the nutritional state of the cell. As nutrients become limited in the cell, CodY is no longer bound by these cofactors, and

repression of genes involved in secondary metabolic pathways and nutrient acquisition is alleviated. CodY not only regulates alternative metabolic pathways, but also impacts many diverse physiological processes such as competence, sporulation, virulence and motility (20-23, 27, 31-34). CodY is a known repressor of toxin synthesis in *C. difficile* and regulates synthesis of the toxin-specific sigma factor, TcdR (35). By repressing toxin synthesis via TcdR, CodY links virulence to the nutritional state of the bacterium. In *C. perfringens*, CodY also regulates toxin expression and, in addition, regulates production of the sporulation regulator, Spo0A (36). However, the role CodY plays in regulating sporulation in *C. difficile* is not known. Prior work evaluating CodY in *C. difficile* was performed under conditions that did not favor sporulation, which likely limited the detection of sporulation factors (37).

This study was undertaken to determine the role of CodY in the initiation of *C. difficile* sporulation and to examine possible strain dependent effects of CodY. We disrupted *codY* in historical and epidemic ribotype strains and observed increased sporulation frequency in both backgrounds. The sporulation frequency of the epidemic 027 *codY* mutant was markedly higher than the historical 012 mutant, signifying strain-dependent effects of CodY. Through gene expression analysis, we observed increased expression of sporulation-specific factors, such as *spo0A* and *sigE,* at earlier time points in both strains. Additionally, we investigated the potential regulation of the *app*, *opp,* and *sinRI* loci by CodY through transcriptional analyses and reporter fusions. The *codY* mutants exhibited differential expression of sporulation-associated genes, indicating possible strain-dependent effects. Overall, these results demonstrate that CodY is a repressor of

sporulation in *C. difficile* and that CodY can impact sporulation frequency in a strain-dependent manner.

MATERIALS AND METHODS

Bacterial strains and growth conditions. The strains and plasmids used in this study can be found in **Table 1**. Brain heart infusion-supplemented (BHIS) broth, BHIS agar plates or tryptose-yeast extract (TY) broth are frequently used to culture *C. difficile* strains (35, 38). BHIS medium was supplemented with 2 to 10 µg thiamphenicol ml^{-1}, or 5 µg erythromycin ml^{-1} (Sigma-Aldrich), as needed. Taurocholate (Sigma-Aldrich) was supplemented to the culture media at 0.1% as needed to induce germination of *C. difficile* spores (39, 40). Fructose was added to overnight cultures at 0.5% to prevent sporulation, as needed. *C. difficile* was cultured anaerobically in a vinyl chamber (Coy Laboratory Products) at 37°C with an atmosphere of 10% H_2, 5% CO_2, and 85% N_2 as previously described (41, 42). *Escherichia coli* strains were cultured at 37°C in LB (43) or BHIS supplemented with 20 µg chloramphenicol ml^{-1} and 100 µg ampicillin ml^{-1} as needed to maintain plasmid selection. To counter-select against *E. coli* following conjugation, media were supplemented with 50 µg kanamycin ml^{-1} (44, 45). *Bacillus subtilis* strains were cultured at 37°C in LB (43) or BHIS supplemented with 5 µg chloramphenicol ml^{-1} and 5 mM potassium nitrate, as needed. To counter-select against *B. subtilis* after conjugation, the media were supplemented with 50 µg kanamycin ml^{-1} (46).

Strain and plasmid construction. The oligonucleotides used in this study can be found in **Table 2**. Cloning and construction details of plasmids used in this study can be found in **Supplementary File S1**. Primer design was based on the strain 630 genomic sequence

TABLE 1 Bacterial strains and plasmids

Plasmid or strain	Relevant genotype or feature(s)	Source and/or reference
Strains		
E. coli HB101	F⁻ *mcrB mrr hsdS20*(r_B^- m_B^-) *recA13 leuB6 ara-14 proA2 lacY1 galK2 xyl-5 mtl-1 rpsL20*	B. Dupuy
E. coli MC101	HB101/pRK24	B. Dupuy
E. coli DH5α (maximum efficiency)	F⁻ ϕ80*lacZ*ΔM15 Δ(*lacZYA-argF*)*U169 recA1 endA1 hsdR17*(r_K^- m_K^+) *phoA supE44* λ⁻ *thi-1 gyrA96 relA1*	Invitrogen
E. coli MC553	HB101/pRK24/pMC421	This study
E. coli MC558	HB101/pRK24/pMC426	This study
E. coli MC568	HB101/pRK24/pMC451	This study
E. coli MC570	HB101/pRK24/pMC453	This study
E. coli MC605	HB101/pRK24/pMC463	This study
E. coli MC639	HB101/pRK24/pMC474	This study
E. coli MC641	HB101/pRK24/pMC476	This study
E. coli MC642	HB101/pRK24/pMC477	This study
E. coli MC643	HB101/pRK24/pMC478	This study
E. coli MC645	HB101/pRK24/pMC480	This study
E. coli MC646	HB101/pRK24/pMC481	This study
E. coli MC766	HB101/pRK24/pMC535	This study
E. coli MC767	HB101/pRK24/pMC536	This study
E. coli LB-EC99	HB101/pRK24/pLB103	This study
C. difficile 630Δ*erm*	Erm^s derivative of strain 630[a]	N. Minton; 92
C. difficile UK1	Clinical isolate	55
C. difficile MC310	630Δ*erm spo0A::ermB*	19
C. difficile MC327	630Δ*erm*/pBL103	This study
C. difficile MC364	630Δ*erm codY::ermB*	This study
C. difficile MC442	630Δ*erm codY::ermB* Tn916::*codY*	This study
C. difficile MC443	UK1 *codY::ermB* Tn916::*codY*	This study
C. difficile MC448	630Δ*erm*/pMC358	46
C. difficile MC560	630Δ*erm*/pMC421	This study
C. difficile MC565	630Δ*erm*/pMC426	This study
C. difficile MC572	630Δ*erm*/pMC451	This study
C. difficile MC574	630Δ*erm*/pMC453	This study
C. difficile MC576	630Δ*erm codY::ermB*/pMC451	This study
C. difficile MC578	630Δ*erm codY::ermB*/pMC453	This study
C. difficile MC589	630Δ*erm codY::ermB*/pMC358	This study
C. difficile MC596	630Δ*erm codY::ermB*/pMC421	This study
C. difficile MC599	630Δ*erm codY::ermB*/pMC424	This study
C. difficile MC601	630Δ*erm*/pMC426	This study
C. difficile MC608	630Δ*erm codY::ermB*/pMC463	This study
C. difficile MC610	630Δ*erm*/pMC463	This study
C. difficile MC611	630Δ*erm codY::ermB*/pMC463	This study
C. difficile MC647	630Δ*erm*/pMC477	This study
C. difficile MC649	630Δ*erm*/pMC476	This study
C. difficile MC650	630Δ*erm*/pMC474	This study
C. difficile MC651	630Δ*erm*/pMC478	This study
C. difficile MC653	630Δ*erm*/pMC480	This study
C. difficile MC654	630Δ*erm*/pMC481	This study
C. difficile MC655	630Δ*erm codY::ermB*/pMC474	This study
C. difficile MC657	630Δ*erm codY::ermB*/pMC476	This study
C. difficile MC658	630Δ*erm codY::ermB*/pMC477	This study
C. difficile MC659	630Δ*erm codY::ermB*/pMC478	This study
C. difficile MC662	630Δ*erm codY::ermB*/pMC481	This study
C. difficile MC768	630Δ*erm*/pMC535	This study
C. difficile MC769	630Δ*erm*/pMC536	This study
C. difficile LB-CD16	UK1 *codY::ermB*	57
C. difficile RT1075	630Δ*erm sigD::ermB*	65
B. subtilis BS49	CU2189::Tn*916*	P. Mullany
B. subtilis MC406	BS49 Tn*916*::pND3	This study

(Continued on following page)

TABLE 1 (Continued)

Plasmid or strain	Relevant genotype or feature(s)	Source and/or reference
Plasmids		
pRK24	Tra^+ Mob^+ *bla tet*	93
pMC123	*E. coli-C. difficile* shuttle vector; *bla catP*	51
pMC358	pMC123 *phoZ*	46
pMC421	pMC123 P$sinR_{600}$(630Δ*erm*)::*phoZ*	This study
pMC426	pMC123 P$oppB_{400}$(630Δ*erm*)::*phoZ*	This study
pMC451	pMC123 P$appA_{600}$(630Δ*erm*)::*phoZ*	This study
pMC453	pMC123 P$appA_{600}$(UK1)::*phoZ*	This study
pMC463	pMC123 P$oppB_{400}$(UK1)::*phoZ*	This study
pMC474	pMC123 P$oppB_{250}$(630Δ*erm*)::*phoZ*	This study
pMC476	pMC123 P$oppB_{170}$(630Δ*erm*)::*phoZ*	This study
pMC477	pMC123 P$oppB_{150}$(630Δ*erm*)::*phoZ*	This study
pMC478	pMC123 P$oppB_{250}$(UK1)::*phoZ*	This study
pMC480	pMC123 P$oppB_{170}$(UK1)::*phoZ*	This study
pMC481	pMC123 P$oppB_{150}$(UK1)::*phoZ*	This study
pMC535	pMC123 P$sinR_{400(C\text{-}290A)}$(630Δ*erm*)::*phoZ*	This study
pMC536	pMC123 P$oppB_{400(G\text{-}181A)}$(630Δ*erm*)::*phoZ*	This study
pBL18	Tn*916* integrational vector; *ermB*	This study
pBL26	pBL18 *catP*	This study
pBL103	Group II intron targeted to *codY*	57
pND3	pBL26 *codY*	This study
pJIR1456	*E. coli-C. difficile* shuttle vector; *catP*	94
pMMOrf	Marnier transposon vector	95
pMMOrf-Cat	pMMOrf *catP*	This study
pSMB47[b]	Tn*916* integrational vector; *catP ermB*	96

[a] Erm^s, erythromycin sensitive.
[b] GenBank accession number U69267.

TABLE 2 Oligonucleotides

Primer	Sequence[a]	Use (location[b])	Source or reference
oMC44	5′-CTAGCTGCTCCTATGTCTCACATC-3′	*rpoC* qPCR (CD0067)	45
oMC45	5′-CCAGTCTCTCCTGGATCAACTA-3′	*rpoC* qPCR (CD0067)	45
oMC112	5′-GGCAAATGTAAGATTTCGTACTCA-3′	*tcdB* qPCR (CD0660)	19
oMC113	5′-TCGACTACAGTATTCTCTGAC-3′	*tcdB* qPCR (CD0660)	19
oMC152	5′-GTTATGGAAGTCAAGGACATGCAC-3′	*ilvC* qPCR (CD1565)	37
oMC153	5′-GCTTCTGCTACACTCTTAACTTCA-3′	*ilvC* qPCR (CD1565)	37
oMC331	5′-CTCAAAGCGCAATAAATCTAGGAGC-3′	*spo0A* qPCR (CD1214)	19
oMC332	5′-TTGAGTCTCTTGAACTGGTCTAGG-3′	*spo0A* qPCR (CD1214)	19
oMC339	5′-GGGCAAATATACTTCCTCCTCCAT-3′	*sigE* qPCR (CD2643)	19
oMC340	5′-TGACTTTACACTTTCATCTGTTTCTAGC-3′	*sigE* qPCR (CD2643)	19
oMC349	5′-CCTTTGTGCTAGCCTTATTGTTAGG-3′	*oppB* qPCR (CD0853)	19
oMC350	5′-AAGTATGAGTACTAAGGCAACCCA-3′	*oppB* qPCR (CD0853)	19
oMC365	5′-GGAAGTAACTGTTGCCAGAGAAGA-3′	*sigF* qPCR (CD0772)	19
oMC366	5′-CGCTCCTAACTAGACCTAAATTGC-3′	*sigF* qPCR (CD0772)	19
oMC425	5′-CTGTGACTTTGTAGCTTGG-3′	*codY* PCR (CD1275)	This study
oMC426	5′-CTGCTAAAGGCATTTTCTCACTC-3′	*codY* PCR (CD1275)	This study
oMC427	5′-GTGGTGTTAATACATCAGAACTTCC-3′	*sigG* qPCR (CD2642)	19
oMC428	5′-CAAACTGTTGTCTGGCTTCTTC-3′	*sigG* qPCR (CD2642)	19
oMC429	5′-GCCTGTGCTTCCAATGATAAAG-3′	*appA* qPCR (CD2672)	19
oMC430	5′-ATATCTGGGTCACTTGCCATAG-3′	*appA* qPCR (CD2672)	19
oMC527	5′-AGGCAGGTTTACATCCAACATA-3′	*sinR* qPCR (CD2214)	19
oMC528	5′-AGTGGTATGTCTAAAGCAGTAGC-3′	*sinR* qPCR (CD2214)	19
oMC529	5′-GCCTTGGTATATAACTCAAATCGAAAGT-3′	*sinI* qPCR (CD2215)	19
oMC530	5′-ATCTGTGATATCAGATTTAGTTCTCTTGAAT-3′	*sinI* qPCR (CD2215)	19
oMC547	5′-TGGATAGGTGGAGAAGTCAGT-3′	*tcdA* qPCR (CD0663)	19
oMC548	5′-GCTGTAATGCTTCAGTGGTAGA-3′	*tcdA* qPCR (CD0663)	19
oMC1008	5′-GCGGGATCCTTATTATCCCTCCACTTTAGATTATATTC-3′	P*sinR* cloning (CD2214)	This study
oMC1009	5′-GCGGAATTCATTAAATTATTTTATAAGATTATTACTCTACTATA-3′	P*sinR* cloning (CD2214)	This study
oMC1012	5′-GCGGGATCCACCCCAACCCCCCTTTG-3′	P*oppB* cloning (CD0853)	This study
oMC1015	5′-GCGGAATTCACTGTGTACATAGTTTTAGAATAAAG-3′	P*oppB* cloning (CD0853)	This study
oMC1025	5′-GCGGGATCCATTCTTATAAAACCTCCATAAAATAATAT-3′	P*appA* cloning (CD2672)	This study
oMC1026	5′-GCGGAATTCCTTCTTCCTTTGATAAATCTTGATG-3′	P*appA* cloning (CD2672)	This study
oMC1074	5′-GCGGAATTCAATTTTATAGAAAATAATGAAGAATAGAATATA-3′	P*oppB* cloning (CD0853)	This study
oMC1076	5′-GCGGAATTCAATTTTTAAAAAGTTTGTTTACACAG-3′	P*oppB* cloning (CD0853)	This study
oMC1077	5′-GCGGAATTCACACAGTTAATAAATGATGCTAAA-3′	P*oppB* cloning (CD0853)	This study
oMC1178	5′-GAAAATTTTTTTAATTTTAAAAATATATTCTACATATC-3′	P*sinR* cloning (CD2214)	This study
oMC1179	5′-GATATGTAGAATATATTTTTAAAATTAAAAAAATTTTC-3′	P*sinR* cloning (CD2214)	This study
oMC1180	5′-GTATAAATAAAATAATTTGATAAAATTTTAACAATTTTT-3′	P*oppB* cloning (CD0853)	This study
oMC1181	5′-AAAAATTGTTAAAATTTTATCAAATTATTTTATTTATAC-3′	P*oppB* cloning (CD0853)	This study
3′ catP	5′-AAACGCGTTTAACTATTTATCAATTCCTGCAAT-3′	*catP* cloning	J. Sorg
5′ catP2	5′-AAACGCGTAATTAGATGCTAAAAATTTGTAATT-3′	*catP* cloning	J. Sorg
oLB275	5′-AAGGATCCAGAGTGAAAATTGAAAAAAATC-3′	*codY* cloning (CD1274)	This study
oLB276	5′-CCCAAGCTTCTAATCTAAACCTATAAAATATAG-3′	*codY* cloning (CD1275)	This study
oLB344	5′-AAGCGCTCATGAGCCCGAAG-3′	*codY* cloning (CD1275)	This study
tcdRqF	5′-AGCAAGAAATAACTCAGTAGATGATT-3′	*tcdR* qPCR (CD0659)	53
tcdRqR	5′-TTATTAAATCTGTTTCTCCCTCTTCA-3′	*tcdR* qPCR (CD0659)	53
ITR	5′-CCCACATGCATGCTAACAGGTTGGCTGATAAGTCCCCGGTCT-3′	*catP* cloning	This study

[a] Underlined regions denote restriction enzyme cut sites.
[b] Locus number in reference to the 630 genome (NC_009089.1). qPCR, quantitative PCR.

(NC_009089.1), and all sequences matched the corresponding sequence in the 027 isolate, R20291 (NC_0133161.1). All plasmids were confirmed by sequencing (Eurofins MWG Operon). Genomic DNA was prepared as previously described (37, 41). To generate strain MC364 (630 *codY::ermB*), pBL103 was transferred into *C. difficile* 630Δ*erm* and colonies screened for Targetron insertion, as previously described (44, 45). To generate the *codY* complemented strains MC442 and MC443, pND3 was integrated into the Tn*916* region within the chromosome of *B. subtilis* strain BS49 and selected for on BHIS plates containing 5 μg chloramphenicol ml^{-1}, as previously described (47-49). Promoter-*phoZ* fusion plasmids were transferred by conjugation from *E. coli* into *C. difficile* 630Δ*erm* and MC364 as previously described (45, 46).

Motility assays. *C. difficile* strains were grown overnight in BHIS medium supplemented with 0.1% taurocholate and 0.2% fructose, and subsequently back-diluted to BHIS to obtain active, logarithmic phase cultures. When the cultures reached an OD_{600} of 0.5, 5 μl was inoculated into the center of one-half concentration BHI plates containing 0.3% agar. The diameter of cell growth was measured every 24 h thereafter for seven days. The results represent four independent experiments. Results are presented as the means and standard errors of the means, and the two-tailed Student's *t* test was performed for statistical comparison of mutant outcomes to the parent strain.

Sporulation efficiency assays. *C. difficile* strains were started as low-density cultures in BHIS medium supplemented with 0.1% taurocholate (Sigma-Aldrich) and 0.5% fructose, and grown to mid-log phase. Cultures were subsequently back-diluted to an optical density at 600 nm (OD_{600}) of 0.5 in 70:30 sporulation medium (50) or BHIS. The cultures were then immediately diluted 1:10 into the main culture flask containing 70:30 or BHIS broth

to reach a starting OD_{600} of 0.05. All cultures were anaerobically incubated at 37°C while being monitored for growth and spore production. Micrographs were taken and enumerated as previously described, with minor modifications (19). Approximately 24 hours following the start of stationary phase (T_{24}), 1 ml samples were taken from the cultures. Samples were pelleted at 21,130 x *g* max for 30 s and resuspended in 0.01 ml of supernatant. Two µl of each concentrated culture was placed on a thin layer of 0.7% agarose previously applied to a slide and imaged with an X100 Ph3 oil immersion objective on a Nikon Eclipse Ci-L microscope. Two to three fields of view were acquired for each strain at T_{24} using a DS-Fi2 camera. A minimum of 1000 cells from each strain were examined and used to calculate the percentage of spores (number of spores divided by the total imaged population).

In addition to microscopy, cultures were tested to determine the ratio of ethanol-resistant spores formed in the population. Cultures were diluted and plated onto BHIS with 0.1% taurocholate to determine the maximum viable cells in the population, which occurred two or five hours after the start of stationary phase for 70:30 and BHIS cultures, respectively. To assess the frequency of spore formation, 500 µl samples were taken at T_{24} and mixed 1:1 with 95% ethanol for 15 minutes. Ethanol-treated cultures were plated on BHIS containing 0.1% taurocholate and the number of ethanol resistant CFU were enumerated after incubation for 24 h. The number of ethanol resistant CFU/ml was divided by the maximum viable population and multiplied by 100 to calculate the percentage of ethanol resistant CFU/ml in the culture. A minimum of three biological replicates were performed for each strain and condition tested. Sporulation efficiency results were averaged and the standard error of the mean was calculated. Data were analyzed by a one-

way ANOVA followed by Dunnett's multiple comparison test using Graphpad Prism 6. $P \leq 0.05$ was considered statistically significant.

Quantitative reverse transcription PCR analysis (qRT-PCR). qRT-PCR was performed as previously described with minor modifications (19). Cultures of *C. difficile* were grown in 70:30 medium as described above. Samples for RNA isolation were collected at mid-logarithmic growth (OD_{600} of 0.5), the onset of stationary phase (T_0) and at stationary phase (T_4) and diluted into 1:1 acetone-ethanol. RNA was isolated as previously described (37, 51). The Tetro cDNA synthesis kit (Bioline) was used for cDNA synthesis. cDNA was generated from four biological replicates and qRT-PCR was performed using a Sensi-Fast SYBR and Fluorescein kit (Bioline) and 50 ng of cDNA as template on a Bio-Rad CFX96 real-time system. To control for genomic contamination, cDNA reactions containing no reverse transcriptase were used. qRT-PCR reactions were performed in technical triplicates. qRT-PCR primers were generated with the PrimerQuest tool available through Integrated DNA Technologies. Primer efficiencies were determined for each set of qRT-PCR primers. Results were calculated with the comparative cycle threshold method (52) with the expression of the amplified transcript being normalized to the internal control transcript, *rpoC*. To evaluate the statistical significance of the results, a two-way repeated measures ANOVA, followed by a Dunnett's multiple comparisons test, was used to compare parent strain expression with its respective *codY* mutant and complemented strain at each time point using Graphpad Prism 6. $P \leq 0.05$ was considered statistically significant.

Western blot analysis. Western blots were performed as previously described, with minor modifications (53). Strains were grown in BHIS medium supplemented with 0.1%

taurocholate and 0.5% fructose until the cultures reached mid-log phase. Cultures were then back-diluted 1:50 into fresh 70:30 medium. Following incubation at 37°C for 8 h, a 6 ml sample of each culture was pelleted and resuspended in 1 ml of 1x Laemmli sample buffer (Bio-Rad). Cells were mechanically disrupted using a Mini-BeadBeater and 0.1 mm silica beads (Biospec Products). Following bead beating, samples were centrifuged for 15 min at 16,100 x *g*. Culture supernatants were boiled for 10 min at 95-100°C and run on a 4-15% gradient precast SDS-PAGE gel (Bio-Rad). Proteins were transferred to a 0.45 µm nitrocellulose membrane for 1 h at 100 V with the Mini-Trans Blot module (Bio-Rad). Following transfer, membranes were probed with mouse anti-TcdA (Novus Biologicals) and mouse anti-RNA polymerase β subunit (Abcam). Membranes were then probed with secondary goat anti-mouse antibody, AlexaFluor 488 (Life Technologies). Imaging and relative quantification of the blots were performed on a ChemiDoc imager (Bio-Rad). Quantification was performed only on full-length protein. Four biological replicates for each strain were analyzed, and a representative image is shown.

Alkaline phosphatase assays. Alkaline phosphatase assays were performed as previously described, with minor modifications (46, 54). Cultures of *C. difficile* containing *phoZ* reporter constructs were grown overnight in BHIS supplemented with 0.1% taurocholate, 0.5% fructose and 2 µg thiamphenicol ml^{-1}. Active cultures were diluted to an OD_{600} of 0.5 in 70:30 medium. Cultures were further diluted 1:10 into a culture flask containing 70:30 medium and 2 µg thiamphenicol ml^{-1} to reach a starting OD_{600} of 0.05. At an OD_{600} of 0.5 (mid-log phase), duplicate 1 ml samples were taken. Four hours after the transition to stationary phase (T_4), duplicate 250 µl samples were taken. The samples were pelleted, the supernatants were discarded and cell pellets were stored at -20°C overnight. To prepare the

samples for assay, pellets were thawed on ice and washed in 0.5 ml of chilled Wash buffer (10 mM Tris-HCl, pH 8.0, 10 mM $MgS0_4$), pelleted and resuspended in 0.8 ml Assay buffer (1M Tris-HCl, pH 8.0, 0.1 mM $ZnCl_2$). Samples were vortexed for 15 s following the addition of 0.05 ml of 0.1% SDS and 0.05 ml chloroform. A blank sample without cells was used as a baseline measurement of optical density for all experiments. Samples were incubated at 37°C for 5 min and transferred to ice for an additional 5 min. Samples were then allowed to return to room temperature. The colorimetric assay was started by the addition of 0.1 ml of 0.4% *p*NP (*p*-nitrophenyl phosphate in 1 M Tris-HCl, pH 8.0; Sigma-Aldrich) to each sample. The samples were mixed and incubated in a 37°C water bath until the development of a light yellow color. Upon color development, 0.1 ml of Stop solution (1 M KH_2PO_4) was added and the samples were transferred to ice to stop the phosphatase reaction. Samples were then centrifuged at 4°C for 5 min at max speed in a benchtop centrifuge. The absorbance of each sample was measured at OD_{420} and $OD_{550.}$ To calculate the units of activity, normalized to cell volume, the following formula was applied: $\frac{[\mathrm{OD420}-(1.75\ \mathrm{x\ OD550})]\ 1000}{t\ (\mathrm{min})\ \mathrm{x\ OD600\ x\ vol.cells\ (ml)}}$. Technical duplicates were averaged for each assay set. At least four biological replicates were performed for each experiment. The data are presented as the means and standard error of the mean for the experimental replicates. Data were analyzed by a two-way ANOVA followed by Tukey's multiple comparison test using Graphpad Prism 6. $P \leq 0.05$ was used.

Germination assays. Spore purification and germination assays were performed as previously described with minor modifications (40, 55). Strains were grown in BHIS medium with 0.2% fructose. 200 µl of active culture was spread onto a 70:30 plate as a confluent lawn, with approximately six plates prepared per strain. Plates were left in the

chamber for a minimum of 48 hours to allow for spores to form. After 48 hours, plates were removed from the chamber and the lawns were scraped into 15 ml of ice cold sterile water. Spore suspensions were incubated overnight at 4°C. Spore suspensions were then centrifuged in a swing-bucket rotor at 1811 x *g* for 10 minutes, and the supernatants were decanted. The pellets were washed five times with ice cold sterile water, and after the fifth wash, the spore pellets were resuspended in 30 ml of ice cold sterile water. 3 ml aliquots of the spore suspension were layered over individual 10 ml beds of 50% sucrose. Spores were centrifuged through the sucrose for 20 minutes in a swing-bucket rotor at 3200 x *g* to remove cellular debris. Following centrifugation, the sucrose was removed and spore pellets were resuspended in 1 ml of ice cold water and pooled. Spores were again pelleted at 1811 x *g* for 10 minutes. The supernatant was decanted and spores were washed five times with 10 ml of ice cold sterile water to removed residual sucrose. Following the last wash, spores were resuspended in 1 ml of sterile water and checked for purity by phase contrast microscopy, and the OD_{600} of each preparation was assessed. Spore preparations were standardized to an approximate OD_{600} of 3.0. For the germination assay, spores were first heat activated at 60°C for 30 minutes and then diluted 1:10 into BHIS with or without 5 mM of the germinant taurocholate. The OD_{600} was monitored for 20 minutes starting from when the spores were diluted into BHIS. Germination is represented as a ratio of the OD_{600} at a timepoint (t) over the OD_{600} at the start of the assay (t_0), plotted against time. Germination assays were performed in triplicate. The data are presented as the averaged ratios for each timepoint, and the standard error of the mean is shown. A two-way repeated measures ANOVA, followed by a Dunnett's multiple comparisons test, was used to

compare the parent strain with its respective *codY* mutant and complemented strain at individual timepoints. *, $P \leq 0.05$.

RESULTS

Generation of *codY* mutants and assessment of growth phenotypes and toxin production

To assess the role of CodY in the sporulation of *C. difficile*, we first generated a *codY* mutant in the 630Δ*erm* strain (012 ribotype). In prior work, we examined a single cross-over mutant that disrupted the *codY* locus in the related strain, JIR8094 (37, 56). Due to the instability of the single-crossover, and the virulence and motility defects of the JIR8094 strain (53), a *codY* Targetron mutant in the 630Δ*erm* background was used in this study. We utilized the same Targetron construct used previously to generate a *codY* mutant in the UK1 background (027 ribotype) (57). The Targetron insertion into *codY* of strain 630Δ*erm* was verified through PCR and sequencing of the locus (**Fig. S2**). We further verified the inactivation and complementation of *codY* by examining expression of *codY* (**Fig. S3**) and the CodY-repressed gene, *ilvC*, which encodes a component of branched chain amino acid (BCAA) synthesis (**Fig. S4)**(56, 58). We observed little change in expression of *codY* in the Targetron-disrupted mutants (**Fig. S3**); however, disruption of *codY* had clear effects on the expression of CodY-dependent genes, indicating that no functional CodY was present (**Fig. S4**). In MC364 (hereafter 630 *codY*) and LB-CD16 (hereafter UK1 *codY*) (**Fig. S4**), we observed an increase in the expression of *ilvC* during logarithmic growth and at T_0 when compared to their respective parent strains. These results demonstrate that *ilvC* is derepressed in the absence of CodY, as anticipated. In the

codY-complemented strains MC442 (630 *codY* Tn916::*codY*) and MC443 (UK1 *codY* Tn*916*::*codY*), we observed significantly higher *codY* transcription than in the parent strains (**Fig. S3**). Higher expression of *codY* was not expected for the complemented strains, given that a single copy of *codY* was restored to the genome. Greater expression of *codY* in the complemented strains suggests that native placement of the gene is required for proper regulation of transcription. Disregulation of *codY* expression may also explain the incomplete restoration of some CodY-dependent transcription and phenotypes observed.

We evaluated the growth phenotype of both 630 *codY*, UK1 *codY* and their respective complements, MC442 and MC443, in TY broth and 70:30 sporulation medium (**Fig. 1A-D**). As observed with previous *codY* mutants, the disruption of *codY* leads to a slight growth defect in TY medium in both the 630Δ*erm* and UK1 strain sets (**Fig. 1A, C**) (56). This growth defect was not as pronounced as previously described because the antibiotic selection required for maintenance of the single insertion in previous *codY* mutants has been eliminated (56). When *codY* is complemented on the chromosome in either strain background, the growth defect in TY medium is corrected (**Fig. 1A, C**). In 70:30 sporulation broth, the UK1 strains exhibited no growth defect, unlike the 630 *codY* mutant, which exhibited a short exponential growth phase and extended transition phase (**Fig. 1B, D**). The dissimilar growth profiles of the 630 *codY* and UK1 *codY* mutants suggests that CodY-responsive gene expression differs between the strains (59-61).

C. difficile encodes two large toxins, TcdA and TcdB, which are essential for virulence (1-4, 62). Previous studies demonstrated that toxin production is controlled by the global nutritional regulatory factors, CcpA and CodY, in strain JIR8094 (56, 63). When

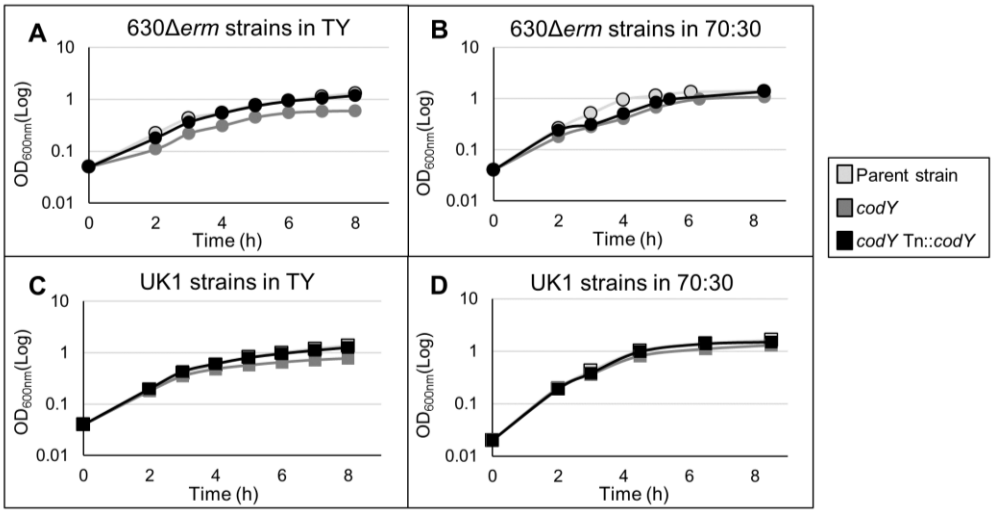

Figure 1. Impact of *codY* on growth in different media and alternate strain backgrounds. A representative growth curve of 630Δ*erm*, MC364 (630 *codY*) and MC442 (630 *codY*, Tn*916::codY)* is shown in TY **(A)** and 70:30 sporulation media **(B).** A representative growth curve of UK1, LB-CD16 (UK1 *codY*) and MC443 (UK1 *codY*, Tn*916*::*codY*) is shown in TY **(C)** and 70:30 sporulation media **(D).**

bound to the cofactors GTP and BCAAs, CodY represses toxin gene expression by binding to the promoter region of *tcdR*. TcdR is a toxin-specific sigma factor that is encoded within the pathogenicity locus (PaLoc) and directs expression of both *tcdA* and *tcdB* (64). We performed qRT-PCR and Western blot analyses of the *codY* mutants grown in 70:30 sporulation medium to confirm the loss of toxin repression and subsequential increase in toxin protein (37, 56). As predicted, *tcdR* expression was increased earlier during growth of the *codY* mutants in both strains, as compared to the respective parent strains. (**Fig. S5A, B**). We also evaluated the expression profiles of *tcdA* and *tcdB*, whose transcription depends on the toxin sigma factor, TcdR (64). The expression of *tcdA* and *tcdB* in 630 *codY* and UK1 *codY* was also elevated during mid-logarithmic growth phase, compared to the parent strains (**Fig. 2A, B and S5C, D**). To further assess the effects of CodY on toxin regulation and production, we performed Western blots to examine the accumulation of TcdA protein. 630 *codY*, UK1 *codY*, and the respective parent strains were grown to stationary phase in 70:30 sporulation medium, and whole-cell lysates were probed for TcdA and the RNA polymerase β subunit (RNAP, **Fig. 2C**). In both *codY* mutants, more full-length TcdA (308 kDa) was present than in the parent controls grown in 70:30 medium (a ~19-fold increase in 630 *codY* and a ~5-fold increase in UK1 *codY* over their respective parent strains). Together these results demonstrate that toxin gene transcription and synthesis are higher in the absence of CodY, consistent with previous reports (37, 56).

Toxin gene expression is also regulated by the flagellar-specific sigma factor, SigD (53). Toxin production is greatly decreased in the related, nonmotile 012 strain, JIR8094, due to a significant decrease in *sigD* expression (53). Because both the toxin and motility phenotypes share some regulatory components, and CodY influences motility in the related

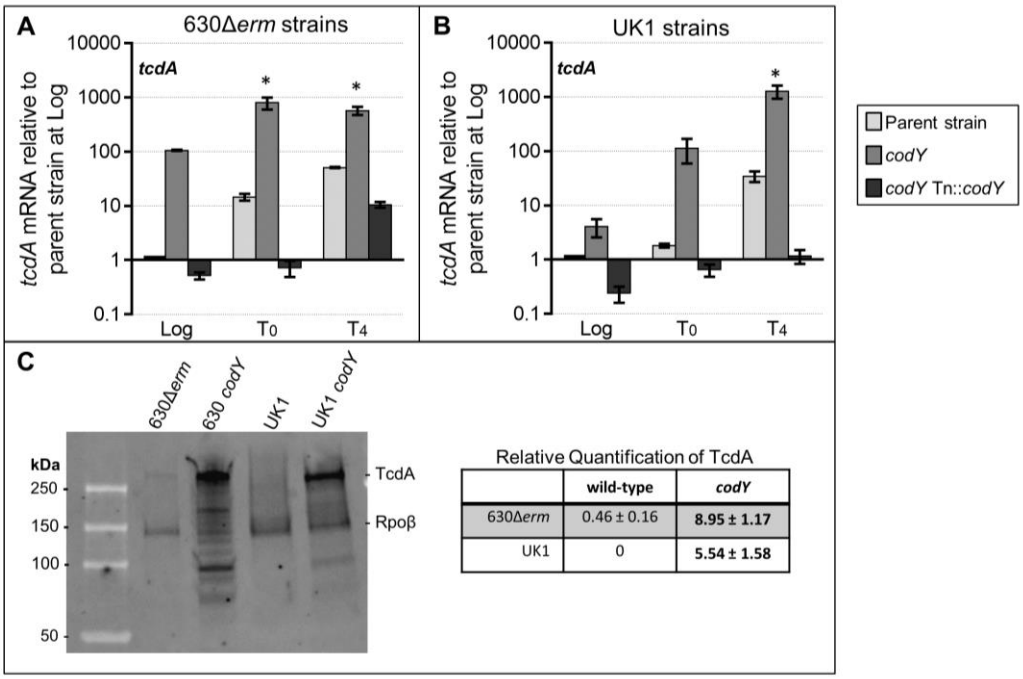

Figure 2. Transcript and protein levels of *tcdA* are increased in *codY* mutants. qRT-PCR analysis of *tcdA* in **A**) 630Δ*erm*, MC364 (630 *codY*) and MC442 (630 *codY* Tn*916*::*codY*), and **B**) UK1, and LB-CD16 (UK1 *codY*) and MC443 (UK1 *codY* Tn*916*::*codY*) strains grown in 70:30 liquid sporulation media. Samples for RNA were collected during logarithmic growth (OD_{600} ~0.5), transition to stationary phase (T_0), and four hours after the transition into stationary phase (T_4). The means and SEM of four biological replicates are shown. A two-way repeated measures ANOVA, followed by Dunnett's multiple comparison test, was used to compare parent strains with their *codY* mutant or the parent strain with the respective complemented strain at the designated timepoints. *, $P \leq 0.05$. **C**) A representative TcdA and Rpoβ western blot of strains grown to stationary phase in 70:30 liquid sporulation media. The relative quantification means and SEM of four biological replicates are shown. A two-tailed Student's *t* test was used to compare parent strain with *codY* mutant. Bolded text indicates significance. $P \leq 0.05$.

organism, *Clostridium perfringens* (36), we asked whether CodY controls motility in the motile 630Δ*erm* (012 ribotype) and UK1 strains (027 ribotype). Motility assays were performed on soft agar plates, and diameters measured every 24 h over seven days; a motility defective *sigD* mutant was included as a negative control (65). As shown in **Fig. S6**, the 630 *codY* mutant consistently displayed lower motility than its parent strain, but no significant difference in motility was observed between the UK1 and UK1 *codY* strains (mean final diameters: 630Δ*erm*, 51 ± 1.7 mm; 630*codY*, 42.3 ± 0.7 mm; UK1, 48.0 ± 1.2 mm; UK1*codY*, 52.0 ± 2.1 mm). CodY is not known to directly regulate the motility sigma factor, SigD, or any other known factors that affect motility in *C. difficile* (37, 53). Considering that the growth rate defect of the 630 *codY* mutant is more pronounced than for the UK1 *codY* mutant (**Fig. 1**), the slower growth of 630 *codY* is likely contributing to the decreased motility observed.

codY mutants demonstrate increased sporulation frequency and expression of sporulation-specific factors

To evaluate the impact of CodY on sporulation, we grew the *codY* mutants and the respective parent strains in 70:30 sporulation broth and assessed sporulation frequency 24 hours after the onset of stationary phase (T_{24}). Samples were visualized by phase contrast microscopy, and the sporulation frequency was calculated by direct counting as described in the Materials and Methods. As shown in **Fig. 3**, the 630 *codY* mutant exhibited a two-fold increase in sporulation frequency when compared to the parent strain, 630Δ*erm* (~1.8% vs. 0.9%; *P= 0.15*). In contrast, the UK1 *codY* mutant demonstrated a ~1,400-fold increase over UK1 (~57% vs. 0.04%). Similar results were obtained when cultures were

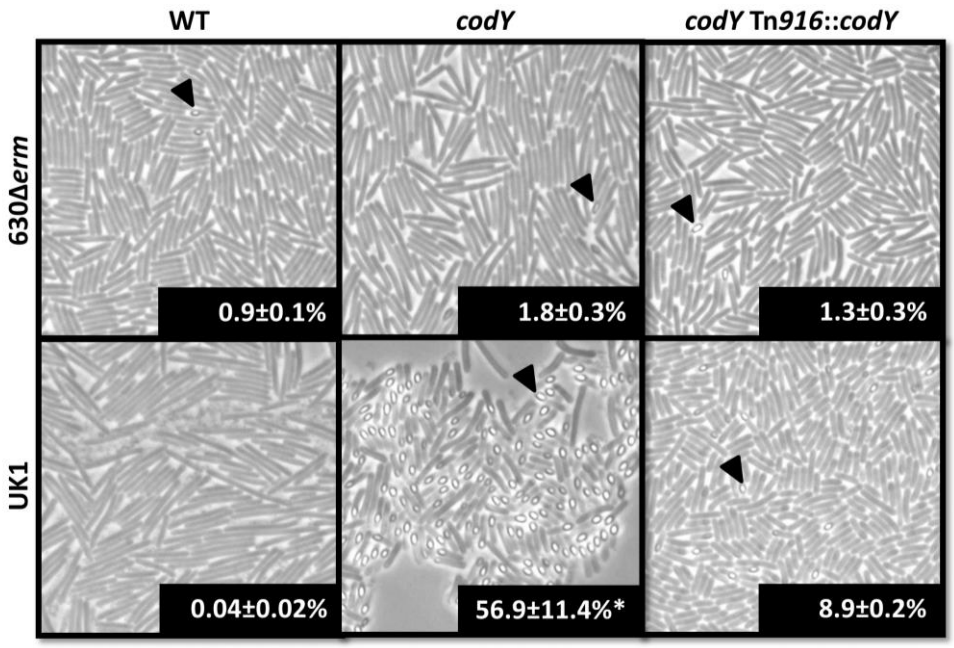

Figure 3. Disruption of *codY* leads to increased sporulation frequency. Phase contrast microscopy of 630Δ*erm,* MC364 (630 *codY*), MC442 (630 *codY* Tn::*codY*), UK1, LB-CD16 (UK1 *codY*), and MC443 (UK1 *codY* Tn::*codY*) grown in 70:30 liquid sporulation medium at T_{24}. Percentage of phase bright spores was evaluated through direct counting of phase contrast micrographs. Filled arrows indicate phase-bright spores. The means and SEM for spore counts of four biological replicates are shown. Sporulation frequencies of the parent strains were compared to the respective *codY* mutants and complemented strains using a one-way ANOVA. (*, $P \leq 0.05$).

examined for the frequency of ethanol-resistant spore formation within the viable population for cells grown in 70:30 sporulation broth; few spores were produced in any strain grown in BHIS medium for 24 h. (**Table 3**). These results indicate that CodY represses sporulation in both *C. difficile* strains. However, the effects of CodY on sporulation are dramatically different in the two strains, suggesting that CodY-dependent gene regulation can vary by strain background.

Since the *codY* mutants demonstrate increased sporulation frequency, we asked whether this increase was a consequence of earlier or higher expression of sporulation regulatory factors. To do so, we assessed the relative gene expression of the key sporulation regulator, *spo0A,* in the parent and *codY* mutant strains during growth in sporulation medium (**Fig. 4**). Spo0A is the master regulator of sporulation and is essential for initiation of sporulation in *C. difficile* (8, 9, 66). During exponential phase growth, the 630 *codY* mutant had 2-fold higher *spo0A* expression than the parent strain, consistent with earlier initiation of sporulation (**Fig. 4A**). By T_0 (transition to stationary phase) and T_4 (four hours after transition to stationary phase), *spo0A* expression was similar for the 630 *codY* mutant and the parent strain. For the UK1 *codY* mutant, *spo0A* transcript levels were higher than the wild-type during logarithmic growth (~1.6-fold) and at T_0 (~3.6 fold), also signifying early entry into sporulation (**Fig. 4B**). But by T_4, UK1 *codY* had lower *spo0A* expression than the wild-type, consistent with *spo0A* gene expression patterns in later stages of sporulation (19).

To evaluate the progression of sporulation in the *codY* mutants, we measured the expression of sporulation-specific sigma factors, *sigF*, *sigE* and *sigG* (**Fig. 4C-H**). *sigF* and *sigE* are dependent on Spo0A for transcription, and they are the early sporulation sigma

TABLE 3 Ethanol-resistant spore formation[a]

Strain background (growth medium)	Frequency of ethanol-resistant spore formation (% ± SEM) in:		
	WT strain	*codY* mutant	*codY* Tn*916*::*codY* strain
630Δ*erm* (70:30 medium)	0.03 ± 0.01	0.18 ± 0.02	0.14 ± 0.08
630Δ*erm* (BHIS)	0.03 ± 0.01	0.003 ± 0.00	0.0001 ± 0.00
UK1 (70:30 medium)	0.0005 ± 0.00	**22.02 ± 5.99**	0.53 ± 0.19
UK1 (BHIS)	0.02 ± 0.01	0.05 ± 0.00	0.05 ± 0.03

[a] Data were analyzed by one-way ANOVA, followed by Dunnett's test for multiple comparisons. Bold text indicates a P value of ≤0.05. Comparisons were made between the parent strain and its respective *codY* mutant or the parent and complemented strains.

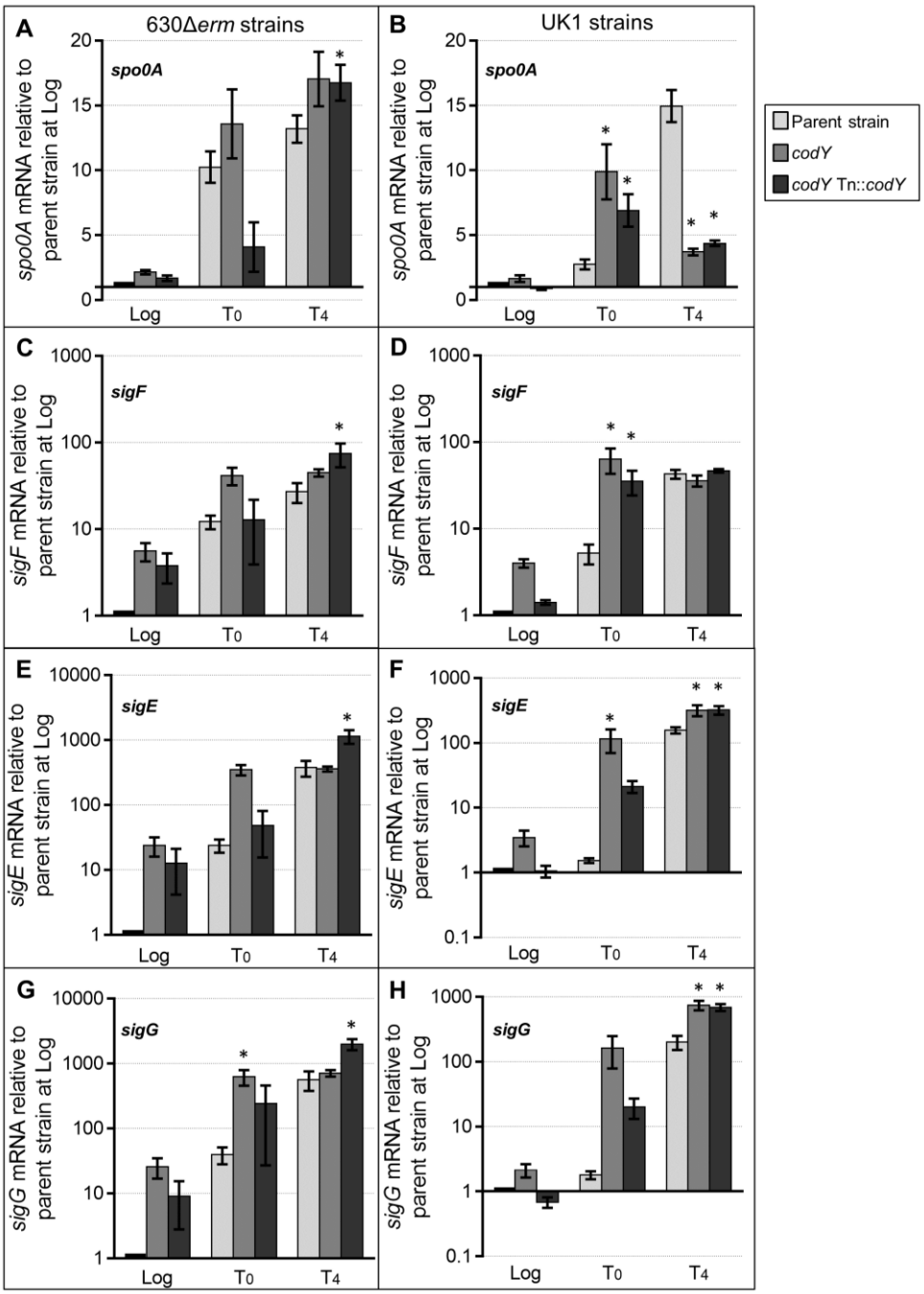

Figure 4. Increased expression of sporulation specific factors in *codY* mutants. qRT-PCR analysis of *spo0A* (**A**,**B**), *sigF* (**C**,**D**), *sigE* (**E**,**F**), and *sigG* (**G**,**H**) expression in 630Δ*erm*, MC364 (630 *codY*), MC442 (630 *codY* Tn*916*::*codY*) (**A**,**C**,**E**,**G**) or UK1, LB-CD16 (UK1 *codY*), and MC443 (UK1 *codY* Tn*916*::*codY*) (**B**,**D**,**F**,**H**) grown in 70:30

sporulation media. Samples for RNA isolation was collected during logarithmic growth (OD_{600} ~0.5), transition to stationary phase (T_0), and four hours after the transition into stationary phase (T_4). The means and SEM of four biological replicates are shown. A two-way repeated measures ANOVA followed by Dunnett's multiple comparison test was used to compare parent strain with the *codY* mutant or the parent strain with the respective complemented strain at the designated timepoints. *, $P \leq 0.05$.

factors for the forespore and mother cell compartments, respectively, while SigG is the late-stage sporulation factor for the forespore (11, 17, 18, 66). *sigF* gene expression was significantly higher in log-phase and at T_0 in the 630 and UK1 *codY* mutants, compared to their parent strains (630 *codY* ~5-fold higher at log, ~3-fold higher at T_0; UK1 *codY* ~4-fold higher at log, ~12-fold higher at T_0; **Fig. 4C-D**). Likewise, *sigE* gene expression was higher in the *codY* mutants at log-phase and at T_0 (630 *codY* ~24-fold higher at log, ~15-fold higher at T_0; UK1 *codY* ~3-fold higher at log, ~77-fold higher at T_0; **Fig. 4E-F**). The premature transcription of *sigF* and *sigE*, and the higher overall expression of these factors, are consistent with earlier entry into sporulation and a greater sporulation frequency within the population. Likewise, transcription of *sigG* was higher during exponential phase in both *codY* mutants, relative to the parent strains (**Fig. 4G-H**). The premature and higher expression levels of both early and late-stage sporulation factors in *codY* mutant cultures provide additional evidence that CodY inhibits entry into sporulation. These data suggest that a higher percentage of the *codY* mutant population is progressing through sporulation, and that sporulation initiates at an earlier growth stage in the *codY* mutants than in the parent strains.

codY mutants differentially express the putative sporulation regulatory genes, *sinR* and *sinI*

In previous work, we investigated the transcriptome of a *codY* mutant and employed IDAP-seq to determine the genes regulated by CodY in *C. difficile* (37). Although higher expression of some sporulation-specific genes was observed in that study, the CodY-regulated sporulation genes that were identified only play a role in sporulation after Spo0A

activation. Since that study, additional genes have been associated with entry into sporulation, including *sigH* (67), *ccpA* (63, 68), the *opp* and *app* permeases (19), *rstA* (69) and *sinRI* (19). Of these, only *opp* and *sinRI* are recognized as being directly regulated by CodY, as demonstrated by IDAP-seq (37). We further examined the expression of *sinRI* and *opp*, to understand how CodY impacts expression of these genes before and during the initiation of sporulation, and to determine if there are differences in expression of these genes that may explain the different sporulation phenotypes of strains.

In *B. subtilis*, SinR functions as a repressor of sporulation (70). In that system, SinI is an alternative binding partner for SinR and prevents SinR from inhibiting sporulation (71). At present, there are no published reports that define the role of SinR or the putative SinI in *C. difficile*, but preliminary studies of these factors show that they are expressed during the initiation of sporulation in *C. difficile* (19). Using qRT-PCR, we evaluated the expression of the putative *sinR* and *sinI* under sporulation conditions for 630 *codY*, UK1 *codY* and their respective parent strains. As a nutritional state regulator, CodY typically represses transcription of genes during exponential phase and that repression is relieved during the transition to stationary phase growth (27, 37). Transcription of *sinR* and *sinI* during logarithmic growth was 2-fold higher in 630 *codY* compared to 630Δ*erm*, indicating that CodY represses *sinRI* expression (**Fig. 5A, C)**. However, in the UK1 background, the *codY* mutant exhibited 5-fold lower relative *sinR* expression during exponential growth, and 18-fold lower at T_4 suggesting that CodY positively affects *sinRI* transcription in the UK1 strain (**Fig. 5B, D**). The dissimilarity in CodY regulation of *sinRI* in these two strains may explain the differences in sporulation frequency between the UK1 *codY* and 630 *codY*

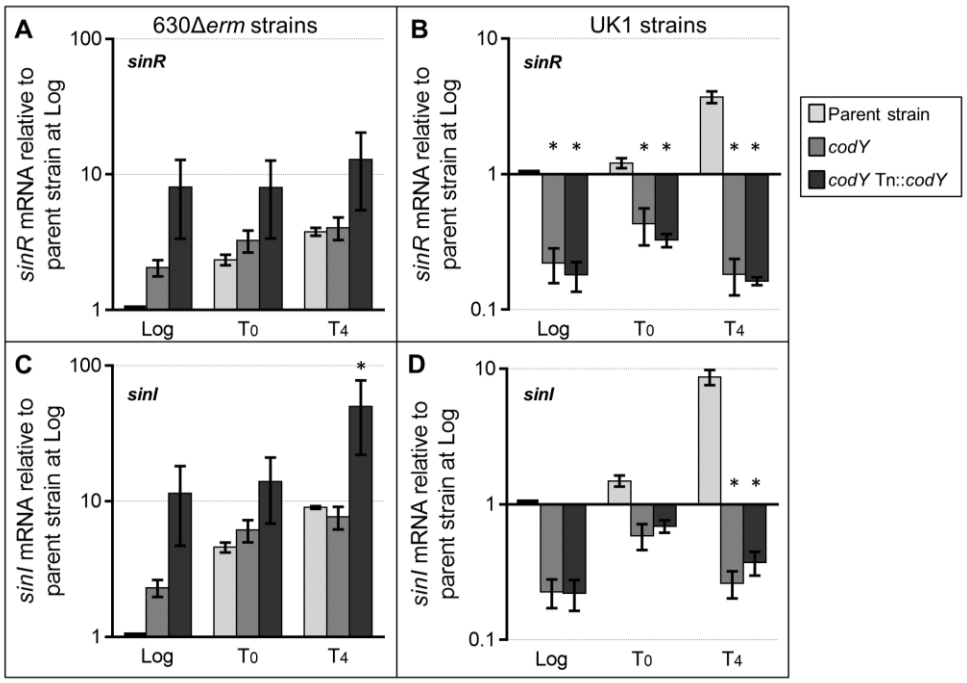

Figure 5. Expression of *sinRI* is differentially regulated by CodY. qRT-PCR expression analysis of *sinR and sinI* in strains 630Δ*erm*, MC364 (630 *codY*), MC442 (630 *codY* Tn*916*::*codY*) (**A**,**C**) and UK1, LB-CD16 (UK1 *codY*) and MC443 (UK1 *codY* Tn*916*::*codY*) (**B**,**D**) grown in 70:30 sporulation media. Samples for RNA isolation were taken during logarithmic growth (OD_{600} ~0.5), transition to stationary phase (T_0), and four hours post the transition into stationary phase (T_4). The means and SEM of at least four biological replicates are shown. A two-way repeated measures ANOVA followed by Dunnett's multiple comparison test was used to compare the parent and *codY* mutant strain or the parent strain with the respective complemented strain at the designated timepoints. *, $P \leq 0.05$.

mutants, but the functions of SinR and SinI in *C. difficile* sporulation initiation need to be defined to understand their impact.

Prior work demonstrated that CodY binds to the region upstream of the *sinR* coding sequence and identified a putative CodY binding site near the promoter (**Fig. S7**)(37). Despite the differences in *sinRI* transcription, no sequence changes were found within the putative *sin* promoters of the UK1 and 630 genomes (**Fig. S7**). To further evaluate how *sinR* is regulated by CodY, we constructed a transcriptional fusion of the promoter region of *sinR* to *phoZ*, an alkaline phosphatase reporter (46). A plasmid containing the P*sinR*$_{600}$*::phoZ* reporter fusion was introduced by conjugation into the 630Δ*erm* and 630 *codY* strains. These strains were grown in 70:30 sporulation medium, and cultures were sampled during exponential phase and four hours after the transition to stationary phase to assay for alkaline phosphatase activity. We observed a significant increase in alkaline phosphatase activity generated from the putative *sinR* promoter in the *codY* mutant (**Table 4**). Although there is an increase in promoter activity in the 630 *codY* mutant compared to the parent strain, there was no change in activity between log phase and stationary phase (T_4) cultures of the parent strain. Therefore, alleviation of CodY repression at stationary phase is not sufficient to increase transcription from the *sin* promoter, most likely because other factors, such as CcpA and SigD, are also involved in regulating *sinR* transcription (68, 72). In addition, alteration of what we predicted as the CodY binding site (31, 37) (P*sinR*$_{600(C\text{-}290A)}$*::phoZ)* did not result in increased alkaline phosphate activity compared to the wild-type promoter (**Table 4**), suggesting that either the mutated base pair is not important for CodY binding or that CodY does not bind to this region of the predicted

TABLE 4 Alkaline phosphatase activity from the *sinR* promoter[a]

Promoter fusion or gene (strain background[s])	Time point	Alkaline phosphatase activity (mean ± SEM) for genotype:	
		630Δ*erm*	630 *codY*
P*sinR*$_{600}$::*phoZ* (MC560/MC596)	Log	7.2 ± 0.9	**11.9 ± 1.1**
	T_4	7.0 ± 0.7	10.9 ± 1.5
P*sinR*$_{600(C\text{-}290A)}$::*phoZ* (MC769)	Log	8.6 ± 1.0	ND[b]
	T_4	9.0 ± 1.0	ND
phoZ (MC448/MC589)	Log	0.6 ± 0.1	0.8 ± 0.1
	T_4	0.7 ± 0.1	0.9 ± 0.2

[a] Data were analyzed by two-way ANOVA followed by Tukey's test for multiple comparisons. Values are expressed in alkaline phosphatase activity units. Bold text indicates a *P* value of ≤0.05 for comparisons between data from the same promoter fusion at different time points or comparisons between data from the same promoter fusion with and without CodY. MC560 was run as a positive control for all experiments; $n = 8$. Log, logarithmic growth phase; T_4, stationary phase.

[b] ND, not determined.

promoter region. Overall, these data demonstrate that there is a functional promoter immediately upstream of *sinR* that is directly or indirectly regulated by CodY.

Expression of the *opp* permease is regulated in part by CodY

In prior work, we demonstrated that disruption of the oligopeptide permeases, Opp and App, results in higher sporulation frequency in *C. difficile* (19). It was also established that CodY represses expression of the *opp* operon during growth in rich medium, and that CodY directly binds to the *opp* promoter region (37). Based on these data, we hypothesized that CodY relieves repression of *opp* at the onset of stationary phase, which would allow greater peptide uptake and potentially postpone the initiation of sporulation. We assessed expression of *oppB,* the first gene of the *opp* operon, in the *codY* mutants to determine how CodY affects regulation of this transporter as the cells initiate sporulation. In the 630 *codY* mutant, *oppB* transcription was ~3-fold higher during logarithmic growth compared to the parent strain, supporting the past finding that CodY is a repressor of *oppB* expression (**Fig. 6A**). However, no change in *oppB* expression was observed in the UK1 *codY* mutant during exponential growth (**Fig. 6B**). By late stationary phase (T_4), *opp* transcription was 2- to 5-fold lower in the 630 *codY* and UK1 *codY* mutants, relative to the parent strains. Thus, CodY appears to modestly repress log-phase expression of *oppB* in strain 630, but not in UK1. But, as cells advanced to late stationary phase, CodY had a positive effect on *oppB* transcription in both strains, resulting in lower *oppB* expression in the absence of CodY (**Fig. 6 A, B**). As CodY is unlikely to act as both a positive and negative regulator of the same locus at different growth stages, the increase in *opp* transcription observed in late

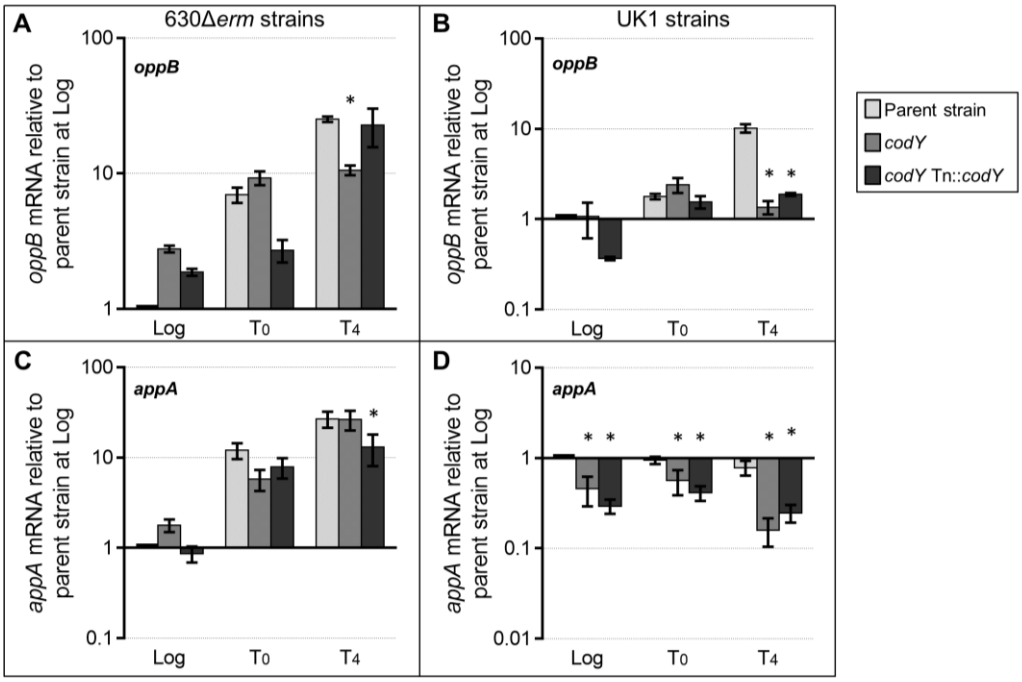

Figure 6. Expression of the peptide permeases, *opp* and *app*. qRT-PCR expression analysis of *oppB* and *appA* in strains 630Δ*erm*, MC364 (630 *codY*), MC442 (630 *codY* Tn*916*::*codY*) (**A,C**) and UK1, LB-CD16 (UK1 *codY*), and MC443 (UK1 *codY* Tn*916*::*codY*) (**B,D**) grown in 70:30 sporulation medium. Samples for RNA isolation were taken at logarithmic growth (OD_{600} ~0.5), transition to stationary phase (T_0), and four hours post the transition into stationary phase (T_4). The means and SEM of four biological replicates are shown. A two-way repeated measures ANOVA followed by Dunnett's multiple comparison test was used to compare parent strain with the *codY* mutant or the parent strain with the respective complemented strain at the designated timepoints. *, $P \leq 0.05$.

stationary phase may be facilitated by another CodY-dependent factor, rather than by CodY directly.

The differential regulation of *opp* in the 630 *codY* and UK1 *codY* strains during logarithmic growth suggests that CodY interacts differently with the *opp* promoters of these strains. Sequence analysis of the putative *opp* promoter regions revealed two nucleotide differences between the UK1 and 630 strains (**Fig. S7**). No sequence changes were found within the previously identified CodY binding site at -175 to -189 nt upstream of the translational start site (37). To investigate the differential regulation of *opp* further, we evaluated expression during exponential phase from the putative *oppB* promoters of strains 630 and UK1 using *phoZ* transcriptional fusions. Promoter fusions were created using promoter sequences amplified from the 630Δ*erm* and UK1 genomes, in order to assess the impact of sequence differences on *opp* expression. The P*oppB::phoZ* reporter fusions were brought into 630Δ*erm* and 630 *codY* by conjugation, allowing us to evaluate the effects of promoter differences on CodY-dependent regulation in an isogenic background. As shown in **Table 5**, a fusion containing the 400 bp upstream of the *oppB* translational start (P$oppB_{400}$*::phoZ*) derived from strain 630 or UK1 generated similar alkaline phosphatase (AP) activity in a wild-type background, and expectedly higher AP activity when expressed in a *codY* mutant. The activity of the P$oppB_{400}$*::phoZ* fusion derived from UK1 sequence was modestly lower than the activity for the 630-derived fusion, suggesting that sequence differences in this region can affect promoter function in the absence of CodY. Additional constructs were created using shorter segments of the promoter region to assess CodY-dependent activity (P$oppB_{250}$*::phoZ*, P$oppB_{170}$*::phoZ*, and P$oppB_{150}$*::phoZ*; **Fig. S7, Table 5**). The P$oppB_{250}$*::phoZ* fusion, which encompasses the

TABLE 5 Alkaline phosphatase activity of the *opp* and *app* promoter regions during logarithmic growth[a]

Promoter fusion or gene	Strain background(s)	Promoter template	Alkaline phosphatase activity (mean ± SEM) for genotype: 630Δ*erm*	630Δ*erm codY*
P*oppB*$_{400}$::*phoZ*	MC565/MC601	630Δ*erm*	244.5 ± 13.3	**503.5 ± 39.9**
	MC608/MC611	UK1	271.5 ± 8.5	**446.0 ± 13.5**
P*oppB*$_{400(G\text{-}181A)}$::*phoZ*	MC769	630Δ*erm*	142.2 ± 3.1	ND[b]
P*oppB*$_{250}$::*phoZ*	MC650/MC655	630Δ*erm*	245.1 ± 15.4	**373.3 ± 41.0***
	MC651/MC659	UK1	287.6 ± 24.5	**422.2 ± 22.4**
P*oppB*$_{170}$::*phoZ*	MC649/MC657	630Δ*erm*	101.7 ± 4.3	118.4 ± 11.1
	MC653	UK1	107.1 ± 10.6	ND
P*oppB*$_{150}$::*phoZ*	MC647/MC658	630Δ*erm*	1.6 ± 0.2	1.8 ± 0.1
	MC654/MC662	UK1	1.1 ± 0.1	1.5 ± 0.1
P*appA*$_{600}$::*phoZ*	MC572/MC576	630Δ*erm*	21.7 ± 3.5	16.6 ± 2.1
	MC574/MC578	UK1	14.5 ± 2.2	12.4 ± 1.7
phoZ	MC448/MC589		0.6 ± 0.1	0.8 ± 0.1

[a] Data were analyzed by two-way ANOVA followed by Tukey's test for multiple comparisons. Values are expressed in alkaline phosphatase activity units. Bold text indicates a *P* value of ≤0.05 for the comparison of promoter activities between strains carrying the same fusion with and without CodY. Underlined text indicates a *P* value of ≤0.05 for the comparison of promoter activities from fusions of the same length in the same background strain. An asterisk indicates a *P* value of ≤0.05 for the comparison between P*oppB*$_{400}$ and P*oppB*$_{250}$ in the same strain background. MC565 was run as a positive control for all experiments; $n = 8$.

[b] ND, not determined.

CodY site and an overlapping CcpA site (68), retained CodY-dependent repression. The AP activity from the P*oppB*$_{250}$*::phoZ* fusion was lower than the AP activity from the P*oppB*$_{400}$*::phoZ* fusion in the *codY* mutant background. However, this effect was only observed in the promoter regions derived from the 630 background, not the UK1 sequence. There are no sequence differences present in the nt -400 to -250 region, which suggests there is a CodY-dependent, sequence-independent influence on *opp* gene expression that is strain-specific. A shorter segment, P*oppB*$_{170}$*::phoZ*, generated significantly lower, but similar, AP activity in the wild-type and *codY* mutant backgrounds, confirming that the CodY binding site lies upstream of this region. These data suggest that there is a CodY-dependent regulatory region present between nt -170 and -250. Unexpectedly, mutation of a conserved nucleotide within the predicted CodY site (31, 37) (P*oppB*$_{400G\text{-}181A}$*::phoZ*) resulted in decreased promoter activity (**Table 5**). It is possible based on this result, that the promoter mutation increased the affinity between the binding site and CodY. However, it remains unclear if this region is important for CodY-dependent regulation or other regulators of *opp*, such as CcpA. These data suggest that in addition to CodY and CcpA-dependent repression of the *opp* promoter, the region between nt -170 and -250 is also important for activating transcription. A shorter segment, P*oppB*$_{150}$*::phoZ*, has no transcriptional activity, indicating that promoter elements are upstream of this segment. Thus, the important CodY/CcpA binding sites are predicted to overlap in the *opp* promoter element to repress transcription, and this arrangement is conserved between the UK1 and 630 strains.

codY mutants differentially express the App permease

Previously, we demonstrated that the oligopeptide permease, App, is involved in the inhibition of sporulation in *C. difficile* (19). An *app* null mutant sporulates at a higher frequency than an *opp* null mutant, indicating that *app* has a greater impact on the cellular pathways that lead to sporulation initiation (19). Though *app* was not identified in previous analyses of CodY-dependent genes in strain 630 (37), we investigated if CodY influenced *app* expression because of the effect App has on sporulation. To this end, we evaluated expression of the first gene in the *app* operon, *appA*, in the *codY* mutants and their parent strains. As shown in **Fig. 6C**, expression of *appA* is slightly higher (~1.7 fold) in the 630 *codY* strain during exponential phase, but no significant difference in expression was detected as cells progressed to stationary phase. However, expression of *app* was 2- to 5-fold lower in UK1 *codY* throughout growth, relative to the parent strain (**Fig. 6D**), illustrating that CodY positively impacts *app* transcription in UK1. To determine if the differences in *app* transcription between UK1 *codY* and 630 *codY* were due to the variations in the promoter sequences in these strains, the UK1 and 630 putative promoter regions were fused to the *phoZ* reporter and expressed in strain 630 (**Table 5**). No significant differences in activity for the UK1 or 630 derived *app* promoters were observed, suggesting that the positive effect of CodY on *app* transcription in UK1 is strain-specific and not a direct CodY effect. This result is similar to the differential effects of CodY on *sinRI* transcription that were observed between UK1 and 630. Overall, these data strongly suggest that CodY impacts the expression of additional regulators in UK1, resulting in indirect regulatory effects of CodY and a greater impact on sporulation in the UK1 strain.

CodY may have a small effect on *C. difficile* germination

In *C. perfringens*, CodY has a positive effect on germination, as evidenced by the decreased germination capacity previously observed for a *codY* mutant in that species (36). To determine if germination is similarly affected by CodY in *C. difficile*, we performed germination assays using purified spores, as previously described (36, 40, 55). In contrast to *C. perfringens*, the absence of CodY resulted in slightly increased spore germination, as measured by a decrease in optical density in the presence of the germinant, taurocholate (**Fig. 7A and B**). This suggests that CodY may have a small positive effect on the germination process. Whether the effects of CodY on germination of these strains has an impact on the outcome of disease remains to be elucidated.

DISCUSSION

As a strict anaerobe, *C. difficile* must form a spore to effectively persist and spread in the aerobic environment outside of the host. The cellular and environmental factors that initiate and regulate the entry into sporulation in *C. difficile* are not well understood (11). While the morphological changes that occur during sporulation are conserved between *B. subtilis* and *C. difficile*, the regulatory pathways that control the initiation of sporulation are not (10, 73). How the master regulator of sporulation, Spo0A, and its activity are controlled in *C. difficile* is an important question, as regulation of Spo0A activity is essential for triggering and appropriately timing the entry into sporulation (8, 17). Previous work indicated that nutrient deprivation is a trigger for sporulation in *C. difficile* (19, 68). We hypothesized that the global nutritional regulator, CodY, would play a role in sporulation in *C. difficile*, as is the case for other spore-forming bacteria (28, 36). Herein, we have shown that CodY is a negative regulator of sporulation in *C. difficile* and that its

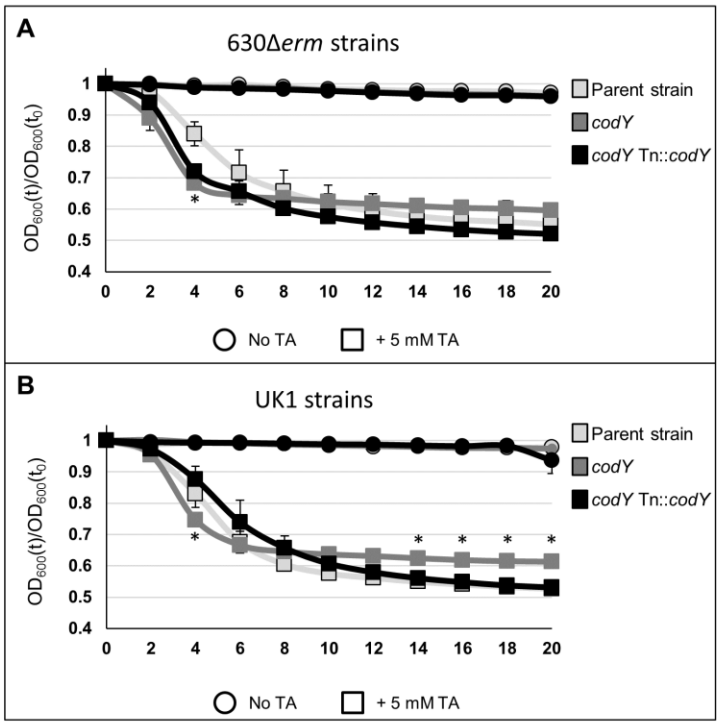

Figure 7. Germination phenotypes of *codY* mutants. The germination of *C. difficile* heat-activated spores suspended in BHIS (circles) or BHIS with 5 mM taurocholate (TA, squares) was monitored over time. The germination of 630Δ*erm*, MC364 (630 *codY*) and MC442 (630 *codY*, Tn*916::codY*) (**A**) or UK1, LB-CD16 (UK1 *codY*) and MC443 (UK1 *codY*, Tn*916::codY*) (**B**) is shown as a ratio of the OD_{600} at a given time point (t) divided by the OD_{600} at the initial time point (t_0). The means and SEM of three biological replicates are shown. Where error bars are not visible, they are obscured by symbols. A two-way repeated measures ANOVA followed by Dunnett's multiple comparison test was used to compare parent strain with the *codY* mutant or the parent strain with the respective complemented strain at the designated timepoints. *, $P \leq 0.05$.

impact on sporulation differs in the 012 (630) and 027 (UK1) ribotypes. Further, we demonstrate that CodY regulates expression of the oligopeptide permease, *opp*, and the putative sporulation regulator, *sinR*.

CodY is known to suppress sporulation in *B. subtilis* (28, 74), *B. thuringiensis* (75), and in the more closely related bacterium, *C. perfringens* (36). When the *C. difficile codY* gene was disrupted and sporulation efficiency was assessed in strains 630 and UK1, sporulation efficiency increased in both backgrounds. But when compared to their respective parent strains, the degree by which CodY impacted sporulation frequency was greater in the 027 ribotype than the 012 ribotype (**Fig. 3**). 630 *codY* demonstrated a two-fold increase in sporulation frequency over its parent strain, in comparison to UK1 *codY*, which had a ~1,400-fold increase over its parent strain. While the data demonstrate that CodY is a negative regulator of sporulation, the sporulation frequency of a UK1 *codY* mutant was 31-fold greater than that of a 630 *codY* mutant. These results indicate that conditions that affect the activity of CodY have a greater impact on sporulation regulation in the UK1 background.

We propose that the variability in *codY* mutant sporulation in different strains results from inherent differences in the regulation of nutrient acquisition. This idea is supported by the data demonstrating differences in peptide transporter expression between the two strains. The ability of the bacterium to acquire nutrients is directly linked to regulation of *tcdA* and *tcdB* expression (34, 37, 56, 76, 77), and as a consequence, lower nutrient acquisition would increase toxin expression. Several studies have assessed strains for differences in toxin production *in vitro* as a measure of potential virulence, though these studies have had mixed results (78-81). Based on the evidence, it is possible that some

strains produce toxin earlier during infection, and possibly at higher levels, because they import nutrients less efficiently. Lower nutrient uptake would cause derepression of CodY and CcpA-responsive genes, and increased SigD activity, all of which would result in higher toxin expression (53, 56, 63, 72). A comparison of gene expression for *C. difficile* grown *in vitro* and *in vivo* found a substantially greater impact of *in vivo* conditions on metabolism and sporulation than *in vitro* (82). This discrepancy highlights the need for greater understanding of the nutritional environment present during *C. difficile* infections, which could be used to improve conditions for examining these physiological processes *in vitro*.

Previous studies of *Bacillus* species revealed that CodY regulates genes that are directly involved in sporulation initiation, including *spo0A*, *rapA*, *rapC*, *rapE*, *sinIR*, *sigH*, and *kinB* (21, 28, 74, 83, 84). Of these initiation factors, only SinR and SinI have homologs in *C. difficile* and are also directly regulated by CodY (37). Upon determining that CodY represses sporulation in *C. difficile*, we investigated potential mechanisms by which CodY could directly or indirectly affect sporulation initiation. We evaluated the transcription and promoter activity of three known or suspected effectors of sporulation, the putative transcriptional repressor, *sinR* and the oligopeptide permeases, *app* and o*pp* (19). In previous work evaluating Opp and App in *C. difficile*, we hypothesized that imported peptides worked through an unknown and indirect mechanism to influence *sinRI* transcription (19). In *B. subtilis*, SinR works as a repressor of sporulation by directly inhibiting the transcription of Spo0A (70). In turn, the co-transcribed SinI antagonizes SinR, thereby preventing SinR-dependent repression of *spo0A*, which in turn allows sporulation initiation to progress (71). We evaluated the expression of *sinRI* in the *codY*

mutants to determine if CodY could repress sporulation by influencing *sinRI* transcription. In the 630 *codY* mutant, expression of *sinRI* is higher during logarithmic growth than is observed in the parent strain, suggesting that CodY acts as a repressor of *sinRI* (**Fig. 5A, C**). In contrast, in the UK1 *codY* mutant, we observed a decrease in the expression of *sinRI*, compared to its parent strain, which suggests that CodY positively regulates *sinRI* transcription in the UK1 strain (**Fig. 5B, D**). The sequences of the *sinR* promoter regions in UK1 and 630 are identical; therefore, we conclude that other differences in CodY-mediated regulation affect the expression of *sinR* in these strains (**Fig. S7, Table 4**). The roles of SinR and SinI in *C. difficile* sporulation are still not known; this information is necessary to determine how CodY, SinRI and sporulation initiation are connected.

In numerous Gram-positive species, CodY directly represses expression of peptide import mechanisms, including the *opp* oligopeptide permease (20-23, 74, 85). We examined expression of the oligopeptide permeases, *opp* and *app*, which have been indirectly linked to sporulation in *C. difficile* (19). During logarithmic growth the 630 *codY* strain had higher expression of *opp* (**Fig. 6A**), in agreement with prior studies that demonstrated CodY-dependent repression of *opp* (37). However, the absence of CodY in either ribotype results in less *opp* transcription during stationary phase, suggesting that CodY has a positive influence on *opp* expression at later stages of growth (**Fig. 6A, B**). One explanation for differential *opp* expression at various growth stages is that the increased sporulation of the *codY* mutants may result in an earlier decline of *opp* expression between the time points examined, which would not be detected in our experiment. To further examine the effect of CodY on *opp*, we constructed P*oppB::phoZ* reporter fusions using the promoters from both strains and examined their activity with and without CodY.

We observed higher promoter activity in the absence of CodY, indicating that CodY represses *opp* in both ribotypes (**Table 5**). Overall, we showed that CodY acts as a repressor of the *opp* oligopeptide transporter operon. Based on these results and previous studies of the oligopeptide permeases, we propose that Opp and App function to import peptides and that these peptides, in turn, can modulate CodY activity by increasing the availability of branched-chain amino acids (**Fig. 8**).

Lastly, we evaluated the transcription of *appA*, the first gene of the *app* operon, in both ribotypes. App is an oligopeptide permease that was previously shown to affect sporulation in *C. difficile*, but does not appear to be directly regulated by CodY (19, 37). We observed differential regulation of *appA* expression in the UK1 and 630 *codY* mutants (**Fig. 6C, D**). But, further examination of promoter activity using P*appA::phoZ* reporter fusions revealed no difference in activity from the *app* promoter of either strain, with or without CodY (**Table 5**). These results indicate that although CodY affects *app* expression, CodY is not a direct regulator of *app*. The information available does not explain the differences observed in *app* expression between the UK1 *codY* and 630 *codY* strains. Thus far, only SigH has been implicated as a regulator of *app* expression, though more regulators are likely involved (67).

The control of *opp, app, sinR* and *sinI* gene expression in response to nutrient availability is not unprecedented. A null mutation in the *B. subtilis scoC* gene (previously known as *hpr*), which encodes the pleiotropic transcriptional regulator, ScoC, relieves catabolite repression of sporulation, and *scoC* transcription increases in the presence of glucose (86). ScoC directly downregulates *opp*, *app* and *sinIR* expression (87, 88), suggesting that ScoC may inhibit sporulation in high nutrient conditions by repressing the

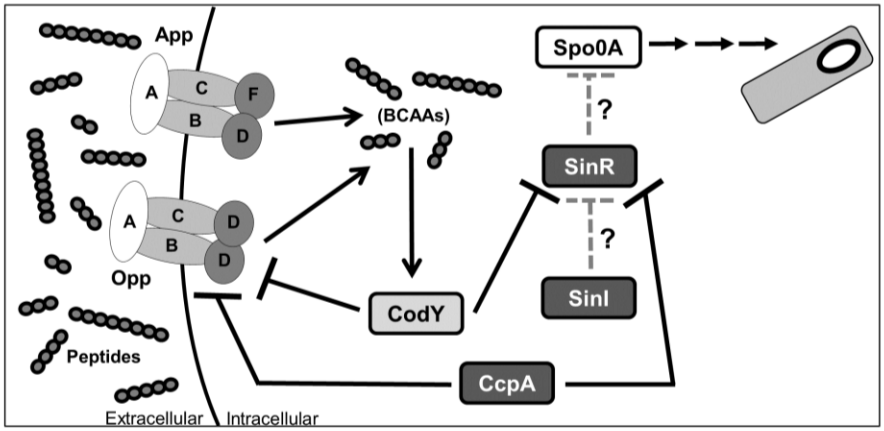

Figure 8. Abbreviated model of nutritional influence on sporulation. In nutrient rich conditions, CodY and CcpA act as repressors of the *opp* oligopeptide transporter operon, the putative *sinRI* regulatory genes and numerous genes involved in nutrient acquisition. As nutrient levels decrease, CodY and CcpA transcriptional repression is alleviated. The oligopeptide transporters, Opp and App, import peptides and the branched chain amino acids (BCAAs) derived from imported peptides bind to CodY, increasing its DNA-binding capacity. SinR is hypothesized to act as a transcriptional repressor of the sporulation master regulator, Spo0A. The putative SinI of *C. difficile* is thought to act as a repressor of SinR. Grey hatched arrows show hypothesized regulatory effects.

expression of genes involved in early sporulation events. Further, CodY directly represses *scoC* transcription, and CodY and ScoC independently co-regulate several loci, including *opp* (89, 90). Altogether, these results imply that multiple regulators control *B. subtilis* sporulation through nutrient-dependent alteration of early sporulation gene expression. Although *B. subtilis* and *C. difficile* do not share identical nutritional requirements, similar complex regulatory mechanisms may be utilized by *C. difficile*. No clear *scoC* gene has been identified in the *C. difficile* genome. But, CodY regulates many genes indirectly (74, 91) (**Fig. 6, Table 5**). Hence, it is possible that in *C. difficile* a ScoC-like regulator could control *opp*, *app* and *sinRI* expression in concert with CodY.

The regulatory mechanisms through which CodY affects sporulation are not fully elucidated, in part because many sporulation initiation factors in *C. difficile* are unknown or understudied. We are only beginning to understand the relationship between sporulation and nutrition in *C. difficile*, and many questions remain about the role CodY plays in this process, such as: what are the *in vivo* effects of CodY on sporulation and pathogenesis? Does the SinRI locus function as predicted, and what role does it play in sporulation? And do differences in CodY-dependent regulation play a role in the pathogenesis of current and emerging epidemic strains compared with historical epidemic isolates? If CodY more sensitively controls the expression of factors that affect sporulation initiation or controls different factors in the 027 strains than other isolates, this would conceivably influence the infectivity and pathogenesis of these strains, and thereby, contribute to the prevalence of the 027 ribotype.

In summary, we have demonstrated that CodY is a repressor of sporulation in *C. difficile* and that CodY is involved in the regulation of genes associated with sporulation,

including *sinR* and the *opp* permease operon. In addition, the evidence suggests that CodY has strain-dependent effects that result in differences in gene regulation that impact initiation of sporulation. This is a significant step in understanding how the process of sporulation is regulated in response to the nutritional status of the bacterium and understanding the potential differences between epidemic and historical strains.

ACKNOWLEDGEMENTS

We thank Charles Moran, Abraham Sonenshein, and members of the McBride lab for suggestions and discussions throughout the course of this work. This research was supported by the U.S. National Institutes of Health through research grants DK087763, DK101870, AI109526 and AI116933 to S.M.M, T32 AI106699 to KLN. LB and ND were supported by R01GM042291. We thank Jeremy Boss for the use of the Bio-Rad CFX96 real-time PCR detection system and Joseph Sorg for primers used for construction of the *codY* complement. The content of this article is solely the responsibility of the authors and does not necessarily reflect the official views of the National Institutes of Health.

REFERENCES

1. **Lyras D, O'Connor JR, Howarth PM, Sambol SP, Carter GP, Phumoonna T, Poon R, Adams V, Vedantam G, Johnson S, Gerding DN, Rood JI.** 2009. Toxin B is essential for virulence of *Clostridium difficile*. Nature **458:**1176-1179.

2. **Kuehne SA, Cartman ST, Heap JT, Kelly ML, Cockayne A, Minton NP.** 2010. The role of toxin A and toxin B in *Clostridium difficile* infection. Nature **467:**711-713.

3. **Kuehne SA, Cartman ST, Minton NP.** 2011. Both, toxin A and toxin B, are important in *Clostridium difficile* infection. Gut Microbes **2:**252-255.

4. **Lyerly DM, Saum KE, MAcDONALD DK, Wilkins TD.** 1985. Effects of *Clostridium difficile* toxins given intragastrically to animals. Infection and immunity **47:**349-352.

5. **CDC.** 2013. Antibiotic Resistance Threats in the United States, 2013.

6. **Kyne L, Hamel MB, Polavaram R, Kelly CP.** 2002. Health care costs and mortality associated with nosocomial diarrhea due to *Clostridium difficile*. Clin Infect Dis **34:**346-353.

7. **O'Brien JA, Lahue BJ, Caro JJ, Davidson DM.** 2007. The emerging infectious challenge of *Clostridium difficile*-associated disease in Massachusetts hospitals: clinical and economic consequences. Infect Control Hosp Epidemiol **28:**1219-1227.

8. **Deakin LJ, Clare S, Fagan RP, Dawson LF, Pickard DJ, West MR, Wren BW, Fairweather NF, Dougan G, Lawley TD.** 2012. The *Clostridium difficile spo0A* gene is a persistence and transmission factor. Infect Immun **80:**2704-2711.

9. **Rosenbusch KE, Bakker D, Kuijper EJ, Smits WK.** 2012. *C. difficile* 630Delta*erm* Spo0A regulates sporulation, but does not contribute to toxin production, by direct high-affinity binding to target DNA. PLoS One **7:**e48608.

10. **Paredes CJ, Alsaker KV, Papoutsakis ET.** 2005. A comparative genomic view of clostridial sporulation and physiology. Nat Rev Microbiol **3:**969-978.

11. **Edwards AN, McBride SM.** 2014. Initiation of sporulation in *Clostridium difficile*: a twist on the classic model. FEMS Microbiol Lett **358:**110-118.

12. **Underwood S, Guan S, Vijayasubhash V, Baines SD, Graham L, Lewis RJ, Wilcox MH, Stephenson K.** 2009. Characterization of the sporulation initiation pathway of *Clostridium difficile* and its role in toxin production. J Bacteriol **191:**7296-7305.

13. **Burbulys D, Trach KA, Hoch JA.** 1991. Initiation of sporulation in *B. subtilis* is controlled by a multicomponent phosphorelay. Cell **64:**545-552.

14. **Perego M, Cole SP, Burbulys D, Trach K, Hoch JA.** 1989. Characterization of the gene for a protein kinase which phosphorylates the sporulation-regulatory proteins Spo0A and Spo0F of *Bacillus subtilis*. J Bacteriol **171:**6187-6196.

15. **Perego M, Hanstein C, Welsh KM, Djavakhishvili T, Glaser P, Hoch JA.** 1994. Multiple protein-aspartate phosphatases provide a mechanism for the integration of diverse signals in the control of development in *B. subtilis*. Cell **79:**1047-1055.

16. **Ferrari FA, Trach K, LeCoq D, Spence J, Ferrari E, Hoch JA.** 1985. Characterization of the *spo0A* locus and its deduced product. Proc Natl Acad Sci U S A **82:**2647-2651.

17. **Fimlaid KA, Bond JP, Schutz KC, Putnam EE, Leung JM, Lawley TD, Shen A.** 2013. Global Analysis of the Sporulation Pathway of *Clostridium difficile*. PLoS Genet **9:**e1003660.

18. **Pereira FC, Saujet L, Tome AR, Serrano M, Monot M, Couture-Tosi E, Martin-Verstraete I, Dupuy B, Henriques AO.** 2013. The Spore Differentiation Pathway in the Enteric Pathogen *Clostridium difficile*. PLoS Genet **9:**e1003782.

19. **Edwards AN, Nawrocki KL, McBride SM.** 2014. Conserved oligopeptide permeases modulate sporulation initiation in *Clostridium difficile*. Infect Immun **82:**4276-4291.

20. **Bennett HJ, Pearce DM, Glenn S, Taylor CM, Kuhn M, Sonenshein AL, Andrew PW, Roberts IS.** 2007. Characterization of *relA* and *codY* mutants of *Listeria monocytogenes*: identification of the CodY regulon and its role in virulence. Mol Microbiol **63:**1453-1467.

21. **Chateau A, van Schaik W, Joseph P, Handke LD, McBride SM, Smeets FM, Sonenshein AL, Fouet A.** 2013. Identification of CodY targets in *Bacillus anthracis* by genome-wide in vitro binding analysis. J Bacteriol **195:**1204-1213.

22. **Majerczyk CD, Dunman PM, Luong TT, Lee CY, Sadykov MR, Somerville GA, Bodi K, Sonenshein AL.** 2010. Direct targets of CodY in *Staphylococcus aureus*. J Bacteriol **192:**2861-2877.

23. **Pohl K, Francois P, Stenz L, Schlink F, Geiger T, Herbert S, Goerke C, Schrenzel J, Wolz C.** 2009. CodY in *Staphylococcus aureus*: a Regulatory Link between Metabolism and Virulence Gene Expression. Journal of Bacteriology **191:**2953-2963.

24. **Hendriksen WT, Bootsma HJ, Estevão S, Hoogenboezem T, De Jong A, De Groot R, Kuipers OP, Hermans PW.** 2008. CodY of *Streptococcus pneumoniae*:

link between nutritional gene regulation and colonization. Journal of bacteriology **190:**590-601.

25. **Slack FJ, Mueller JP, Strauch MA, Mathiopoulos C, Sonenshein AL.** 1991. Transcriptional regulation of a *Bacillus subtilis* dipeptide transport operon. Mol Microbiol **5:**1915-1925.

26. **Slack FJ, Serror P, Joyce E, Sonenshein AL.** 1995. A gene required for nutritional repression of the *Bacillus subtilis* dipeptide permease operon. Molecular microbiology **15:**689-702.

27. **Sonenshein AL.** 2005. CodY, a global regulator of stationary phase and virulence in Gram-positive bacteria. Curr Opin Microbiol **8:**203-207.

28. **Ratnayake-Lecamwasam M, Serror P, Wong KW, Sonenshein AL.** 2001. *Bacillus subtilis* CodY represses early-stationary-phase genes by sensing GTP levels. Genes Dev **15:**1093-1103.

29. **Handke LD, Shivers RP, Sonenshein AL.** 2008. Interaction of *Bacillus subtilis* CodY with GTP. J Bacteriol **190:**798-806.

30. **Shivers RP, Sonenshein AL.** 2004. Activation of the *Bacillus subtilis* global regulator CodY by direct interaction with branched-chain amino acids. Molecular Microbiology **53:**599-611.

31. **Belitsky BR, Sonenshein AL.** 2008. Genetic and biochemical analysis of CodY-binding sites in *Bacillus subtilis*. J Bacteriol **190:**1224-1236.

32. **Guedon E, Serror P, Ehrlich SD, Renault P, Delorme C.** 2001. Pleiotropic transcriptional repressor CodY senses the intracellular pool of branched-chain amino acids in *Lactococcus lactis*. Mol Microbiol **40:**1227-1239.

33. **Majerczyk CD, Sadykov MR, Luong TT, Lee C, Somerville GA, Sonenshein AL.** 2008. *Staphylococcus aureus* CodY negatively regulates virulence gene expression. J Bacteriol **190:**2257-2265.

34. **Karlsson S, Burman LG, Akerlund T.** 2008. Induction of toxins in *Clostridium difficile* is associated with dramatic changes of its metabolism. Microbiology **154:**3430-3436.

35. **Dupuy B, Sonenshein AL.** 1998. Regulated transcription of *Clostridium difficile* toxin genes. Mol Microbiol **27:**107-120.

36. **Li J, Ma M, Sarker MR, McClane BA.** 2013. CodY is a global regulator of virulence-associated properties for *Clostridium perfringens* type D strain CN3718. MBio **4:**e00770-00713.

37. **Dineen SS, McBride SM, Sonenshein AL.** 2010. Integration of metabolism and virulence by *Clostridium difficile* CodY. J Bacteriol **192:**5350-5362.

38. **Smith CJ, Markowitz SM, Macrina FL.** 1981. Transferable tetracycline resistance in *Clostridium difficile*. Antimicrob Agents Chemother **19:**997-1003.

39. **Sorg JA, Dineen SS.** 2009. Laboratory maintenance of *Clostridium difficile*. Curr Protoc Microbiol **Chapter 9:**Unit9A 1.

40. **Sorg JA, Sonenshein AL.** 2008. Bile salts and glycine as cogerminants for *Clostridium difficile* spores. J Bacteriol **190:**2505-2512.

41. **Bouillaut L, McBride SM, Sorg JA.** 2011. Genetic manipulation of *Clostridium difficile*. Curr Protoc Microbiol **Chapter 9:**Unit 9A 2.

42. **Edwards AN, Suarez JM, McBride SM.** 2013. Culturing and maintaining *Clostridium difficile* in an anaerobic environment. J Vis Exp doi:10.3791/50787**:**e50787.

43. **Luria SE, Burrous JW.** 1957. Hybridization between *Escherichia coli* and *Shigella.* J Bacteriol **74:**461-476.

44. **Purcell EB, McKee RW, McBride SM, Waters CM, Tamayo R.** 2012. Cyclic diguanylate inversely regulates motility and aggregation in *Clostridium difficile*. J Bacteriol **194:**3307-3316.

45. **McBride SM, Sonenshein AL.** 2011. The *dlt* operon confers resistance to cationic antimicrobial peptides in *Clostridium difficile*. Microbiology **157:**1457-1465.

46. **Edwards AN, Pascual RA, Childress KO, Nawrocki KL, Woods EC, McBride SM.** 2015. An alkaline phosphatase reporter for use in *Clostridium difficile*. Anaerobe.

47. **Haraldsen JD, Sonenshein AL.** 2003. Efficient sporulation in *Clostridium difficile* requires disruption of the *sigmaK* gene. Mol Microbiol **48:**811-821.

48. **Mullany P, Wilks M, Puckey L, Tabaqchali S.** 1994. Gene cloning in *Clostridium difficile* using Tn*916* as a shuttle conjugative transposon. Plasmid **31:**320-323.

49. **Mullany P, Williams R, Langridge GC, Turner DJ, Whalan R, Clayton C, Lawley T, Hussain H, McCurrie K, Morden N, Allan E, Roberts AP.** 2012. Behavior and target site selection of conjugative transposon Tn*916* in two different strains of toxigenic *Clostridium difficile.* Appl Environ Microbiol **78:**2147-2153.

50. **Putnam EE, Nock AM, Lawley TD, Shen A.** 2013. SpoIVA and SipL are *Clostridium difficile* spore morphogenetic proteins. J Bacteriol **195:**1214-1225.

51. **McBride SM, Sonenshein AL.** 2011. Identification of a genetic locus responsible for antimicrobial peptide resistance in *Clostridium difficile*. Infect Immun **79:**167-176.

52. **Schmittgen TD, Livak KJ.** 2008. Analyzing real-time PCR data by the comparative C(T) method. Nat Protoc **3:**1101-1108.

53. **McKee RW, Mangalea MR, Purcell EB, Borchardt EK, Tamayo R.** 2013. The second messenger cyclic Di-GMP regulates *Clostridium difficile* toxin production by controlling expression of *sigD.* J Bacteriol **195:**5174-5185.

54. **Woods EC, Nawrocki KL, Suarez JM, McBride SM.** 2016. The *Clostridium difficile* Dlt pathway is controlled by the ECF sigma factor, *sigmaV*, in response to lysozyme. Infect Immun doi:10.1128/IAI.00207-16.

55. **Sorg JA, Sonenshein AL.** 2010. Inhibiting the initiation of *Clostridium difficile* spore germination using analogs of chenodeoxycholic acid, a bile acid. J Bacteriol **192:**4983-4990.

56. **Dineen SS, Villapakkam AC, Nordman JT, Sonenshein AL.** 2007. Repression of *Clostridium difficile* toxin gene expression by CodY. Mol Microbiol **66:**206-219.

57. **Mooyottu S, Kollanoor-Johny A, Flock G, Bouillaut L, Upadhyay A, Sonenshein AL, Venkitanarayanan K.** 2014. Carvacrol and trans-cinnamaldehyde reduce *Clostridium difficile* toxin production and cytotoxicity in vitro. International journal of molecular sciences **15:**4415-4430.

58. **Sonenshein AL, Hoch JA, Losick R.** 1993. *Bacillus subtilis* and Other Gram-Positive Bacteria doi:doi:10.1128/9781555818388. American Society of Microbiology.

59. **He M, Sebaihia M, Lawley TD, Stabler RA, Dawson LF, Martin MJ, Holt KE, Seth-Smith HM, Quail MA, Rance R, Brooks K, Churcher C, Harris D, Bentley SD, Burrows C, Clark L, Corton C, Murray V, Rose G, Thurston S, van Tonder A, Walker D, Wren BW, Dougan G, Parkhill J.** 2010. Evolutionary dynamics of *Clostridium difficile* over short and long time scales. Proc Natl Acad Sci U S A **107:**7527-7532.

60. **Sebaihia M, Wren BW, Mullany P, Fairweather NF, Minton N, Stabler R, Thomson NR, Roberts AP, Cerdeno-Tarraga AM, Wang H, Holden MT, Wright A, Churcher C, Quail MA, Baker S, Bason N, Brooks K, Chillingworth T, Cronin A, Davis P, Dowd L, Fraser A, Feltwell T, Hance Z, Holroyd S, Jagels K, Moule S, Mungall K, Price C, Rabbinowitsch E, Sharp S, Simmonds M, Stevens K, Unwin L, Whithead S, Dupuy B, Dougan G, Barrell B, Parkhill J.** 2006. The multidrug-resistant human pathogen *Clostridium difficile* has a highly mobile, mosaic genome. Nat Genet **38:**779-786.

61. **Stabler RA, He M, Dawson L, Martin M, Valiente E, Corton C, Lawley TD, Sebaihia M, Quail MA, Rose G, Gerding DN, Gibert M, Popoff MR, Parkhill J, Dougan G, Wren BW.** 2009. Comparative genome and phenotypic analysis of *Clostridium difficile* 027 strains provides insight into the evolution of a hypervirulent bacterium. Genome Biol **10:**R102.

62. **Just I, Gerhard R.** 2004. Large clostridial cytotoxins. Rev Physiol Biochem Pharmacol **152:**23-47.

63. **Antunes A, Martin-Verstraete I, Dupuy B.** 2011. CcpA-mediated repression of *Clostridium difficile* toxin gene expression. Mol Microbiol **79:**882-899.

64. **Mani N, Dupuy B.** 2001. Regulation of toxin synthesis in *Clostridium difficile* by an alternative RNA polymerase sigma factor. Proc Natl Acad Sci U S A **98:**5844-5849.

65. **Bordeleau E, Purcell EB, Lafontaine DA, Fortier LC, Tamayo R, Burrus V.** 2015. Cyclic di-GMP riboswitch-regulated type IV pili contribute to aggregation of *Clostridium difficile*. J Bacteriol **197:**819-832.

66. **Saujet L, Pereira FC, Serrano M, Soutourina O, Monot M, Shelyakin PV, Gelfand MS, Dupuy B, Henriques AO, Martin-Verstraete I.** 2013. Genome-Wide Analysis of Cell Type-Specific Gene Transcription during Spore Formation in *Clostridium difficile*. PLoS Genet **9:**e1003756.

67. **Saujet L, Monot M, Dupuy B, Soutourina O, Martin-Verstraete I.** 2011. The key sigma factor of transition phase, SigH, controls sporulation, metabolism, and virulence factor expression in *Clostridium difficile*. J Bacteriol **193:**3186-3196.

68. **Antunes A, Camiade E, Monot M, Courtois E, Barbut F, Sernova NV, Rodionov DA, Martin-Verstraete I, Dupuy B.** 2012. Global transcriptional control by glucose and carbon regulator CcpA in *Clostridium difficile*. Nucleic Acids Res **40:**10701-10718.

69. **Edwards AN, Tamayo R, McBride SM.** 2016. A Novel Regulator Controls *Clostridium difficile* Sporulation, Motility and Toxin Production. Mol Microbiol doi:10.1111/mmi.13361**:**n/a-n/a.

70. **Mandic-Mulec I, Doukhan L, Smith I.** 1995. The *Bacillus subtilis* SinR protein is a repressor of the key sporulation gene *spo0A*. J Bacteriol **177:**4619-4627.

71. **Bai U, Mandic-Mulec I, Smith I.** 1993. SinI modulates the activity of SinR, a developmental switch protein of *Bacillus subtilis*, by protein-protein interaction. Genes Dev **7:**139-148.

72. **El Meouche I, Peltier J, Monot M, Soutourina O, Pestel-Caron M, Dupuy B, Pons JL.** 2013. Characterization of the SigD regulon of *C. difficile* and its positive control of toxin production through the regulation of *tcdR*. PLoS One **8:**e83748.

73. **McBride SM.** 2014. More Than One Way to Make a Spore. Microbe **9:**153-157.

74. **Molle V, Nakaura Y, Shivers RP, Yamaguchi H, Losick R, Fujita Y, Sonenshein AL.** 2003. Additional targets of the *Bacillus subtilis* global regulator CodY identified by chromatin immunoprecipitation and genome-wide transcript analysis. J Bacteriol **185:**1911-1922.

75. **Qi M, Mei F, Wang H, Sun M, Wang G, Yu Z, Je Y, Li M.** 2015. Function of global regulator CodY in *Bacillus thuringiensis* BMB171 by comparative proteomic analysis. J Microbiol Biotechnol **25:**152-161.

76. **Karlsson S, Burman LG, Akerlund T.** 1999. Suppression of toxin production in *Clostridium difficile* VPI 10463 by amino acids. Microbiology **145 (Pt 7):**1683-1693.

77. **Karlsson S, Lindberg A, Norin E, Burman LG, Akerlund T.** 2000. Toxins, butyric acid, and other short-chain fatty acids are coordinately expressed and down-regulated by cysteine in *Clostridium difficile*. Infect Immun **68:**5881-5888.

78. **Smits WK.** 2013. Hype or hypervirulence: a reflection on problematic *C. difficile* strains. Virulence **4:**592-596.

79. **Warny M, Pepin J, Fang A, Killgore G, Thompson A, Brazier J, Frost E, McDonald LC.** 2005. Toxin production by an emerging strain of *Clostridium difficile* associated with outbreaks of severe disease in North America and Europe. Lancet **366:**1079-1084.

80. **Merrigan M, Venugopal A, Mallozzi M, Roxas B, Viswanathan VK, Johnson S, Gerding DN, Vedantam G.** 2010. Human hypervirulent *Clostridium difficile* strains exhibit increased sporulation as well as robust toxin production. J Bacteriol **192:**4904-4911.

81. **Vohra P, Poxton IR.** 2011. Comparison of toxin and spore production in clinically relevant strains of *Clostridium difficile*. Microbiology **157:**1343-1353.

82. **Janoir C, Deneve C, Bouttier S, Barbut F, Hoys S, Caleechum L, Chapeton-Montes D, Pereira FC, Henriques AO, Collignon A, Monot M, Dupuy B.** 2013. Adaptive Strategies and Pathogenesis of *Clostridium difficile* from In Vivo Transcriptomics. Infect Immun **81:**3757-3769.

83. **Mueller JP, Bukusoglu G, Sonenshein AL.** 1992. Transcriptional regulation of *Bacillus subtilis* glucose starvation-inducible genes: control of *gsiA* by the ComP-ComA signal transduction system. J Bacteriol **174:**4361-4373.

84. **Lazazzera BA, Kurtser IG, McQuade RS, Grossman AD.** 1999. An autoregulatory circuit affecting peptide signaling in *Bacillus subtilis.* J Bacteriol **181:**5193-5200.

85. **Slack FJ, Mueller JP, Sonenshein AL.** 1993. Mutations that relieve nutritional repression of the *Bacillus subtilis* dipeptide permease operon. J Bacteriol **175:**4605-4614.

86. **Shafikhani SH, Nunez E, Leighton T.** 2003. ScoC mediates catabolite repression of sporulation in *Bacillus subtilis*. Curr Microbiol **47:**327-336.

87. **Koide A, Perego M, Hoch JA.** 1999. ScoC regulates peptide transport and sporulation initiation in *Bacillus subtilis.* J Bacteriol **181:**4114-4117.

88. **Caldwell R, Sapolsky R, Weyler W, Maile RR, Causey SC, Ferrari E.** 2001. Correlation between *Bacillus subtilis scoC* phenotype and gene expression determined using microarrays for transcriptome analysis. J Bacteriol **183:**7329-7340.

89. **Barbieri G, Albertini AM, Ferrari E, Sonenshein AL, Belitsky BR.** 2016. Interplay of CodY and ScoC in the regulation of major extracellular protease genes of *Bacillus subtilis*. Journal of bacteriology**:**JB. 00894-00815.

90. **Belitsky BR, Barbieri G, Albertini AM, Ferrari E, Strauch MA, Sonenshein AL.** 2015. Interactive regulation by the *Bacillus subtilis* global regulators CodY and ScoC. Molecular microbiology **97:**698-716.

91. **Belitsky BR, Sonenshein AL.** 2013. Genome-wide identification of *Bacillus subtilis* CodY-binding sites at single-nucleotide resolution. Proceedings of the National Academy of Sciences **110:**7026-7031.

92. **Hussain HA, Roberts AP, Mullany P.** 2005. Generation of an erythromycin-sensitive derivative of *Clostridium difficile* strain 630 (630Δ*erm*) and demonstration that the conjugative transposon Tn*916*ΔE enters the genome of this strain at multiple sites. Journal of Medical Microbiology **54:**137-141.

93. **Thomas CM, Smith CA.** 1987. Incompatibility group P plasmids: genetics, evolution, and use in genetic manipulation. Annual Reviews in Microbiology **41:**77-101.

94. **Lyras D, Rood JI.** 1998. Conjugative Transfer of RP4-oriT Shuttle Vectors from *Escherichia coli* to *Clostridium perfringens*. Plasmid **39:**160-164.

95. **Lampe DJ, Churchill ME, Robertson HM.** 1996. A purified mariner transposase is sufficient to mediate transposition in vitro. The EMBO Journal **15:**5470-5479.

96. **Manganelli R, Provvedi R, Berneri C, Oggioni MR, Pozzi G.** 1998. Insertion vectors for construction of recombinant conjugative transposons in *Bacillus subtilis* and *Enterococcus faecalis*. FEMS microbiology letters **168:**259-268.

CHAPTER 3

The Impact of Ethanolamine Utilization on Pathogenesis of *Clostridium difficile*

Kathryn L. Nawrocki and Shonna M. McBride

The work presented in this chapter is in preparation for publication

K.L.N. performed all experiments, made figures and wrote the manuscript.

ABSTRACT

The gastrointestinal (GI) tract is a competitive environment with potential pathogens and members of the microbiota vying for nutrients. The ability to utilize nutrients specific to the GI tract can give pathogenic bacteria a competitive advantage that can lead to successful colonization and establishment of disease. The nutrients required for *Clostridium difficile* to establish itself within the GI tract have not been determined. In other enteric pathogens, ethanolamine (ETA), a membrane-derived intestinal metabolite, provides a growth advantage and functions as a signal to initiate production of virulence factors. We have investigated the capacity of *C. difficile* to utilize ETA, and the impact of ETA on virulence factor expression and pathogenesis. *C. difficile* contains a putative 19-gene ETA utilization (*eut*) cluster. Using targeted mutagenesis, we made an insertional disruption in *eutA*, an ammonia lyase reactivating factor, and observed that this gene cluster does facilitate the utilization of ETA in *C. difficile*. To investigate pathogenesis, we infected hamsters with the *eutA* mutant. The *eutA* mutation decreases the time to morbidity in hamsters. The inability to utilize ETA does not affect growth in the hamster model because equivalent numbers of CFUs were enumerated from the ceca of hamsters infected with the wild-type and *eutA* mutant strains. These hamster studies suggest that the ability to utilize ETA may delay the onset of disease. Overall, our data suggest that ETA is a true nutrient source and impacts pathogenesis of *C. difficile*.

INTRODUCTION

Clostridium difficile is a Gram-positive, spore-forming, obligate anaerobe. *C. difficile* resides asymptomatically in 2-5% of the population, but it can cause severe

intestinal disease following antibiotic disruption of the host microbiota (1-3). *C. difficile* is a leading cause of nosocomial infections in the United States, resulting in healthcare-associated costs close to $4.8 billion annually (4, 5). C. *difficile* causes intestinal disease through the production of two large toxins, TcdA and TcdB (6-8). *tcdA* and *tcdB*, along with 3 other accessory genes, are encoded in a region referred to as the pathogenicity locus (PaLoc) (9). TcdA and TcdB inactivate host Rho and Rac GTPases through glycosylation, leading to host cell death (10-14). *C. difficile* strains that do not produce TcdA and TcdB do not cause disease (6, 15).

Many important processes involved in the survival, transmission, and virulence of *C. difficile* are linked with its metabolism. Toxin production in *C. difficile* is influenced by growth and environmental conditions. The toxins are predominately regulated by two global nutritional regulators, CcpA and CodY (16-19). CcpA mediates catabolite repression of the PaLoc (16, 19). CodY also represses toxin production in times of nutrient excess (17). Therefore, expression of these toxins is closely linked with *C. difficile* metabolism. In addition to toxin production, the process of sporulation in *C. difficile* is also linked to environmental conditions. Persistence and transmission in the aerobic environment outside of the host is dependent on the formation of a metabolically dormant spore (20, 21). Sporulation in *C. difficile* is directly controlled by the master regulator, Spo0A (20, 22). The regulatory pathways that control the activation of Spo0A are not fully understood in *C. difficile* (23, 24), but research suggests a strong link between nutritional state and sporulation. In previous work, we determined that CodY, Opp, and App, inhibit sporulation (25, 26). App and Opp are oligopeptide permeases that are hypothesized to indirectly inhibit sporulation by the importation of peptides in *C. difficile* (25). The

complete metabolic relationship between the host, the host microbiota, and *C. difficile* is still under investigation.

Ethanolamine (ETA) is an readily available gastrointestinal metabolite. ETA is derived from phosphatidylethanolamine, an abundant phospholipid present in prokaryotic and eukaryotic cellular membranes (27-29). Studies have connected ETA metabolism with pathogenesis in other gastrointestinal pathogens (30-35). ETA can provide a growth advantage to pathogenic enteric species over the host microbiota (30, 31, 35). Additionally, ETA can act as a signal for niche recognition and lead to virulence factor production (32, 33, 36). Due to the connection between virulence and ETA in other species, we decided to further examine the role of ETA metabolism in *C. difficile* pathogenesis.

The first step of ETA metabolism is the breakdown of ETA into acetaldehyde and ammonia by the ammonia lyase EutBC (37, 38). Acetaldehyde can be further processed into acetyl-CoA by EutE, an aldehyde oxidoreductase (39), or into ethanol by EutG, an alcohol dehydrogenase (40). Genomic studies have shown that many bacteria encode *eutBC,* but the number and organization of the *eut* accessory genes, like *eutE* and *eutG* varies (41). Sequence analysis indicates that *C. difficile* encodes a 19-gene ethanolamine utilization cluster (Fig **1**) (42). While *C. difficile* contains one of the largest ethanolamine utilization gene clusters, little to no research has examined this metabolic pathway and its role in *C. difficile* pathogenesis.

Therefore, this study was undertaken to understand ETA metabolism of *C. difficile* and its effect on pathogenesis. We disrupted *eutA*, an ETA ammonia lyase reactivating factor, and determined that *C. difficile* utilizes ETA in minimal media studies. In the hamster model of infection, we observed that hamsters infected with the *eutA* mutant

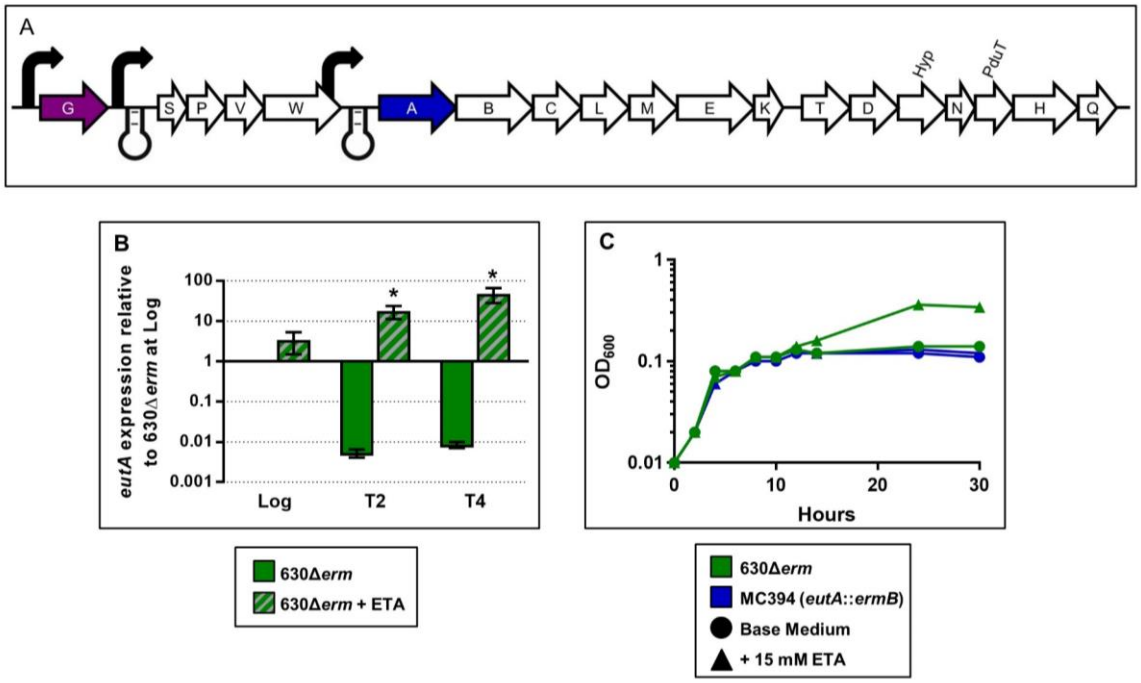

Figure 1. *Clostridium difficile* utilizes ethanolamine. (**A**) Ethanolamine utilization (*eut*) gene cluster in *C. difficile* 630. The *eut* gene cluster contains 19 predicted open reading frames. Putative promoters and terminator structures were identified through sequence analysis (59, 60). *eutA*, marked in blue, and *eutG*, marked in purple, were disrupted. (**B**) qRT-PCR analysis of *eutA* expression of 630Δ*erm* grown in 70:30 liquid medium with and without the addition of 15 mM ethanolamine hydrochloride (ETA). Expression of *eutA* in 630Δ*erm* grown in medium with and without ETA was compared at each timepoint by a two-tailed *t*-test. The Holm-Sidak method was used to correct for multiple comparisons. * indicates $p \leq 0.05$. (**C**) Representative growth curve of 630Δ*erm* and MC394 (*eutA*::*ermB*) in a modified minimal medium with and without the addition of 15 mM ETA.

became moribund at an earlier time in infection. We observed no difference between the wild-type and mutant strain in the amount of *C. difficile* CFU present in the cecal content collected at the time of morbidity. This was an indication that ETA is an important nutrient source in the host and ETA metabolism may delay the onset of disease. Additionally, we studied the effect of ETA metabolism *in vitro* with transcriptional analyses, but did not observe any change in toxin and colonization factor expression in the presence of ETA. These *in vitro* results may not accurately recapitulate *in vivo* conditions, or ETA and its metabolism may not affect toxin or colonization factor production. Overall, our results demonstrate that *C. difficile* utilizes ETA, and that ETA is an important nutrient source in the host.

MATERIALS AND METHODS

Bacterial strains and growth conditions. Table 1 provides a list of the strains and plasmids used in this study. *C. difficile* strains were routinely cultured in brain heart infusion-supplemented (BHIS) broth and BHIS agar plates (43). Two to 10 µg thiamphenicol ml^{-1}, or 5 µg erythromycin ml^{-1} (Sigma-Aldrich) was used to supplement BHIS medium, as needed. To induce the germination of *C. difficile* spores, media was supplemented with 0.1% taurocholate (Sigma-Aldrich) (44). 0.5% D-fructose was added to the overnight cultures to prevent sporulation, as needed (45). An anaerobic vinyl chamber (Coy Laboratory Products) at 37°C with an atmosphere of 10% H_2, 5% CO_2, and 85% N_2 was used to culture *C. difficile* (46). Minimal medium growth curves were performed using in a modified minimal media based on a complete defined medium (47). The modified minimal medium used contained 75% less amino acids than the original,

Table 1. Bacterial Strains and Plasmids

Plasmid or Strain	Relevant genotype or features	Source, construction or reference
Strains		
E. coli		
	HB101	F^- *mcrB mrr hsdS20*(r_B^- m_B^-) *recA13 leuB6 ara-14 proA2 lacY1 galK2 xyl-5 mtl-1 rpsL20* — B. Dupuy
	MC101	HB101 pRK24 — B. Dupuy
	DH5α Max Efficiency	F^- Φ80*lac*ZΔM15 Δ(*lac*ZYA-*arg*F) U169 *rec*A1 *end*A1 *hsd*R17 (rk^-, mk^+) *pho*A *sup*E44 λ^- *thi*$^-$1 *gyr*A96 *rel*A1 — Invitrogen
	MC341	HB101 pRK24 pMC263 — This study
	MC344	HB101 pRK24 pMC266 — This study
C. difficile		
	630Δ*erm*	Erm^S derivative of strain 630 — N. Minton (78)
	MC310	630Δ*erm spo0A::ermB* — (25)
	MC346	630Δ*erm eutG::ermB* — This study
	MC394	630Δ*erm eutA::ermB* — This study
Plasmids	pCE240	*C. difficile* Targetron construct based on pJIR750ai (group II intron, *ermB*::RAM *ltrA*) *catP* — C. Ellermeier (79)
	pRK24	Tra^+, Mob^+; *bla, tet* — (80)
	pCR2.1	*bla kan* — Invitrogen
	pMC111	pCE240 Group II intron targeted to *dltD* — (50)
	pMC123	*E. coli-C. difficile* shuttle vector; *bla*, *catP* — (81)
	pMC253	pCR2.1 Group II intron targeting region for *eutA* — This study
	pMC256	pCR2.1 Group II intron targeting region for *eutG* — This study
	pMC257	pCE240 Group II intron targeted to *eutA* — This study
	pMC260	pCE240 Group II intron targeted to *eutG* — This study
	pMC263	pMC123 Group II intron targeted to *eutA, ermB*::RAM *ltrA catP* — This study
	pMC266	pMC123 Group II intron targeted to *eutG*, *ermB*::RAM ltrA catP — This study

except for L-cysteine and L-tryptophan, which were added as previously described (47). Modified minimal media was supplemented with 15 mM ethanolamine hydrochloride (Sigma-Aldrich) and 5 mM D-glucose. 99.9% ethanolamine (Sigma-Aldrich) was used to supplement 70:30 liquid medium in the transcriptional unit study only. *Escherichia coli* strains were cultured at 37°C in LB (48) supplemented with 20 µg chloramphenicol ml^{-1} and 100 µg ampicillin ml^{-1}. Following conjugation, 50 µg kanamycin ml^{-1} was used to counter-select against *E. coli* (49).

Strain and plasmid construction. Oligonucleotides used in this study are listed in **Table 2**. Construction details of plasmids used in this study can be found in Figure **S1**. 630 genomic sequence (NC_009089.1) was used for primer design. Plasmids were confirmed by sequencing (Eurofins MWG Operon). Null mutations were generated in 630Δ*erm* as previously described (49, 50). pMC263 was conjugated into *C. difficile* 630Δ*erm* to generate MC394 (*eutA*::*ermB)*. pMC266 was conjugated into *C. difficile* 630Δ*erm* to generate MC346 (*eutG*::*ermB)*. Colonies were screened by PCR to verify intron insertion into the target gene. MC394 (*eutA*::*ermB)* was further verified by Southern blot and whole genome sequencing (Yerkes Nonhuman Genomics Core).

Transcriptional unit study. 630Δ*erm* was grown in 70:30 sporulation medium supplemented with 15 mM ethanolamine hydrochloride (Sigma-Aldrich). Samples for RNA were taken six hours following inoculation. RNA was isolated as previously described using a Qiagen RNeasy kit. RNA preparations were treated with the Ambion DNAse Turbo Kit to remove contaminating genomic DNA. A Bioline Tetro cDNA

Table 2. Oligonucleotides

Primer	Sequence (5'→3')	Use/location[a]	Source or reference
EBS universal	**5'-CGAAATTAGAAACTTGCGTTCAGTAAAC-3'**	Targetron cloning	Sigma-Aldrich
oMC44	**5'-CTAGCTGCTCCTATGTCTCACATC-3'**	*rpoC* qPCR (CD0067)	(50)
oMC45	**5'-CCAGTCTCTCCTGGATCAACTA-3'**	*rpoC* qPCR (CD0067)	(50)
oMC112	**5'-GGCAAATGTAAGATTTCGTACTCA-3'**	*tcdB* qPCR (CD0660)	(25)
oMC113	**5'-TCGACTACAGTATTCTCTGAC-3'**	*tcdB* qPCR (CD0660)	(25)
oMC339	**5'-GGGCAAATATACTTCCTCCTCCAT-3'**	*sigE* qPCR (CD2643)	(25)
oMC340	**5'-TGACTTTACACTTTCATCTGTTTCTAGC-3'**	*sigE* qPCR (CD2643)	(25)
oMC547	**5'-TGGATAGGTGGAGAAGTCAGT-3'**	*tcdA* qPCR (CD0663)	(25)
oMC548	**5'-GCTGTAATGCTTCAGTGGTAGA-3'**	*tcdA* qPCR (CD0663)	(25)
oMC655	**5'-GAAATAGTACCAGACCCACCAATA-3'**	*eutG* PCR (CD1907)	This study
oMC657	**5'-CTAAAGAAGATATACATACAGGAGCAGT-3'**	*eutA* PCR (CD1912)	This study
oMC658	**5'-TAAATCAGGTCCTGCTGTTGC-3'**	*eutA* PCR (CD1912)	This study
oMC659	**5'-ATCAGGAGATAAATTAGCAGGTCTT-3'**	*eutB* PCR (CD1913)	This study
oMC660	**5'-GCCACTGCAGGATTATTTCTTATATC-3'**	*eutB* PCR (CD1913)	This study
oMC661	**5'-GTTGATGATGAACCACTGTTAAGG-3'**	*eutV* PCR (CD1910)	This study
oMC662	**5'-TTCAACAGCTTCAAATCCATCAC-3'**	*eutV* PCR (CD1910)	This study
oMC663	**5'-TGTACTAAGTAAATTTGATGATGAAGCA-3'**	*eutW* PCR (CD1911)	This study
oMC664	**5'-TGACCAGTTTATATTCCTGTGTTAAAG-3'**	*eutW* PCR (CD1911)	This study
oMC665	**5'-AAAAGCTTTTGCAACCCACGTCGATCGTGAAGGAAGGCTTGTAGTGCGCCCAGATAGGGT-3'**	*eutA* intron retargeting (CD1912)	This study

oMC666	**5'-CAGATTGTACAAATGTGGTGATAACAGATAAGTCCTTGTAAATAACTTACCTTTCTTTGT-3'**	*eutA* intron retargeting (CD1912)	This study
oMC667	**5'-CGCAAGTTTCTAATTTCGGTTCTTCCTCGATAGAGGAAAGTGTCT-3'**	*eutA* intron retargeting (CD1912)	This study
oMC674	**5'-AAAAGCTTTTGCAACCCACGTCGATCGTGAATCTACCTCGTTAGTGCGCCCAGATAGGGTG-3'**	*eutG* intron retargeting (CD1907)	This study
oMC675	**5'-CAGATTGTACAAATGTGGTGATAACAGATAAGTCTCGTTAATTAACTTACCTTTCTTTGT-3'**	*eutG* intron retargeting (CD1907)	This study
oMC676	**5'-CGCAAGTTTCTAATTTCGGTTGTAGATCGATAGAGGAAAGTGTCT-3'**	*eutG* intron retargeting (CD1907)	This study
oMC855	**5'-TCATAGCTAACCCTAATGAAGACAT-3'**	*eutS* PCR (CD1908)	This study
oMC856	**5'-GCAACATCTGCTGCTATTATTGA-3'**	*eutS* PCR (CD1908)	This study
oMC859	**5'-TCCTAAGGATGCAGAAGCTTATTT-3'**	*eutC* PCR (CD1914)	This study
oMC860	**5'-CAGCATGGTCTGCTCTAAATCT-3'**	*eutC* PCR (CD1914)	This study
oMC861	**5'-ACTGCAGACTGTGATGATGTT-3'**	*eutL* PCR (CD1915)	This study
oMC862	**5'-CAGCACCTGCATACATTGATTT-3'**	*eutL* PCR (CD1915)	This study
oMC863	**5'-GGAGATGTCGGTGCTGTAAA-3'**	*eutM* PCR (CD1916)	This study
oMC864	**5'-TGTTCTTAATGTACCAACTCTGGA-3'**	*eutM* PCR (CD1916)	This study
oMC865	**5'-TGGTGAAGATAAGGAAGCCAATA-3'**	*eutE* PCR (CD1917)	This study
oMC866	**5'-GATGTTGGGTTTGTTGAAGGTATAA-3'**	*eutE* PCR (CD1917)	This study
oMC867	**5'-GCAGCAGATGCAATGGTTAAA-3'**	*eutK* PCR (CD1918)	This study
oMC868	**5'-CAGCTCCAACATCTCCTCTTAC-3'**	*eutK* PCR (CD1918)	This study
oMC869	**5'-TTTGGCGCTAAATTGGATGAAA-3'**	*eutT* PCR (CD1919)	This study
oMC870	**5'-TTCCTTAACAAGCTTTGGCATATC-3'**	*eutT* PCR (CD1919)	This study
oMC871	**5'-ATAGAAGTTGAAGCATCAGGAAGAC-3'**	*eutD* PCR (CD1920)	This study
oMC872	**5'-CATGCATATTGACCTGGTTGAGATA-3'**	*eutD* PCR (CD1920)	This study

oMC873	**5'-CCTAAAGCTGTGATTGTATTTGAACAAG-3'**	*eut hyp* PCR (CD1921)	This study
oMC874	**5'-ATTTCCAAGTGCTATATTCGATAGTCC-3'**	*eut hyp* PCR (CD1921)	This study
oMC877	**5'-AGGCGTTGTTGAAAGTAGTAAAGT-3'**	*pduT* PCR (CD1923)	This study
oMC878	**5'-ACTGTCTACTGATGGTATTACAGTCT-3'**	*pduT* PCR (CD1923)	This study
oMC879	**5'-TGGTCTTGGAGAACAATTTGAAGA-3'**	*eutH* PCR (CD1924)	This study
oMC880	**5'-ATCAGCAAGAACTGGTGCTAAA-3'**	*eutH* PCR (CD1924)	This study
oMC882	**5'-CCTAATCTTGGGCTTTCCTCTAAT-3'**	*eutQ* PCR (CD1925)	This study
oMC972	**5'-ATAAGAGCCACAGTGGTTGG-3'**	*eutA* qPCR (CD1912)	This study
oMC973	**5'-CTGGCAAGTTCTTAAGTGGAAAC-3'**	*eutA* qPCR (CD1912)	This study
fliCqF	**5'-TACAAGTTGGAGCAAGTTATGGAAC-3'**	*fliC* qPCR (CD0239)	(82)
fliCqR	**5'-GTTGTTATACCAGCTGAAGCCATTA-3'**	*fliC* qPCR (CD0239)	(82)
OBD522	**5'-ATCTGTAGGAGAACCTATGGGAAC-3'**	Intron probe	(53)
OBD523	**5'-CACGTAATAAATATCTGGACGTAAAA-3'**	Intron probe	(53)
qRTpilA1F	**5'-TGGCAGTTCCAGCTTTATTTAGTAAT-3'**	*pilA1* qPCR (CD3513)	(83)
qRTpilA1R	**5'-AAGATAATGCTGCACTCTTAACTGAA-3'**	*pilA1* qPCR (CD3513)	(83)

[a] Locus number in reference to the 630 genome (NC_009089.1)

[b] Underlined regions denote restriction enzyme cut sites

synthesis kit was used to synthesize cDNA from the isolated RNA. This reaction was performed in duplicate, except reverse transcriptase (RT) was withheld in one sample to generate the minus RT control. The minus RT reaction controls for DNA contamination in the RNA preparation. Genomic DNA from 630Δ*erm* was collected using a modified Bust n' Grab protocol (51), as previously described (52). PCR reactions were performed using Phusion (NEB). Primers were designed to amplify adjacent open reading frames.

Southern blot. The Southern blot was performed as previously described (25, 53). Genomic DNA was prepared from an overnight culture of 630Δ*erm* or MC394 (*eutA*::*ermB*) using a modified Bust n' Grab protocol (51), as previously described (52). Six µg of genomic DNA from 630Δ*erm* and MC394 (*eutA*::*ermB*) was digested with *HindIII*. Digests were run out on a 0.7% agarose gel and transferred to Hybond-N+ nylon membranes (GE Healthcare) via capillary action. A DIG high prime labeling and detection kit (Roche) was used to perform the Southern blot. The membrane was probed using an intron-specific probe that was generated by PCR using OBD522 and OBD523, as previously described (53).

Single-nucleotide polymorphisms (SNP) analysis. MC394 (*eutA*::ermB) and its parent strain, 630Δ*erm,* underwent SNP analysis in lieu of complementation. A modified Bust n' Grab protocol (51, 52) was used to prepare genomic DNA. Libraries were generated from genomic DNA using the Illumina NexteraXT DNA kit; dual barcoding and sequencing primers were added according to the manufacturer protocol. Libraries were validated by microelectrophoresis on an Agilent 2100 Bioanalyzer, quantified, pooled, and clustered on

an Illumina miSeq V3 flowcell. The clustered flowcell was sequenced on an Illumina miSeq in 275-base paired-read reactions. Per sample reads were mapped to the *C. difficile* 630 reference genome (GenBank no. AM180355). CLC Genomics Workbench v9.0 was used for all variant analysis as previously described (54).

Quantitative reverse transcription PCR analysis (qRT-PCR). qRT-PCR was performed as described previously with minor modifications (25). *C. difficile* was grown in 70:30 medium with and without the addition of 15 mM ethanolamine hydrochloride (Sigma-Aldrich). Samples for RNA were collected at logarithmic growth (OD_{600} of ~0.5), mid stationary phase (2 hours after reaching an OD_{600} of ~1.0, T_2), and at late stationary phase (4 hours after reaching an OD_{600} of ~1.0, T_4). RNA isolation was performed as previously described (18, 50). Samples for RNA isolation were diluted in 1:1 acetone-ethanol. RNA was isolated using a Qiagen RNeasy kit as previously described. Samples were treated with the Ambion DNAse Turbo Kit to remove any contaminating genomic DNA. cDNA synthesis was performed using a Bioline Tetro cDNA synthesis kit. Using the Bioline Sensi-Fast SYBR and Fluroescein kit, qRT-PCR was performed with 50 ng of cDNA as template on a Roche Lightcycler 96. qRT-PCR reactions were performed in technical triplicates. As a negative control, cDNA reactions containing no reverse transcriptase were performed. The PrimerQuest tool provided by Integrated DNA Technologies was used to generate qRT-PCR primers. The primer efficiencies were determined using genomic DNA. qRT-PCR results were calculated with the comparative cycle threshold method (55), with the expression of the amplified transcript being normalized to the internal control transcript, *rpoC*. All qRT-PCR data were analyzed with

a two-way repeated measures ANOVA, except for the *eutA* expression study. The *eutA* expression study was analyzed by a two-tailed *t* test and multiple comparisons were corrected for by Holm-Sidak.

Hamster studies. Hamster studies were conducted as previously described with minor modifications (56). Male and female Syrian golden hamsters (*Mesocricetus auratus*) weighing between 70 to 110 grams were purchased from Charles River Laboratories. Hamsters were kept in an animal biosafety level 2 room within the Emory University Division of Animal Resources. Hamsters were housed individually with sterile rodent pellets and sterile water provided *ad libitum*. Hamsters were orally gavaged with clindamycin (30mg/kg) to induce susceptibility to *C. difficile* seven days prior to inoculation (Day -7). Hamsters were inoculated by oral gavage with 5000 spores of 630Δ*erm* or MC394 (*eutA*::*ermB*) (Day 0). Spores were prepared as previously described (25, 56). Following inoculation, hamsters were monitored for signs of disease, such as diarrhea or wet tail, weight loss, and lethargy. Hamsters were considered moribund if they lost ≥ 15% of their body weight and/or exhibited severe disease symptoms. Hamsters meeting these criteria were euthanized. Hamsters were weighed and fecal pellets were collected at least once daily. Cecal contents were collected post-mortem. Fecal and cecal contents were diluted in 1X PBS and plated onto to taurocholate cycloserine cefoxitin fructose agar (TCCFA) plates to determine the number of *C. difficile* CFU {Wilson, 1981 #457;George, 1979 #456}. Inoculated TCCFA plates were incubated anaerobically for 48 hours prior to CFU enumeration. Fecal CFU enumeration data were analyzed with a general linear model on a Poisson distribution. Cecal CFU enumeration data were analyzed

with a two-tailed *t* test. To determine the number of spores present in the cecal content, a suspension of cecal content in 1x PBS was diluted 1:1 in 57% ethanol and incubated for 15 minutes at room temperature. The samples were then diluted in 1X PBS containing 0.1% taurocholate and plated onto TCCFA plates. Plates were incubated anaerobically at 37°C for at least 48 hours before enumeration. Cecal spore counts were compared using a two-tailed *t* test. Hamsters treated with clindamycin, but not inoculated with *C. difficile* spores, served as negative controls. Survival data were analyzed using log-rank regression. Three independent hamster experiments were conducted with cohorts of 5 to 6 hamsters per *C. difficile* strain; a total of 17 hamsters per strain were used.

Ethanol resistance assay. Ethanol resistance assays, as an indication of spore formation, were performed as previously described with minor modifications (52). Strains were grown overnight in BHIS broth supplemented with 0.2% D-fructose to prevent sporulation and 0.1% taurocholate to germinate any spores present in the inoculum. Active cultures were diluted into BHIS to an OD_{600} of 0.5. 250 µl of each culture was spread onto 70:30 agar plates supplemented with 0, 15, or 30 mM ethanolamine hydrochloride. Upon inoculation, plates were incubated anaerobically at 37°C for 24 hours. To evaluate ethanol resistance, samples from plates were scraped into 5 ml of BHIS to an OD_{600} of 1.0. The resuspended cells were serially diluted in BHIS and plated onto BHIS agar containing 0.1% taurocholate to determine the number of viable cells. To determine the number of ethanol resistant spores, 500 µl of each sample was diluted 1:1 in 57% ethanol to reach a final concentration of 28.5% ethanol. Samples were mixed and incubated for 15 minutes at room temperature. Ethanol treated samples were serially diluted in 1X PBS containing 0.1% taurocholate to

assist with the germination of spores. Serial dilutions were plated onto BHIS containing 0.1% taurocholate. Sporulation frequency was calculated by dividing the number of ethanol-resistant spores by the number of viable cells. MC310 (*spo0A*::*ermB*), a sporulation mutant, was used as a negative control to verify vegetative cell death following ethanol treatment. The mean sporulation frequencies and standard deviations were calculated from four independent experiments. Data were analyzed with a two-way repeated measures ANOVA.

Phase contrast microscopy and direct count sporulation frequency. Samples for phase contrast microscopy were prepared as previously described (25). Samples were scraped from the 70:30 agar plates and resuspended in BHIS broth. Three µl of each sample was pipetted on to a 100 µl 0.7% agarose pad on a glass slide. Coverslips were placed over the samples. Micrographs were taken with a DS-Fi2 camera on a Nikon Eclipse Ci-L microscope with an X100 Ph3 oil-immersion objective. Direct count sporulation frequency was performed as previously described (52). A minimum of 1000 cells were counted per strain and condition. Sporulation frequency was calculated by dividing the number of spores by the total number of cells present (spores and vegetative cells). MC310 (spo0A::ermB), a sporulation defective mutant, was used as a negative control. The mean sporulation frequencies and standard deviations were calculated from four independent experiments. Phase contrast sporulation frequency data were analyzed using a two-way repeated measures ANOVA.

Accession numbers. *C. difficile* strain 630 (GenBank accession NC_009089.1).

Statistical analysis. Statistical analyses were performed using GraphPad Prism version 7.0 for Windows. R version 3.3.1 for Windows was used to analyze the fecal CFU/ml over time data.

RESULTS

Ethanolamine is a viable nutrient source for *C. difficile*

To be able to assess the role of ETA metabolism in *C. difficile* pathogenesis, we first had to generate ETA metabolism mutants and verify that *C. difficile* utilizes ETA. First, we identified the putative ethanolamine utilization (*eut*) gene cluster in *C. difficile*. *C. difficile* contains a *eut* gene cluster consisting of 19 predicted open reading frames (Fig **1A**). Sequence analysis performed by us and others have identified the locations of the promoters and transcriptional antiterminator structures in this region (59, 60). We performed a transcriptional unit study of the *eut* cluster to identify probable operons in this region (Fig **S2**). We showed that the *eut* cluster consists of at least two transcriptional units, the first spanning from *eutG* to *eutW,* and the second spanning from *eutA* to *eutQ* (Fig **S2B**). We then confirmed that the *eut* cluster is actively transcribed in the presence of ETA using qRT-PCR (Fig **1B**). We found that over time in the presence of ETA transcription of *eutA* was increased. We examined other genes within the cluster and saw similar results (data not shown).

Following the identification of the *eut* cluster, we generated two ETA utilization mutants using Targetron mutagenesis. We inserted an *ermB* cassette into *eutA*, which encodes a reactivating factor for EutBC (Fig **1A**). This was verified with a Southern blot

(Fig **S3**). The insertion in *eutA* was polar (data not shown). We also inserted an *ermB* cassette into *eutG*, which encodes an alcohol dehydrogenase (Fig **1A**). We tested whether these mutants were capable of utilizing ETA in a modified minimal medium growth curve (Fig **1C, S4**). When the parent strain, 630Δ*erm*, was grown in modified minimal medium without supplementation, growth stalled after a few hours. The initial spike in growth is likely due to media transfer from the original culture. In medium supplemented with ETA, 630Δ*erm* reached a higher optical density, demonstrating that *C. difficile* can utilize ETA (Fig **1C**). We also grew our *eut* mutants in the same conditions. The *eutA* mutant did not exhibit a growth advantage in media supplemented with ETA, demonstrating that *eutA* and its downstream genes are required for ETA utilization (Fig **1C**). Unlike the *eutA* mutant, the *eutG* mutant exhibited the same phenotype as the parent strain, indicating that *eutG* is not essential for ETA metabolism in the conditions tested (Fig **S4**). From these minimal medium growth curves, we were able to determine that *C. difficile* does utilize ETA and that the genes spanning from *eutA* to *eutQ* are needed for its utilization.

We attempted to complement our *eutA* mutant through *codA* allelic replacement (61), but were unsuccessful. In lieu of complementation, we performed whole genome sequencing and single nucleotide analysis (SNP analysis) on our *eutA* mutant and its parent strain. The only differences detected between the two strains were of our own making. This indicates that the phenotypes observed with the *eutA* mutant are caused by the disruption of *eutA* alone.

Lastly, we performed additional modified minimal medium growth curves with 630Δ*erm* to determine if ETA is a primary nutrient source. Many metabolic pathways are regulated through catabolite repression, wherein alternate metabolic pathways are shut

down while more energy efficient metabolites, such as glucose, are utilized first (19, 62). When 630Δ*erm* is grown with ETA or glucose the growth rate is higher than the base modified minimal medium (Fig **S5**). When we supplement the media with both ETA and glucose, we see a growth phenotype that mimics the glucose supplementation growth curve (Fig **S5**). The absence of a diauxic growth trend when ETA and glucose are present demonstrates that ETA is primary nutrient source, and that the *eut* cluster does not appear to be under catabolite repression.

Ethanolamine metabolism *in vivo* alters disease progression

ETA is a major component of phospholipid bilayers and is naturally found in the gastrointestinal tract (31, 35, 63). Intestinal epithelial turnover and a diet rich in processed foods can create a gastrointestinal environment with high concentrations of ETA (27, 59, 64). In other enteric pathogens, ETA is a virulence signal and a niche nutrient that can lead to a growth advantage over the microbiota (32-35, 63). Therefore, we decided to investigate the impact of ETA metabolism in the hamster model of *C. difficile* infection.

Male and female hamsters were inoculated with 5000 spores of 630Δ*erm* or MC394 (*eutA*::*ermB*) seven days following a single dose of clindamycin and monitored for disease symptoms. Hamsters that were inoculated with MC394 (*eutA*::*ermB*) became moribund earlier than hamsters infected with the parent strain. The median time to morbidity for hamsters infected with MC394 (*eutA*::*ermB*) was 33.9 hours, versus 43.56 hours for hamsters infected with 630Δ*erm* (Fig **2A**). This demonstrates that the inability to utilize ETA decreases the time to morbidity.

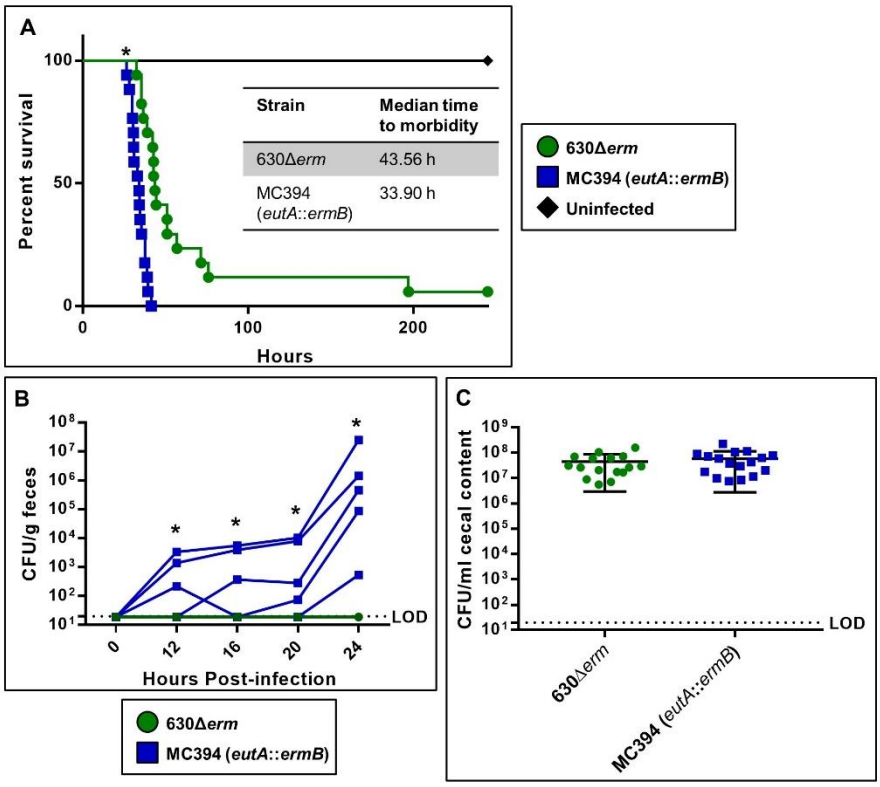

Figure 2. MC394 (*eutA*::*ermB*) is more virulent than 630Δ*erm*. Hamsters were orally gavaged with approximately 5000 spores of 630Δ*erm* (n=17) and MC394 (*eutA*::*ermB*) (n=17) seven days after clindamycin treatment. (**A**) Time to morbidity is shown in a Kaplan-Meier survival curve. * indicates $p \leq 0.0001$ by Log-rank test. Median time to morbidity for each strain is shown. (**B**) Over the first 24 hours post-infection, *C. difficile* CFU were enumerated from fecal samples. Five hamsters per strain were evaluated. The dotted line is the limit of detection (LOD) which is set at 20 CFU/ml. MC394 (*eutA*::*ermB*) fecal CFU were compared to the parent strain CFU with a general linearized model on a Poisson distribution. Mean CFU/g feces were compared between strains. * indicates $p \leq 0.001$. (**C**) *C. difficile* CFU were enumerated from cecal samples collected post-mortem. Mean and standard deviation are shown for each strain. The dotted line is the LOD at 20

CFU/ml. MC394 (*eutA*::*ermB*) cecal CFU were compared to the parent strain with a two-tailed *t* test. * indicates $p \leq 0.05$.

During the first 24 hours following inoculation, we collected fecal samples from 10 hamsters (5 hamsters per strain) to determine if and when C. *difficile* could be detected during the course of infection. We were able to detect CFU in the feces of the hamsters infected with MC394 (*eutA*::*ermB*) as early as 12 hours post-infection (Fig **2B**). We were unable to detect the parent strain until after 24 hours post-infection (data not shown). These data suggest that MC394 (*eutA*::*ermB*) either has an initial growth advantage in the host, or produces spores at an earlier time during infection. It was unexpected that the inability to utilize ETA would lead to potential growth advantage. To further evaluate the potential growth advantage of MC394 (*eutA*::*ermB*), we plated cecal contents to enumerate the *C. difficile* population present at the time of morbidity. In the cecal contents, there was no difference in the number of CFU present between the two strains (Fig **2C**). Because the mutant does not appear to have a growth advantage, we next examined effects of ETA metabolism on virulence factor production and sporulation in an attempt to explain the enhanced virulence of the *eutA* mutant.

Toxin production is not impacted by ethanolamine *in vitro*

C. difficile produces two large toxins, TcdA and TcdB, that are responsible for the majority of disease symptoms (6-8). Due to the increased virulence observed when hamsters were infected with a strain unable to utilize ETA, we decided to determine if toxin expression was altered by ETA and its metabolism. MC394 (*eutA*::*ermB*) and 630Δ*erm* were grown in liquid 70:30 medium supplemented with ETA. RNA was isolated at three different time points: logarithmic growth, mid stationary phase, and late stationary phase. We examined toxin expression and did not observe any significant changes between the

strains or in the presence of ETA (Fig **3A,B**). This indicates that ETA and its metabolism do not impact toxin expression under the conditions tested.

Immune activating colonization factors are not impacted by ethanolamine *in vitro*

C. difficile flagella and pilin are detected by the innate immune system and can elicit a response (65-68). Additionally, a connection between pilin expression and ETA has been reported in *Escherichia coli* O157:H7 (32). Due to the significant difference in the time to morbidity observed in hamster model, we decided to investigate if ETA or its metabolism could alter the expression of *pilA1* and *fliC*. Strains were grown in liquid 70:30 medium supplemented with ETA. We examined *pilA1* expression and observed no difference with and without ETA or between strains (Fig **4A**). When we examined *fliC* expression in the same conditions, we also saw no difference in expression between the strains or in the presence of ETA (Fig **4B**). Overall, these data demonstrate that *pilA1* and *fliC* expression are not altered by ETA or its metabolism under the conditions tested.

Sporulation is not altered by the presence of ethanolamine

Sporulation is an essential process for *C. difficile* to survive outside of the host gastrointestinal tract (20, 21). Prior work has indicated that degree of spore formation in the animal model can have an effect on the outcome of infection (25). Additionally, we detected *C. difficile* CFU in hamster feces at an earlier timepoint infection. Therefore, we evaluated if ETA and its metabolism had any impact on the process of sporulation *in vitro*. We investigated if the number of spores present in hamster cecal content was different depending on the strain. We treated the cecal sample with 28.5% ethanol to kill any

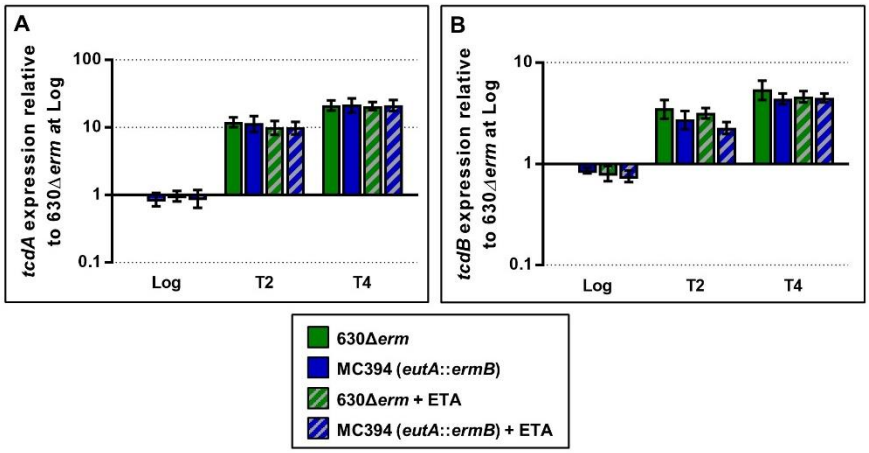

Figure 3. No change in toxin expression occurs in the presence of ethanolamine *in vitro*. qRT-PCR analysis of *tcdA* (A) and *tcdB* (B) expression in 630Δ*erm* and MC394 *(eutA::ermB)* grown in 70:30 liquid sporulation medium supplemented with 15 mM ETA. Samples for RNA isolation were collected during logarithmic growth (Log, OD_{600} of 0.5), two hours after the transition to stationary phase (T2, mid stationary), and four hours after the transition into stationary phase (T4, late stationary). The means and standard deviations of four biological replicates are shown. Data were analyzed with a two-way repeated measures ANOVA.

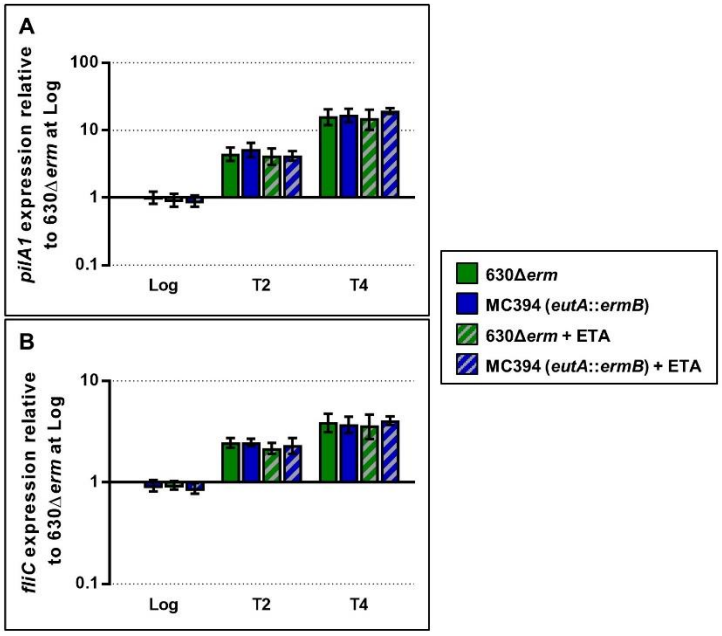

Figure 4. No changes in expression of the immune-activating colonization factors, *pilA1* and *fliC*, occur in the presence of ethanolamine. qRT-PCR analysis of *pilA1* (A) and *fliC* (B) expression in 630Δ*erm* and MC394 *(eutA::ermB)* grown in 70:30 liquid sporulation medium supplemented with 15 mM ETA. Samples for RNA isolation were collected during logarithmic growth (Log, OD_{600} of 0.5), two hours after the transition to stationary phase (T2, early stationary), and four hours after the transition into stationary phase (T4, late stationary). The means and standard deviations of four biological replicates are shown. Data were analyzed with a two-way repeated measures ANOVA.

vegetative cells and plated onto TCCFA plates. We noted no difference between the number of spores present in the cecal content of hamsters infected with MC394 (*eutA*::*ermB*) or 630Δ*erm* (Fig **S6**). This demonstrates that ETA and ETA metabolism do not have an effect on sporulation *in vivo* at time of death.

In addition to the *in vivo* study, we also examined the impact of ETA on sporulation *in vitro*. We grew MC394 (*eutA*::*ermB*) and 630Δ*erm* in 70:30 liquid medium and monitored the expression of *sigE* over time. SigE is a sporulation specific sigma factor, and its expression is linked with the progression of sporulation (69, 70). We observed no change in expression between the strains or in the presence of ETA (Fig **5**). Lastly, we examined if there was any change in sporulation on 70:30 agar. MC394 (*eutA*::*ermB*) and 630Δ*erm* were plated onto 70:30 plates supplemented with ETA. We examined sporulation by phase contrast microscopy and ethanol resistance assays. An examination of the micrographs showed no change in sporulation between strains or in the presence of ETA following a 24-hour incubation (Fig **S7**). The ethanol resistance assay did not show any difference in spore formation between the strains or in the presence of ETA (Table **3**). Overall, these data show that ETA and its metabolism do not have an effect on sporulation *in vivo* and *in vitro* at the timepoints tested.

DISCUSSION

ETA and its metabolism have been shown to provide an advantage to enteric pathogens in the host. For example, the ability to utilize ETA allows *Salmonella* to gain an advantage over the host microbiota (30, 35). Additionally, research into ETA metabolism has shown that EutR regulates not only the *eut* genes in *Escherichia coli*, but also the locus

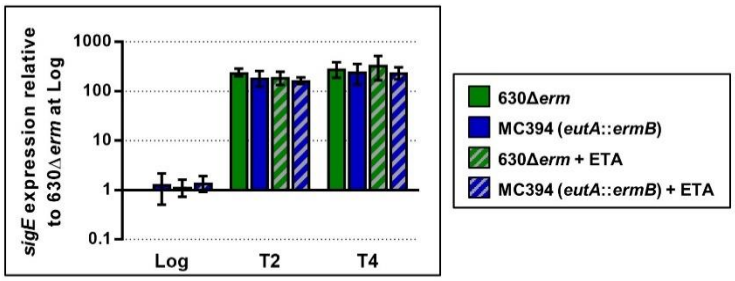

Figure 5. No change occurs in the expression of the sporulation-specific sigma factor, *sigE*, in the presence of ethanolamine. qRT-PCR analysis of *sigE* expression in 630Δ*erm* and MC394 *(eutA::ermB)* grown in 70:30 liquid sporulation medium supplemented with 15 mM ETA. Samples for RNA isolation were collected during logarithmic growth (Log, OD_{600} of 0.5), two hours after the transition to stationary phase (T2, early stationary), and four hours after the transition into stationary phase (T4, late stationary). The means and standard deviations of four biological replicates are shown. Data were analyzed with a two-way repeated measures ANOVA.

Table 3. Ethanol resistant spore formation

Growth Condition	630Δ*erm* [a,b]	MC394 (*eutA*::ermB) [a,b]	MC310 (*spo0A*::*ermB*) [a,b]
70:30 plate	9.09 ± 3.60%	9.34 ± 1.68%	0.00 ± 0.00%
+ 15 mM ETA	7.50 ± 2.06%	9.34 ± 1.68%	
+ 30 mM ETA HCl	7.94 ± 2.28%	11.06 ± 2.31%	

[a] The frequencies of ethanol resistant spore formation are shown ± the standard deviation.
[b] Data were analyzed by a two-way repeated measures ANOVA.

of enterocyte effacement (LEE) (36). Knowing the importance of ETA to bacterial pathogenesis in the gastrointestinal tract, we investigated the role of ETA metabolism in *C. difficile* pathogenesis.

Before we were able to address our main question of interest, we first had to demonstrate that *C. difficile* utilized ETA. We were able to disrupt *eutA*, and generate a polar mutation that altered the expression of the genes downstream (Fig **1A,** data not shown). We demonstrated that the *eut* cluster has increased expression in the presence of ETA (Fig **1B**, **S2**). This finding was in line with other studies investigating the regulation of *eut* clusters in both Gram-positives and Gram-negatives (33, 71-73). With our modified minimal medium studies, we were able to demonstrate that *C. difficile* can utilize ETA (Fig **1C**), and that the *eut* cluster does not appear to be under catabolite repression (Fig **S5**). While it would have been ideal to determine if *C. difficile* utilizes ETA as either as a carbon and/or a nitrogen source, due to the fastidious nature of *C. difficile,* we were unable to reduce the minimal media enough to test this (74, 75). Overall, we were able to establish that the *eut* cluster is responsible for ETA utilization in *C. difficile*.

After establishing that *C. difficile* utilizes ETA, we wanted to determine the role of ETA metabolism in the host. We hypothesized that we would see a virulence defect when hamsters were infected with MC394 (*eutA*::*ermB*), our mutant unable to utilize ETA. However, we instead found that the inability to utilize ETA makes *C. difficile* more virulent in the hamster model of infection (Fig **2A**). Our original hypothesis was further refuted when we were able to detect MC394 (*eutA*::*ermB*) CFU as early as 12 hours post infection. We were not able to detect the parent strain until 24 hours or later (Fig **2B**, data not shown). Instead of the predicted defect in growth, cecal contents for hamsters infected with the two

strains contained similar amounts of CFU, indicating no growth difference between the strains at the time of death (Fig **2C**). Overall, it is possible that the inability to utilize ETA may alter growth early in infection, but it does not impact the number of CFU that can be reached in the cecum at time of death.

We attempted to investigate why MC394 (*eutA*::*ermB*) was more virulent in the animal model, but studies *in vitro* did not yield any clear results. First, we investigated toxin expression, since the toxins are the main effectors of disease, and it is know that they are regulated predominantly by nutritional regulators (6, 16, 17). When we investigated toxin expression in the presence of ETA, we found no difference in expression (Fig **3A,B**). We had similar results when we investigated the expression of *pilA1* and *fliC* (Fig **4A,B**). Either ETA metabolism does not have an effect on virulence factor production, or our *in vitro* system does not accurately represent the host environment. More extensive studies examining toxin and colonization factor expression in different media types supplemented with ETA could address this concern.

Sporulation is an essential process for the survival of *C. difficile* in aerobic environments, and is a key component of *C. difficile* transmission (20). We investigated the effects of ETA and its metabolism on sporulation. We observed no difference in the number of ethanol resistant spores present in the cecal contents of infected hamsters post mortem (Fig **S6**). Additionally, *in vitro* tests examining sporulation through ethanol resistance assays and phase contrast microscopy demonstrated no difference in sporulation in the presence of ETA (Fig **5**, **S7**, **Table 3**). ETA and it metabolism do not appear to have an effect on *C. difficile* sporulation *in vitro* or *in vivo* at the timepoints investigated.

Overall, our original hypothesis was incorrect, the inability to utilize ETA did not cause a defect in the hamster model of infection. Based on this study, we put forth a new hypothesis, that ETA is utilized by *C. difficile*, and that the inability to utilize ETA alters the time frame of infection (Fig **6**). We propose that in the hamster model, mutants unable to utilize ETA run out of nutrient sources earlier in the course of infection, and begin to produce toxins and sporulate. The early production of toxins leads to earlier death in hamsters infected with the *eutA* mutant (Fig **6**). We do not suggest that toxins or other immune stimulating factors are increased above normal levels during infection, since we saw no effect on expression of these factors in the presence of ETA *in vitro*.

The relationship between the host and *C. difficile* is not fully elucidated. Recent studies, including ours, have begun to understand the nutritional relationship between the host, the resident microbiota, and *C. difficile* (25, 76, 77). Still, many questions remain surrounding our ETA study, such as: does ETA metabolism have a suppressive effect on infection? Does the inability to utilize ETA lead to early spore and toxin production in the hamster model? If and how could ETA impact toxin production? What role does ETA and its metabolism play in asymptomatic colonization? While more questions than answers remain, we have demonstrated that ETA is a nutrient source for *C. difficile* and that the *eut* cluster is responsible for its metabolism. Additionally, we have shown that ETA metabolism has an important, if not fully elucidated, role in *C. difficile* pathogenesis. This is an important step in understanding how the nutritional state of the host can alter the pathogenesis of *C. difficile*.

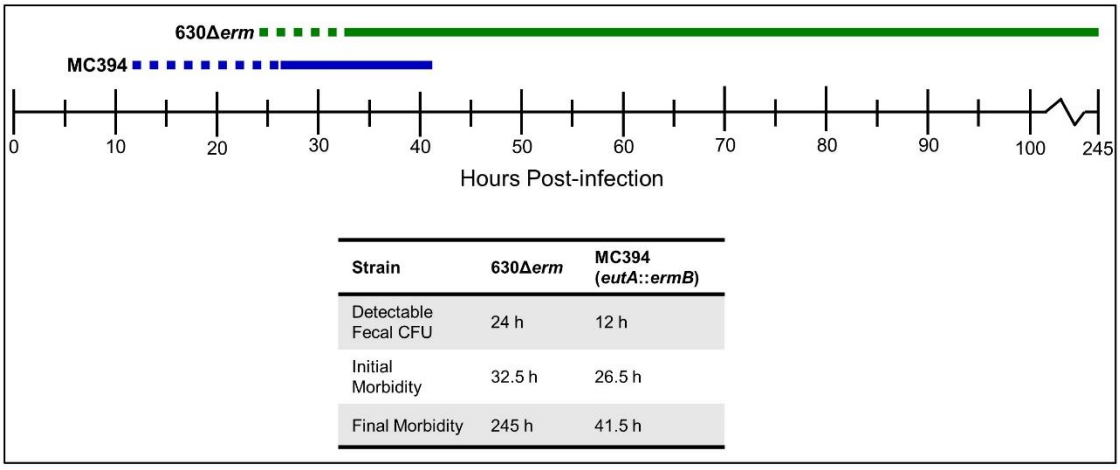

Strain	630Δ*erm*	MC394 (*eutA*::*ermB*)
Detectable Fecal CFU	24 h	12 h
Initial Morbidity	32.5 h	26.5 h
Final Morbidity	245 h	41.5 h

Figure 6. Timeline schematic of hamster infection with 630Δ*erm* and MC394 (*eutA::ermB*). Hamsters were inoculated with approximately 5000 spores of 630Δ*erm* (n=17) and MC394 (*eutA*::*ermB*) (n=17) at hour zero. Dotted lines indicate when *C. difficile* CFU were first detected in fecal samples up to the first morbidity event. Solid lines indicate the span of time between the first and last morbidity event for each strain. Hamsters infected with MC394 (*eutA*::*ermB*) had an altered time course of infection.

ACKNOWLEDGEMENTS

We thank members of the McBride lab, Charles Moran, Joanna Goldberg, David Weiss, and Philip Rather for their helpful suggestions and discussions during the course of this work. We also thank the Institute for Quantitative Theory and Methods Statistics Help Desk at Emory University for their guidance in using R.

FUNDING INFORMATION

This research was supported by the U.S. National Institutes of Health through research grants DK087763, DK101870, AI109526 and AI116933 to S.M.M., and T32 AI106699 to K.L.N. The content of this manuscript is solely the responsibility of the authors and does not necessarily reflect the official views of the National Institutes of Health.

REFERENCES

1. **Rivera EV, Woods S.** 2003. Prevalence of asymptomatic Clostridium difficile colonization in a nursing home population: a cross-sectional study. J Gend Specif Med **6:**27-30.
2. **Bartlett JG, Chang TW, Moon N, Onderdonk AB.** 1978. Antibiotic-induced lethal enterocolitis in hamsters: studies with eleven agents and evidence to support the pathogenic role of toxin-producing Clostridia. Am J Vet Res **39:**1525-1530.
3. **Bartlett JG, Moon N, Chang TW, Taylor N, Onderdonk AB.** 1978. Role of Clostridium difficile in antibiotic-associated pseudomembranous colitis. Gastroenterology **75:**778-782.
4. **Dubberke ER, Olsen MA.** 2012. Burden of Clostridium difficile on the healthcare system. Clin Infect Dis **55 Suppl 2:**S88-92.

5. **Magill SS, Edwards JR, Bamberg W, Beldavs ZG, Dumyati G, Kainer MA, Lynfield R, Maloney M, McAllister-Hollod L, Nadle J, Ray SM, Thompson DL, Wilson LE, Fridkin SK.** 2014. Multistate Point-Prevalence Survey of Health Care–Associated Infections. New England Journal of Medicine **370:**1198-1208.

6. **Kuehne SA, Cartman ST, Heap JT, Kelly ML, Cockayne A, Minton NP.** 2010. The role of toxin A and toxin B in *Clostridium difficile* infection. Nature **467:**711-713.

7. **Lyerly DM, Krivan HC, Wilkins TD.** 1988. Clostridium difficile: its disease and toxins. Clin Microbiol Rev **1:**1-18.

8. **Lyerly DM, Saum KE, MAcDONALD DK, Wilkins TD.** 1985. Effects of *Clostridium difficile* toxins given intragastrically to animals. Infection and immunity **47:**349-352.

9. **Braun V, Hundsberger T, Leukel P, Sauerborn M, von Eichel-Streiber C.** 1996. Definition of the single integration site of the pathogenicity locus in Clostridium difficile. Gene **181:**29-38.

10. **Just I, Selzer J, Wilm M, von Eichel-Streiber C, Mann M, Aktories K.** 1995. Glucosylation of Rho proteins by Clostridium difficile toxin B.

11. **Just I, Wilm M, Selzer J, Rex G, von Eichel-Streiber C, Mann M, Aktories K.** 1995. The enterotoxin from Clostridium difficile (ToxA) monoglucosylates the Rho proteins. Journal of Biological Chemistry **270:**13932-13936.

12. **Qa'Dan M, Ramsey M, Daniel J, Spyres LM, Safiejko-Mroczka B, Ortiz-Leduc W, Ballard JD.** 2002. Clostridium difficile toxin B activates dual caspase-

dependent and caspase-independent apoptosis in intoxicated cells. Cellular microbiology **4:**425-434.

13. **He D, Hagen S, Pothoulakis C, Chen M, Medina N, Warny M, LaMont J.** 2000. Clostridium difficile toxin A causes early damage to mitochondria in cultured cells. Gastroenterology **119:**139-150.

14. **Brito GA, Fujji J, Carneiro-Filho BA, Lima AA, Obrig T, Guerrant RL.** 2002. Mechanism of Clostridium difficile toxin A–induced apoptosis in T84 cells. Journal of Infectious Diseases **186:**1438-1447.

15. **Kuehne SA, Cartman ST, Minton NP.** 2011. Both, toxin A and toxin B, are important in *Clostridium difficile* infection. Gut Microbes **2:**252-255.

16. **Antunes A, Martin-Verstraete I, Dupuy B.** 2011. CcpA-mediated repression of Clostridium difficile toxin gene expression. Mol Microbiol **79:**882-899.

17. **Dineen SS, Villapakkam AC, Nordman JT, Sonenshein AL.** 2007. Repression of Clostridium difficile toxin gene expression by CodY. Mol Microbiol **66:**206-219.

18. **Dineen SS, McBride SM, Sonenshein AL.** 2010. Integration of metabolism and virulence by Clostridium difficile CodY. J Bacteriol **192:**5350-5362.

19. **Antunes A, Camiade E, Monot M, Courtois E, Barbut F, Sernova NV, Rodionov DA, Martin-Verstraete I, Dupuy B.** 2012. Global transcriptional control by glucose and carbon regulator CcpA in Clostridium difficile. Nucleic Acids Res **40:**10701-10718.

20. **Deakin LJ, Clare S, Fagan RP, Dawson LF, Pickard DJ, West MR, Wren BW, Fairweather NF, Dougan G, Lawley TD.** 2012. The *Clostridium difficile spo0A* gene is a persistence and transmission factor. Infect Immun **80:**2704-2711.

21. **Jump RL, Pultz MJ, Donskey CJ.** 2007. Vegetative Clostridium difficile survives in room air on moist surfaces and in gastric contents with reduced acidity: a potential mechanism to explain the association between proton pump inhibitors and C. difficile-associated diarrhea? Antimicrobial agents and chemotherapy **51:**2883-2887.

22. **Rosenbusch KE, Bakker D, Kuijper EJ, Smits WK.** 2012. *C. difficile* 630Delta*erm* Spo0A regulates sporulation, but does not contribute to toxin production, by direct high-affinity binding to target DNA. PLoS One **7:**e48608.

23. **Paredes CJ, Alsaker KV, Papoutsakis ET.** 2005. A comparative genomic view of clostridial sporulation and physiology. Nat Rev Microbiol **3:**969-978.

24. **Underwood S, Guan S, Vijayasubhash V, Baines SD, Graham L, Lewis RJ, Wilcox MH, Stephenson K.** 2009. Characterization of the sporulation initiation pathway of *Clostridium difficile* and its role in toxin production. J Bacteriol **191:**7296-7305.

25. **Edwards AN, Nawrocki KL, McBride SM.** 2014. Conserved oligopeptide permeases modulate sporulation initiation in *Clostridium difficile*. Infect Immun **82:**4276-4291.

26. **Nawrocki KL, Edwards AN, Daou N, Bouillaut L, McBride SM.** 2016. CodY-Dependent Regulation of Sporulation in Clostridium difficile. J Bacteriol **198:**2113-2130.

27. **Larson TJ, Ehrmann M, Boos W.** 1983. Periplasmic glycerophosphodiester phosphodiesterase of Escherichia coli, a new enzyme of the glp regulon. J Biol Chem **258:**5428-5432.

28. **Zhang Y-M, Rock CO.** 2008. Membrane lipid homeostasis in bacteria. Nat Rev Micro **6:**222-233.

29. **van Meer G, Voelker DR, Feigenson GW.** 2008. Membrane lipids: where they are and how they behave. Nat Rev Mol Cell Biol **9:**112-124.

30. **Anderson CJ, Clark DE, Adli M, Kendall MM.** 2015. Ethanolamine signaling promotes Salmonella niche recognition and adaptation during infection. PLoS Pathog **11:**e1005278.

31. **Bertin Y, Girardeau JP, Chaucheyras-Durand F, Lyan B, Pujos-Guillot E, Harel J, Martin C.** 2011. Enterohaemorrhagic Escherichia coli gains a competitive advantage by using ethanolamine as a nitrogen source in the bovine intestinal content. Environ Microbiol **13:**365-377.

32. **Gonyar LA, Kendall MM.** 2014. Ethanolamine and choline promote expression of putative and characterized fimbriae in enterohemorrhagic Escherichia coli O157:H7. Infect Immun **82:**193-201.

33. **Kendall MM, Gruber CC, Parker CT, Sperandio V.** 2012. Ethanolamine controls expression of genes encoding components involved in interkingdom signaling and virulence in enterohemorrhagic Escherichia coli O157:H7. MBio **3**.

34. **Srikumar S, Fuchs TM.** 2011. Ethanolamine utilization contributes to proliferation of Salmonella enterica serovar Typhimurium in food and in nematodes. Appl Environ Microbiol **77:**281-290.

35. **Thiennimitr P, Winter SE, Winter MG, Xavier MN, Tolstikov V, Huseby DL, Sterzenbach T, Tsolis RM, Roth JR, Baumler AJ.** 2011. Intestinal inflammation allows Salmonella to use ethanolamine to compete with the microbiota. Proc Natl Acad Sci U S A **108:**17480-17485.

36. **Luzader DH, Clark DE, Gonyar LA, Kendall MM.** 2013. EutR is a direct regulator of genes that contribute to metabolism and virulence in enterohemorrhagic Escherichia coli O157: H7. Journal of bacteriology **195:**4947-4953.

37. **Bradbeer C.** 1965. The clostridial fermentations of choline and ethanolamine. 1. Preparation and properties of cell-free extracts. J Biol Chem **240:**4669-4674.

38. **Bradbeer C.** 1965. The clostridial fermentations of choline and ethanolamine. II. Requirement for a cobamide coenzyme by an ethanolamine deaminase. J Biol Chem **240:**4675-4681.

39. **Roof DM, Roth JR.** 1988. Ethanolamine utilization in Salmonella typhimurium. J Bacteriol **170:**3855-3863.

40. **Stojiljkovic I, Baumler AJ, Heffron F.** 1995. Ethanolamine utilization in Salmonella typhimurium: nucleotide sequence, protein expression, and mutational analysis of the cchA cchB eutE eutJ eutG eutH gene cluster. J Bacteriol **177:**1357-1366.

41. **Tsoy O, Ravcheev D, Mushegian A.** 2009. Comparative genomics of ethanolamine utilization. J Bacteriol **191:**7157-7164.

42. **Pitts AC, Tuck LR, Faulds-Pain A, Lewis RJ, Marles-Wright J.** 2012. Structural insight into the Clostridium difficile ethanolamine utilisation microcompartment. PLoS One **7:**e48360.

43. **Smith CJ, Markowitz SM, Macrina FL.** 1981. Transferable tetracycline resistance in Clostridium difficile. Antimicrob Agents Chemother **19:**997-1003.

44. **Sorg JA, Sonenshein AL.** 2008. Bile salts and glycine as cogerminants for Clostridium difficile spores. J Bacteriol **190:**2505-2512.

45. **Putnam EE, Nock AM, Lawley TD, Shen A.** 2013. SpoIVA and SipL are Clostridium difficile spore morphogenetic proteins. J Bacteriol **195:**1214-1225.

46. **Bouillaut L, McBride SM, Sorg JA.** 2011. Genetic manipulation of Clostridium difficile. Curr Protoc Microbiol **Chapter 9:**Unit 9A 2.

47. **Karlsson S, Burman LG, Akerlund T.** 1999. Suppression of toxin production in Clostridium difficile VPI 10463 by amino acids. Microbiology **145 (Pt 7):**1683-1693.

48. **Luria SE, Burrous JW.** 1957. Hybridization between *Escherichia coli* and *Shigella.* J Bacteriol **74:**461-476.

49. **Purcell EB, McKee RW, McBride SM, Waters CM, Tamayo R.** 2012. Cyclic diguanylate inversely regulates motility and aggregation in Clostridium difficile. J Bacteriol **194:**3307-3316.

50. **McBride SM, Sonenshein AL.** 2011. The dlt operon confers resistance to cationic antimicrobial peptides in Clostridium difficile. Microbiology **157:**1457-1465.

51. **Harju S, Fedosyuk H, Peterson KR.** 2004. Rapid isolation of yeast genomic DNA: Bust n' Grab. BMC Biotechnol **4:**8.

52. **Edwards AN, Tamayo R, McBride SM.** 2016. A novel regulator controls Clostridium difficile sporulation, motility and toxin production. Mol Microbiol **100:**954-971.

53. **Saujet L, Pereira FC, Serrano M, Soutourina O, Monot M, Shelyakin PV, Gelfand MS, Dupuy B, Henriques AO, Martin-Verstraete I.** 2013. Genome-Wide Analysis of Cell Type-Specific Gene Transcription during Spore Formation in Clostridium difficile. PLoS Genet **9:**e1003756.

54. **Childress KO, Edwards AN, Nawrocki KL, Woods EC, Anderson SE, McBride SM.** 2016. The Phosphotransfer Protein CD1492 Represses Sporulation Initiation in Clostridium difficile. Infect Immun doi:10.1128/IAI.00735-16.

55. **Schmittgen TD, Livak KJ.** 2008. Analyzing real-time PCR data by the comparative C(T) method. Nat Protoc **3:**1101-1108.

56. **Woods EC, Nawrocki KL, Suarez JM, McBride SM.** 2016. The Clostridium difficile Dlt pathway is controlled by the ECF sigma factor, sigmaV, in response to lysozyme. Infect Immun doi:10.1128/IAI.00207-16.

57. **Wilson KH, Silva J, Fekety FR.** 1981. Suppression of Clostridium difficile by normal hamster cecal flora and prevention of antibiotic-associated cecitis. Infect Immun **34:**626-628.

58. **George WL, Sutter VL, Citron D, Finegold SM.** 1979. Selective and differential medium for isolation of Clostridium difficile. J Clin Microbiol **9:**214-219.

59. **Fox KA, Ramesh A, Stearns JE, Bourgogne A, Reyes-Jara A, Winkler WC, Garsin DA.** 2009. Multiple posttranscriptional regulatory mechanisms partner to

control ethanolamine utilization in Enterococcus faecalis. Proc Natl Acad Sci U S A **106:**4435-4440.

60. **Ramesh A, DebRoy S, Goodson JR, Fox KA, Faz H, Garsin DA, Winkler WC.** 2012. The mechanism for RNA recognition by ANTAR regulators of gene expression. PLoS Genet **8:**e1002666.

61. **Cartman ST, Kelly ML, Heeg D, Heap JT, Minton NP.** 2012. Precise manipulation of the Clostridium difficile chromosome reveals a lack of association between the tcdC genotype and toxin production. Appl Environ Microbiol **78:**4683-4690.

62. **Görke B, Stülke J.** 2008. Carbon catabolite repression in bacteria: many ways to make the most out of nutrients. Nature Reviews Microbiology **6:**613-624.

63. **Winter SE, Thiennimitr P, Winter MG, Butler BP, Huseby DL, Crawford RW, Russell JM, Bevins CL, Adams LG, Tsolis RM, Roth JR, Baumler AJ.** 2010. Gut inflammation provides a respiratory electron acceptor for Salmonella. Nature **467:**426-429.

64. **Snoeck V, Goddeeris B, Cox E.** 2005. The role of enterocytes in the intestinal barrier function and antigen uptake. Microbes Infect **7:**997-1004.

65. **Pechine S, Collignon A.** 2016. Immune responses induced by Clostridium difficile. Anaerobe doi:10.1016/j.anaerobe.2016.04.014.

66. **Pechine S, Gleizes A, Janoir C, Gorges-Kergot R, Barc MC, Delmee M, Collignon A.** 2005. Immunological properties of surface proteins of Clostridium difficile. J Med Microbiol **54:**193-196.

67. **Pechine S, Janoir C, Boureau H, Gleizes A, Tsapis N, Hoys S, Fattal E, Collignon A.** 2007. Diminished intestinal colonization by Clostridium difficile and immune response in mice after mucosal immunization with surface proteins of Clostridium difficile. Vaccine **25:**3946-3954.

68. **Maldarelli GA, De Masi L, Rosenvinge EC, Carter M, Donnenberg MS.** 2014. Identification, immunogenicity, and cross-reactivity of type IV pilin and pilin-like proteins from Clostridium difficile. Pathogens and disease **71:**302-314.

69. **Fimlaid KA, Bond JP, Schutz KC, Putnam EE, Leung JM, Lawley TD, Shen A.** 2013. Global Analysis of the Sporulation Pathway of *Clostridium difficile*. PLoS Genet **9:**e1003660.

70. **Pereira FC, Saujet L, Tome AR, Serrano M, Monot M, Couture-Tosi E, Martin-Verstraete I, Dupuy B, Henriques AO.** 2013. The Spore Differentiation Pathway in the Enteric Pathogen *Clostridium difficile*. PLoS Genet **9:**e1003782.

71. **Garsin DA.** 2010. Ethanolamine utilization in bacterial pathogens: roles and regulation. Nat Rev Micro **8:**290-295.

72. **Del Papa MF, Perego M.** 2008. Ethanolamine activates a sensor histidine kinase regulating its utilization in Enterococcus faecalis. J Bacteriol **190:**7147-7156.

73. **Roof DM, Roth JR.** 1992. Autogenous regulation of ethanolamine utilization by a transcriptional activator of the eut operon in Salmonella typhimurium. J Bacteriol **174:**6634-6643.

74. **Karasawa T, Ikoma S, Yamakawa K, Nakamura S.** 1995. A defined growth medium for Clostridium difficile. Microbiology **141:**371-375.

75. **Yamakawa K, Kamiya S, Meng X, Karasawa T, Nakamura S.** 1994. Toxin production by Clostridium difficile in a defined medium with limited amino acids. Journal of medical microbiology **41:**319-323.

76. **Ferreyra JA, Wu KJ, Hryckowian AJ, Bouley DM, Weimer BC, Sonnenburg JL.** 2014. Gut microbiota-produced succinate promotes C. difficile infection after antibiotic treatment or motility disturbance. Cell host & microbe **16:**770-777.

77. **Ng KM, Ferreyra JA, Higginbottom SK, Lynch JB, Kashyap PC, Gopinath S, Naidu N, Choudhury B, Weimer BC, Monack DM.** 2013. Microbiota-liberated host sugars facilitate post-antibiotic expansion of enteric pathogens. Nature **502:**96-99.

78. **Hussain HA, Roberts AP, Mullany P.** 2005. Generation of an erythromycin-sensitive derivative of Clostridium difficile strain 630 (630Δerm) and demonstration that the conjugative transposon Tn916ΔE enters the genome of this strain at multiple sites. Journal of Medical Microbiology **54:**137-141.

79. **Ho TD, Ellermeier CD.** 2011. PrsW is required for colonization, resistance to antimicrobial peptides, and expression of extracytoplasmic function sigma factors in Clostridium difficile. Infect Immun **79:**3229-3238.

80. **Thomas CM, Smith CA.** 1987. Incompatibility group P plasmids: genetics, evolution, and use in genetic manipulation. Annual Reviews in Microbiology **41:**77-101.

81. **McBride SM, Sonenshein AL.** 2011. Identification of a genetic locus responsible for antimicrobial peptide resistance in Clostridium difficile. Infect Immun **79:**167-176.

82. **McKee RW, Mangalea MR, Purcell EB, Borchardt EK, Tamayo R.** 2013. The second messenger cyclic Di-GMP regulates Clostridium difficile toxin production by controlling expression of sigD. J Bacteriol **195:**5174-5185.

83. **Purcell EB, McKee RW, Bordeleau E, Burrus V, Tamayo R.** 2016. Regulation of Type IV Pili Contributes to Surface Behaviors of Historical and Epidemic Strains of Clostridium difficile. Journal of bacteriology **198:**565-577.

CHAPTER 4

Discussion

Clostridium difficile is now the leading cause of health-care associated infections in the United States (1, 2). Approximately $4.8 billion is spent annually in the United States to address the *C. difficile* disease in health-care facilities (3). A major issue in the healthcare-associated setting is the spore morphotype of *C. difficile*. *C. difficile* spores are intrinsically resistant to many disinfectants and antibiotics (4-6). The production of viable spores is essential for the transmission and survival of *C. difficile*. *C. difficile* spores are orally ingested and then germinate in the presence of bile salts in the host gastrointestinal tract (7, 8). Following germination, toxins are produced that cause disease symptoms in the gastrointestinal tract (9, 10). These toxins are the main effectors of disease (11, 12). Prior to exiting the intestine, vegetative cells must undergo sporulation in order to survive outside the host (13). Through the production of a resilient spore, this obligate anaerobe is able to survive and persist in the aerobic environment. Even though the process of sporulation is essential for survival, the signals that trigger *C. difficile* vegetative cells to differentiate into a spore are unknown. Overall this work focused on understanding how nutritional status of the cell alters sporulation and pathogenesis in *C. difficile*.

CodY-dependent Regulation of Sporulation in *Clostridium difficile*

To further evaluate the role of nutritional state in sporulation in *C. difficile*, we investigated the effect of CodY on the process of sporulation. CodY is a highly conserved global nutritional regulator found in Gram-positive organisms (14-18). In many Gram-positive bacteria, CodY regulates a wide range of genes involved in secondary metabolism,

nutrient acquisition, sporulation, and virulence (14-17, 19-30). CodY functions as transcriptional repressor in nutrient rich conditions when bound to GTP or branched chain amino acids, making CodY a direct link between transcription and the metabolite pool in the cell. In *C. difficile*, CodY has been described as a regulator of toxin and amino acid synthesis (31, 32). These initial CodY studies were not performed under sporulating conditions. This limited the detection of sporulation specific genes. In conjunction with prior work on Opp and App, we evaluated the effect of CodY on sporulation in *C. difficile*.

We disrupted *codY* in two different *C. difficile* strains, a historical and an epidemic isolate, and evaluated spore production. The disruption of *codY* in the historical lab strain only caused a marginal two-fold increase in sporulation frequency when compared to the parent strain. In contrast, sporulation frequency was increased in the epidemic *codY* mutant by ~1,400-fold when compared to the parent strain. These data indicate that CodY is a negative regulator of sporulation in *C. difficile*, but that CodY-dependent effects on sporulation may differ between strains. Additionally, we examined if CodY regulates any known effectors of sporulation. We demonstrated that CodY regulates the activity of the *oppB* promoter region using promoter fusion studies. Overall, we were able to show that CodY is negative regulator of sporulation in *C. difficile* that potentially mediates the effect Opp has on sporulation.

This work furthered the understanding of the relationship between the nutritional state of the cell and sporulation. More experiments, such as RNA-seq, could be performed to gain greater perspective on the CodY regulon under sporulating conditions. Additionally, experiments should be performed to determine how the CodY-dependent response to the nutritional state varies between historical and epidemic isolates.

The Impact of Ethanolamine Utilization on Pathogenesis of *Clostridium difficile*

Ethanolamine is a common gastrointestinal metabolite. It can be derived from phosphatidylethanolamine, an abundant phospholipid present in cellular membranes (33-35). Many studies have connected ethanolamine utilization to pathogenesis in a variety of gastrointestinal pathogens (36-41). Ethanolamine can provide a growth advantage to invading pathogens over the host microbiota. Additionally, it has been shown that ethanolamine can also act as a direct single for niche recognition and virulence factor production (36-39, 41, 42). Through sequence analysis, we identified an ethanolamine utilization gene cluster in *C. difficile*. We hypothesized that ethanolamine metabolism would be important for *C. difficile* in the host environment, and that a mutant unable to utilize ethanolamine would be at a disadvantage in the host.

We insertionally disrupted *eutA*, which encodes for an ammonia lyase reactivating factor; this mutation was polar, decreasing expression of the downstream *eut* genes. We verified with minimal medium growth curves that *C. difficile* utilizes ethanolamine. We evaluated the role of ethanolamine metabolism in the hamster model of infection. Hamsters infected with the ethanolamine metabolism mutant succumbed to infection at an earlier time than those infected with the parent strain. Additionally, we were able to enumerate CFU from fecal samples from hamsters infected with the ethanolamine metabolism mutant at an earlier timepoint in infection. These data suggest that ethanolamine metabolism is important in the host and potentially delays the onset of disease. These results were unexpected and led to revision of our hypothesis. Therefore, we now hypothesize that the ethanolamine metabolism mutant experiences starvation-like conditions at an earlier

timepoint during infection because it cannot utilize ethanolamine. As the ethanolamine mutant begins to starve in the host, toxin is produced and a portion of the population undergoes sporulation. Toxin production acts as a means to gain more nutrients from the host. The induction of sporulation is a bet-hedging mechanism that safeguards a portion of the population until growth conditions become more favorable.

Overall this work demonstrated the importance of ethanolamine and its metabolism during *C. difficile* infection. Additional hamster studies could be performed to verify that sporulation is initiated earlier in infection when *C. difficile* is unable to utilize ethanolamine. Toxin ELISAs could performed on fecal and cecal content of hamsters infected with the ethanolamine utilization mutant. This would further evaluate the timeline of disease and determine if toxin production is influenced by ethanolamine and its metabolism.

Overall Conclusions

In conclusion, we have examined the relationship between nutritional state, pathogenesis, and sporulation in *C. difficile*. First, a potential link between nutritional state and sporulation was demonstrated in our lab. The oligopeptide permeases, Opp and App, have an inhibitory effect on sporulation in *C. difficile*. Since there is no likely quorum-signaling peptide candidate encoded by *C. difficile*, we hypothesize that these permeases facilitate the transport of peptides into the cell. This action supplements the intracellular metabolite pool and indirectly inhibits sporulation. Additionally, we demonstrated that the process of sporulation is linked to nutritional state by CodY, a global nutritional regulator. The direct mechanism of how CodY negatively regulates sporulation is unclear. Lastly, we

investigated the role of ethanolamine and its metabolism on sporulation and pathogenesis in *C. difficile*. *In vitro* results examining sporulation and toxin expression in the presence of ethanolamine indicated that ethanolamine and its metabolism had no effect. In contrast, the *in vivo* results suggest that ethanolamine and its metabolism may have an effect on the timing of sporulation and toxin production during infection. Overall, we concluded that *C. difficile* utilizes ethanolamine and that ethanolamine and its metabolism play an important, if undetermined, role in *C. difficile* pathogenesis. Collectively, these results shed light onto the role of cellular nutrition on pathogenesis and sporulation in *C. difficile*. Further investigations into how the processes of sporulation and pathogenesis are impacted by nutrition may ultimately lead to the development of novel therapeutics that can limit sporulation and pathogenesis of *C. difficile*.

REFERENCES

1. **Magill SS, Edwards JR, Bamberg W, Beldavs ZG, Dumyati G, Kainer MA, Lynfield R, Maloney M, McAllister-Hollod L, Nadle J, Ray SM, Thompson DL, Wilson LE, Fridkin SK.** 2014. Multistate Point-Prevalence Survey of Health Care–Associated Infections. New England Journal of Medicine **370:**1198-1208.
2. **Miller BA, Chen LF, Sexton DJ, Anderson DJ.** 2011. Comparison of the burdens of hospital-onset, healthcare facility-associated *Clostridium difficile* Infection and of healthcare-associated infection due to methicillin-resistant Staphylococcus aureus in community hospitals. Infect Control Hosp Epidemiol **32:**387-390.
3. **Lessa FC, Gould CV, McDonald LC.** 2012. Current status of *Clostridium difficile* infection epidemiology. Clin Infect Dis **55 Suppl 2:**S65-70.

4. **Edwards AN, Karim ST, Pascual RA, Jowhar LM, Anderson SE, McBride SM.** 2016. Chemical and Stress Resistances of *Clostridium difficile* Spores and Vegetative Cells. Frontiers in Microbiology **7:**1698.

5. **Baines SD, O'Connor R, Saxton K, Freeman J, Wilcox MH.** 2009. Activity of vancomycin against epidemic *Clostridium difficile* strains in a human gut model. J Antimicrob Chemother **63:**520-525.

6. **Ali S, Moore G, Wilson AP.** 2011. Spread and persistence of *Clostridium difficile* spores during and after cleaning with sporicidal disinfectants. J Hosp Infect **79:**97-98.

7. **Giel JL, Sorg JA, Sonenshein AL, Zhu J.** 2010. Metabolism of bile salts in mice influences spore germination in *Clostridium difficile*. PLoS One **5:**e8740.

8. **Sorg JA, Sonenshein AL.** 2008. Bile salts and glycine as cogerminants for *Clostridium difficile* spores. J Bacteriol **190:**2505-2512.

9. **Lyerly DM, Krivan HC, Wilkins TD.** 1988. *Clostridium difficile*: its disease and toxins. Clin Microbiol Rev **1:**1-18.

10. **Voth DE, Ballard JD.** 2005. *Clostridium difficile* toxins: mechanism of action and role in disease. Clin Microbiol Rev **18:**247-263.

11. **Kuehne SA, Cartman ST, Heap JT, Kelly ML, Cockayne A, Minton NP.** 2010. The role of toxin A and toxin B in *Clostridium difficile* infection. Nature **467:**711-713.

12. **Kuehne SA, Cartman ST, Minton NP.** 2011. Both, toxin A and toxin B, are important in *Clostridium difficile* infection. Gut Microbes **2:**252-255.

13. **Deakin LJ, Clare S, Fagan RP, Dawson LF, Pickard DJ, West MR, Wren BW, Fairweather NF, Dougan G, Lawley TD.** 2012. The *Clostridium difficile spo0A* gene is a persistence and transmission factor. Infect Immun **80:**2704-2711.

14. **Bennett HJ, Pearce DM, Glenn S, Taylor CM, Kuhn M, Sonenshein AL, Andrew PW, Roberts IS.** 2007. Characterization of *relA* and *codY* mutants of *Listeria monocytogenes*: identification of the CodY regulon and its role in virulence. Mol Microbiol **63:**1453-1467.

15. **Chateau A, van Schaik W, Joseph P, Handke LD, McBride SM, Smeets FM, Sonenshein AL, Fouet A.** 2013. Identification of CodY targets in *Bacillus anthracis* by genome-wide in vitro binding analysis. J Bacteriol **195:**1204-1213.

16. **Majerczyk CD, Dunman PM, Luong TT, Lee CY, Sadykov MR, Somerville GA, Bodi K, Sonenshein AL.** 2010. Direct targets of CodY in *Staphylococcus aureus*. J Bacteriol **192:**2861-2877.

17. **Pohl K, Francois P, Stenz L, Schlink F, Geiger T, Herbert S, Goerke C, Schrenzel J, Wolz C.** 2009. CodY in *Staphylococcus aureus*: a Regulatory Link between Metabolism and Virulence Gene Expression. Journal of Bacteriology **191:**2953-2963.

18. **Hendriksen WT, Bootsma HJ, Estevão S, Hoogenboezem T, De Jong A, De Groot R, Kuipers OP, Hermans PW.** 2008. CodY of *Streptococcus pneumoniae*: link between nutritional gene regulation and colonization. Journal of bacteriology **190:**590-601.

19. **Slack FJ, Mueller JP, Strauch MA, Mathiopoulos C, Sonenshein AL.** 1991. Transcriptional regulation of a *Bacillus subtilis* dipeptide transport operon. Mol Microbiol **5:**1915-1925.

20. **Slack FJ, Serror P, Joyce E, Sonenshein AL.** 1995. A gene required for nutritional repression of the *Bacillus subtilis* dipeptide permease operon. Molecular microbiology **15:**689-702.

21. **Sonenshein AL.** 2005. CodY, a global regulator of stationary phase and virulence in Gram-positive bacteria. Curr Opin Microbiol **8:**203-207.

22. **Belitsky BR, Sonenshein AL.** 2008. Genetic and biochemical analysis of CodY-binding sites in *Bacillus subtilis*. J Bacteriol **190:**1224-1236.

23. **Guedon E, Serror P, Ehrlich SD, Renault P, Delorme C.** 2001. Pleiotropic transcriptional repressor CodY senses the intracellular pool of branched-chain amino acids in *Lactococcus lactis*. Mol Microbiol **40:**1227-1239.

24. **Majerczyk CD, Sadykov MR, Luong TT, Lee C, Somerville GA, Sonenshein AL.** 2008. *Staphylococcus aureus* CodY negatively regulates virulence gene expression. J Bacteriol **190:**2257-2265.

25. **Karlsson S, Burman LG, Akerlund T.** 2008. Induction of toxins in *Clostridium difficile* is associated with dramatic changes of its metabolism. Microbiology **154:**3430-3436.

26. **Dupuy B, Sonenshein AL.** 1998. Regulated transcription of *Clostridium difficile* toxin genes. Mol Microbiol **27:**107-120.

27. **Ratnayake-Lecamwasam M, Serror P, Wong KW, Sonenshein AL.** 2001. *Bacillus subtilis* CodY represses early-stationary-phase genes by sensing GTP levels. Genes Dev **15:**1093-1103.

28. **Handke LD, Shivers RP, Sonenshein AL.** 2008. Interaction of *Bacillus subtilis* CodY with GTP. J Bacteriol **190:**798-806.

29. **Shivers RP, Sonenshein AL.** 2004. Activation of the *Bacillus subtilis* global regulator CodY by direct interaction with branched-chain amino acids. Molecular Microbiology **53:**599-611.

30. **Li J, Ma M, Sarker MR, McClane BA.** 2013. CodY is a global regulator of virulence-associated properties for *Clostridium perfringens* type D strain CN3718. MBio **4:**e00770-00713.

31. **Dineen SS, McBride SM, Sonenshein AL.** 2010. Integration of metabolism and virulence by *Clostridium difficile* CodY. J Bacteriol **192:**5350-5362.

32. **Dineen SS, Villapakkam AC, Nordman JT, Sonenshein AL.** 2007. Repression of *Clostridium difficile* toxin gene expression by CodY. Mol Microbiol **66:**206-219.

33. **Larson TJ, Ehrmann M, Boos W.** 1983. Periplasmic glycerophosphodiester phosphodiesterase of *Escherichia coli*, a new enzyme of the glp regulon. J Biol Chem **258:**5428-5432.

34. **Zhang Y-M, Rock CO.** 2008. Membrane lipid homeostasis in bacteria. Nat Rev Micro **6:**222-233.

35. **van Meer G, Voelker DR, Feigenson GW.** 2008. Membrane lipids: where they are and how they behave. Nat Rev Mol Cell Biol **9:**112-124.

36. **Anderson CJ, Clark DE, Adli M, Kendall MM.** 2015. Ethanolamine signaling promotes Salmonella niche recognition and adaptation during infection. PLoS Pathog **11:**e1005278.

37. **Bertin Y, Girardeau JP, Chaucheyras-Durand F, Lyan B, Pujos-Guillot E, Harel J, Martin C.** 2011. Enterohaemorrhagic *Escherichia coli* gains a competitive advantage by using ethanolamine as a nitrogen source in the bovine intestinal content. Environ Microbiol **13:**365-377.

38. **Gonyar LA, Kendall MM.** 2014. Ethanolamine and choline promote expression of putative and characterized fimbriae in enterohemorrhagic *Escherichia coli* O157:H7. Infect Immun **82:**193-201.

39. **Kendall MM, Gruber CC, Parker CT, Sperandio V.** 2012. Ethanolamine controls expression of genes encoding components involved in interkingdom signaling and virulence in enterohemorrhagic *Escherichia coli* O157:H7. MBio **3**.

40. **Srikumar S, Fuchs TM.** 2011. Ethanolamine utilization contributes to proliferation of *Salmonella enterica* serovar Typhimurium in food and in nematodes. Appl Environ Microbiol **77:**281-290.

41. **Thiennimitr P, Winter SE, Winter MG, Xavier MN, Tolstikov V, Huseby DL, Sterzenbach T, Tsolis RM, Roth JR, Baumler AJ.** 2011. Intestinal inflammation allows *Salmonella* to use ethanolamine to compete with the microbiota. Proc Natl Acad Sci U S A **108:**17480-17485.

42. **Luzader DH, Clark DE, Gonyar LA, Kendall MM.** 2013. EutR is a direct regulator of genes that contribute to metabolism and virulence in

enterohemorrhagic *Escherichia coli* O157: H7. Journal of bacteriology **195:**4947-4953.

CHAPTER 5

Appendix I - Supplemental Material for Chapter 2

Supplementary File S1: Vector Construction

pMC421: A 600 bp fragment containing the upstream region of the *sinR* (CD2214) operon was amplified from *C. difficile* 630Δ*erm* genomic DNA using primers oMC1008 and oMC1009. This region was cloned into pMC358 using *Bam*HI and *Eco*RI.

pMC426: A 400 bp fragment containing the upstream region of the *oppB* (CD0853) operon was amplified from *C. difficile* 630Δ*erm* genomic DNA using primers oMC1012 and oMC1015. This region was cloned into pMC358 using *Bam*HI and *Eco*RI.

pMC451: A 600 bp fragment containing the upstream region of the *appA* (CD2672) operon was amplified from *C. difficile* 630Δ*erm* genomic DNA using primers oMC1025 and oMC1026. This region was cloned into pMC358 using *Bam*HI and *Eco*RI.

pMC453: A 600 bp fragment containing the upstream region of the *appA* operon was amplified from *C. difficile* UK1 genomic DNA using primers oMC1025 and oMC1026. This region was cloned into pMC358 using *Bam*HI and *Eco*RI.

pMC463: A 400 bp fragment containing the upstream region of the *oppB* operon was amplified from *C. difficile* UK1 genomic DNA using primers oMC1012 and oMC1015. This region was cloned into pMC358 using *Bam*HI and *Eco*RI.

pMC474: A 250 bp fragment containing the upstream region of the *oppB* (CD0853) operon was amplified from *C. difficile* 630Δ*erm* genomic DNA using primers oMC1012 and oMC1074. This region was cloned into pMC358 using *Bam*HI and *Eco*RI.

MC476: A 170 bp fragment containing the upstream region of the *oppB* (CD0853) operon was amplified from *C. difficile* 630Δ*erm* genomic DNA using primers oMC1012 and oMC1076. This region was cloned into pMC358 using *Bam*HI and *Eco*RI.

pMC477: A 150 bp fragment containing the upstream region of the *oppB* (CD0853) operon was amplified from *C. difficile* 630Δ*erm* genomic DNA using primers oMC1012 and oMC1077. This region was cloned into pMC358 using *Bam*HI and *Eco*RI.

pMC478: A 250 bp fragment containing the upstream region of the *oppB* (CD0853) operon was amplified from *C. difficile* UK1 genomic DNA using primers oMC1012 and oMC1074. This region was cloned into pMC358 using *Bam*HI and *Eco*RI.

pMC480: A 170 bp fragment containing the upstream region of the *oppB* (CD0853) operon was amplified from *C. difficile* UK1 genomic DNA using primers oMC1012 and oMC1076. This region was cloned into pMC358 using *Bam*HI and *Eco*RI.

pMC481: A 150 bp fragment containing the upstream region of the *oppB* (CD0853) operon was amplified from *C. difficile* UK1 genomic DNA using primers oMC1012 and oMC1077. This region was cloned into pMC358 using *Bam*HI and *Eco*RI.

pMC535: A 600 bp fragment containing the upstream region of the *sinR* (CD2214) operon was generated through splicing and overlap extension PCR from *C. difficile* 630Δ*erm* genomic DNA to generate a C to A transversion 290 bp upstream the *sinR* translational start site using primers oMC1008, oMC1009, oMC1178, and oMC1179. This region was cloned into pMC358 using *Bam*HI and *Eco*RI

pMC536: A 600 bp fragment containing the upstream region of the *sinR* (CD2214) operon was generated through splicing and overlap extension PCR from *C. difficile* 630Δ*erm* genomic DNA to generate a C to A transversion 290 bp upstream the *sinR* translational

start site using primers oMC1008, oMC1009, oMC1178, and oMC1179. This region was cloned into pMC358 using *Bam*HI and *Eco*RI

pBL18: pSMB47 was digested with *Eco*RI and *Nco*I. The ends were blunted and the plasmid was self-ligated generating pBL18.

pBL26: The *catP* gene of pMMOrf-Cat was amplified using 5'catP2 and ITR primers. This region was cloned into pBL18 using *Sph*I.

pMMOrf-Cat: 950 bp region containing *catP* and its promoter was amplified from pJIR1456 using 5'catP2 and 3'catP. This region was cloned into the *Sma*I site of pMMOrf.

pND3: A 983 bp fragment containing the promoter and coding sequencing of *codY* was amplified from *C. difficile* JIR8094 genomic DNA using primers oLB275 and oLB276. This region was cloned into pBL26 using *Bam*HI and *Hind*III.

Supplemental Figure S2 – Chapter 2

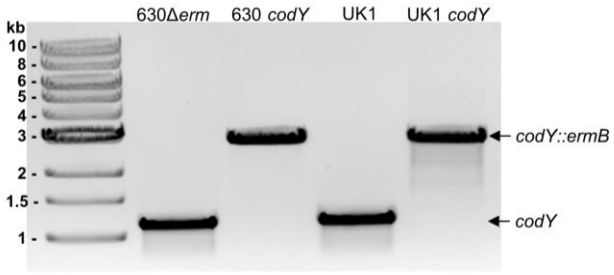

Figure S2. Confirmation of *codY* disruption. PCR amplification of *codY* from 630Δ*erm*, MC364 (630Δ*erm codY::ermB*), UK1, and LB-CD16 (UK1 *codY::ermB*) genomic DNA using primers oMC425/426, demonstrating insertion of the Targetron-based intron in mutants.

Supplemental Figure S3 – Chapter 2

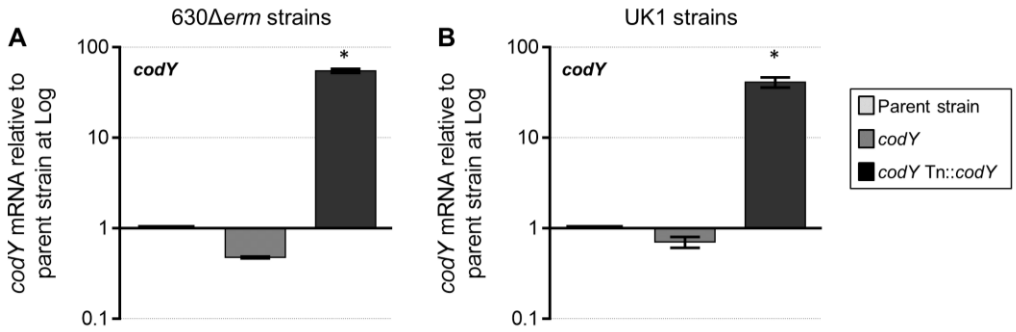

Figure S3. Analysis of *codY* expression. qRT-PCR expression analysis of *codY* for (A) 630Δ*erm*, MC364 (630Δ*erm codY::ermB*) and MC442 (630Δ*erm codY* Tn::*codY*) and B) UK1, LB-CD16 (UK1 *codY::ermB*), and MC443 (UK1 *codY* Tn::*codY*). Strains were grown in 70:30 liquid sporulation medium and samples for RNA isolation were taken during logarithmic growth (OD_{600} ~0.5). The means and standard error of the means of four biological replicates are shown. A one-way ANOVA followed by Dunnett's multiple comparison test was used to compare the parent strain with the *codY* mutant or the parent strain with the respective complemented strain. *, $P \leq 0.05$.

Supplemental Figure S4 – Chapter 2

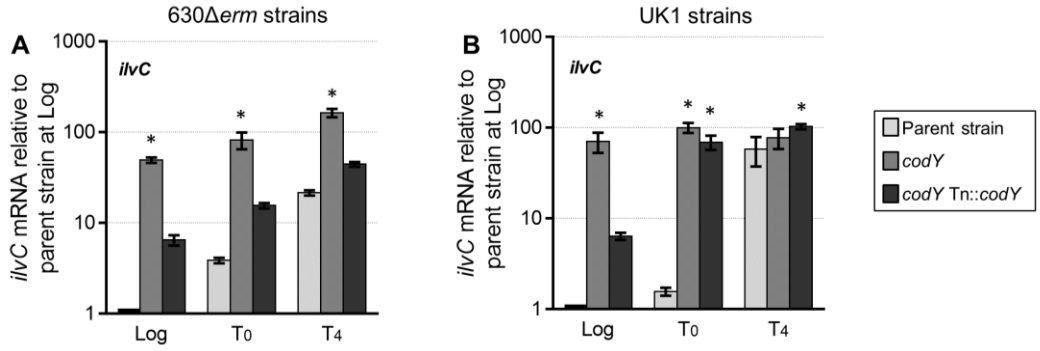

Figure S4. Loss of CodY-dependent regulation of *ilvC*. qRT-PCR expression analysis of *ilvC* in A) 630Δ*erm*, MC364 (630Δ*erm codY::ermB*), MC442 (630Δ*erm codY* Tn::*codY*) and (B) UK1, LB-CD16 (UK1 *codY::ermB*) and MC443 (UK1 *codY* Tn::*codY*) grown in 70:30 liquid sporulation media. Samples for RNA isolation were taken during logarithmic growth (OD_{600} ~0.5), transition to stationary phase (T_0), and four hours after the transition into stationary phase (T_4). The means and standard error of the means of four biological replicates are shown. A two-way repeated measures ANOVA, followed by Dunnett's multiple comparison test was used to compare parent strain with the *codY* mutant or the parent strain with the respective complemented strain. *, $P \leq 0.05$.

Supplemental Figure S5 – Chapter 2

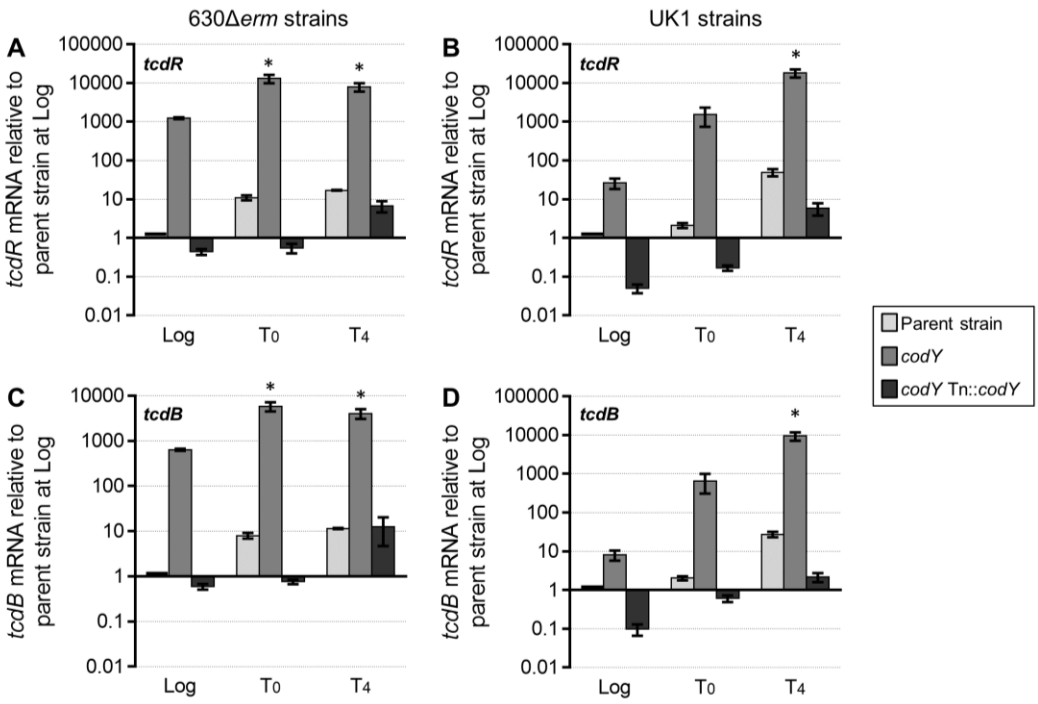

Figure S5. Expression of the toxin-specific sigma factor, *tcdR*, and toxin gene, *tcdB*, is increased in *codY* mutants. qRT-PCR analysis of *tcdR* and *tcdB* in (A,C) 630Δ*erm*, MC364 (630Δ*erm codY::ermB*), MC442 (630Δ*erm codY* Tn::*codY*) and (B,D) UK1, LB-CD16 (UK1 *codY::ermB*), and MC443 (UK1 *codY* Tn::*codY*) grown in 70:30 sporulation media. Samples for RNA were collected during logarithmic growth (OD_{600} ~0.5), transition to stationary phase (T_0), and four hours post the transition to stationary phase (T_4). The means and standard error of the means of four biological replicates are shown. A two-way repeated measures ANOVA followed by Dunnett's multiple comparison test was used to compare parent strain with the *codY* mutant or the parent strain with the respective complemented strain. *, $P \leq 0.05$.

Supplemental Figure S6 – Chapter 2

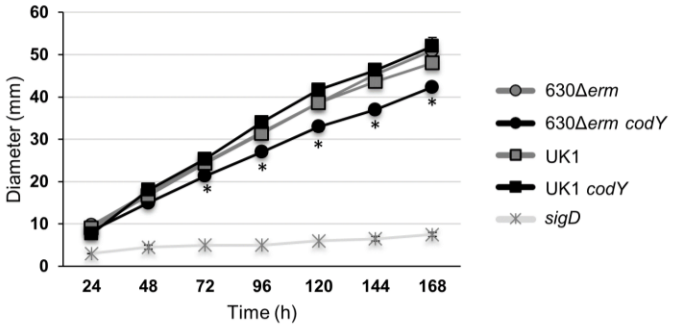

Figure S6. Motility phenotypes of *codY* mutants. (A) Motility of 630Δ*erm*, MC364 (630 *codY*), UK1, LB-CD16 (UK1 *codY*) and the non-motile strain, *sigD* (RT1075) on the surface of one-half concentration BHI with 0.3% agar plate. The diameters of motility (mm) were measured every 24 h for a total of 168 h. The means and SEM of four biological replicates are shown. *, $P \leq 0.05$ by a two-tailed Student's *t* test.

Supplemental Figure S7 – Chapter 2

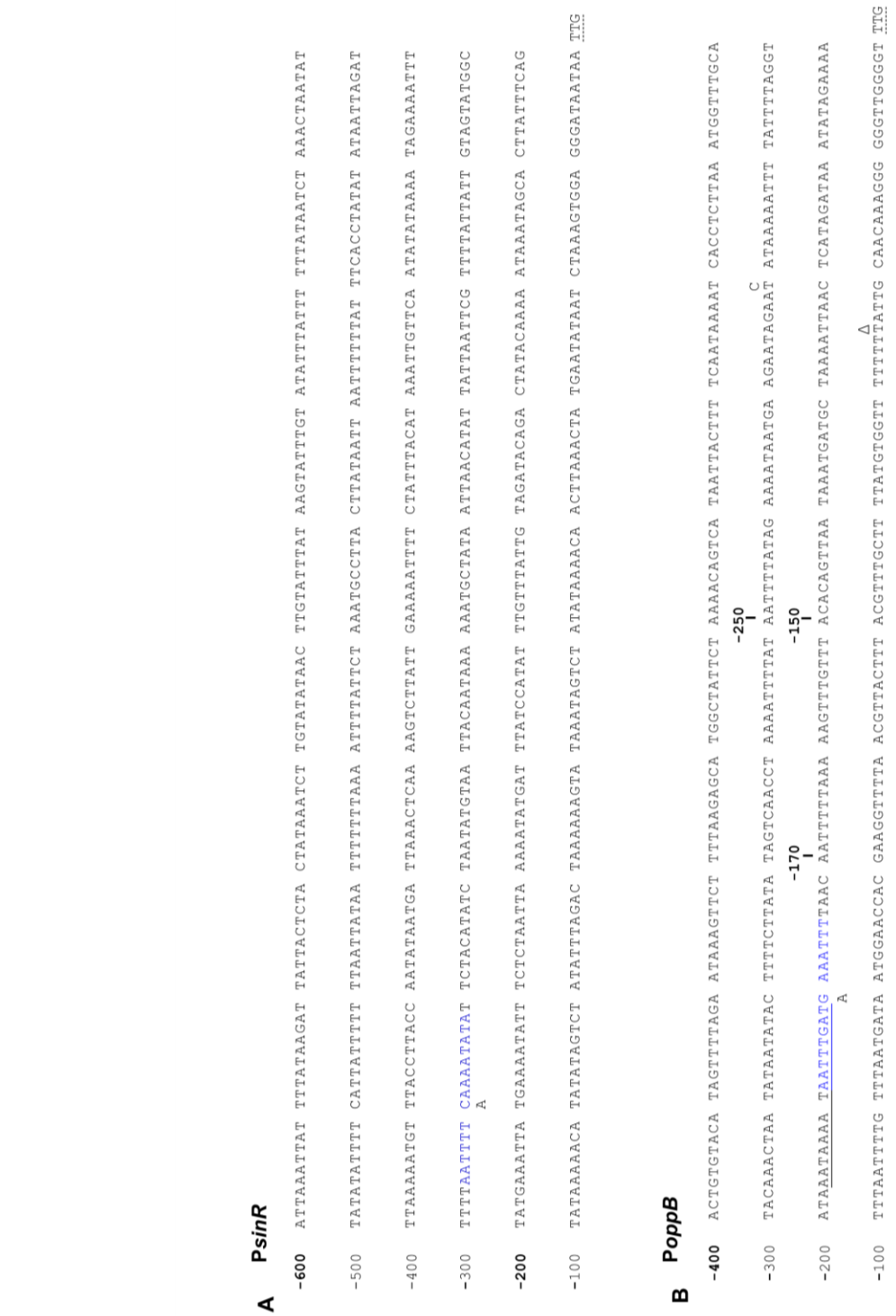

Figure S7. The promoter region of *sinR* and *oppB*. 600 bp DNA sequence upstream of the predicted *sinR* translational start site from the 630 genome (**A**). 400 bp DNA sequence

upstream of the predicted *oppB* translational start site from the 630 genome (**B**). Sequence differences in the UK1 strain are noted above the 630 sequence. Δ denotes a deletion. Alterations made by site-directed mutagenesis are noted below the sequence. The putative translation start site is marked by a dashed underline. The previously identified CcpA (67) and CodY (32, 37) binding sites are marked by a solid underline and blue font, respectively. The evaluated promoter fusion lengths are indicated by bolded markers.

CHAPTER 6

Appendix II - Supplemental Material for Chapter 3

Supplementary File S1: Vector Construction

pMC253: The group II intron of pMC111 was retargeted to *eutA* through splice by overlap extension (SOE) PCR using primers oMC665, oM666, oMC667 and EBSu. The primers used were generated by JPintronator. This retargeted group II intron was TA cloned into pCR2.1 generating pMC253.

pMC256: The group II intron of pMC111 was retargeted to *eutG* through SOE PCR using primers oMC674, oM675, oMC676 and EBSu. The primers used were generated by Intron Site Finder. This retargeted group II intron was TA cloned into pCR2.1 generating pMC256.

pMC257: The group II intron targeted to *eutA* in pMC253 was cloned into pCE240 using *BsrGI* and *HindIII* to generate pMC257.

pMC260: The group II intron targeted to *eutG* in pMC256 was cloned into pCE240 using *BsrGI* and *HindIII* generating pMC260.

pMC263: pMC257 was digested with *AcuI*, *SfoI*, and *SphI*. The resulting 5.8kb fragment was cloned into pMC123 digested with *SphI* and *SnaBI* generating pMC263.

pMC266: pMC260 was digested with *AcuI*, *SfoI*, and *SphI*. The resulting 5.8kb fragment was cloned into pMC123 digested with *SphI* and *SnaBI* generating pMC266.

Supplmental Figure S2 – Chapter 3

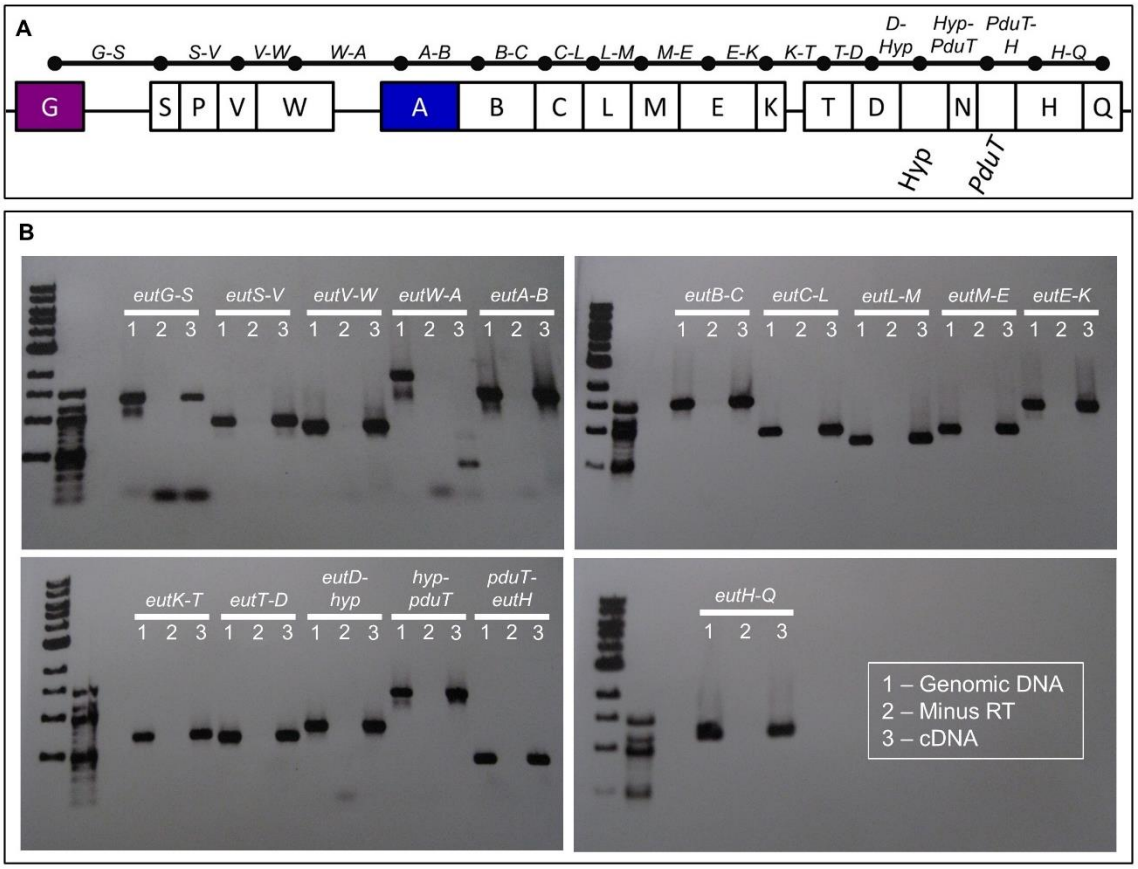

Figure S2. Determination of transcriptional units within the *eut* gene cluster. (A) Primers were designed to generate a product if adjacent open reading frames were present on the same transcript. (B) Transcriptional units were determined by PCR. The column number refers to template type, (1) 630Δ*erm* genomic DNA (positive control), (2) minus reverse transcriptase cDNA reaction of RNA isolated from 630Δ*erm* grown in 70:30 broth with 15 mM ethanolamine (negative control), (3) cDNA produced from RNA isolated from 630Δ*erm* grown in 70:30 broth with 15 mM ethanolamine.

Supplmental Figure S3 – Chapter 3

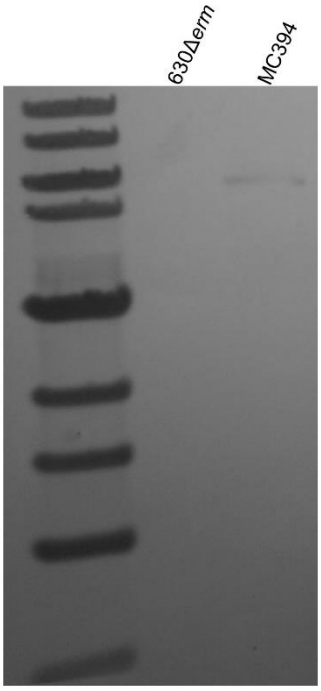

Figure S3. Confirmation of *eutA* disruption. A Southern blot of *HindIII* digested genomic DNA from *C. difficile* 630Δ*erm* and MC394 (*eutA*::*ermB*) using an intron-specific probe is shown.

Supplmental Figure S4 – Chapter 3

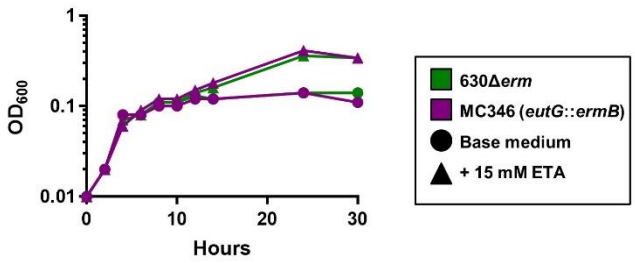

Figure S4. *eutG* is not essential for ethanolamine utilization in *C. difficile*. A representative modified minimal medium growth curve of 630Δ*erm* and MC346 (*eutG*::*ermB*) with and without the addition of 15 mM ethanolamine hydrochloride (ETA) is shown.

Supplmental Figure S5 – Chapter 3

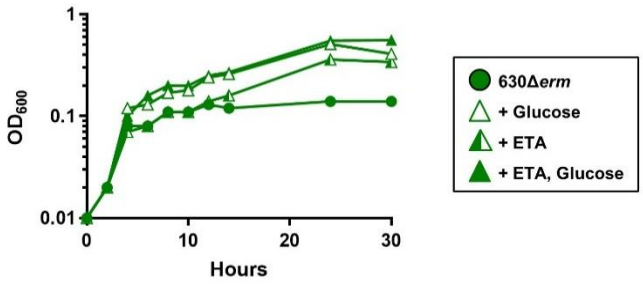

Figure S5. Ethanolamine can be utilized as a primary nutrient source. A Representative growth curve of 630Δ*erm* in modified minimal medium supplemented with 15 mM ETA and 5 mM D-glucose is shown.

Supplmental Figure S6 – Chapter 3

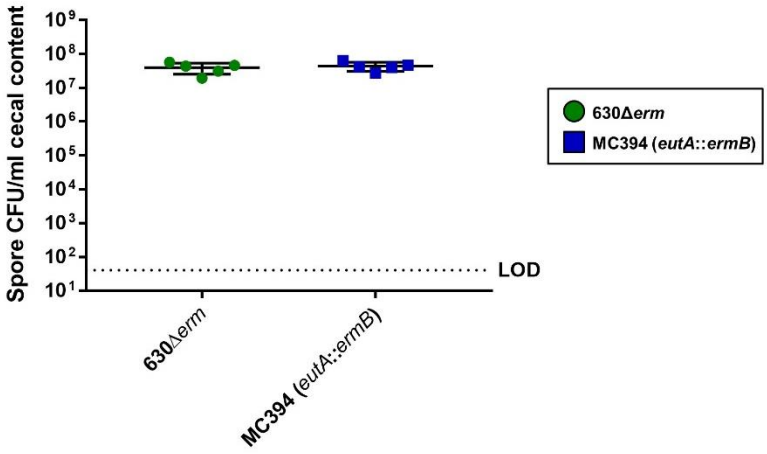

Figure S6. MC394 (*eutA*::*ermB*) exhibits no change in spore production *in vivo*. Spores were enumerated from post-mortem hamster cecal content following treatment with ethanol to eliminate vegetative cells. Five hamsters per strain were used. The mean and standard deviation is shown for each strain. The limit of detection (LOD) is demarcated by the dotted line at 40 spore CFU/ml. MC394 (*eutA*::*ermB*) cecal spore counts were compared to the parent strain with a two-tailed *t*-test. * indicates $p \leq 0.05$.

Supplmental Figure S7 – Chapter 3

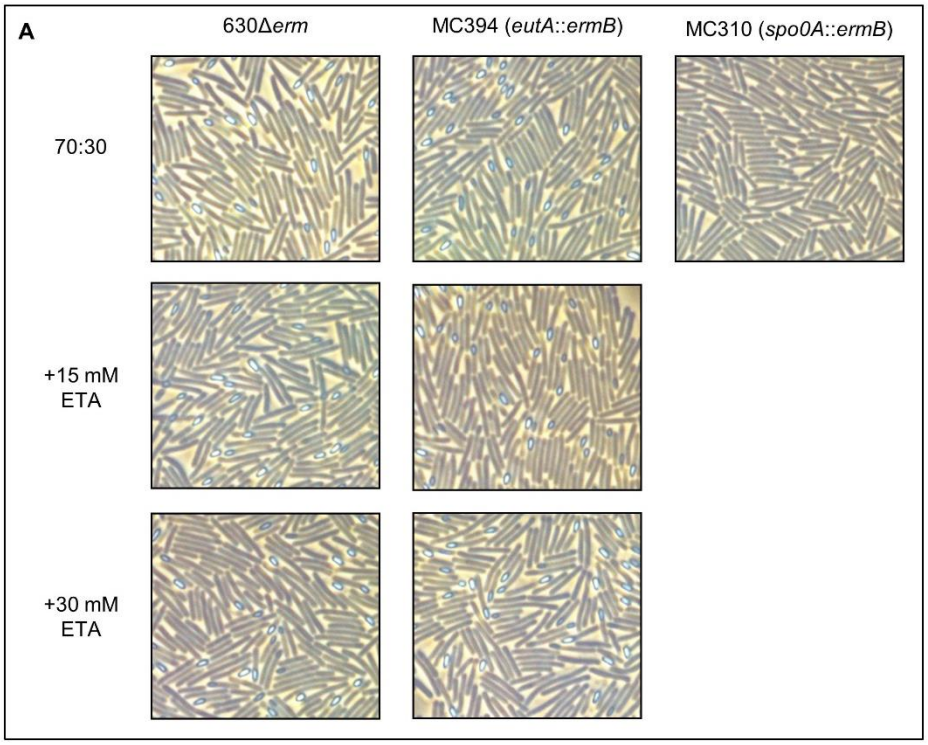

B

Growth Condition	630Δ*erm*	MC394 (*eutA*::*ermB*)	MC310 (*spo0A*::*ermB*)
70:30	19.3 ± 5.7%	18.6 ± 2.5%	0.0 ± 0.0%
+ 15 mM ETA	15.1 ± 2.3%	18.4 ± 3.7%	
+ 30 mM ETA	17.9 ± 0.9%	20.9 ± 2.0%	

Figure S7. No effect on sporulation frequency *in vitro* in the presence of ethanolamine. (A) Phase contrast microscopy was performed on 630Δ*erm*, MC394 (*eutA*::*ermB*), and MC310 (*spo0A*::*ermB*, negative control) grown for 24 hours on 70:30 sporulation plates supplemented with 15 or 30 mM ETA. A representative image is shown for each strain and condition. Arrowheads indicate phase-bright spores. (B) Sporulation frequency was determined by direct count. The means and standard deviations of four biological replicates

are shown. Sporulation frequencies of 630Δ*erm* and MC394 (*eutA*::*ermB*) were compared using a two-way ANOVA. *, $P \leq 0.05$.

CHAPTER 7

Appendix III - Conserved Oligopeptide Permeases Modulate Sporulation Initiation in *Clostridium difficile*

Adrianne N. Edwards, Kathryn L. Nawrocki and Shonna M. McBride

This work was published in 2014 in *Infection and Immunity*.

K.L.N. performed qRT-PCR experiments and assisted with manuscript revision.

Article Citation:

Edwards, A. N., Nawrocki, K. L., & McBride, S. M. (2014). Conserved oligopeptide permeases modulate sporulation initiation in *Clostridium difficile*. *Infection and Immunity*, *82*(10), 4276-4291. doi: 10.1128/IAI.02323-14 PMCID 4187847

ABSTRACT

The anaerobic gastrointestinal pathogen *Clostridium difficile* must form a metabolically dormant spore to survive in oxygenic environments and be transmitted from host to host. The regulatory factors by which *C. difficile* initiates and controls the early stages of sporulation in *C. difficile* are not highly conserved with other *Clostridium* or *Bacillus* species. Here, we investigated the role of two conserved oligopeptide permeases, Opp and App, in the regulation of sporulation in *C. difficile*. These permeases are known to positively affect sporulation in *Bacillus* species through the import of sporulation-specific quorum-sensing peptides. In contrast to other spore-forming bacteria, we discovered that inactivating these permeases in *C. difficile* resulted in earlier expression of early sporulation genes and increased sporulation *in vitro*. Furthermore, disruption of *opp* and *app* resulted in greater virulence and increased spores recovered from feces in the hamster model of *C. difficile* infection. Our data suggest that Opp and App indirectly inhibit sporulation, likely through the activities of the transcriptional regulator, SinR, and its inhibitor, SinI. Taken together, these results indicate that the Opp and App transporters serve a different function in controlling sporulation and virulence in *C. difficile* than in *Bacillus subtilis* and suggest that nutrient availability plays a significant role in pathogenesis and sporulation *in vivo*. This study suggests a link between the nutritional status of the environment and sporulation initiation in *C. difficile*.

INTRODUCTION

Clostridium difficile is an anaerobic, Gram-positive pathogen that causes a significant gastrointestinal disease in humans and other mammals. Because *C. difficile* is an obligate anaerobe, its survival outside of the host requires the formation of a

metabolically inactive spore, which can withstand harsh environmental conditions. The ability of *C. difficile* to form a spore is critical to the spread and recurrence of the disease (1). Spore formation also contributes to *C. difficile* resistance to traditional antibiotic therapies. Despite the importance of spore formation in the pathogenesis of *C. difficile*, little is understood about how the initiation of sporulation is regulated.

Sporulation is a complex process governed by multiple regulators and feedback processes in bacteria; however, the regulatory components and environmental signals that control the initiation of sporulation in well-studied spore formers are not well conserved in *C. difficile* (2-7). In all studied spore-forming bacteria, including *C. difficile* (1, 8), the initiation of sporulation is controlled by the activity of the highly conserved transcription factor, Spo0A, which functions as the master regulator of sporulation. In *Bacillus* species, Spo0A activity is tightly regulated through a phosphorylation-mediated signal transduction pathway in response to nutrient availability (9). One mechanism that controls Spo0A phosphorylation and thereby the activity of Spo0A in *B. subtilis* and other species, is the uptake of small, quorum-signaling peptides known as Phr peptides (10). The Phr peptides are imported by the Opp (Spo0K) and App oligopeptide permeases and contribute to the induction of sporulation or genetic competence when bacterial population densities are high (11-13). The Phr peptides are encoded by multiple *phr* genes and are initially secreted as pro-proteins that are subsequently processed to form pentapeptides (10, 13). Once imported by Opp or App, the Phr peptides directly target the Rap phosphatases, which would otherwise inhibit sporulation by dephosphorylating components of the Spo0A phosphorelay pathway (10, 14).

Opp (also known as Spo0K in spore-forming bacteria and Ami in *Streptococcus* species) and App are membrane-associated five-protein complexes of the ABC-transporter family and are found in both Gram-positive and Gram-negative species. These transporters contain an extracellular ligand-binding lipoprotein (OppA/AppA), two transmembrane proteins (OppBC/AppBC) that form a membrane-spanning pore and two cytoplasmic ATPases (OppDF/AppDF) that drive the transport of the peptide into the cell (15, 16). The Opp and App oligopeptide transport systems influence many cellular processes besides sporulation, including competence in *Bacillus* and *Streptococcus* species (11, 17, 18), plasmid transfer in *Enterococcus faecalis* (19, 20) and the expression of virulence factors in *Bacillus thuringiensis* (21, 22). But the primary function of Opp and App in bacteria is to import small, heterogeneous peptides, varying from 3 to 20 amino acids, relatively nonspecifically as nutrient sources (23-27). These imported peptides may be utilized as carbon or nitrogen sources and can also serve as substrates for the generation of ATP in Clostridial species via the Stickland reaction (28-32).

The *C. difficile* genome encodes orthologs of the Opp and App oligopeptide transporter systems and two Rap phosphatase orthologs; however, no clear Phr ortholog is detectable by sequence analysis. In this study, we asked whether the conserved oligopeptide transporter systems have a role in regulating the initiation of sporulation of *C. difficile*. By studying *opp* and *app* null mutants, we determined that the absence of App or both Opp and App results in increased sporulation *in vitro,* as well as earlier and increased expression of sporulation genes. Our results indicate that the loss of either or both putative transporters results in a hypervirulent phenotype as well as increased spore formation during infection in a hamster model. Further, we observed that the increase in sporulation

in *opp app* mutants is associated with differential expression of the genes encoding SinR, a transcriptional regulator, and the predicted SinI, a putative inhibitor of SinR. Together these data suggest that the *C. difficile* Opp and App transporters indirectly inhibit sporulation by facilitating the uptake of peptides, and thus, the availability of intracellular nutrients.

MATERIALS AND METHODS

Bacterial strains and growth conditions. The bacterial strains and plasmids used in this study are listed in Table 1. *Clostridium difficile* strains were routinely cultured in BHIS broth or on BHIS agar plates (33). Media for growth of *C. difficile* were supplemented with 2-10 μg thiamphenicol ml^{-1}, 5 μg erythromycin ml^{-1} or 30 μg lincomycin ml^{-1} (Sigma-Aldrich) as needed. Counterselection of *E. coli* after conjugation with *C. difficile* was done using 50 μg kanamycin ml^{-1} as previously detailed (34). Taurocholate was added to cultures (0.1%) to induce germination of *C. difficile* spores as indicated (Sigma-Aldrich) (35, 36). *C. difficile* strains were cultured in an anaerobic chamber maintained at 37°C (Coy Laboratory Products) with an atmosphere of 10% H_2, 5% CO_2 and 85% N_2 as previously described (37, 38). Growth experiments with oligopeptides composed of 5 or 10 random amino acids (Peptide 2.0) were added to minimal defined medium (39) containing no other amino acid sources. *Escherichia coli* strains were grown at 37°C in LB (40) or BHIS medium, and supplemented with 20 μg chloramphenicol ml^{-1} or 100 μg ampicillin ml^{-1} as needed.

Sporulation efficiency assays. Sporulation assays were performed in 70:30 sporulation broth medium (36). *C. difficile* cultures were started in BHIS medium supplemented with

TABLE 1 Bacterial strains and plasmids

Plasmid or strain	Relevant genotype or features	Source or reference
Strains		
E. coli		
DH5α Max Efficiency	F$^-$ ϕ80d*lacZ*ΔM15 Δ(*lacZYA-argF*)*U169 recA1 endA1 hsdR17* (r_K^- m_K^+) *phoA supE44* λ$^-$ *thi-1 gyrA96 relA1*	Invitrogen
MC101	HB101/pRK24	B. Dupuy
MC135	HB101 containing pRK24 and pMC123	48
MC253	HB101 containing pRK24 and pMC199	This study
MC263	HB101 containing pRK24 and pMC213	This study
MC274	HB101 containing pRK24 and pMC217	This study
MC277	HB101 containing pRK24 and pMC211	This study
MC295	HB101 containing pRK24 and pMC230	This study
MC306	HB101 containing pRK24 and pJS107::*spo0A178*::TargeTron	69
MC329	HB101 containing pRK24 and pMC238	This study
MC330	HB101 containing pRK24 and pMC240	This study
C. difficile		
630	Clinical isolate	97
630Δ*erm*	Erm^s derivative of strain 630	N. Minton and 98
R20291	Clinical isolate	41
MC282	630Δ*erm* pMC211	This study
MC283	630Δ*erm* pMC217	This study
MC296	630Δ*erm oppB*::*ermB*	This study
MC301	630Δ*erm appA*::*ermB*	This study
MC307	630Δ*erm oppB*::*ermB appA*::*ermB*	This study
MC310	630Δ*erm spo0A*::*ermB*	This study
MC322	630Δ*erm oppB*::*ermB*/pMC213	This study
MC323	630Δ*erm oppB*::*ermB appA*::*ermB*/pMC213	This study
MC324	630Δ*erm*/pMC123	This study
MC331	630Δ*erm appA*::*ermB*/pMC238	This study
MC332	630 Δ*erm oppB*::*ermB*/pMC240	This study
MC334	630Δ*erm oppB*::*ermB appA*::*ermB*/pMC238	This study
MC337	63 Δ*erm oppB*::*ermB*/pMC123	This study
MC338	630Δ*erm appA*::*ermB*/pMC123	This study
MC339	630Δ*erm oppB*::*ermB appA*::*ermB*/pMC123	This study
Plasmids		
pRK24	Tra$^+$ Mob$^+$ *bla tet*	99
pBL100	Untargeted group II intron-TargeTron vector	29
pCR2.1	*bla kan*	Invitrogen
pCE240	*C. difficile* TargeTron construct based on pJIR750ai (group II intron, *ermB*::RAM *ltrA*) *catP*	C. Ellermeier (44)
pJS107-*spo0A*-178TT	Group II intron targeted to *spo0A*	69
pMC123	*E. coli-C. difficile* shuttle vector, *bla catP*	48
pMC199	pBL100 with group II intron targeted to *oppB*	This study
pMC211	pMC123 with *cprA* promoter	This study
pMC213	pMC123 with P*oppBCAD* operon	This study
pMC217	pMC211 with CD0852	This study
pMC220	pCR2.1 with group II intron targeted to *appA*	This study
pMC226	pCE240 with *appA*-targeted intron	This study
pMC230	pMC123 with *appA*-targeted intron, *ermB*::RAM *ltrA catP*	This study
pMC237	pCR2.1 with P*appFDABC* operon	This study
pMC238	pMC123 with P*appFDABC* operon	This study
pMC239	pCR2.1 with P*oppBCADF* from R20291	This study
pMC240	pMC123 with P*oppBCADF* from R20291	This study

0.1% taurocholate and 0.5% fructose until mid-log phase (active growth) to allow for germination of any spores within the starting inoculum. Cultures were then back-diluted and equilibrated to an OD_{600} = 0.1 into 70:30 medium. These cultures were further diluted 1:10 into 70:30 medium, incubated at 37°C, and monitored for the production of spores. Samples were taken at the point of maximum cell density (T_2; approximately 2 h after the onset of stationary phase), serially diluted and plated onto BHIS with 0.1% taurocholate to determine the total colony forming units (CFU) from which spores could form. To determine the number of spores present, 500 µl samples were taken from each culture, mixed 1:1 with 95% ethanol and incubated for 1 hour to kill all non-spores (vegetative cells) present. Ethanol treated samples were then serially diluted, plated onto BHIS containing 0.1% taurocholate and incubated for 24-48 h to enumerate spore CFU. The sporulation frequency was determined by dividing the number of spores by the total CFU at T_2 for each culture (spore ratio) and multiplied by 100 (percentage of spores formed). The sporulation defective *spo0A* mutant was used as a negative control to ensure that all vegetative cells were killed during ethanol treatment. Cultures were assessed at the time of inoculation and at the start of stationary phase (T_0) to ensure no contaminating spores were present in the starter cultures.

Strain and plasmid construction. Oligonucleotides used in this study are listed in Table 2. Details of DNA cloning and vector construction are outlined in the Supplementary file S1. *C. difficile* strain 630 (GenBank accession NC_009089.1) was used as a template for primer design, unless otherwise specified. Strain 630Δ*erm* was used as a template for PCR amplification, except where strain R20291 (NC_013316.1) template was specified (41). Isolation of plasmid DNA, PCR and cloning was performed using standard protocols.

Genomic DNA was prepared and genetic manipulation of *C. difficile* was performed as previously described (37, 42). Null mutations in *C. difficile* were created by retargeting the group II intron from pCE240 using the intron retargeting primers listed in Table 2, as previously described (43-45). The double *opp app* mutant (MC307) was created by using the *oppB*-specific group II intron in MC301 (*app* single mutant) and selecting for the second intron integration event on BHIS plates containing lincomycin (30 μg ml^{-1}). To complement the *opp* and *app* disruptions, plasmids containing the *oppBCAD* (pMC213) or *appFDABC* (pMC238) operons and upstream promoter regions were transferred into *C. difficile* mutants from *E. coli* by conjugation as previously described, except that 50 μg kanamycin ml^{-1} was used to counterselect against *E. coli* post-conjugation (46). Cloned DNA fragments were verified by sequencing (Eurofins MWG Operon) prior to use.

Phase Contrast Microscopy. *C. difficile* strains were grown in 70:30 sporulation medium as described above. At the indicated time points, 1 ml of culture was removed from the anaerobic chamber, centrifuged at full speed for 30 sec and resuspended in ~10 μl of supernatant. Slides were prepared by placing 2 μl of the concentrated culture onto a thin layer of 0.7% agarose applied directly to the surface of the slide. Phase contrast microscopy was performed using a 100X-Ph3 oil immersion objective on a Nikon Eclipse Ci-L. At least three fields of view for each strain were acquired with a DS-Fi2 camera and used to calculate the percentage of spores (the number of spores divided by the total number of spores, prespores and vegetative cells) from two independent experiments.

Fluorescence Microscopy. *C. difficile* strains were grown in 70:30 sporulation medium as described above. At approximately 4 h after the onset of stationary phase (~T_4), 2 ml of culture was removed from the anaerobic chamber, pelleted and resuspended in 50 μl of

TABLE 2 Oligonucleotides

Primer	Sequence[a] (5′ → 3′)	Purpose (operon)	Source or reference
EBS universal	5′-CGAAATTAGAAACTTGCGTTCAGTAAAC-3′		Sigma-Aldrich
oMC44	5′-CTAGCTGCTCCTATGTCTCACATC-3′	*rpoC* qPCR (CD0067)	46
oMC45	5′-CCAGTCTCTCCTGGATCAACTA-3′	*rpoC* qPCR (CD0067)	46
oMC112	5′ -GGCAAATGTAAGATTTCGTACTCA- 3′	*tcdB* qPCR (CD0660)	
oMC113	5′ -TCGACTACAGTATTCTCTGAC- 3′	*tcdB* qPCR (CD0660)	
oMC152	5′-GTTATGGAAGTCAAGGACATGCAC-3′	*ilvC* qPCR (CD1565)	42
oMC153	5′-GCTTCTGCTACACTCTTAACTTCA-3′	*ilvC* qPCR (CD1565)	42
oMC158	5′-CCAGAAGAATCTATGGTAAAGGTTG-3′	*hisZ* qPCR (CD1547)	42
oMC159	5′-ACCATCTTCCCATCTTGGTACA-3′	*hisZ* qPCR (CD1547)	42
oMC215	5′-GCGAATTCGACATGGAAGTAGAAGTTAAGG-3′	P*cprA* cloning	
oMC331	5′-CTCAAAGCGCAATAAATCTAGGAGC-3′	*spo0A* qPCR (CD1214)	
oMC332	5′-TTGAGTCTCTTGAACTGGTCTAGG-3′	*spo0A* qPCR (CD1214)	
oMC339	5′-GGGCAAATATACTTCCTCCTCCAT-3′	*sigE* qPCR (CD2643)	
oMC340	5′-TGACTTTACACTTTCATCTGTTTCTAGC-3′	*sigE* qPCR (CD2643)	
oMC346	5′-GCGGATCCAATTTTCATCCTTTCTTTTGTCAAAC-3′	P*cprA* cloning	
oMC349	5′-CCTTTGTGCTAGCCTTATTGTTAGG-3′	*oppB* qPCR (CD0853)	
oMC350	5′-AAGTATGAGTACTAAGGCAACCCA-3′	*oppB* qPCR (CD0853)	
oMC363	5′-GACTTGCTCTGTGTTAGTTCCATC-3′	*spoIID* qPCR (CD0124)	
oMC364	5′-TGTTTATAGATACTGGGCTCTCTGG-3′	*spoIID* qPCR (CD0124)	
oMC365	5′-GGAAGTAACTGTTGCCAGAGAAGA-3′	*sigF* qPCR (CD0772)	
oMC366	5′-CGCTCCTAACTAGACCTAAATTGC-3′	*sigF* qPCR (CD0772)	
oMC371	5′-AAAAGCTTTTGCAACCCACGTCGATCGTGAA ATATACAGTCAAGTGCGCCCAGATAGGGTG-3′	*oppB* (CD0853) intron retargeting	
oMC372	5′- CAGATTGTACAAATGTGGTGATAACAGATAAGTC AGTCAATATAACTTACCTTTCTTTGT-3′	*oppB* (CD0853) intron retargeting	
oMC373	5′-CGCAAGTTTCTAATTTCGGTTTATATTCGATAGA GGAAAGTGTCT-3′	*oppB* (CD0853) intron retargeting	
oMC427	5′-GTGGTGTTAATACATCAGAACTTCC-3′	*sigG* qPCR (CD2642)	
oMC428	5′-CAAACTGTTGTCTGGCTTCTTC-3′	*sigG* qPCR (CD2642)	
oMC429	5′-GCCTGTGCTTCCAATGATAAAG-3′	*appA* qPCR (CD2672)	
oMC430	5′-ATATCTGGGTCACTTGCCATAG-3′	*appA* qPCR (CD2672)	
oMC431	5′-GTTGGAGAATCAGGATGTGGTA-3′	*appD* qPCR (CD2671)	
oMC432	5′-GCTGGGTTTAAAGATGTCATTGG-3′	*appD* qPCR (CD2671)	
oMC439	5′- GCCGGATCCCGTTTGCTTTTATGTGGTTT-3′	*oppB*::*ermB* verification	
oMC440	5′- GCCGGATCCCTGTTGGTGTGTTAATCCATTTTC-3′	*oppBCAD* cloning	
oMC441	5′-GCCTGCAGGCTTTTACAGTAGTACTTTTGTCC-3′	*oppBCAD* cloning	
oMC506	5′-GCCGGATCCAACCATTTAAGAGGTGATTT-3′	CD0852 cloning	
oMC507	5′-GACCTGCAGCTTTCTCCAAATACACCTAT-3′	CD0852 cloning	
oMC527	5′-AGGCAGGTTTACATCCAACATA-3′	*sinR* qPCR (CD2214)	
oMC528	5′-AGTGGTATGTCTAAAGCAGTAGC-3′	*sinR* qPCR (CD2214)	
oMC544	5′-AAAAGCTTTTGCAACCCACGTCGATCGTGAA GTTAACGTAGAAGTGCGCCCAGATAGGGTG-3′	CD2672 (*appA*) intron retargeting	
oMC545	5′-CAGATTGTACAAATGTGGTGATAACAGATAAGTC GTAGAAAATAACTTACCTTTCTTTGT-3′	CD2672 (*appA*) intron retargeting	
oMC546	5′-CGCAAGTTTCTAATTTCGGTTTTAACTCGATAGA GGAAAGTGTCT-3′	CD2672 (*appA*) intron retargeting	
oMC547	5′-TGGATAGGTGGAGAAGTCAGT-3′	*tcdA* qPCR (CD0663)	
oMC548	5′-GCTGTAATGCTTCAGTGGTAGA-3′	*tcdA* qPCR (CD0663)	
oMC553	5′-TGAATGCACCAGAACCAACT-3′	*appA*::*ermB* verification	
oMC587	5′-GTCGGATCCGGCTTTACATAACATGGTAGAGTAGTA-3′	*appFDABC* cloning	
oMC588	5′-AGCGAATTCAACAGCATGAAATCCCATCTTAATC-3′	*appFDABC* cloning	
oMC589	5′-GACACATGAACCAACATACATGG-3′	*oppC* qPCR (CD0854)	
oMC590	5′-AGATGCTGAACCACTTATACTACC-3′	*oppC* qPCR (CD0854)	
oMC591	5′-GATAAGAAGGCAGATACGCCTAAA-3′	*oppA* qPCR (CD0855)	
oMC592	5′-GCTAGACAAGGAACCACCTTATTA-3′	*oppA* qPCR (CD0855)	
oMC593	5′-ATTTCAAGACCCTATGACATCTCTC-3′	*oppD* qPCR (CD0856)	
oMC594	5′-TCTCAGGATTATCAATTCCAACCA-3′	*oppD* qPCR (CD0856)	
oMC595	5′-CATGAATCTACTGGTGGAGAAGTAA-3′	*oppF* qPCR (CD0857)	
oMC596	5′-CTGCAATTGTCATACGTGGATTT-3′	*oppF* qPCR (CD0857)	
oMC597	5′-TGCAGGAAGAACCATTCTTAGAT-3′	*appF* qPCR (CD2670)	
oMC598	5′-ATGTTCTATAACTGCCTCGGATATT-3′	*appF* qPCR (CD2670)	

(Continued on fo

TABLE 2 (Continued)

Primer	Sequence[a] (5′ → 3′)	Purpose (operon)	Source or reference
oMC599	5′-GGTTAATATGGGACTTGATAAACCAG-3′	*appB* qPCR (CD2673)	
oMC600	5′-CATAATTTGTTCTGTAACGGGCATA-3′	*appB* qPCR (CD2673)	
oMC601	5′-CTTCAAGAACCTAGCTTAAAGCATATC-3′	*appC* qPCR (CD2674)	
oMC602	5′-ATAACACCTACAGCAGTACCAAATA-3′	*appC* qPCR (CD2674)	
oMC612	5′-ACAGAAGAAGGTGTTGAAGGATATG-3′	*appA* (3′) qPCR	
oMC613	5′-TTATGCCCAAATCTACCTGTGTTAT-3′	*appA* (3′) qPCR	
oMC654	5′-GCCTGCAGCCTGTTCAAGTATTTTTATACTAAAC-3′	*oppF* cloning	
oMC683	5′-GTATCTGACAACATCAATTGCCTAAA-3′	CD0341 qPCR	
oMC684	5′-TCAGCTTGAGATTCAATTTCTTCATT-3′	CD0341 qPCR	
oMC733	5′-AGGTTTGGAGCAATCAAGAAAGA-3′	*murG* qPCR (CD2651)	
oMC734	5′-TGCTCATGTATTATGGCTGGTATTT-3′	*murG* qPCR (CD2651)	
oMC735	5′-CCTGGTAATTGGTCTTGGAAATAGA-3′	*gpr* qPCR (CD2470)	
oMC736	5′-CCTCAGTGAAATCATCATCATAGTCTTTA-3′	*gpr* qPCR (CD2470)	
oMC739	5′-AAGTGTGGCATTTGTAGACCATAATA-3′	*acnB* qPCR (CD0833)	
oMC740	5′-ACCATTTCCTGGCTTAGAGAAATAAA-3′	*acnB* qPCR (CD0833)	
oMC741	5′-CTCTGCAAATGTAGGTCATGGTAATAA-3′	*gabT* qPCR (CD2158)	
oMC742	5′-TTCCACAAGCTTCTCAGCTAATTT-3′	*gabT* qPCR (CD2158)	
oMC745/oBD522	5′-ATCTGTAGGAGAACCTATGGGAAC-3′	Intron forward primer for Southern blotting	47
oMC746/oBD523	5′-CACGTAATAAATATCTGGACGTAAAA-3′	Intron reverse primer for Southern blotting	47
oMC747	5′-TCAACGGAAGATCAGGATGATTTA-3′	*sigK* qPCR (CD1230)	
oMC748	5′-CATATGTTGCTAATCGAGTTCCTTTAT-3′	*sigK* qPCR (CD1230)	
oMC756	5′-TGGCAAGTAACAATAACAACAACAG-3′	*sspA* qPCR (CD2688)	
oMC757	5′-CCATTTGTTGTTCAGCCATTTCA-3′	*sspA* qPCR (CD2688)	

[a] Underlining indicates sequence-specific sites within gene of interest for intron retargeting.

BHI medium. The membrane-specific dyes, FM4-64 and MitoTracker Green, were added to a final concentration of 165 µM and 100 nM, respectively, and incubated for 30 min at room temperature. Slides were prepared by first applying a thin layer of 1.0 % agarose to the slide, followed by application of 8 µl of the concentrated culture onto the agarose bed. Fluorescence microscopy was performed using a 100X 1.49 NA oil immersion objective on a Nikon Structured Illumination Microscope (N-SIM). At least three fields of view for each strain were used to calculate the percentage of cells entering sporulation from two independent experiments. The percentage of sporulating cells was defined as the number of cells possessing polar septa or partially/completely engulfed forespores divided by the total number of cells.

Southern Blot Analysis. Genomic DNA from *C. difficile* strains 630Δ*erm*, MC296, MC301 and MC307 were isolated from overnight cultures as previously described (42). 6 µg of DNA from each strain was digested with HindIII (NEB), separated on a 0.7% agarose gel and transferred onto Hybond-N+ nylon membranes (GE Healthcare). DNA was then fixed to the membranes by UV crosslinking. Southern blot analysis was performed using the DIG high prime labeling and detection kit (Roche). An intron-specific probe was prepared by PCR using primers OBD522 and OBD523 as previously described (47).

Spore Preparation and Quantification. To prepare spores for animal studies, strains for spore preparation were grown in BHIS broth overnight and 100 µl spread onto 70:30 agar plates (36). Plates were then incubated for 48 h to allow spores to form. Following incubation, cells were scraped from the plates, resuspended in 5 ml of phosphate-buffered saline (PBS), pelleted at 3000 x g for 15 min, and resuspended in 5 ml of PBS. The resuspended cells were then combined 1:1 with 95% ethanol and incubated at room

temperature for 1 h to kill all non-spores present. Spores were then pelleted, washed twice in PBS and resuspended in 5 ml of fresh PBS. Spore suspensions were then heated to 70°C for 20 min, followed by addition of 1% BSA to prevent spores from sticking to each other and plastic or glass surfaces. Spore preparations were serially plated in PBS with 1% BSA to determine the number of CFU present and diluted prior to use. Spores were stored in glass tubes at room temperature.

Quantitative reverse transcription PCR analysis (qRT-PCR). Samples of *C. difficile* grown in 70:30 sporulation medium were harvested into 1:1 ethanol:acetone and RNA purified as previously described (42, 48). RNA isolated from hamster cecal contents was treated identically except cells were mechanically disrupted using a bead-beater for twice as long (a total of 6 min per sample). cDNA synthesis was performed with random hexamers using the Tetro cDNA Synthesis Kit (Bioline) and either 50 ng (samples isolated from *in vitro* cultures) or 200 ng (samples isolated from cecal contents) cDNA per reaction was used for qPCR analysis. qPCR analysis was performed using the SensiMix SYBR & Fluorescein Kit (Bioline) and a BioRad CFX96 Real Time System as previously described (49). Mock cDNA synthesis reaction mixtures containing no reverse transcriptase were performed to control for genomic contamination in subsequent amplifications. Primers used for qPCR reactions were designed using the PrimerQuest tool by IDT (http://www.idtdna.com/Scitools/Applications/Primerquest) and primer efficiencies were determined for each primer set prior to use. qPCR reactions were performed in technical triplicate for each cDNA sample and primer pair. qPCR was performed on cDNA isolated from a minimum of three biological replicates. Results are presented as the means and standard error of the means of the data obtained. Results were calculated by the

comparative cycle threshold method (50), with the amplified target sequence normalized to the internal control transcript, *rpoC*. The two-tailed Student's *t* test was used to compare the transcriptional ratios of the variable to control sets as indicated.

Animal Studies. Female Syrian golden hamsters (*Mesocricetus auratus*) between 70-120 g were purchased from Charles River Laboratories and maintained in an ABSL-2 facility in the Emory University Division of Animal Resources. Animals were housed individually in sterile cages and were fed a standard rodent diet and water *ad libitum*. Five days prior to inoculation with *C. difficile*, hamsters were administered a single dose of clindamycin (30 mg kg^{-1}) by oral gavage to perturb the intestinal microbiota and induce susceptibility to infection (51, 52). At 5 days post-antibiotic treatment, hamsters were administered approximately 500 spores of a single strain of *C. difficile* and monitored for symptoms of disease (weight loss, lethargy, diarrhea and "wet tail"). Hamsters were weighed at least once per day and fecal samples were collected daily for enumeration of spores. Cohorts of 5-6 animals were tested per strain, and experiments were performed a minimum of two times. Negative control animals that were treated with clindamycin, but not administered *C. difficile* were included in all experiments. Animals were considered moribund if 1) they had lost 15% or more of their starting weight or 2) if they presented with diarrhea, lethargy and wet tail. Animals meeting either of these criteria were euthanized to prevent unnecessary suffering. Hamsters were euthanized by CO_2 asphyxiation followed by thoracotomy as a secondary method of euthanasia. At the time of death, animals infected with either the 630Δ*erm* or MC307 strains were necropsied and cecal contents were collected and stored in an 1:1 acetone:ethanol solution at -80°C. All animal studies were performed with prior approval from the Emory University Institutional Animal Care and

Use Committee (IACUC). Differences in spores recovered from fecal samples were analyzed by ANOVA (Single Factor; Microsoft Excel). Differences in hamster survival between those infected with *C. difficile* 630Δ*erm* and either MC296 (*opp*), MC301 (*app*) or MC307 (*opp app*) were analyzed using the Log-rank test (Graphpad Prism).

Accession numbers. *C. difficile* strain 630 (GenBank accession NC_009089.1); *C. difficile* strain R20291 (NC_013316.1). The accession numbers for individual genes mentioned in the text are listed in Table 2.

RESULTS

Identification of Opp and App transporters in *C. difficile*

The *opp* and *app* operons were identified on the chromosome of the sequenced strain 630 as CD0853-CD0857 and CD2670-CD2674, respectively (53, 54). The *app* genes are arranged in two apparently divergently transcribed operons (*appABC* and *appDF*), while the *opp* genes appear to be organized as a single transcription unit (*oppBCADF*) (Fig. 1). Similar to oligopeptide transporters found in other Gram-positive bacteria, both the *app* and *opp* regions encode an apparent extracellular substrate binding protein (*appA/oppA*), two apparent integral membrane permeases (*appBC*/*oppBC*) and two apparent cytoplasmic ATP-binding proteins (*appDF/oppDF*). Orthologs of the *opp* and *app* oligopeptide transporters are common to many bacterial species and often two or more analogous transport systems are encoded in the genomes of Gram-positive bacteria (17, 55-58). In the latter cases, the systems may have overlapping or redundant functions (57). Although the predicted App and Opp protein sequences are orthologous to oligopeptide transport

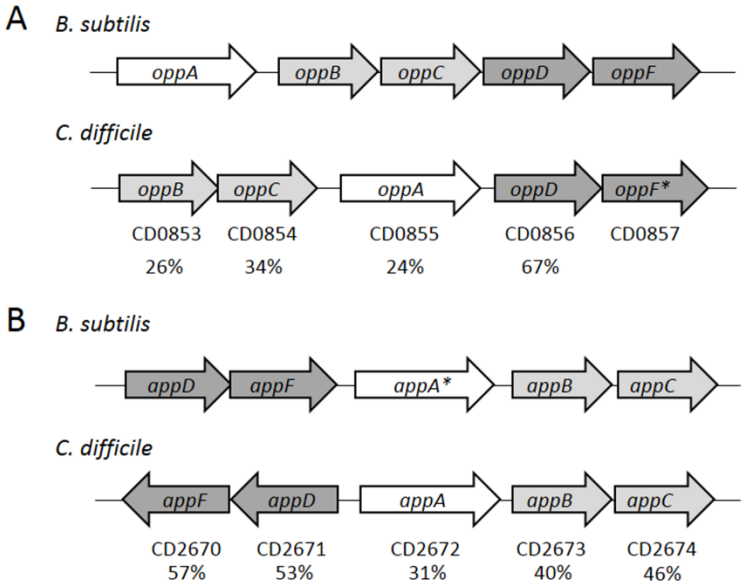

Figure 1. Identification of oligopeptide transporter systems in *C. difficile*. Comparison of the *opp* (A) and *app* (B) operons in *B. subtilis* 168 (GenBank accession no. AL009126) and *C. difficile* 630 (AM180355). OppA/AppA are solute-binding lipoproteins, OppBC/AppBC are transmembrane proteins and OppDF/AppDF are ATP-binding proteins. An asterisk (*) indicates a pseudogene; OppF is annotated as a pseudogene in *C. difficile* 630 as well as AppA in *B. subtilis* 168 (57). Numbers below the arrows represent percent identity in proteins to the corresponding *B. subtilis* sequences.

systems found in other bacteria (Fig. 1), the individual App and Opp proteins of *C. difficile* have only modest amino acid identity to one another (*e.g.*, 29% identity between OppA and AppA); therefore, the specific functions of these transporters in *C. difficile* could not be assumed from their sequence similarities. In previous *C. difficile* studies, the *opp* operon was found to be repressed by the global transcriptional regulators CodY and CcpA and by glucose, implying that the Opp transporter is involved in adaptation to nutrient limiting conditions (42, 59). In addition, SigH, the alternative sigma factor involved in the transition to stationary phase, was shown to differentially affect transcription of the *app* and *opp* genes (60). In a *sigH* mutant, transcription of the *opp* genes was decreased while *app* transcripts were increased, suggesting that the transporters are regulated differently during the adaptation to stationary phase in TY medium (60). However, our transcriptional analysis of *app* and *opp* expression in cells grown in sporulation medium (70:30 broth; (36)) revealed that expression of *appA* and *oppB* genes increases similarly throughout the transition to stationary phase (Supplementary File S2A).

Disruption of the *opp* and *app* operons results in increased spore formation

In the model spore-forming Firmicute, *Bacillus subtilis*, the Opp (Spo0K) and App transporters are responsible for the uptake of small, quorum-signaling peptides that stimulate competence and sporulation (12, 57). In *B. subtilis*, the absence of functional App and Opp transporters results in a significant sporulation defect (61, 62). *C. difficile* does not encode orthologs of either the PhrA peptide or the competence stimulating factor, PhrC (CSF) (18), but unrelated peptides with similar activities could potentially be transported by the oligopeptide transporters. To test whether the Opp and App transporter systems have

a role in regulating the entry into sporulation in *C. difficile*, we introduced insertional mutations into the first genes of the *app* and *opp* operons (*appA* and *oppB*). To do so, we used a Targetron-based group II intron, which was retargeted for integration into *appA* at nucleotide 439 and into *oppB* at nucleotide 178 of the coding sequences, respectively (see Methods). The locations of the insertions were confirmed by Southern blot analysis (Supplementary File S3). Both the *appA* and *oppB* insertional mutations greatly reduced expression of all the downstream genes in each operon, as evidenced by qRT-PCR analysis (Supplementary File S2B and C).

The *app* and *opp* null mutants (MC296 and MC301) were tested for the frequency of spore formation after 24 h of growth in 70:30 sporulation medium by measuring the number of ethanol-resistant spores recovered and normalizing this to the number of viable cells present at T_2 as described in the Materials and Methods (36). We observed a sporulation frequency of ~0.1% in the parent strain, 630Δ*erm* (Fig. 2A). Low sporulation frequencies in *C. difficile* have been observed in other studies (1, 63, 64); however, the percentage of spore formation reported is widely variable depending on the strain, media and methods used to enumerate spores (63). As shown in Figure 2A, the *opp* mutant had the same low frequency of spore formation as the parent strain. In contrast, the *app* null mutant produced an average of 10-fold more ethanol-resistant spores than did the parent strain (Fig. 2A). To determine if the Opp and App transporter systems have overlapping or redundant roles in mediating sporulation frequency, a double mutant strain containing both the *oppB* and *appA* insertional disruptions was created (MC307). The *opp app* double mutant produced ~20-fold more spores than did the parent strain (Fig. 2A). These data suggest that the App transporter influence sporulation frequency in *C. difficile* while

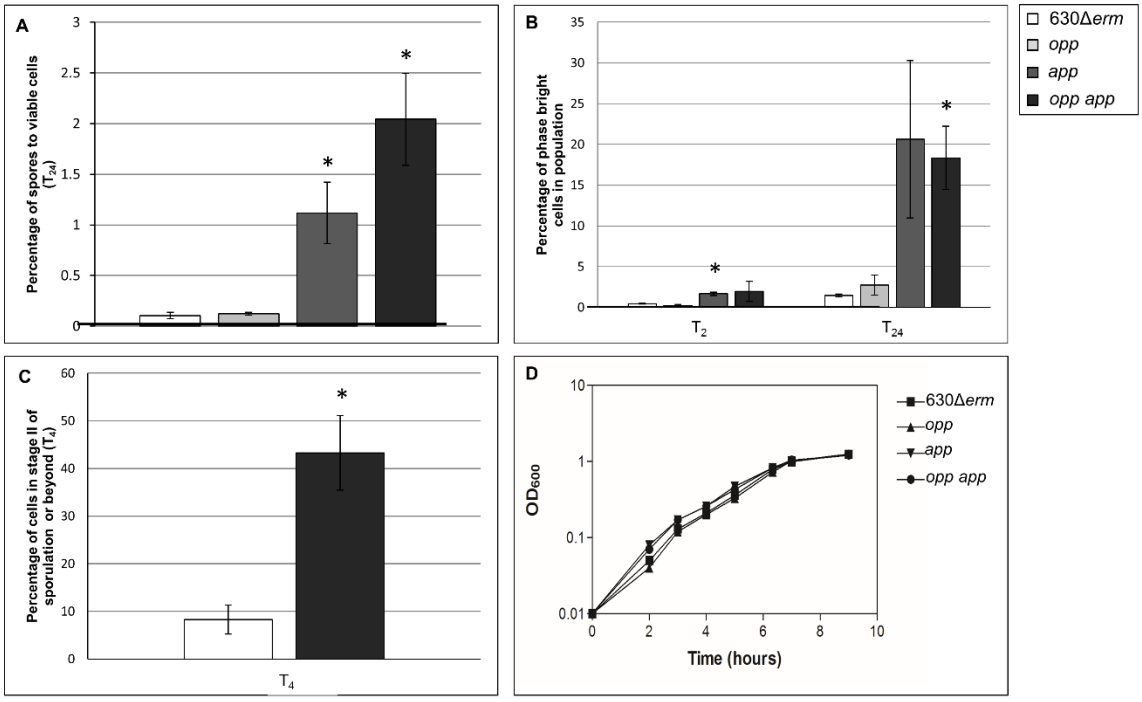

Figure 2. Disruption of the *opp* and *app* operons results in an increase in sporulation frequencies. (A) Sporulation frequency (CFU ml^{-1} ethanol resistant spores) of 630Δ*erm*, MC296 (*opp*), MC301 (*app*) and MC307 (*opp app*) grown in 70:30 sporulation medium at T_{24}. (B) Percentage of phase-bright spores assessed by phase-contrast microscopy. (C) Percentage of cells that have a polar septum or partially/completely engulfed forespores assessed by fluorescence microscopy using the membrane-specific dye, FM4-64. (D) Representative growth curve of 630Δ*erm*, MC296 (*opp*), MC301 (*app*) and MC307 (*opp app*) grown in 70:30 sporulation medium. The means and standard error of the means for spore counts of at least two biological replicates are shown (*, $P \leq 0.05$ by two-tailed Student's *t* test).

the Opp transporter does not appear to affect sporulation *in vitro*.

Using phase-contrast microscopy, we followed the rate of sporulation in the parent and the transporter mutant strains (Fig. 3A). Phase-dark prespores and phase-bright spores were visible by the second hour of stationary phase (T_2) in all strains; however, the *app* and *opp app* mutants produced more spores than the wild-type by T_2 (3.7-fold and 4.3-fold higher, respectively) and T_{24} (14.1-fold and 12.5-fold higher, respectively; Fig. 2B). To further define sporulation initiation in the parent strain and the *opp app* mutant, we performed fluorescence microscopy using the membrane-specific dye FM4-64 (65, 66). This technique enables the identification of cells that have asymmetric sporulation septa (Stage II) as well as partial or complete engulfment of the prespore (Stage III). At T_4, more cells were in Stage II or beyond in the transporter mutant (43.2 ± 7.8%) than in the wild-type strain (8.3 ± 3.0%; Fig. 2C and 3B). There was no significant difference in growth rate of the parent, *app*, *opp* or *opp app* strain in 70:30 or BHIS media (Fig. 2C; data not shown). These results indicate that these oligopeptide transporters are not essential for growth or for detection of population density under the conditions tested. Surprisingly, the increased sporulation rate of *C. difficile* App transporter mutants contrasts dramatically with the roles of analogous transporters in other spore-forming species, suggesting that peptide transport plays a distinctly different role in *C. difficile* spore formation (21, 57).

The sporulation phenotypes of the *opp* and *opp app* transporter mutants were fully rescued when plasmid copies of the *opp* operon were used to complement the disrupted transporters. Expression of the *app* operons from their native promoters on a plasmid did not effectively complement either the *app* or the *opp app* double mutant

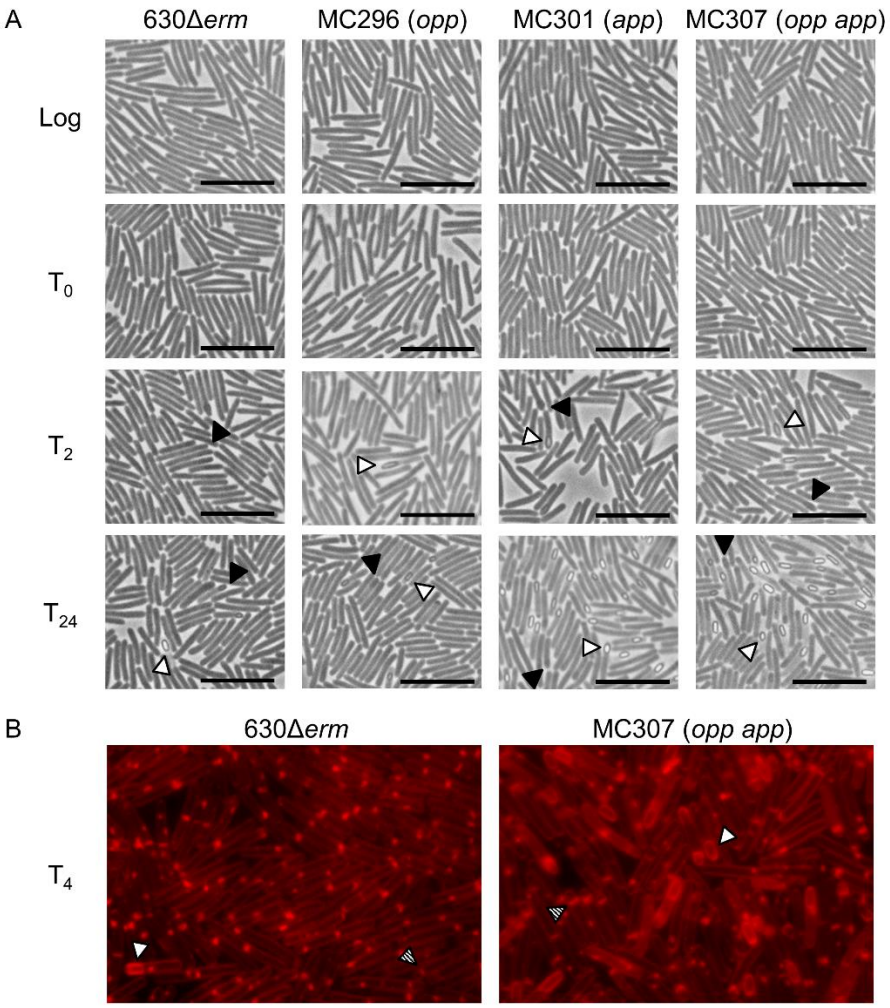

Figure 3. Oligopeptide transporter mutants hypersporulate and form spores earlier than the wild-type strain. (A) Phase contrast microscopy of 630Δ*erm*, MC296 (*opp*), MC301 (*app*) and MC307 (*opp app*) grown in 70:30 sporulation medium. Filled arrowheads indicate phase-dark prespores, while open arrowheads point to phase-bright mature spores. Scale bars represent 10 μm. (B) Fluorescence microscopy of 630 Δ*erm* and MC307 (*opp app*) grown in 70:30 sporulation medium and stained with FM4-64. Open arrowheads designate partially or completely engulfed forespores, and patterned arrowheads represent cells with polar septa. For both phase contrast and fluorescence microscopy, samples were removed at indicated times and prepared for microscopy as described in the Materials and Methods.

(Supplementary File S4). We performed transcriptional analysis to determine the levels of *opp* and *app* expression from plasmids in the complemented strains. Transcript levels of *oppB* were increased ~25-fold in the respective complemented strains (MC322 and MC323) while *appA* and *appD* transcript levels were upregulated ~60-120-fold in the respective complemented strains (MC331 and MC334; Supplementary File S5). These data reveal that expression of the *app* operons in *trans* results in significantly increased levels of *app* transcript compared to the native *app* during log phase growth. Increased *app* transcription may result in a dysfunctional App system that may cause additional stress on the strains harboring plasmid copies of the *app* operons. We were unable to complement the transporter mutants in single copy on the chromosome with current technologies due to size constraints (>5 kb) and toxicity issues. Notably, the sporulation frequency was increased in all strains containing a plasmid, including those with only the vector control (data not shown). This increase in sporulation may be due to the energy burden of the plasmid or the addition of thiamphenicol to the medium for plasmid maintenance, although these possibilities are not mutually exclusive.

Loss of Opp and App affects the expression of genes required for initiation of spore formation

The increased sporulation frequencies of the *app* and *opp app* transporter mutants may result from earlier and/or higher transcription of key sporulation-specific genes or other post-exponential phase control genes during growth. To determine if sporulation-dependent gene expression correlates with the increased sporulation phenotype of the *app* and *opp app* mutants, we analyzed early sporulation gene expression during growth in

70:30 sporulation medium, starting with the master regulator of sporulation, Spo0A. Spo0A is a DNA-binding protein that directly and indirectly regulates many stationary phase processes, including sporulation. *spo0A* transcription is regulated by multiple global regulators, including positive autoregulation of its own transcription, and Spo0A activity in other spore-formers is tightly controlled at multiple levels by transcriptional, post-transcriptional and post-translational mechanisms (3, 59, 60, 67, 68). Expression of *spo0A* was slightly elevated (~1.5-fold) in the *opp app* double mutant during exponential growth phase compared to the parent strain (Fig. 4A). We also analyzed gene expression of *murG*, which is a direct target of active Spo0A (69). *murG* transcript levels increased in the *app* and *opp app* mutants at at the T_4 and T_8 timepoints (~3-fold compared to the parent strain; Fig. 4B), indicating that more Spo0A is active and Spo0A-dependent gene expression is upregulated in the absence of the App transporter.

To determine if subsequent sporulation-specific gene transcription differs in the transporter mutants, we used qRT-PCR to analyze the expression of sporulation sigma factors and genes dependent upon activation of each sigma factor. qRT-PCR analysis was performed to assess expression and activities of the sporulation sigma factors. SigF (σ^F) controls early forespore-specific sporulation gene expression (47, 69, 70). Transcript analysis revealed that the level of *sigF* mRNA is increased in the *app* and the *opp app* transporter mutants at T_4 and T_8 (~4-fold and ~2-fold, respectively; Fig. 4C), and expression of a σ^F-dependent gene, *gpr*, is also up at T_4 (~8-fold) and T_8 (~10-fold) compared to the parent strain (Fig. 4D). *gpr* transcript levels were ~4-8-fold higher in the *app* single mutant and the *opp app* double mutant at T_2. These data indicate that σ^F gene expression and activity is increased in the App transporter mutants in stationary phase.

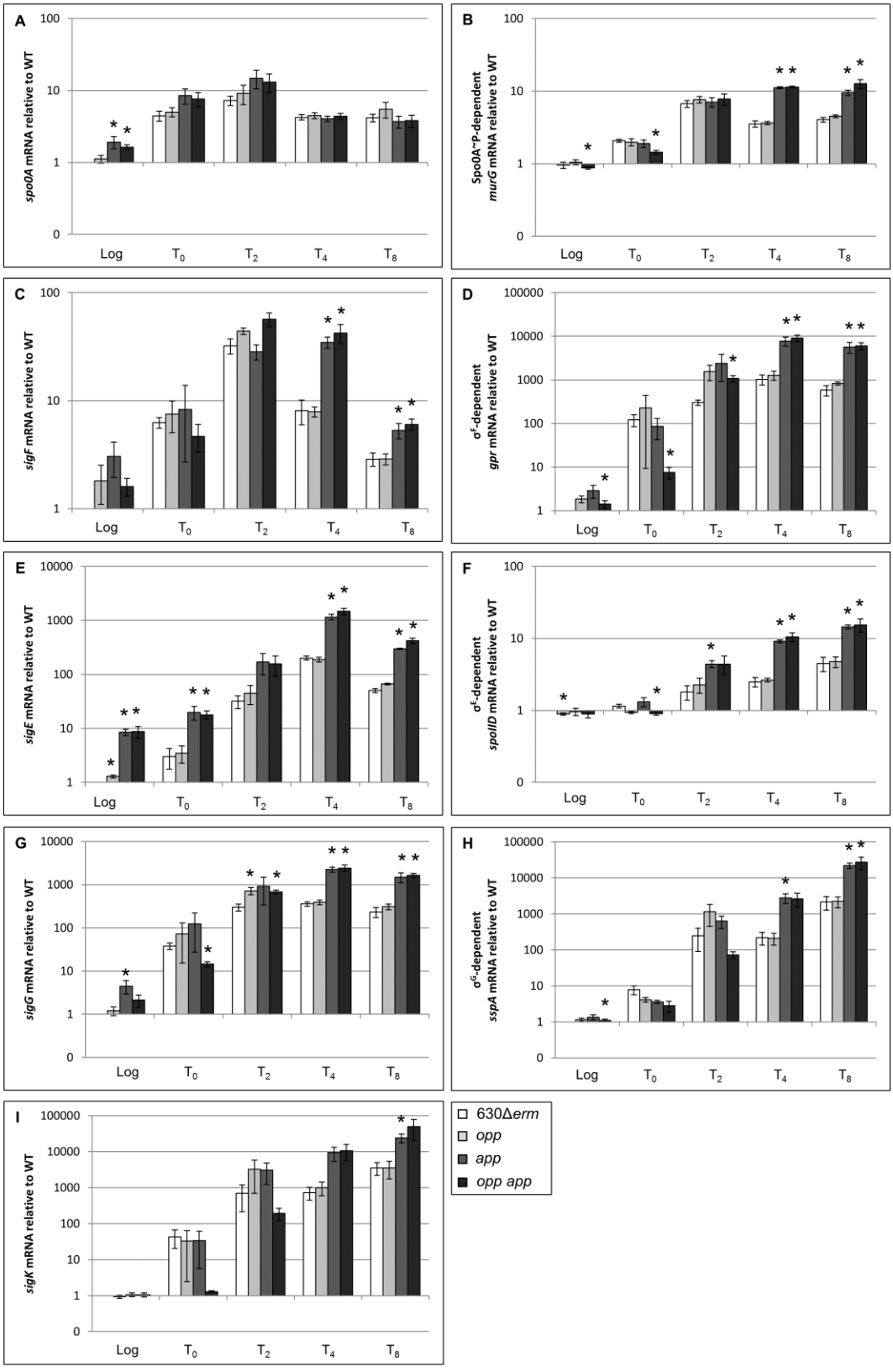
A
spo0A mRNA relative to WT
B
Spo0A~P-dependent murG mRNA relative to WT
C
sigF mRNA relative to WT
D
σF-dependent gpr mRNA relative to WT
E
sigE mRNA relative to WT
F
σE-dependent spoIID mRNA relative to WT
G
sigG mRNA relative to WT
H
σG-dependent sspA mRNA relative to WT
I
sigK mRNA relative to WT
Log
T0
T2
T4
T8
630Δerm
opp
app
opp app

Figure 4. Effects of oligopeptide transporters on the regulation of sporulation-specific gene transcription. qRT-PCR analysis of *spo0A* (A), the Spo0A-dependent gene, *murG* (B), *sigF* (C), the σ^F-dependent gene, *gpr* (D), *sigE* (E), the σ^E-dependent gene *spoIID* (F), *sigG* (G), the σ^G-dependent gene *sspA* (H) and *sigK* (I) expression in 630Δ*erm*, MC296 (*opp*), MC301 (*app*) and MC307 (*opp app*) grown in 70:30 sporulation medium to an OD_{600} of 0.5, 1.0 (T_0) and two, four and eight hours after T_0 (T_2, T_4 and T_8) as described in the Materials and Methods. The means and standard error of the means of at least three biological replicates are shown (*, $P \leq 0.05$ by a two-tailed Student's *t* test).

SigE (σ^E) is responsible for transcription of early sporulation-specific genes in the mother cell compartment (71), and *sigE* transcription is directly upregulated only by active Spo0A (47, 69, 70, 72). The *app* and *opp app* mutants expressed more *sigE* transcript than the parent cells during logarithmic and stationary phases of growth (~5-10-fold; Fig. 4E). In addition, analysis of the σ^E-dependent transcript, *spoIID*, showed that σ^E-dependent gene expression is increased ~3-fold at stationary phase in the *app* and *opp app* mutant compared to the parent or *opp* mutant strains (Fig. 4F; (73)). These data indicate that early sporulation-specific gene expression proceeds earlier and is increased at stationary phase in the *app* and *opp app* mutants.

To further understand sporulation progression in the transporter mutants, we analyzed expression of additional mid-to-late stage sporulation genes. In contrast to *B. subtilis*, the order and synchronization of sporulation sigma factor expression and activation are not tightly regulated in *C. difficile* (47, 69, 70). But increased expression of these sigma factors and genes dependent on their activation is positively correlated with the later stages of spore development. Transcription of *sigG*, the forespore-specific late sigma factor, was higher (~2-3-fold) in the App transporter mutants by T_2, and was increased even further (~6-7-fold) by later time points (Fig. 4G). Transcription of the σ^G-dependent gene, *sspA*, was also increased in stationary phase in the *app* and *opp app* mutants (~10-13-fold; Fig. 4H). σ^K, the late-stage mother cell sigma factor, contains a 14.6 kb *skin*^{cd} element that must be excised prior to translation (74). σ^K activity is necessary for efficient sporulation but is not strictly required for the formation of heat-resistant spores (70). Expression of *sigK* in the App transporter mutants was upregulated ~7-15-fold at T_4 and T_8 (Fig. 4I). Together, these results demonstrate that sporulation genes are expressed

earlier and at higher levels in the *app* and *opp app* mutants, consistent with their increased sporulation phenotype observed *in vitro*.

In *B. subtilis*, transcription of *opp* and *app* is repressed by the DNA-binding negative regulator of sporulation, ScoC (75). *C. difficile* contains a putative *scoC* ortholog (CD0852) encoded upstream of the *opp* operon. Preliminary data suggests that overexpression of CD0852 in *C. difficile* negatively impacts sporulation (Edwards and McBride, unpublished data). qRT-PCR analysis revealed that *oppB*, *appA* and *appD* transcript levels at stationary phase of growth (T_2) were unchanged between the wild-type strain and a CD0852 overexpressing strain (Supplementary File S2D), suggesting that the *opp* and *app* operons are not under the same regulatory control in *C. difficile* as they are in *B. subtilis.* Altogether, these results indicate that the Opp and App transporters play a different role in controlling sporulation in *C. difficile* than in other spore-forming bacteria, such as *B. subtilis.*

Absence of Opp and App transporters influences expression of the transcriptional regulator, SinR, and its putative inhibitor, SinI

As the Opp and App transporters are not predicted to have direct DNA binding domains or regulatory capabilities, the changes in gene expression observed in the transporter mutants likely result from the lack of peptides feeding into nutritional and/or regulatory pathways. The two global regulatory proteins known to control cellular responses to nutrient availability in *C. difficile* are CodY and CcpA (39, 42, 76-78). CodY is a DNA-binding transcriptional regulator that controls expression of hundreds of genes in response to the intracellular availability of GTP and branched-chain amino acids (76, 79). CcpA mediates

carbon catabolite repression in many Gram-positive bacteria, including *C. difficile*, and controls expression of a wide range of genes involved in sugar uptake, fermentation and amino acid metabolism (59, 77). Both CodY and CcpA directly control the transcription of gene products required for sporulation initiation and toxin synthesis in *C. difficile* and other sporulating pathogens (59, 76, 77, 80, 81). To determine if either of these global regulatory proteins is involved in mediating the increase in spore formation observed in the *app* and *opp app* mutants, we investigated the effects of the transporter mutations on CodY-mediated and CcpA-mediated gene regulation. qRT-PCR analysis of samples taken during logarithmic and stationary phase growth in 70:30 sporulation medium revealed that expression of multiple CodY- and CcpA-dependent genes was not greatly influenced in the transporter mutants (Supplementary File S6), suggesting that inactivation of the transporters is likely not signaling through CodY or CcpA to control sporulation. However, we found that expression of the CcpA-dependent *sinR* transcript was greatly elevated in logarithmic and stationary phases (~30-80-fold) in the *app* and *opp app* mutants (Fig. 5A; (59)). In other species, SinR acts as a repressor of sporulation by directly inhibiting Spo0A transcription (82). Although transcription of *sinR* is elevated, the SinR protein can be held inactive in a complex with its repressor, SinI (83). *C. difficile* encodes a *sinI*-like regulator adjacent to *sinR*. Transcription of the putative *sinI* was also amplified in the *app* and *opp app* mutants (~80-125-fold; Fig. 5B), suggesting that the inhibitory effects of SinR on sporulation are negated by SinI in *C. difficile*. These results suggest that the function of the App transporter influences *sinR* and *sinI* gene expression, and potentially initiation of spore formation, under the conditions tested.

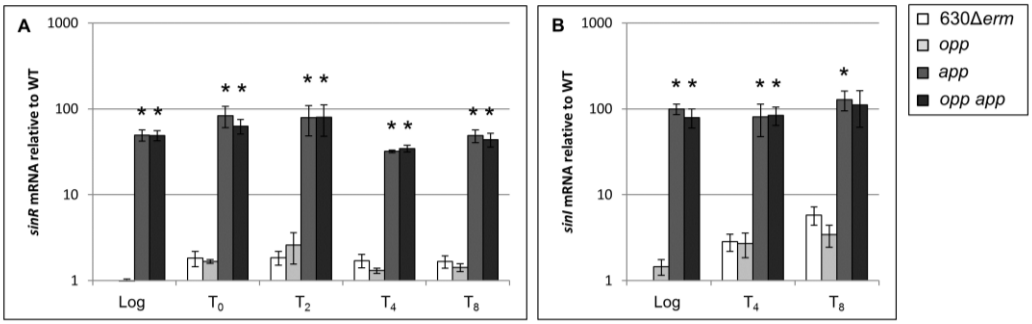

Figure 5. Effects of oligopeptide transporters on regulation of *sinR* and *sinI* gene expression. qRT-PCR analysis of expression of *sinR* (A) and *sinI* (B) in 630Δ*erm*, MC296 (*opp*), MC301 (*app*) and MC307 (*opp app*) grown in 70:30 sporulation medium to an OD_{600} of 0.5, 1.0 (T_0) and two, four and/or eight hours after T_0 (T_2, T_4 and T_8) as described in the Materials and Methods. The means and standard error of the means of at least three biological replicates are shown (*, $P \leq 0.05$ by a two-tailed Student's *t* test).

Loss of Opp and App transporters results in increased virulence and spore formation in an animal model of *C. difficile* infection (CDI)

The conditions that lead to sporulation of *C. difficile* within the intestinal environment are not known. What is known is that *C. difficile* initiates sporulation *in vivo* within hours after germination and that *de novo* spores can be detected within 12 hours post-inoculation (84, 85). To determine if the Opp and App transporters influence sporulation frequency in the intestinal environment, we examined the effects of the *opp, app* and *opp app* mutations on spore production and virulence in the hamster model of CDI, a model that has been used for more than 35 years to study acute disease caused by *C. difficile* (52, 86, 87). Female Syrian golden hamsters were infected by gavage with approximately 500 spores of either the parental strain or the transporter mutants. Animals were closely monitored for symptoms of disease, and fecal samples were retrieved to quantify the number of spores shed during infection as described in the Materials and Methods. As shown in Figure 6A, hamsters infected with the *opp, app* and *opp app* null mutants shed greater numbers of spores in feces than those infected with the parent strain at 24 hours post-infection. On average, *opp app* infected animals shed approximately 8.5 times the number spores per gram of feces than wild-type infected animals. The number of vegetative cells present in feces was not calculated, as exposure to oxygen could not be eliminated from our test conditions. Likewise, the number of spores located throughout the gastrointestinal tract was not assessed. All of the hamsters infected with transporter mutant strains succumbed to disease more rapidly than those infected with the parent strain (*P*-value < 0.02, log rank test; mean time to morbidity: 630Δ*erm*, 45.1 ± 6.4 h; MC296 (*opp*), 38.4 ± 6.6 h; MC301

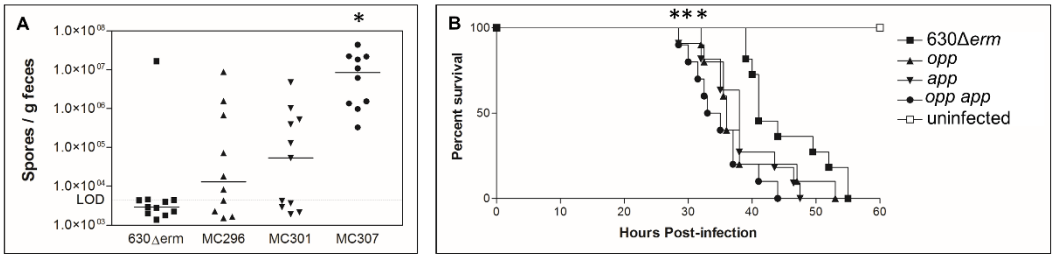

Figure 6. Effects of oligopeptide transporters on fecal spore output and virulence in the hamster model of CDI. (A) Total number of *C. difficile* spores per gram of feces recovered 24 h post-infection from two independent experiments of clindamycin-treated Syrian golden hamsters inoculated with 500 spores of *C. difficile* 630Δ*erm*, MC296 (*opp*), MC301 (*app*) or MC307 (*opp app*). Fecal samples were weighed, resuspended in 1X PBS, and plated onto TCCFA plates (95, 96), and *C. difficile* colonies were enumerated after 48 h. The line represents the median for each strain while the limit of detection (LOD) is demarcated by the dotted line (4.51 x 10^3 CFU/g). (B) Kaplan-Meier survival curve representing the cumulative results from the same two independent experiments described in (A). Hamsters infected with mutant strains succumbed more rapidly than those infected with the parent strain (Mean time to morbidity: 630Δerm, 45.1 ± 6.4 h; MC296 (opp), 38.4 ± 6.6 h; MC301 (app), 38.2 ± 5.8 h; and MC307 (opp app), 35.0 ± 4.9 h; *P*-value < 0.02 for all mutants, log rank test).

(*app*), 38.2 ± 5.8 h; and MC307 (*opp app*), 35.0 ± 4.9 h; Fig. 6B). Hamsters infected with the transporter mutant strains lost weight and displayed symptoms earlier than wild-type infected animals, but no statistically significant difference in weight loss at the time of death between hamsters infected with different strains was observed (data not shown). All animals lost a minimum of 6% of their bodyweight during infection. As described in other studies, a few animals did not exhibit wet tail prior to becoming moribund (88). The hypervirulent phenotypes of the transporter mutants demonstrate that these transporters are not required for growth *in vivo*, but instead may indirectly function to influence toxin production or other virulence phenotypes in the host. Interestingly, the *opp* mutant exhibited a similar phenotype to the *app* mutant in the hamster model of CDI, despite the fact that no significant phenotype was observed *in vitro.* These data demonstrate that the strain 630 *opp* operon, containing *oppF* as a pseudogene, has an important function *in vivo*.

Production of both toxin A and toxin B by *C. difficile* 630 is required for full virulence in the hamster model of CDI; however, toxin A or toxin B alone is sufficient to cause disease (89). It was previously established that toxin production in *C. difficile* is upregulated in response to nutrient limitation, including amino acid starvation (39, 76-78, 90). We asked whether expression of the toxin genes, *tcdA* and *tcdB*, were upregulated in the transporter mutants *in vitro*, potentially explaining the observed hypervirulent phenotype. qRT-PCR analysis of the *tcdA* and *tcdB* transcripts revealed that there was no difference in toxin expression between the parent strain, *opp*, *app*, and *opp app* mutants, except for a modest decrease in *tcdA* transcript levels in the *app* and the *opp app* mutants in late stationary phase, when grown in 70:30 medium (Fig. 7A and B). To determine if toxin production is upregulated *in vivo*, RNA was isolated from cecal contents obtained at

the time of death from hamsters infected with the parental or *opp app* mutant strains. As a control, we analyzed RNA isolated from the cecal contents of an uninfected animal. We recovered insignificant levels of *rpoC* transcript and were unable to detect specific *C. difficile* gene transcripts in uninfected controls (data not shown). qRT-PCR analysis revealed that *tcdA* and *tcdB* gene expression was slightly decreased in hamsters infected with the *opp app* double mutant compared to those infected with the parent strain (Fig. 7C). Additionally, transcript levels of the sporulation-specific gene, *sigE*, and the negative transcriptional regulator, *sinR*, in RNA isolated from cecal contents were slightly increased in the *opp app* double mutant (Fig. 7C). These results suggest that the hypervirulent phenotype observed in hamsters infected with the oligopeptide transporter mutants is not directly correlated with toxin production but may be related to the increased sporulation phenotype characterized *in vitro* and *in vivo*.

DISCUSSION

As an obligate anaerobe, the ability of *C. difficile* to form dormant spores is required for the effective spread of this pathogen from host to host. Although spore morphology and the stages of spore formation are similar among the spore-forming Firmicutes, the regulatory pathways and environmental triggers that control the initiation of sporulation are not conserved in *C. difficile* (2). While spore formation begins in response to nutrient deprivation and cell density in the well-studied model organism *B. subtilis* (91), these signals were not previously proven to influence sporulation of *C. difficile* (59, 77). Oligopeptide transporters have been shown to activate sporulation in other bacteria through

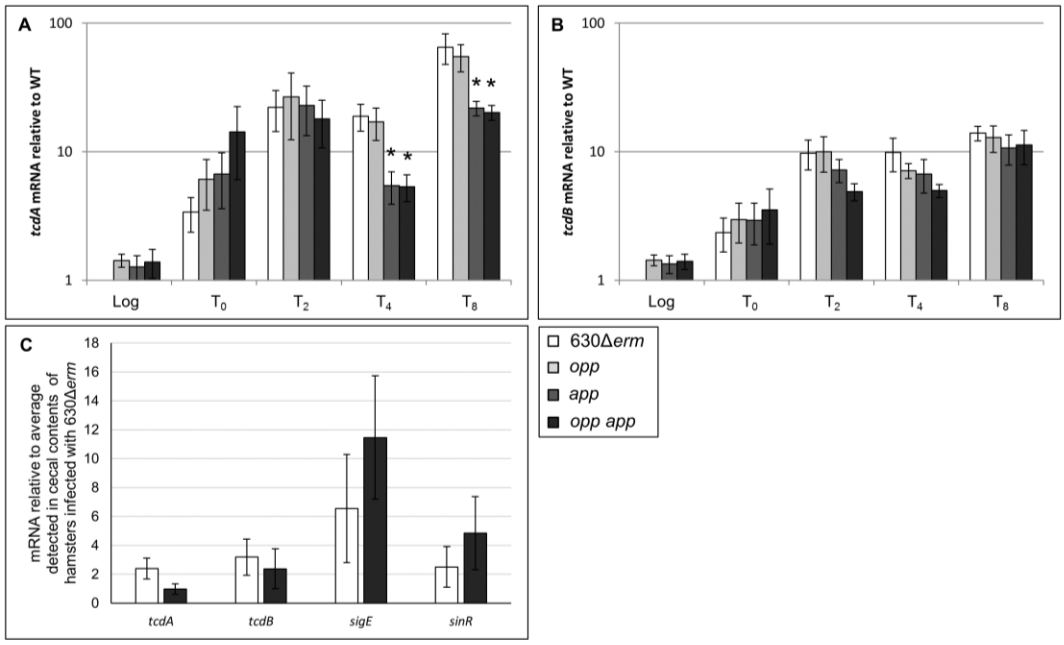

Figure 7. Effects of oligopeptide transporters on toxin gene expression. (A, B) qRT-PCR analysis of *tcdA* (A) and *tcdB* (B) expression in 630Δ*erm*, MC296 (*opp*), MC301 (*app*) and MC307 (*opp app*) grown in 70:30 sporulation medium to an OD_{600} of 0.5, 1.0 (T_0) and two, four and eight hours after T_0 (T_2, T_4 and T_8) as described in the Materials and Methods. The means and standard error of the means of four biological replicates are shown (*, $P \leq 0.05$ by a two-tailed Student's *t* test). (C) qRT-PCR analysis of *tcdA*, *tcdB*, *sigE* and *sinR* gene expression in cecal contents from hamsters infected with either 630Δ*erm* or MC307 (*opp app*). The means and standard error of the means of samples from at least 10 animals per strain are shown (*, $P \leq 0.05$ by a two-tailed Student's *t* test).

the import of specific quorum sensing peptides that indirectly upregulate early sporulation-specific gene transcription (11-13). In the current work, we demonstrate that the Opp and App transporters play a significant role in *C. difficile* sporulation and pathogenesis *in vitro* and *in vivo*, but the role of these transporters in *C. difficile* sporulation differs from that in *B. subtilis*.

Our initial hypothesis was that the *C. difficile* oligopeptide transporters could be stimulating sporulation in a cell density-dependent manner through the uptake of small secreted quorum-signaling peptides, similar to the Phr peptides found in spore-forming *Bacillus* species (11-13). Surprisingly, the Opp and App transporters negatively impact both the initiation of spore formation and the total number of spores formed both *in vitro* and *in vivo* (Fig. 2A-C, 3 and 6A). The data indicate that in *C. difficile* these transporters are not required for cell density-dependent signaling. This conclusion is supported by the absence of *phr* orthologs in the *C. difficile* genome (2, 53, 54). Furthermore, addition of spent medium to exponentially growing wild-type *C. difficile* did not affect early sporulation gene expression (data not shown). One hypothesis is that *C. difficile* could import a signaling peptide that inhibits sporulation at low cell density; however, this is unlikely given the ecological niche that *C. difficile* inhabits. Alternatively, other quorum-sensing mechanisms, such as *agr*, may potentially fill the role of the Phr system. *C. difficile* may not maintain high population density within the gastrointestinal tract due to frequent diarrhea which results in the transient availability of nutrients and other metabolites. We favor the hypothesis that the Opp and App transporters serve to import general oligopeptides that influence the intracellular nutrient availability (Fig. 8). In an effort to demonstrate directly the function of the transporters, we examined the efficacy of peptide

uptake (random 5 and 10-amino acid peptides) in the wild-type and mutant strains in the absence of other amino acid sources; however, both the wild-type and transporter mutants were unable to utilize 5 or 10-amino acid peptides as their sole source of amino acids in minimal defined medium (data not shown) (39). Our data suggest that without the Opp and App transporters, sporulation-specific gene programming is initiated, likely due to intracellular signals of poor nutritional and environmental conditions. Finally, the regulation of *opp* and *app* expression is different in *C. difficile* and *B. subtilis* (Supplementary File S2D), suggesting that *opp* and *app* are not influencing sporulation similarly in both species.

In contrast to *B. subtilis*, mutants defective in the Opp and App transporters express the genes for certain sporulation regulatory proteins (Spo0A, σ^F and σ^E) prematurely, suggesting that their normal activities cause uptake of peptide nutrients that block initiation of sporulation (Fig. 4). Although the complete genetic pathway through which transporter activity signals sporulation initiation remains unclear, our data suggests that these signals may involve both SinR and SinI (Fig. 5). In *B. subtilis*, SinR functions as a homo-tetramer and directly represses a number of genes involved in sporulation initiation, including *spo0A* (82). However, SinR repression is relieved by SinI, which inhibits SinR-mediated repression by disrupting the SinR homotetramer and forming an inactive heterodimer with SinR (83). In *C. difficile*, *sinR* and *sinI* (CD2214 and CD2215) appear to form an operon. Our preliminary data indicate that the increase in *sinI* transcript levels was greater than the increase in *sinR* levels in the *app* and *opp app* mutants as cells entered sporulation (Fig. 5). These data suggest that *sinR* and *sinI* are differentially expressed, as they are in *B. subtilis* (92). A greater increase in SinI compared to SinR levels would allow for efficient

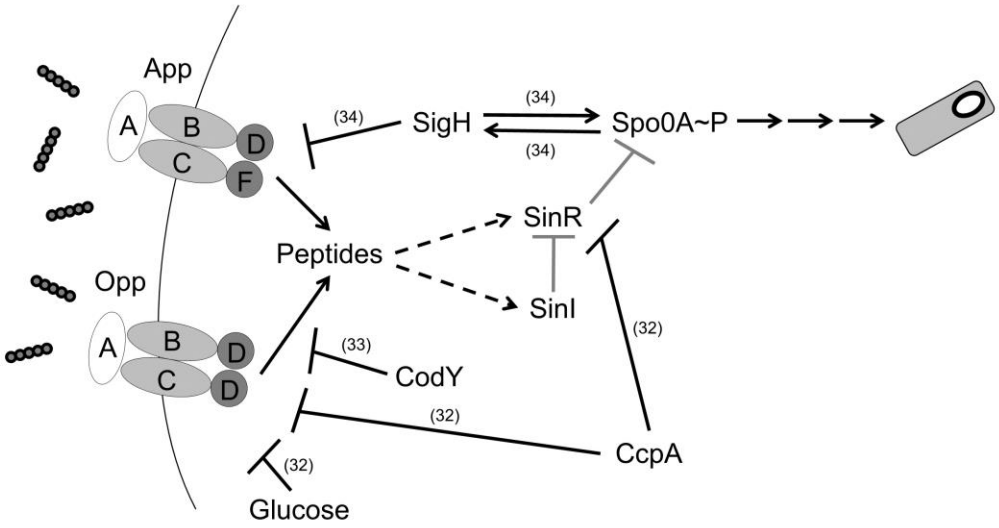

Figure 8. Proposed model of Opp and App influence on sporulation initiation in *C. difficile*. Opp and App mediate uptake of peptides as a nutrient source. The acquisition of peptides indirectly influences both *sinR* and *sinI* gene expression, through an unknown mechanism, which represses sporulation-specific gene expression. Gray arrows represent putative regulatory effects while hatched arrows indicate indirect effects. References for experimentally proven interactions are denoted in parentheses.

deactivation of SinR-mediated *spo0A* repression if these proteins function like the *B. subtilis* orthologs. Even a minimal increase in *spo0A* transcription and subsequent activation may lead to the increases in transcription observed for the Spo0A~P-dependent gene, *sigE* (Fig. 4E), and influence overall sporulation frequencies in the transporter mutants.

The regulatory pathway through which intracellular amino acid available is signaled to initiate sporulation is unknown. Our data suggest that CodY and CcpA are not involved in this regulatory pathway as expression of many direct targets, including the *tcdA* and *tcdB* genes (76, 77), are unchanged or non-uniformly changed in the transporter mutants (Fig. 7 and Supplementary File S6). Determining the intermediates of the genetic pathway linking Opp and App transporter activity and sporulation initiation would provide further evidence of the environmental signals that regulate the initiation of spore formation and would fill a gap in the regulatory mechanisms governing the early stages of sporulation in *C. difficile* as well as nutrient acquisition.

The Opp and App transporters are not expected to be the only mechanisms by which *C. difficile* could obtain extracellular amino acids. *C. difficile* has orthologs of several individual amino acid importer proteins found in other species, as well as putative di- and tri- peptide transporters. Additional oligopeptide transporters present in other spore-forming species include the Dpp and DtpT transporter systems (93, 94). However, the *C. difficile* genome does not contain a full *dpp* transporter complement. The *C. difficile* genome possesses two DtpT orthologs (CD2260 and CD3036) but their role in peptide uptake is unknown.

In our assays, the Opp transporter did not have a significant effect on sporulation *in vitro*. However, overexpression of the *opp* operon from its native promoter in the *opp app* mutant fully restored wild-type levels of sporulation, indicating that this operon encodes a functional oligopeptide transporter (Supplementary File S4). In addition, the loss of *opp* function *in vivo* was similar to the loss of *app*, and the *opp app* double mutant resulted in more fecal spores and a shorter time to morbidity compared to the single mutants in the hamster model of infection (Fig. 6). Interestingly, a functional *oppF* gene is required in *B. subtilis* for competence but not for sporulation (61, 62). However, no natural competence system in *C. difficile* has been described nor does the genome contain many of the orthologs required for competence in *Bacillus* species (53).

It is unclear why the transporter mutants are hypervirulent despite no apparent increase in toxin expression within the population, *in vitro* or *in vivo* (Fig. 7). Our data do not account for differences in secreted toxin between the transporter mutants and the parent strain. When these experiments were performed we did not anticipate the increased virulence of the mutants or the need to acquire additional samples for toxin assays. However, no difference was observed in the rate of lysis between the parent strain and the transporter mutants *in vitro*, which would result in toxin release. (Supplementary File S7). It is possible that the inability to import peptides as a nutrient source affects growth rates or results in upregulation of other virulence factors, such as motility or adherence, *in vivo*. We did not observe a difference in growth rates (Fig. 2D) or in motility (data not shown) between the parent strain and the transporter mutants *in vitro*. Although inactivation of Opp and App results in increased sporulation and increased virulence *in vivo*, it does not necessarily suggest that these phenotypes are controlled through the same regulatory

pathways. Further studies are needed to determine how nutrient limitation and increased sporulation contribute to more severe disease *in vivo*.

Finally, differences in ecological niches could explain much of the divergence in the genetic mechanisms of spore initiation and patterns of gene expression between bacterial spore-formers. We hypothesize that *C. difficile* does not require a quorum sensing system to signal sporulation because *C. difficile* never inhabits an environment where cell population density directly correlates with nutrient availability. Rather, *C. difficile* relies on directly linking the availability of environmental nutrients, such as amino acids, to the regulatory mechanisms controlling sporulation initiation. This direct link between nutrient availability and sporulation allows *C. difficile* to quickly respond to changing conditions as the organism transits through the gastrointestinal tract. The findings presented here provide the first evidence of a nutritional link to spore formation in *C. difficile* and represent a mechanism that could potentially be exploited to prevent spore formation, and thereby, spread of the pathogen.

ACKNOWLEDGEMENTS

We give special thanks to Charles Moran, Linc Sonenshein and members of the McBride lab for helpful suggestions and discussions during the course of this work, Aimee Shen for the *spo0A* plasmid and Jeremy Boss for use of the BioRad CFX96 Real Time PCR Detection System. This research was supported by the U.S. National Institutes of Health through research grants DK087763 and DK101870 to S.M.M. and was supported in part by the Emory University Integrated Cellular Imaging Microscopy Core. The content of

this manuscript is solely the responsibility of the authors and does not necessarily reflect the official views of the National Institutes of Health.

REFERENCES

1. **Deakin, L. J., S. Clare, R. P. Fagan, L. F. Dawson, D. J. Pickard, M. R. West, B. W. Wren, N. F. Fairweather, G. Dougan, and T. D. Lawley.** 2012. The Clostridium difficile spo0A gene is a persistence and transmission factor. Infection and immunity **80:**2704-2711.

2. **Paredes, C. J., K. V. Alsaker, and E. T. Papoutsakis.** 2005. A comparative genomic view of clostridial sporulation and physiology. Nature reviews. Microbiology **3:**969-978.

3. **Underwood, S., S. Guan, V. Vijayasubhash, S. D. Baines, L. Graham, R. J. Lewis, M. H. Wilcox, and K. Stephenson.** 2009. Characterization of the sporulation initiation pathway of Clostridium difficile and its role in toxin production. Journal of bacteriology **191:**7296-7305.

4. **Jones, S. W., C. J. Paredes, B. Tracy, N. Cheng, R. Sillers, R. S. Senger, and E. T. Papoutsakis.** 2008. The transcriptional program underlying the physiology of clostridial sporulation. Genome biology **9:**R114.

5. **Steiner, E., J. Scott, N. P. Minton, and K. Winzer.** 2012. An agr quorum sensing system that regulates granulose formation and sporulation in Clostridium acetobutylicum. Applied and environmental microbiology **78:**1113-1122.

6. **Durre, P., and C. Hollergschwandner.** 2004. Initiation of endospore formation in Clostridium acetobutylicum. Anaerobe **10:**69-74.

7. **Paredes-Sabja, D., A. Shen, and J. A. Sorg.** 2014. Clostridium difficile spore biology: sporulation, germination, and spore structural proteins. Trends in microbiology **22:**406-416.

8. **Edwards, A. N., and S. M. McBride.** 2014. Initiation of sporulation in Clostridium difficile: a twist on the classic model. FEMS microbiology letters.

9. **Sonenshein, A. L.** 2000. Control of sporulation initiation in Bacillus subtilis. Current opinion in microbiology **3:**561-566.

10. **Perego, M., and J. A. Hoch.** 1996. Cell-cell communication regulates the effects of protein aspartate phosphatases on the phosphorelay controlling development in Bacillus subtilis. Proceedings of the National Academy of Sciences of the United States of America **93:**1549-1553.

11. **Magnuson, R., J. Solomon, and A. D. Grossman.** 1994. Biochemical and genetic characterization of a competence pheromone from B. subtilis. Cell **77:**207-216.

12. **Lazazzera, B. A., J. M. Solomon, and A. D. Grossman.** 1997. An exported peptide functions intracellularly to contribute to cell density signaling in B. subtilis. Cell **89:**917-925.

13. **Perego, M.** 1997. A peptide export-import control circuit modulating bacterial development regulates protein phosphatases of the phosphorelay. Proceedings of the National Academy of Sciences of the United States of America **94:**8612-8617.

14. **Perego, M., C. Hanstein, K. M. Welsh, T. Djavakhishvili, P. Glaser, and J. A. Hoch.** 1994. Multiple protein-aspartate phosphatases provide a mechanism for the integration of diverse signals in the control of development in B. subtilis. Cell **79:**1047-1055.

15. **Hiles, I. D., M. P. Gallagher, D. J. Jamieson, and C. F. Higgins.** 1987. Molecular characterization of the oligopeptide permease of Salmonella typhimurium. Journal of molecular biology **195:**125-142.

16. **Pearce, S. R., M. L. Mimmack, M. P. Gallagher, U. Gileadi, S. C. Hyde, and C. F. Higgins.** 1992. Membrane topology of the integral membrane components, OppB and OppC, of the oligopeptide permease of Salmonella typhimurium. Molecular microbiology **6:**47-57.

17. **Pearce, B. J., A. M. Naughton, and H. R. Masure.** 1994. Peptide permeases modulate transformation in Streptococcus pneumoniae. Molecular microbiology **12:**881-892.

18. **Solomon, J. M., B. A. Lazazzera, and A. D. Grossman.** 1996. Purification and characterization of an extracellular peptide factor that affects two different developmental pathways in Bacillus subtilis. Genes & development **10:**2014-2024.

19. **Ruhfel, R. E., D. A. Manias, and G. M. Dunny.** 1993. Cloning and characterization of a region of the Enterococcus faecalis conjugative plasmid, pCF10, encoding a sex pheromone-binding function. Journal of bacteriology **175:**5253-5259.

20. **Leonard, B. A., A. Podbielski, P. J. Hedberg, and G. M. Dunny.** 1996. Enterococcus faecalis pheromone binding protein, PrgZ, recruits a chromosomal oligopeptide permease system to import sex pheromone cCF10 for induction of conjugation. Proceedings of the National Academy of Sciences of the United States of America **93:**260-264.

21. **Gominet, M., L. Slamti, N. Gilois, M. Rose, and D. Lereclus.** 2001. Oligopeptide permease is required for expression of the Bacillus thuringiensis plcR regulon and for virulence. Molecular microbiology **40:**963-975.

22. **Slamti, L., and D. Lereclus.** 2002. A cell-cell signaling peptide activates the PlcR virulence regulon in bacteria of the Bacillus cereus group. The EMBO journal **21:**4550-4559.

23. **Guyer, C. A., D. G. Morgan, and J. V. Staros.** 1986. Binding specificity of the periplasmic oligopeptide-binding protein from Escherichia coli. Journal of bacteriology **168:**775-779.

24. **Tame, J. R., G. N. Murshudov, E. J. Dodson, T. K. Neil, G. G. Dodson, C. F. Higgins, and A. J. Wilkinson.** 1994. The structural basis of sequence-independent peptide binding by OppA protein. Science **264:**1578-1581.

25. **Kunji, E. R., A. Hagting, C. J. De Vries, V. Juillard, A. J. Haandrikman, B. Poolman, and W. N. Konings.** 1995. Transport of beta-casein-derived peptides by the oligopeptide transport system is a crucial step in the proteolytic pathway of Lactococcus lactis. The Journal of biological chemistry **270:**1569-1574.

26. **Sleigh, S. H., P. R. Seavers, A. J. Wilkinson, J. E. Ladbury, and J. R. Tame.** 1999. Crystallographic and calorimetric analysis of peptide binding to OppA protein. Journal of molecular biology **291:**393-415.

27. **Lanfermeijer, F. C., F. J. Detmers, W. N. Konings, and B. Poolman.** 2000. On the binding mechanism of the peptide receptor of the oligopeptide transport system of Lactococcus lactis. The EMBO journal **19:**3649-3656.

28. **Nisman, B., M. Raynaud, and G. N. Cohen.** 1948. Extension of the Stickland reaction to several bacterial species. Archives of biochemistry **16:**473.

29. **Bouillaut, L., W. T. Self, and A. L. Sonenshein.** 2013. Proline-dependent regulation of Clostridium difficile Stickland metabolism. Journal of bacteriology **195:**844-854.

30. **Stickland, L. H.** 1934. Studies in the metabolism of the strict anaerobes (genus Clostridium): The chemical reactions by which Cl. sporogenes obtains its energy. The Biochemical journal **28:**1746-1759.

31. **Stickland, L. H.** 1935. Studies in the metabolism of the strict anaerobes (genus Clostridium): The oxidation of alanine by Cl. sporogenes. IV. The reduction of glycine by Cl. sporogenes. The Biochemical journal **29:**889-898.

32. **Stickland, L. H.** 1935. Studies in the metabolism of the strict anaerobes (Genus Clostridium): The reduction of proline by Cl. sporogenes. The Biochemical journal **29:**288-290.

33. **Smith, C. J., S. M. Markowitz, and F. L. Macrina.** 1981. Transferable tetracycline resistance in Clostridium difficile. Antimicrobial agents and chemotherapy **19:**997-1003.

34. **Purcell, E. B., R. W. McKee, S. M. McBride, C. M. Waters, and R. Tamayo.** 2012. Cyclic diguanylate inversely regulates motility and aggregation in Clostridium difficile. Journal of bacteriology **194:**3307-3316.

35. **Sorg, J. A., and S. S. Dineen.** 2009. Laboratory maintenance of Clostridium difficile. Current protocols in microbiology **Chapter 9:**Unit9A 1.

36. **Putnam, E. E., A. M. Nock, T. D. Lawley, and A. Shen.** 2013. SpoIVA and SipL are Clostridium difficile spore morphogenetic proteins. Journal of bacteriology.

37. **Bouillaut, L., S. M. McBride, and J. A. Sorg.** 2011. Genetic manipulation of Clostridium difficile. Current protocols in microbiology **Chapter 9:**Unit 9A 2.

38. **Edwards, A. N., J. M. Suarez, and S. M. McBride.** 2013. Culturing and Maintaining Clostridium difficile in an Anaerobic Environment. Journal of visualized experiments : JoVE.

39. **Karlsson, S., L. G. Burman, and T. Akerlund.** 1999. Suppression of toxin production in Clostridium difficile VPI 10463 by amino acids. Microbiology **145 (Pt 7):**1683-1693.

40. **Luria, S. E., and J. W. Burrous.** 1957. Hybridization between *Escherichia coli* and *Shigella*. J Bacteriol **74:**461-476.

41. **Stabler, R. A., M. He, L. Dawson, M. Martin, E. Valiente, C. Corton, T. D. Lawley, M. Sebaihia, M. A. Quail, G. Rose, D. N. Gerding, M. Gibert, M. R. Popoff, J. Parkhill, G. Dougan, and B. W. Wren.** 2009. Comparative genome and phenotypic analysis of Clostridium difficile 027 strains provides insight into the evolution of a hypervirulent bacterium. Genome biology **10:**R102.

42. **Dineen, S. S., S. M. McBride, and A. L. Sonenshein.** 2010. Integration of metabolism and virulence by Clostridium difficile CodY. Journal of bacteriology **192:**5350-5362.

43. **Karberg, M., H. Guo, J. Zhong, R. Coon, J. Perutka, and A. M. Lambowitz.** 2001. Group II introns as controllable gene targeting vectors for genetic manipulation of bacteria. Nature biotechnology **19:**1162-1167.

44. **Ho, T. D., and C. D. Ellermeier.** 2011. PrsW is required for colonization, resistance to antimicrobial peptides, and expression of extracytoplasmic function sigma factors in Clostridium difficile. Infection and immunity **79:**3229-3238.

45. **Heap, J. T., O. J. Pennington, S. T. Cartman, G. P. Carter, and N. P. Minton.** 2007. The ClosTron: a universal gene knock-out system for the genus Clostridium. Journal of microbiological methods **70:**452-464.

46. **McBride, S. M., and A. L. Sonenshein.** 2011. The dlt operon confers resistance to cationic antimicrobial peptides in Clostridium difficile. Microbiology **157:**1457-1465.

47. **Saujet, L., F. C. Pereira, M. Serrano, O. Soutourina, M. Monot, P. V. Shelyakin, M. S. Gelfand, B. Dupuy, A. O. Henriques, and I. Martin-Verstraete.** 2013. Genome-Wide Analysis of Cell Type-Specific Gene Transcription during Spore Formation in Clostridium difficile. PLoS genetics **9:**e1003756.

48. **McBride, S. M., and A. L. Sonenshein.** 2011. Identification of a genetic locus responsible for antimicrobial peptide resistance in Clostridium difficile. Infection and immunity **79:**167-176.

49. **Suarez, J. M., A. N. Edwards, and S. M. McBride.** 2013. The Clostridium difficile cpr Locus is Regulated by a Non-contiguous Two-component System in Response to Type A and B Lantibiotics. Journal of bacteriology.

50. **Schmittgen, T. D., and K. J. Livak.** 2008. Analyzing real-time PCR data by the comparative C(T) method. Nature protocols **3:**1101-1108.

51. **Bartlett, J. G., A. B. Onderdonk, R. L. Cisneros, and D. L. Kasper.** 1977. Clindamycin-associated colitis due to a toxin-producing species of Clostridium in hamsters. The Journal of infectious diseases **136:**701-705.

52. **Chang, T. W., J. G. Bartlett, S. L. Gorbach, and A. B. Onderdonk.** 1978. Clindamycin-induced enterocolitis in hamsters as a model of pseudomembranous colitis in patients. Infection and immunity **20:**526-529.

53. **Sebaihia, M., B. W. Wren, P. Mullany, N. F. Fairweather, N. Minton, R. Stabler, N. R. Thomson, A. P. Roberts, A. M. Cerdeno-Tarraga, H. Wang, M. T. Holden, A. Wright, C. Churcher, M. A. Quail, S. Baker, N. Bason, K. Brooks, T. Chillingworth, A. Cronin, P. Davis, L. Dowd, A. Fraser, T. Feltwell, Z. Hance, S. Holroyd, K. Jagels, S. Moule, K. Mungall, C. Price, E. Rabbinowitsch, S. Sharp, M. Simmonds, K. Stevens, L. Unwin, S. Whithead, B. Dupuy, G. Dougan, B. Barrell, and J. Parkhill.** 2006. The multidrug-resistant human pathogen Clostridium difficile has a highly mobile, mosaic genome. Nature genetics **38:**779-786.

54. **Monot, M., C. Boursaux-Eude, M. Thibonnier, D. Vallenet, I. Moszer, C. Medigue, I. Martin-Verstraete, and B. Dupuy.** 2011. Reannotation of the genome sequence of Clostridium difficile strain 630. Journal of medical microbiology **60:**1193-1199.

55. **Doeven, M. K., J. Kok, and B. Poolman.** 2005. Specificity and selectivity determinants of peptide transport in Lactococcus lactis and other microorganisms. Molecular microbiology **57:**640-649.

56. **Monnet, V.** 2003. Bacterial oligopeptide-binding proteins. Cellular and molecular life sciences : CMLS **60:**2100-2114.

57. **Koide, A., and J. A. Hoch.** 1994. Identification of a second oligopeptide transport system in Bacillus subtilis and determination of its role in sporulation. Molecular microbiology **13:**417-426.

58. **Peltoniemi, K., E. Vesanto, and A. Palva.** 2002. Genetic characterization of an oligopeptide transport system from Lactobacillus delbrueckii subsp. bulgaricus. Archives of microbiology **177:**457-467.

59. **Antunes, A., E. Camiade, M. Monot, E. Courtois, F. Barbut, N. V. Sernova, D. A. Rodionov, I. Martin-Verstraete, and B. Dupuy.** 2012. Global transcriptional control by glucose and carbon regulator CcpA in Clostridium difficile. Nucleic acids research **40:**10701-10718.

60. **Saujet, L., M. Monot, B. Dupuy, O. Soutourina, and I. Martin-Verstraete.** 2011. The key sigma factor of transition phase, SigH, controls sporulation, metabolism, and virulence factor expression in Clostridium difficile. Journal of bacteriology **193:**3186-3196.

61. **Perego, M., C. F. Higgins, S. R. Pearce, M. P. Gallagher, and J. A. Hoch.** 1991. The oligopeptide transport system of Bacillus subtilis plays a role in the initiation of sporulation. Molecular microbiology **5:**173-185.

62. **Rudner, D. Z., J. R. LeDeaux, K. Ireton, and A. D. Grossman.** 1991. The spo0K locus of Bacillus subtilis is homologous to the oligopeptide permease locus and is required for sporulation and competence. Journal of bacteriology **173:**1388-1398.

63. **Burns, D. A., J. T. Heap, and N. P. Minton.** 2010. The diverse sporulation characteristics of Clostridium difficile clinical isolates are not associated with type. Anaerobe **16:**618-622.

64. **Boudry, P., C. Gracia, M. Monot, J. Caillet, L. Saujet, E. Hajnsdorf, B. Dupuy, I. Martin-Verstraete, and O. Soutourina.** 2014. Pleiotropic role of the RNA chaperone protein Hfq in the human pathogen Clostridium difficile. Journal of bacteriology.

65. **Pogliano, J., N. Osborne, M. D. Sharp, A. Abanes-De Mello, A. Perez, Y. L. Sun, and K. Pogliano.** 1999. A vital stain for studying membrane dynamics in bacteria: a novel mechanism controlling septation during Bacillus subtilis sporulation. Molecular microbiology **31:**1149-1159.

66. **McBride, S. M., A. Rubio, L. Wang, and W. G. Haldenwang.** 2005. Contributions of protein structure and gene position to the compartmentalization of the regulatory proteins sigma(E) and SpoIIE in sporulating Bacillus subtilis. Molecular microbiology **57:**434-451.

67. **Chastanet, A., and R. Losick.** 2011. Just-in-time control of Spo0A synthesis in Bacillus subtilis by multiple regulatory mechanisms. Journal of bacteriology **193:**6366-6374.

68. **Errington, J.** 2003. Regulation of endospore formation in Bacillus subtilis. Nature reviews. Microbiology **1:**117-126.

69. **Fimlaid, K. A., J. P. Bond, K. C. Schutz, E. E. Putnam, J. M. Leung, T. D. Lawley, and A. Shen.** 2013. Global Analysis of the Sporulation Pathway of Clostridium difficile. PLoS genetics **9:**e1003660.

70. **Pereira, F. C., L. Saujet, A. R. Tome, M. Serrano, M. Monot, E. Couture-Tosi, I. Martin-Verstraete, B. Dupuy, and A. O. Henriques.** 2013. The Spore Differentiation Pathway in the Enteric Pathogen Clostridium difficile. PLoS genetics **9:**e1003782.

71. **Haldenwang, W. G.** 1995. The sigma factors of Bacillus subtilis. Microbiological reviews **59:**1-30.

72. **Satola, S., P. A. Kirchman, and C. P. Moran, Jr.** 1991. Spo0A binds to a promoter used by sigma A RNA polymerase during sporulation in Bacillus subtilis. Proceedings of the National Academy of Sciences of the United States of America **88:**4533-4537.

73. **Rong, S., M. S. Rosenkrantz, and A. L. Sonenshein.** 1986. Transcriptional control of the Bacillus subtilis spoIID gene. Journal of bacteriology **165:**771-779.

74. **Haraldsen, J. D., and A. L. Sonenshein.** 2003. Efficient sporulation in Clostridium difficile requires disruption of the sigmaK gene. Molecular microbiology **48:**811-821.

75. **Koide, A., M. Perego, and J. A. Hoch.** 1999. ScoC regulates peptide transport and sporulation initiation in Bacillus subtilis. Journal of bacteriology **181:**4114-4117.

76. **Dineen, S. S., A. C. Villapakkam, J. T. Nordman, and A. L. Sonenshein.** 2007. Repression of Clostridium difficile toxin gene expression by CodY. Molecular microbiology **66:**206-219.

77. **Antunes, A., I. Martin-Verstraete, and B. Dupuy.** 2011. CcpA-mediated repression of Clostridium difficile toxin gene expression. Molecular microbiology **79:**882-899.

78. **Dupuy, B., and A. L. Sonenshein.** 1998. Regulated transcription of Clostridium difficile toxin genes. Molecular microbiology **27:**107-120.

79. **Sonenshein, A. L.** 2007. Control of key metabolic intersections in Bacillus subtilis. Nature reviews. Microbiology **5:**917-927.

80. **Chateau, A., W. van Schaik, P. Joseph, L. D. Handke, S. M. McBride, F. M. Smeets, A. L. Sonenshein, and A. Fouet.** 2013. Identification of CodY targets in Bacillus anthracis by genome-wide in vitro binding analysis. Journal of bacteriology **195:**1204-1213.

81. **Chiang, C., C. Bongiorni, and M. Perego.** 2011. Glucose-dependent activation of Bacillus anthracis toxin gene expression and virulence requires the carbon catabolite protein CcpA. Journal of bacteriology **193:**52-62.

82. **Mandic-Mulec, I., L. Doukhan, and I. Smith.** 1995. The Bacillus subtilis SinR protein is a repressor of the key sporulation gene spo0A. Journal of bacteriology **177:**4619-4627.

83. **Bai, U., I. Mandic-Mulec, and I. Smith.** 1993. SinI modulates the activity of SinR, a developmental switch protein of Bacillus subtilis, by protein-protein interaction. Genes & development **7:**139-148.

84. **Janoir, C., C. Deneve, S. Bouttier, F. Barbut, S. Hoys, L. Caleechum, D. Chapeton-Montes, F. Pereira, A. Henriques, A. Collignon, M. Monot, and B. Dupuy.** 2013. Insights into the adaptive strategies and pathogenesis of Clostridium difficile from in vivo transcriptomics. Infection and immunity.

85. **Wilson, K. H., J. N. Sheagren, and R. Freter.** 1985. Population dynamics of ingested Clostridium difficile in the gastrointestinal tract of the Syrian hamster. The Journal of infectious diseases **151:**355-361.

86. **Douce, G., and D. Goulding.** 2010. Refinement of the hamster model of Clostridium difficile disease. Methods Mol Biol **646:**215-227.

87. **Best, E. L., J. Freeman, and M. H. Wilcox.** 2012. Models for the study of Clostridium difficile infection. Gut microbes **3:**145-167.

88. **Razaq, N., S. Sambol, K. Nagaro, W. Zukowski, A. Cheknis, S. Johnson, and D. N. Gerding.** 2007. Infection of hamsters with historical and epidemic BI types of Clostridium difficile. The Journal of infectious diseases **196:**1813-1819.

89. **Kuehne, S. A., S. T. Cartman, J. T. Heap, M. L. Kelly, A. Cockayne, and N. P. Minton.** 2010. The role of toxin A and toxin B in Clostridium difficile infection. Nature **467:**711-713.

90. **Yamakawa, K., T. Karasawa, S. Ikoma, and S. Nakamura.** 1996. Enhancement of Clostridium difficile toxin production in biotin-limited conditions. Journal of medical microbiology **44:**111-114.

91. **Errington, J.** 1993. Bacillus subtilis sporulation: regulation of gene expression and control of morphogenesis. Microbiological reviews **57:**1-33.

92. **Gaur, N. K., K. Cabane, and I. Smith.** 1988. Structure and expression of the Bacillus subtilis sin operon. Journal of bacteriology **170:**1046-1053.

93. **Mathiopoulos, C., J. P. Mueller, F. J. Slack, C. G. Murphy, S. Patankar, G. Bukusoglu, and A. L. Sonenshein.** 1991. A Bacillus subtilis dipeptide transport system expressed early during sporulation. Molecular microbiology **5:**1903-1913.

94. **Caldwell, R., R. Sapolsky, W. Weyler, R. R. Maile, S. C. Causey, and E. Ferrari.** 2001. Correlation between Bacillus subtilis scoC phenotype and gene expression determined using microarrays for transcriptome analysis. Journal of bacteriology **183:**7329-7340.

95. **George, W. L., V. L. Sutter, D. Citron, and S. M. Finegold.** 1979. Selective and differential medium for isolation of Clostridium difficile. Journal of clinical microbiology **9:**214-219.

96. **Wilson, K. H., J. Silva, and F. R. Fekety.** 1981. Suppression of Clostridium difficile by normal hamster cecal flora and prevention of antibiotic-associated cecitis. Infection and immunity **34:**626-628.

97. **Wust, J., and U. Hardegger.** 1983. Transferable resistance to clindamycin, erythromycin, and tetracycline in *Clostridium difficile*. Antimicrob Agents Chemother **23:**784-786.

98. **Hussain, H. A., A. P. Roberts, and P. Mullany.** 2005. Generation of an erythromycin-sensitive derivative of Clostridium difficile strain 630 (630Deltaerm) and demonstration that the conjugative transposon Tn916DeltaE enters the genome of this strain at multiple sites. Journal of medical microbiology **54:**137-141.

99. **Thomas, C. M., and C. A. Smith.** 1987. Incompatibility group P plasmids: genetics, evolution, and use in genetic manipulation. Annu Rev Microbiol **41:**77-101.

CHAPTER 8

APPENDIX IV - An Alkaline Phosphatase Reporter for use in *Clostridium difficile*

Adrianne N. Edwards, Ricardo A. Pascual, Kevin O. Childress, Kathryn L. Nawrocki, Emily C. Woods and Shonna M. McBride

This work was published in 2015 in *Anaerobe.*

K.L.N. performed experiments and generated Figure 2, and assisted with manuscript revision.

Article Citation:

Edwards, A. N., Pascual, R. A., Childress, K. O., Nawrocki, K. L., Woods, E. C., & McBride, S. M. (2015). An alkaline phosphatase reporter for use in *Clostridium difficile*. *Anaerobe, 32*, 98-104. doi: 10.1016/j.anaerobe.2015.01.002. PMCID 4385412

ABSTRACT

Clostridium difficile is an anaerobic, Gram-positive pathogen that causes severe gastrointestinal disease in humans and other mammals. *C. difficile* is notoriously difficult to work with and, until recently, few tools were available for genetic manipulation and molecular analyses. Despite the recent advances in the field, there is no simple or cost-effective technique for measuring gene transcription in *C. difficile* other than direct transcriptional analyses (*e.g.*, quantitative real-time PCR and RNA-seq), which are time-consuming, expensive and difficult to scale-up. We describe the development of an *in vivo* reporter assay that can provide qualitative and quantitative measurements of *C. difficile* gene expression. Using the *Enterococcus faecalis* alkaline phosphatase gene, *phoZ*, we measured expression of *C. difficile* genes using a colorimetric alkaline phosphatase assay. We show that inducible alkaline phosphatase activity correlates directly with native gene expression. The ability to analyze gene expression using a standard reporter is an important and critically needed tool to study gene regulation and design genetic screens for *C. difficile* and other anaerobic clostridia.

INTRODUCTION

Although *Clostridium difficile* is a major nosocomial pathogen that causes severe gastrointestinal disease, the molecular mechanisms that control pathogenesis in this bacterium are poorly understood. The primary reasons that *C. difficile* remains an understudied pathogen are that the bacterium has long been difficult to cultivate and genetically manipulate. First, *C. difficile* is a fastidious organism and a strict anaerobe. Thus, for optimal and consistent growth, *C. difficile* is typically cultivated in rich growth

medium within a strict anaerobic environment. Culture conditions notwithstanding, one of the greatest impediments has been the shortage of genetic tools for use in *C. difficile*.

Many of the molecular biology tools and techniques that are used to genetically manipulate other species have been difficult to adapt for *C. difficile.* However, techniques for studying *C. difficile* molecular biology have been developed in the past decade, including methods for gene disruption and plasmid transfer, random mutagenesis strategies and the application of next-generation sequencing technologies (1-7). Despite the advancements in molecular technologies over the past decade, genetic analysis of *C. difficile* remains a challenge.

The constraints of an anaerobic growth environment have been particularly problematic for the adaption of gene reporter technologies used in other bacteria. Reporter gene fusions are incredibly useful tools in the study of gene regulation and signal transduction, defining regulatory elements and promoters, and for the development of genetic screens (8). The most commonly used reporter gene fusions include colorimetric reporters, such as β-galactosidase (*lacZ*) and β-glucuronidase (*gusA*), fluorescent proteins (*e.g., gfp, dsRed, mCherry*), and chemiluminescent reporters (*i.e.*, luciferase; *luxAB*). Unfortunately, these reporters require oxygen for proper reporter protein folding or full enzymatic activity (9-12) (data not shown), and consequently have little utility in anaerobic bacteria. Antibiotic-based reporters, such as Chloramphenicol Acetyl Transferase (*cat*) and neomycin (*neo*), are excluded because *cat* is one of the few selectable markers available and because *C. difficile* has high intrinsic resistance to aminoglycosides. A cyan fluorescent protein (CFP) reporter (13), a mCherry reporter (14), and anaerobically-functioning fluorescent reporters have been described, including SNAP (15) and LOV-based fusions (16, 17). While these

fluorescent reporters are useful, visualization of activity can be difficult due to photo-bleaching and to high variability of fluorescence within a population of cells (13, 15-17). β-glucuronidase (*gusA*) reporters have been used in the heterologous host, *Clostridium perfringens*, an anaerobe that is somewhat aerotolerant, to measure *C. difficile*-specific gene expression (18). In addition, *gusA* reporters have been used in *C. difficile* (19); however, these assays exhibit low sensitivity and are cost-prohibitive.

While other methods are available for quantifying *C. difficile* gene transcription, including qRT-PCR, microarray and RNA-seq analyses, these techniques are expensive and require an investment in specialized equipment and enzymes. Since these methods are expensive and time-consuming, it is not practical to employ these techniques in large-scale genetic screens. In contrast, colorimetric reporter assays are relatively inexpensive and require a low investment in materials and reagents. In this study, we evaluate the alkaline phosphatase gene, *phoZ*, from *Enterococcus faecalis* as a transcriptional reporter for use in *C. difficile*. We report that *C. difficile* can express an active *phoZ* transcriptional fusion, which functions as a sensitive and quantifiable reporter of gene expression. This alkaline phosphatase reporter provides *C. difficile* researchers with a versatile new tool for assessing gene expression.

MATERIALS AND METHODS

Bacterial strains and growth conditions. The strains and plasmids used in this study are listed in **Table 1**. *Escherichia coli* strains were cultured at 37°C in LB (20) or BHIS medium (21) aerobically or anaerobically, and supplemented with 20 μg chloramphenicol ml^{-1} or 100 μg ampicillin ml^{-1}, as needed. *Enterococcus faecalis* was cultured on BHI or

Table 1
Bacterial Strains and plasmids.

Plasmid or strain	Relevant genotype or features	Source, construction or reference
Strains		
E. faecalis		
V583	Clinical isolate	[40,41]
E. coli		
HB101	F⁻ *mcrB mrr hsdS20*(r_B^- m_B^-) *recA13 leuB6 ara-14 proA2 lacY1 galK2 xyl-5 mtl-1 rpsL20*	B. Dupuy
MC101	HB101 pRK24	B. Dupuy
MC445	HB101 containing pRK24 and pMC358	This study
MC461	HB101 containing pRK24 and pMC368	This study
MC468	HB101 containing pRK24 and pMC375	This study
B. subtilis		
BS49	CU2189::Tn*916*	P. Mullany
MC472	BS49 Tn*916*::pMC370	This study
MC473	BS49 Tn*916*::pMC371	This study
C. difficile		
R20291	Clinical isolate	
630	Clinical isolate	[42]
630Δ*erm*	Erm^S derivative of strain 630	N. Minton [43]
MC324	630Δ*erm* pMC123	[25]
MC448	630Δ*erm* pMC358	This study
MC486	630Δ*erm* pMC368	This study
MC488	630Δ*erm* Tn*916*::*phoZ*	This study
MC489	630Δ*erm* Tn*916*::P*cprA*::*phoZ*	This study
MC499	630Δ*erm* pMC375	This study
Plasmids		
pRK24		Tra^+, Mob^+; *bla, tet*
pUC19	Cloning vector; *bla*	[44]
pSMB47	Tn*916* integrational vector; CmR, ErmR	[45] (GenBank U69267)
pMC123	*E. coli-C. difficile* shuttle vector; *bla, catP*	[37]
pMC211	pMC123 P*cprA*	[25]
pMC358	pMC123 *phoZ*	This study
pMC368	pMC123 P*cprA*::*phoZ*	This study
pMC370	pSMB47 *phoZ*	This study
pMC371	pSMB47 P*cprA*::*phoZ*	This study
pMC375	pMC123 P*dlt*::*phoZ*	This study

BHIS medium as previously described (22). *Clostridium difficile* strains were cultured at 37°C in an anaerobic chamber as previously detailed (23, 24). *C. difficile* strains were grown in BHIS medium supplemented with 2-10 μg thiamphenicol ml^{-1}, 5 μg erythromycin ml^{-1}, 0.5-5 μg nisin ml^{-1} or 100-400 μg XP (BCIP, 5-Bromo-4-chloro-3-indolyl phosphate; Sigma-Aldrich) ml^{-1} as indicated.

Strain and plasmid construction. *E. faecalis* strain V583 (GenBank accession AE016830) was used as a template for *phoZ* amplification. Oligonucleotides used for PCR and qRT-PCR are listed in **Table 2**. Isolation of plasmid DNA, PCR and cloning were performed using standard protocols. The 1477 bp *phoZ* coding sequence and upstream ribosomal binding site were amplified using primers oMC829/oMC830. This fragment was cloned into the *Bam*HI and *Sph*I sites of pMC123 (4) to create pMC358 (**Figure 1A**). pMC368 was created by cloning the P*cprA* fragment from pMC211 (25) as *Eco*RI/*Bam*HI into pMC358. pMC375 was created by amplifying a 600 bp fragment upstream of *dltD* with oMC850/oMC823 and cloning this fragment as *Eco*RI/*Bam*HI into pMC358. pMC370 was created by cloning the *phoZ* fragment from pMC358 as *Bam*HI/*Sph*I into pSMB47 (**Figure 1B**). To construct pMC371, the P*cprA::phoZ* insert was amplified from pMC368 using primers oMC909/oMC830, followed by digestion and cloning as a *Sal*I/*Sph*I fragment into pSMB47. Note that the *cat* cassette of pSMB47 is only functional as a selectable marker in *E. coli*. Sequencing of cloned DNA fragments was performed by Eurofins MWG Operon. Plasmid maps were created using SnapGene Viewer software.

pMC358, pMC368 and pMC375 were introduced into *E. coli* strain MC101 by transformation, resulting in strains MC445, MC461 and MC468, respectively. MC445, MC461 and MC468 were conjugated independently to *C. difficile* strain 630Δ*erm* as

Table 2
Oligonucleotides.

Primer	Sequence (5′→3′)	Use/location
oMC44	5′-CTAGCTGCTCCTATGTCTCACATC-3′	*rpoC* qPCR (CD0067) [4]
oMC45	5′-CCAGTCTCTCCTGGATCAACTA-3′	*rpoC* qPCR (CD0067) [4]
oMC96	5′- CGTTCAGGTCAATTCTCTCTAGGC -3′	*cprA* qPCR (CD1349) [4]
oMC97	5′- GGTCAAGACCATTTGTAGGCTC -3′	*cprA* qPCR (CD1349) [4]
oMC823	5′- gccggatccATTTTCTCTCCTCTAAAAATATTCAAA -3′	P*dltD* cloning (CD2854)
oMC829	5′- gccggatccGTCAATGTATGGGTAGATATGAAGG -3′	*phoZ* cloning (EF2973)
oMC830	5′- gcggcatgcCGTTCTGCTTTTTCTTCATTTTG -3′	*phoZ* cloning (EF2973)
oMC850	5′- gcggaattcTTCTTATATACCATCTGAAATACAGG -3′	P*dltD* cloning (CD2854)
oMC901	5′-CTGAAGCGAAGGCAACTGAA-3′	*phoZ* qPCR (EF2973)
oMC902	5′-GCTTGCTGTCCGACCAAATA-3′	*phoZ* qPCR (EF2973)
oMC909	5′-GCCgtcgacGACATGGAAGTAGAAGTTAAGG-3′	P*cprA* cloning

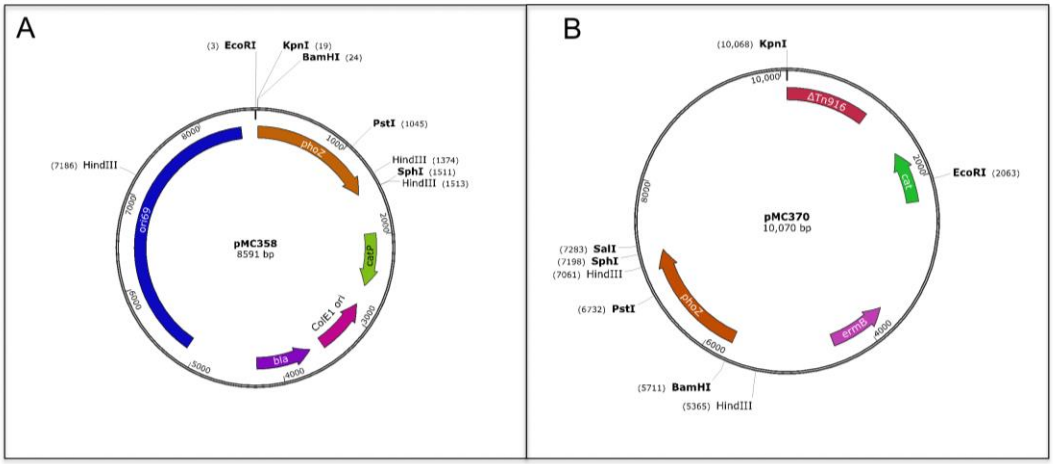

Figure 1. Overview of alkaline phosphatase reporter constructs. Plasmid maps of pMC358 (for construction of plasmid *phoZ* reporters) and pMC370 (for construction of chromosomal *phoZ* reporters).

previously described (26, 27) using 10 μg thiamphenicol ml^{-1} to select for the plasmids in *C. difficile* and 50 μg kanamycin ml^{-1} to counterselect against *E. coli* after conjugation.

pMC370 and pMC371 were integrated into the Tn*916* region within the chromosome of *B. subtilis* strain BS49 and selected for on BHIS plates containing 5 μg erythromycin ml^{-1} as previously described (28, 29), except that 50 μg kanamycin ml^{-1} was added to counterselect against *B. subtilis* after conjugation.

Alkaline Phosphatase Assays. Assays of alkaline phosphatase (AP) activity in *C. difficile* were adapted from previously described assays with some modifications (30, 31). To begin, overnight *C. difficile* cultures were back-diluted to an OD_{600} of approximately 0.05 in BHIS medium (21) with or without addition of nisin, as indicated. Duplicate (2 ml) samples of each culture were taken when the cells reached an OD_{600} of approximately 0.5. Samples were pelleted and the supernatant discarded, then stored at -20°C. To prepare samples for assay, cell pellets were first washed with 0.5 ml of cold Wash buffer (10 mM Tris-HCl, pH 8.0, 10 mM $MgSO_4$), pelleted and resuspended in 1 ml Assay buffer (1 M Tris-HCl, pH 8.0, 0.1 mM $ZnCl_2$). 500 μl of cell suspension was transferred to a separate tube for alkaline phosphatase tests. 300 μl of additional Assay buffer, 50 μl of 0.1% SDS and 50 μl of chloroform were added to the suspension, which was then vortexed for 1 min and incubated at 37°C for 5 min. Sample tubes were then placed on ice for 5 min to cool. To begin the assay, samples were pre-warmed to 37°C, then 100 μl of 0.4% *p*NP (*p*-nitrophenyl phosphate in 1M Tris-HCl, pH 8.0; Sigma-Aldrich) was added to each sample at 10 second intervals. A blank without cells was prepared as a negative control in all experiments. Samples were inverted to mix and placed in a 37°C water bath. Upon development of a light yellow color, 100 μl of stop solution (1 M KH_2PO_4) was added and tubes placed in

an ice bath to stop the phosphatase reaction. Time elapsed (min) for the assay was recorded. Assay samples were then centrifuged at max speed for 5 minutes. Absorbance for each sample was read at OD_{420} and OD_{550}. Units of activity were calculated and normalized to cell volume as follows: $\frac{[OD420-(1.75 \text{ x } OD550)]\ 1000}{t\ (\text{min}) \text{ x } OD600 \text{ x vol.cells (ml)}}$. Technical duplicates were performed and averaged for each AP assay set. A minimum of three biological replicates were performed for each experiment. The results are presented as the means and standard error of the experimental replicates. The two-tailed Student's *t* test was used to compare the results of the variable and control sets as indicated.

Quantitative reverse transcription PCR analysis (qRT-PCR). Cultures for qRT-PCR analysis were harvested in parallel with the alkaline phosphatase assay samples described above. Cultures were harvested into cold 1:1 ethanol:acetone prior to RNA purification as previously described (4, 32). Total RNA was DNase I treated and cDNA synthesized as previously described (33). qRT-PCR primers were designed using the IDT PrimerQuest tool and primer efficiencies were determined for each primer set (http://www.idtdna.com/Scitools/Applications/Primerquest). Technical triplicates were performed for each qPCR reaction set for a minimum of three biological replicates. Relative quantification of transcription was performed using the internal control transcript, *rpoC*, for normalization. The transcriptional ratios of variable and control sets are presented as the means and standard error of the means for the data obtained. The two-tailed Student's *t* test was used to compare the ratios of the variable and control sets as indicated.

RESULTS AND DISCUSSION

Evaluation of alkaline phosphatase activity and construction of vectors for alkaline

phosphatase reporter fusions.

Before evaluating the use of *phoZ* as a reporter, we first assessed the potential for inherent alkaline phosphatase (AP) activity in *C. difficile*. A protein BLAST search revealed no proteins with significant homology to *phoZ* within the genome of any *C. difficile* strain. For good measure, *C. difficile* strains 630Δ*erm* and R20291 were grown overnight on BHIS agar medium with and without the chromogenic substrate XP as described in the Materials and Methods. No apparent blue color development of the colonies was detected following overnight anaerobic growth or aerobic incubation of the plates, indicating that *C. difficile* does not produce significant levels of alkaline phosphatase under the tested conditions (data not shown).

In order for *phoZ* to be useful as an anaerobic reporter, the PhoZ produced under anaerobic conditions needs to be enzymatically active. To determine whether the *E. faecalis phoZ* gene product was functional when produced under anaerobic conditions, *E. faecalis* was grown on BHIS agar with and without XP, anaerobically and aerobically. *E. faecalis* grown aerobically exhibited the blue colony phenotype indicative of AP activity, while the bacteria that were incubated anaerobically appeared white until the plates were allowed to develop in the presence of oxygen (data not shown). However, when cells expressing *phoZ* were assayed anaerobically using the AP substrate *p*NP, significant color change was observed, indicating that PhoZ is enzymatically active anaerobically (data not shown). Thus, the AP protein folds properly anaerobically, but oxidation is required for the XP cleavage product to produce the color-forming precipitate as previously described (34). Accordingly, AP reactions using the *p*NP substrate can be performed under anaerobic conditions, but reactions using the XP substrate will not produce a colored precipitate

without further oxidation.

To investigate *phoZ* as a transcriptional reporter in *C. difficile*, two independent reporter constructs were created. The first was an extrachromosomally-replicating plasmid containing the *phoZ* reporter gene. The *phoZ* gene was amplified from *E. faecalis* and cloned into the *C. difficile-E.coli* shuttle vector pMC123, creating pMC358 (**Figure 1A**). This vector does not have a promoter to drive the expression of *phoZ*, thus no alkaline phosphatase activity should be produced in strains harboring this plasmid. To enable expression of *phoZ* in *C. difficile* the strong promoter, P*dltD*, or the nisin-inducible promoter, P*cpr*, was cloned into pMC358 upstream of *phoZ* to give pMC375 and pMC368, respectively (4, 35, 36). All three plasmids were conjugated into *C. difficile* strain 630Δ*erm* as described in the Materials and Methods.

A second *phoZ* vector was created to permit single-copy chromosomal-based reporter fusions. To this end, *phoZ* and P*cpr::phoZ* were amplified and cloned independently into the plasmid pSMB47 to create pMC370 (**Figure 1B)** and pMC371, respectively. pSMB47 can replicate in *E. coli*, but integrates into the chromosome of *B.subtilis* strain BS49 at the Tn*916* locus and can be conjugated via Tn*916* onto the chromosome of *C. difficile* (37-39).

Alkaline phosphatase is expressed and functional in *C. difficile*.

To investigate the activity of alkaline phosphatase expressed in *C. difficile*, strains carrying the plasmid-based P*dlt::phoZ* (MC499), the promoterless *phoZ* control (MC448) or the empty vector (MC324) were grown on BHIS plates containing XP and thiamphenicol. After overnight anaerobic growth, plates were removed from the anaerobic

chamber and alkaline phosphatase activity was allowed to develop aerobically. As shown in **Figure 2**, *C. difficile* containing the P*dlt::phoZ* fusion turn blue on XP plates. The development of color in colonies was visible within 20 minutes of removing the plate from the anaerobic chamber. Cells carrying the empty vector or the promoterless *phoZ* vector remained white on XP plates. These results demonstrate that the *E. faecalis* PhoZ is active when produced by *C. difficile*.

Alkaline phosphatase transcriptional reporter activity correlates directly with gene-specific transcription.

To determine the amount of alkaline phosphatase activity in *C. difficile* cells expressing *phoZ*, quantitative AP assays were performed. This AP assay was based on previously published assays with minor modifications (30, 31) (see Materials and Methods). *C. difficile* strains expressing the promoterless *phoZ* (MC448) and the P*dlt::phoZ* fusion (MC499) from a plasmid were used to assess the expression and activity of alkaline phosphatase. Each strain was grown in BHIS broth, and culture samples were taken during mid-logarithmic growth (OD_{600} = ~0.5) for AP assays. The strain expressing the P*dlt::phoZ* fusion exhibited a 144-fold increase in AP activity compared to the promoterless *phoZ* construct, indicating that a *C. difficile*-specific promoter can robustly drive measurable *phoZ* expression (**Figure 3A**).

To further determine the sensitivity and linear range of the *phoZ* promoter, we used the inducible *cpr* promoter (4). *C. difficile* strains expressing either the promoterless *phoZ* integrated on the chromosome (MC488) or from a plasmid (MC448), or the P*cpr::phoZ* fusion on the chromosome (MC489) or from a plasmid (MC486) were grown in BHIS

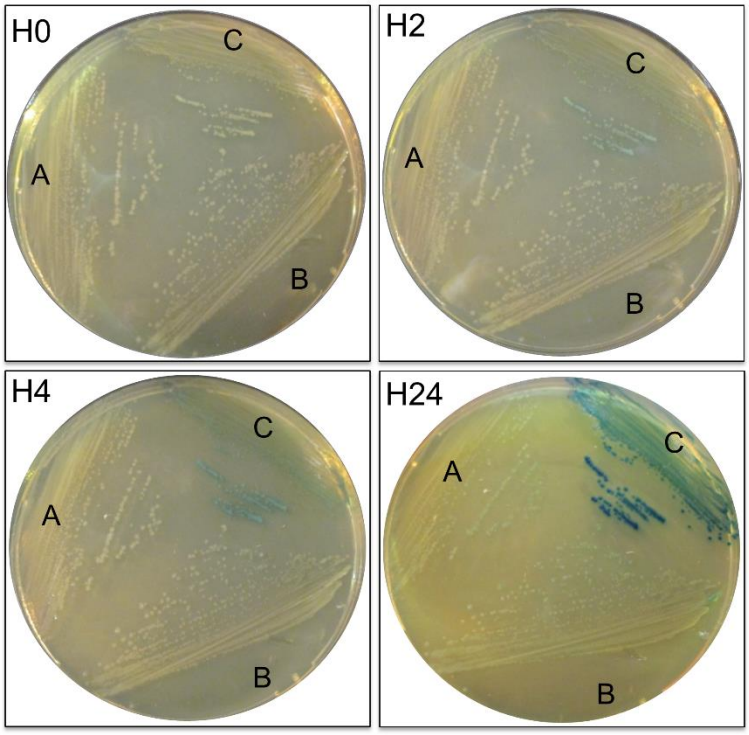

Figure 2. Visualization of alkaline phosphatase activity from *C. difficile* grown on agar plates. *C. difficile* strains A) MC324 (empty vector), B) MC448 (promoterless *phoZ*) and C) MC499 (P*dlt::phoZ*) were grown anaerobically overnight on BHIS agar plates containing 400 µg XP substrate ml^{-1} and 2 µg thiamphenicol ml^{-1}. Plates were removed from the anaerobic chamber and development of color was monitored over 24 hours ("H" indicates the number of hours after removal from the anaerobic chamber). Visible color development was observed within 20 minutes of aerobic atmospheric exposure.

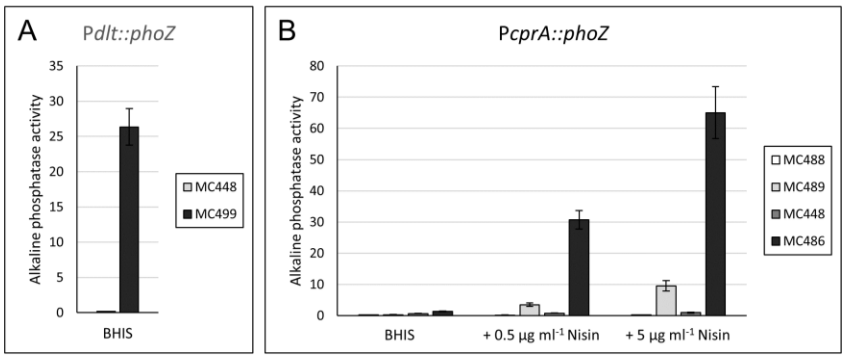

Figure 3. Alkaline phosphatase activity from the *cprA::phoZ* constructs is increased in the presence of nisin. (A) *C. difficile* strains MC448 (promoterless *phoZ* on a plasmid) and MC499 (P*dlt::phoZ* on a plasmid) were grown to an OD_{600} = ~0.5 in BHIS medium. **(B)** *C. difficile* strains MC488 (promoterless *phoZ* on the chromosome), MC489 (P*cprA::phoZ* on the chromosome), MC448 (promoterless *phoZ* on a plasmid) and MC486 (P*cprA::phoZ* on a plasmid) were grown to an OD_{600} = ~0.5 in BHIS medium in the presence or absence of nisin. Alkaline phosphatase activity was determined as described in the Materials and Methods. The means and standard errors of the means of three biological replicates are shown.

broth alone or with the addition of 0.5 μg or 5 μg ml^{-1} nisin. Culture samples were later taken during mid-logarithmic growth (OD_{600} = ~0.5) for AP assays and RNA preparation. Shown in **Figure 3B,** strains expressing the promoterless *phoZ* from the chromosome or from a plasmid exhibit very low alkaline phosphatase activity. As expected, strains expressing either P*cpr::phoZ* fusion had higher AP activity when grown in nisin (~10-20-fold in the presence of 0.5 μg ml^{-1} nisin and ~30-50-fold in the presence of 5 μg ml^{-1} nisin), demonstrating that the *cprA* promoter is induced in a dose-dependent manner in the presence of nisin, as observed previously (4, 35). In addition, AP activity is significantly lower from the P*cprA*::*phoZ* fusion (MC486) in BHIS medium (1.3 AP units) compared to the constitutive, stronger P*dlt::phoZ* fusion (MC499; 26 AP units; compare **Figure 3B** to **3A**). Altogether, these results indicate that the *phoZ* reporter can be used to accurately quantify gene expression in a wide dynamic range with little basal expression.

To determine if AP activity from the P*cprA::phoZ* constructs correlates with native gene expression, qRT-PCR analysis was performed to measure chromosomal *cprA* gene transcription. Expression of native *cprA* was increased ~100-fold in the presence of 0.5 μg ml^{-1} nisin and ~170-200-fold in the presence of 5 μg ml^{-1} nisin (**Figure 4**). To compare chromosomal *cprA* expression to the AP activity measured from the P*cprA::phoZ* fusion in the absence and presence of nisin, we determined the fold change in AP activity and transcript levels in various conditions (**Table 3**). The fold change in P*crpA*::*phoZ* fusion AP activity and in native *cprA* transcription is similar between the chromosomal and plasmid reporter constructs, although the plasmid reporter constructs are more sensitive (**Table 3; bolded numbers**). In addition, this data demonstrates that the presence of an additional *cprA* promoter in the chromosome or on a plasmid does not affect native gene

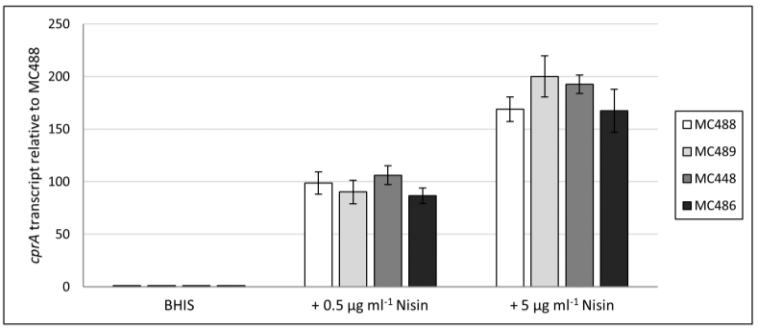

Figure 4. Native *cprA* transcription correlates with P*cprA::phoZ* alkaline phosphatase activity. qRT-PCR analysis of *cprA* expression in C. *difficile* strains MC488 (promoterless *phoZ* on the chromosome), MC489 (P*cprA::phoZ* on the chromosome), MC448 (promoterless *phoZ* on a plasmid) and MC486 (P*cprA::phoZ* on a plasmid) grown to an OD600 = ~0.5 in BHIS medium in the presence or absence of nisin. The means and standard errors of the means of three biological replicates are shown.

Table 3
Fold change of *cprA* gene expression analyzed by alkaline phosphatase activity and qRT-PCR in *C. difficile* grown with and without nisin.

Strain	Relevant genotype	Nisin 0.5 μg ml^{-1}/BHIS[a,d]		Nisin 5 μg ml^{-1}/BHIS[b,d]		Nisin 5 μg ml^{-1}/Nisin 0.5 μg ml^{-1}[c,d]	
		AP	qRT-PCR	AP	qRT-PCR	AP	qRT-PCR
MC488	Tn*916*::*phoZ*	1.1 ± 0.1	89.3 ± 10.5	1.0 ± 0.1	162.7 ± 11.7	1.0 ± 0.0	1.8 ± 0.1
MC489	Tn*916*::P*cprA*::*phoZ*	**17.3 ± 1.1**	**84.7 ± 2.6**	**32.5 ± 7.9**	**193.0 ± 27.1**	**2.7 ± 0.3**	**2.3 ± 0.4**
MC448	p*phoZ*	1.2 ± 0.1	110.0 ± 8.3	1.5 ± 0.2	201.3 ± 18.0	1.2 ± 0.1	1.8 ± 0.1
MC486	pP*cprA*::*phoZ*	**23.3 ± 2.9**	**78.5 ± 5.4**	**48.3 ± 1.4**	**152.0 ± 19.0**	**2.2 ± 0.3**	**1.9 ± 0.2**

[a] Fold change of alkaline phosphatase (AP) activity or transcript levels (qRT-PCR) in cells grown in 0.5 μg ml^{-1} nisin to BHIS medium with no supplement.
[b] Fold change of alkaline phosphatase (AP) activity or transcript levels (qRT-PCR) in cells grown in 5 μg ml^{-1} nisin to BHIS medium with no supplement.
[c] Fold change of alkaline phosphatase (AP) activity or transcript levels (qRT-PCR) in cells grown in 5 μg ml^{-1} nisin to 0.5 μg ml^{-1} nisin.
[d] The means and standard errors of the means of three biological replicates are shown.

expression or its regulation as *cprA* transcription is equal between all strains in the absence or presence of nisin (qRT-PCR data in **Table 3; Figure 4**).

Our data demonstrate that *phoZ* can function as an alkaline phosphatase reporter to provide qualitative or quantitative analysis of gene expression in *C. difficile*. This *phoZ* reporter will be amenable to multiple uses, including the analysis of promoter function, identifying transcriptional regulatory effects, and genetic screens. For genetic screens performed using XP substrate, it is critical to replica plate the bacteria anaerobically prior to the removal,of cells from the chamber, as brief exposure to oxygen can kill vegetative *C. difficile*. In addition measuring *phoZ* reporter activity in sporulating cells may require additional extraction techniques, such as the use of French pressure cell press, for complete cell lysis and accurate measurement of alkaline phosphatase activity. Notably, the use of the reporter on a multi-copy plasmid will facilitate increased expression for analyzing low levels of gene expression or screening for a range of regulatory effects in a variety of conditions. As with any construct expressed on a plasmid, additional considerations must be acknowledged when interpreting the results (e.g. titration of regulatory factors and plasmid burden).

It is important to note that we normalized alkaline phosphatase activity to the optical density of cultures at the time cells were harvested. Because of cell lysis, the optical density of *C. difficile* cells after resuspension in assay buffer was inconsistent and unreliable. However, some strains or mutants could exhibit aberrant cellular morphology that would result in an inaccurate correlation between optical density readings and the number of cells present. In this case, alkaline phosphatase activity can be normalized to total cellular protein (mg ml^{-1}), which can be determined by precipitating cells with

trichloroacetic acid, to remove cross-reacting or interfering substances, and performing a standard protein quantification assay (e.g. bicinchoninic acid assay).

CONCLUSIONS

The use of a standardized reporter for analysis of gene expression and regulatory effects as well as the development of genetic screens is an effective molecular biology tool for studying prokaryotes. Thus, the development of a colorimetric and quantifiable reporter system that functions well in an anaerobe will be useful for the study of *C. difficile* molecular genetics. The *phoZ* reporter is a simple, critically-needed system that will allow cost-effective and time-efficient genetic analysis in *C. difficile* and other anaerobic organisms.

ACKNOWLEDGEMENTS

We give special thanks to Charles Moran for helpful critiques of the manuscript and to Jeremy Boss for use of the BioRad CFX96 Real Time PCR Detection System. This research was supported by the U.S. National Institutes of Health through research grants DK087763, DK101870 and AI109526 to S.M.M.; KLN and RAP were supported through training grants AI106699 and GM099644, respectively. The content of this manuscript is solely the responsibility of the authors and does not necessarily reflect the official views of the National Institutes of Health.

REFERENCES

1. **O'Connor, J. R., D. Lyras, K. A. Farrow, V. Adams, D. R. Powell, J. Hinds, J. K. Cheung, and J. I. Rood.** 2006. Construction and analysis of chromosomal Clostridium difficile mutants. Molecular microbiology **61:**1335-1351.

2. **Heap, J. T., O. J. Pennington, S. T. Cartman, G. P. Carter, and N. P. Minton.** 2007. The ClosTron: a universal gene knock-out system for the genus Clostridium. Journal of microbiological methods **70:**452-464.

3. **Cartman, S. T., M. L. Kelly, D. Heeg, J. T. Heap, and N. P. Minton.** 2012. Precise manipulation of the Clostridium difficile chromosome reveals a lack of association between the tcdC genotype and toxin production. Applied and environmental microbiology **78:**4683-4690.

4. **McBride, S. M., and A. L. Sonenshein.** 2011. Identification of a genetic locus responsible for antimicrobial peptide resistance in Clostridium difficile. Infection and immunity **79:**167-176.

5. **Fimlaid, K. A., J. P. Bond, K. C. Schutz, E. E. Putnam, J. M. Leung, T. D. Lawley, and A. Shen.** 2013. Global Analysis of the Sporulation Pathway of Clostridium difficile. PLoS genetics **9:**e1003660.

6. **Soutourina, O. A., M. Monot, P. Boudry, L. Saujet, C. Pichon, O. Sismeiro, E. Semenova, K. Severinov, C. Le Bouguenec, J. Y. Coppee, B. Dupuy, and I. Martin-Verstraete.** 2013. Genome-wide identification of regulatory RNAs in the human pathogen Clostridium difficile. PLoS genetics **9:**e1003493.

7. **Heap, J. T., O. J. Pennington, S. T. Cartman, and N. P. Minton.** 2009. A modular system for Clostridium shuttle plasmids. Journal of microbiological methods **78:**79-85.

8. **Naylor, L. H.** 1999. Reporter gene technology: the future looks bright. Biochemical pharmacology **58:**749-757.

9. **Hastings, J. W., and Q. H. Gibson.** 1967. The role of oxygen in the photoexcited luminescence of bacterial luciferase. The Journal of biological chemistry **242:**720-726.

10. **Beneke, S., H. Bestgen, and A. Klein.** 1995. Use of the Escherichia coli uidA gene as a reporter in Methanococcus voltae for the analysis of the regulatory function of the intergenic region between the operons encoding selenium-free hydrogenases. Molecular & general genetics : MGG **248:**225-228.

11. **Lie, T. J., and J. A. Leigh.** 2007. Genetic screen for regulatory mutations in Methanococcus maripaludis and its use in identification of induction-deficient mutants of the euryarchaeal repressor NrpR. Applied and environmental microbiology **73:**6595-6600.

12. **Heim, R., D. C. Prasher, and R. Y. Tsien.** 1994. Wavelength mutations and posttranslational autoxidation of green fluorescent protein. Proceedings of the National Academy of Sciences of the United States of America **91:**12501-12504.

13. **Ransom, E. M., K. B. Williams, D. S. Weiss, and C. D. Ellermeier.** 2014. Identification and characterization of a gene cluster required for proper rod shape, cell division, and pathogenesis in Clostridium difficile. Journal of bacteriology **196:**2290-2300.

14. **Ransom, E. M., C. D. Ellermeier, and D. S. Weiss.** 2014. Use of mCherry Red Fluorescent Protein for Studies of Protein Localization and Gene Expression in Clostridium difficile. Applied and environmental microbiology.

15. **Pereira, F. C., L. Saujet, A. R. Tome, M. Serrano, M. Monot, E. Couture-Tosi, I. Martin-Verstraete, B. Dupuy, and A. O. Henriques.** 2013. The Spore Differentiation Pathway in the Enteric Pathogen Clostridium difficile. PLoS genetics **9:**e1003782.

16. **Drepper, T., T. Eggert, F. Circolone, A. Heck, U. Krauss, J. K. Guterl, M. Wendorff, A. Losi, W. Gartner, and K. E. Jaeger.** 2007. Reporter proteins for in vivo fluorescence without oxygen. Nature biotechnology **25:**443-445.

17. **Lobo, L. A., C. J. Smith, and E. R. Rocha.** 2011. Flavin mononucleotide (FMN)-based fluorescent protein (FbFP) as reporter for gene expression in the anaerobe Bacteroides fragilis. FEMS microbiology letters **317:**67-74.

18. **Dupuy, B., and A. L. Sonenshein.** 1998. Regulated transcription of Clostridium difficile toxin genes. Molecular microbiology **27:**107-120.

19. **Mani, N., D. Lyras, L. Barroso, P. Howarth, T. Wilkins, J. I. Rood, A. L. Sonenshein, and B. Dupuy.** 2002. Environmental response and autoregulation of Clostridium difficile TxeR, a sigma factor for toxin gene expression. Journal of bacteriology **184:**5971-5978.

20. **Luria, S. E., and J. W. Burrous.** 1957. Hybridization between *Escherichia coli* and *Shigella.* Journal of bacteriology **74:**461-476.

21. **Smith, C. J., S. M. Markowitz, and F. L. Macrina.** 1981. Transferable tetracycline resistance in Clostridium difficile. Antimicrobial agents and chemotherapy **19:**997-1003.

22. **McBride, S. M., V. A. Fischetti, D. J. Leblanc, R. C. Moellering, Jr., and M. S. Gilmore.** 2007. Genetic diversity among Enterococcus faecalis. PloS one **2:**e582.

23. **Bouillaut, L., S. M. McBride, and J. A. Sorg.** 2011. Genetic manipulation of Clostridium difficile. Current protocols in microbiology **Chapter 9:**Unit 9A 2.

24. **Edwards, A. N., J. M. Suarez, and S. M. McBride.** 2013. Culturing and Maintaining Clostridium difficile in an Anaerobic Environment. Journal of visualized experiments : JoVE.

25. **Edwards, A. N., K. L. Nawrocki, and S. M. McBride.** 2014. Conserved Oligopeptide Permeases Modulate Sporulation Initiation in Clostridium difficile. Infection and immunity **82:**4276-4291.

26. **Dineen, S. S., A. C. Villapakkam, J. T. Nordman, and A. L. Sonenshein.** 2007. Repression of Clostridium difficile toxin gene expression by CodY. Molecular microbiology **66:**206-219.

27. **McBride, S. M., and A. L. Sonenshein.** 2011. The dlt operon confers resistance to cationic antimicrobial peptides in Clostridium difficile. Microbiology **157:**1457-1465.

28. **Haraldsen, J. D., and A. L. Sonenshein.** 2003. Efficient sporulation in Clostridium difficile requires disruption of the sigmaK gene. Molecular microbiology **48:**811-821.

29. **Mullany, P., R. Williams, G. C. Langridge, D. J. Turner, R. Whalan, C. Clayton, T. Lawley, H. Hussain, K. McCurrie, N. Morden, E. Allan, and A. P. Roberts.** 2012. Behavior and target site selection of conjugative transposon Tn916 in two different strains of toxigenic Clostridium difficile. Applied and environmental microbiology **78:**2147-2153.

30. **Brickman, E., and J. Beckwith.** 1975. Analysis of the regulation of Escherichia coli alkaline phosphatase synthesis using deletions and phi80 transducing phages. Journal of molecular biology **96:**307-316.

31. **Manoil, C.** 1991. Analysis of membrane protein topology using alkaline phosphatase and beta-galactosidase gene fusions. Methods in cell biology **34:**61-75.

32. **Dineen, S. S., S. M. McBride, and A. L. Sonenshein.** 2010. Integration of metabolism and virulence by Clostridium difficile CodY. Journal of bacteriology **192:**5350-5362.

33. **Suarez, J. M., A. N. Edwards, and S. M. McBride.** 2013. The Clostridium difficile cpr Locus is Regulated by a Non-contiguous Two-component System in Response to Type A and B Lantibiotics. Journal of bacteriology.

34. **Cotson, S., and S. J. Holt.** 1958. Studies in enzyme cytochemistry. IV. Kinetics of aerial oxidation of indoxyl and some of its halogen derivatives. Proceedings of the Royal Society of London. Series B, Containing papers of a Biological character. Royal Society **148:**506-519.

35. **Purcell, E. B., R. W. McKee, S. M. McBride, C. M. Waters, and R. Tamayo.** 2012. Cyclic diguanylate inversely regulates motility and aggregation in Clostridium difficile. Journal of bacteriology **194:**3307-3316.

36. **McKee, R. W., M. R. Mangalea, E. B. Purcell, E. K. Borchardt, and R. Tamayo.** 2013. The second messenger cyclic Di-GMP regulates Clostridium difficile toxin production by controlling expression of sigD. Journal of bacteriology **195:**5174-5185.

37. **Manganelli, R., R. Provvedi, C. Berneri, M. R. Oggioni, and G. Pozzi.** 1998. Insertion vectors for construction of recombinant conjugative transposons in *Bacillus subtilis* and *Enterococcus faecalis*. FEMS Microbiol Lett **168:**259-268.

38. **Mullany, P., M. Wilks, L. Puckey, and S. Tabaqchali.** 1994. Gene cloning in Clostridium difficile using Tn916 as a shuttle conjugative transposon. Plasmid **31:**320-323.

39. **Wang, H., A. P. Roberts, and P. Mullany.** 2000. DNA sequence of the insertional hot spot of Tn916 in the Clostridium difficile genome and discovery of a Tn916-like element in an environmental isolate integrated in the same hot spot. FEMS microbiology letters **192:**15-20.

40. **Paulsen, I. T., L. Banerjei, G. S. Myers, K. E. Nelson, R. Seshadri, T. D. Read, D. E. Fouts, J. A. Eisen, S. R. Gill, J. F. Heidelberg, H. Tettelin, R. J. Dodson, L. Umayam, L. Brinkac, M. Beanan, S. Daugherty, R. T. DeBoy, S. Durkin, J. Kolonay, R. Madupu, W. Nelson, J. Vamathevan, B. Tran, J. Upton, T. Hansen, J. Shetty, H. Khouri, T. Utterback, D. Radune, K. A. Ketchum, B. A. Dougherty, and C. M. Fraser.** 2003. Role of mobile DNA in the evolution of vancomycin-resistant Enterococcus faecalis. Science **299:**2071-2074.

41. **Sahm, D. F., J. Kissinger, M. S. Gilmore, P. R. Murray, R. Mulder, J. Solliday, and B. Clarke.** 1989. In vitro susceptibility studies of vancomycin-resistant Enterococcus faecalis. Antimicrobial agents and chemotherapy **33:**1588-1591.

42. **Wust, J., and U. Hardegger.** 1983. Transferable resistance to clindamycin, erythromycin, and tetracycline in *Clostridium difficile*. Antimicrob Agents Chemother **23:**784-786.

43. **Hussain, H. A., A. P. Roberts, and P. Mullany.** 2005. Generation of an erythromycin-sensitive derivative of Clostridium difficile strain 630 (630Deltaerm) and demonstration that the conjugative transposon Tn916DeltaE enters the genome of this strain at multiple sites. Journal of medical microbiology **54:**137-141.

44. **Thomas, C. M., and C. A. Smith.** 1987. Incompatibility group P plasmids: genetics, evolution, and use in genetic manipulation. Annu Rev Microbiol **41:**77-101.

45. **Yanisch-Perron, C., J. Vieira, and J. Messing.** 1985. Improved M13 phage cloning vectors and host strains: nucleotide sequences of the M13mp18 and pUC19 vectors. Gene **33:**103-119.

CHAPTER 9

Appendix V - The *Clostridium difficile* Dlt pathway is controlled by the ECF sigma factor, σ^V, in response to lysozyme

Emily C. Woods, Kathryn L. Nawrocki, Jose M. Suárez and Shonna M. McBride

This work was published in 2016 in *Infection and Immunity*.

K.L.N. performed animal experiments and assisted with manuscript revision.

Article Citation:

Woods, E. C., Nawrocki, K. L., Suárez, J. M., & McBride, S. M. (2016). The *Clostridium difficile* Dlt Pathway Is Controlled by the Extracytoplasmic Function Sigma Factor σV in Response to Lysozyme. *Infection and Immunity*, *84*(6), 1902-1916.

doi:10.1128/IAI.00207-16 PMCID 27068095

ABSTRACT

Clostridium difficile (also known as *Peptoclostridium difficile*) is a major nosocomial pathogen and a leading cause of antibiotic-associated diarrhea throughout the world. Colonization of the intestinal tract is necessary for *C. difficile* to cause disease. Host-produced antimicrobial proteins (AMPs), such as lysozyme, are present in the intestinal tract and can deter colonization by many bacterial pathogens, yet *C. difficile* is able to survive in the colon in the presence of these AMPs. Our prior studies established that the Dlt pathway, which increases the surface charge of the bacterium by addition of D-alanine to teichoic acids, is important for *C. difficile* resistance to a variety of AMPs. We sought to determine what genetic mechanisms regulate expression of the Dlt pathway. In this study, we show that a *dlt* null mutant is severely attenuated for growth in lysozyme and that expression of the *dltDABC* operon is induced in response to lysozyme. Moreover, we found that a mutant lacking the extracytoplasmic function (ECF) sigma factor, σ^V, does not induce *dlt* expression in response to lysozyme, indicating that σ^V is required for regulation of lysozyme-dependent D-alanylation of the cell wall. Using reporter gene fusions and 5' RACE analysis, we identified promoter elements necessary for lysozyme-dependent and lysozyme-independent *dlt* expression. In addition, we observed that both a *sigV* mutant and a *dlt* mutant are more virulent in a hamster model of infection. These findings demonstrate that cell wall D-alanylation in *C. difficile* is induced by lysozyme in a σ^V-dependent manner and that this pathway impacts virulence *in vivo*.

INTRODUCTION

Clostridium difficile (*Peptoclostridium difficile*) causes nearly half a million infections in the United States each year, representing a significant public health threat (1). In order to cause infection, *C. difficile* must colonize the colon. As an important interface between the host and microbiota, the colon is an environment rich in host innate immune molecules and bacterial-derived antimicrobials made by the indigenous microbiota (2-6). These innate immune molecules and bacterially produced antimicrobials include a variety of cationic antimicrobial peptides (CAMPs), such as lysozyme, LL-37, defensins, and bacteriocins (2, 4, 7-9). Understanding how *C. difficile* is able to resist killing in this antimicrobial-laden environment could better our understanding of the factors that contribute to the progression of *C. difficile* infections.

A common resistance mechanism to CAMPs in many bacteria is the alteration of the cell surface charge (10-12). One mechanism for increasing the surface charge is through the addition of D-alanine (D-ala) to teichoic acids in the cell wall (10, 12, 13). The addition of D-ala is mediated by four proteins, DltA, DltB, DltC, and DltD, encoded by the *dlt* operon (13). The Dlt pathway confers lysozyme resistance to *Bacillus subtilis* and *Enterococcus faecalis* (14, 15). Previously, we demonstrated that the D-alanylation of the cell wall via the Dlt pathway is important for resistance of *C. difficile* to several CAMPs and other antimicrobials, including nisin, gallidermin, polymyxin B, and vancomycin (12).

How the Dlt pathway is regulated in *C. difficile* is unknown. Expression of *dlt* increases in *C. difficile* in the presence of CAMPs (12), but the mechanisms that control this expression remain unidentified. Although a putative DeoR-family regulator (CD2850) is co-transcribed as part of the *C. difficile dlt* operon, it does not appear to be necessary for

dlt expression *in vitro* (12). The availability of sugars may play a role in regulating *dlt* expression in *C. difficile*, as evidenced by a CcpA binding site located within *dltD* and differential expression of the operon in the presence of glucose (16). In *B. subtilis*, the *dlt* operon is regulated by the alternative sigma factor, σ^D, the sporulation regulatory protein, Spo0A, and the extracytoplasmic function (ECF) sigma factors, σ^X and σ^V (15, 17-19). ECF sigma factors are a class of alternative sigma factors broadly involved in functions at the cell surface (20). ECF sigma factors are typically regulated by anti-sigma factors that are located in the cell membrane, which makes ECF sigma factors uniquely suited to regulate genes, such as *dlt*, that are needed to respond to changes in the cell surface (20). *C. difficile* encodes orthologs of Spo0A, σ^V (also known as *csfV* or *sigV*) and σ^D. Moreover, σ^V is necessary for lysozyme resistance in *C. difficile* (21). In fact, the *C. difficile* σ^V anti-sigma factor, RsiV, binds lysozyme and may serve as a direct lysozyme receptor, as it does in *B. subtilis* (22). An ortholog of σ^X has not been identified in any sequenced *C. difficile* isolate, but *C. difficile* strains encode an additional ECF sigma factor, σ^T (*csfT* or *sigT)*. Based on the presence of alternative sigma factors in *C. difficile* that are comparable to those that regulate *dlt* in *B. subtilis*, we hypothesized that σ^V, σ^T, or σ^D may regulate the *dlt* operon of *C. difficile* in response to CAMPs.

To test this hypothesis, we characterized growth, D-alanylation of the cell wall and gene expression profiles of *dlt*, *sigV*, *sigT* and *sigD* null mutants in the presence of the antimicrobials, lysozyme and polymyxin B. In addition, we characterized expression from the *dlt* promoter to determine regions that are responsible for antimicrobial-dependent expression. Our results demonstrate that σ^V is an important regulator of *dlt* expression and

that σ^V is necessary for controlling D-alanylation of the *C. difficile* cell wall in response to lysozyme.

MATERIALS AND METHODS

Bacterial strains and growth conditions. The bacterial strains and plasmids used in this study are listed in **Table 1**. *Escherichia coli* strains were grown aerobically in Luria broth (Teknova) at 37˚C (23). Cultures were supplemented with 20 µg chloramphenicol ml^{-1} (Sigma-Aldrich) or 100 µg ampicillin ml^{-1} (Cayman Chemical Company) as needed. *C. difficile* strains were grown in brain heart infusion medium supplemented with 2% yeast extract (BHIS; Becton, Dickinson, and Company) or on BHIS agar plates (24) at 37˚C in an anaerobic chamber (Coy Laboratory Products) as previously described (25-27). BHIS medium was supplemented with 0.6–1.0 mg lysozyme ml^{-1} (Fisher Scientific), 150–200 µg polymyxin B ml^{-1} (Sigma-Aldrich), 2 µg thiamphenicol ml^{-1} (Sigma-Aldrich), 0.5 µg kanamycin ml^{-1} or 0.5 µg nisin ml^{-1} (MP Biomedicals) as needed.

Strain and plasmid construction. The oligonucleotides used in this study are listed in **Table 2**. Primers were designed based on *C. difficile* strain 630 (GenBank accession NC_009089.1), unless otherwise specified. Genomic DNA from strain 630Δ*erm* served as template for PCR amplifications, except where the use of strain R20291 (GenBank accession NC_013316.1) is noted. PCR, cloning, and plasmid DNA isolation were performed according to standard protocols (25). To create null mutations in *C. difficile* strain 630Δ*erm*, the group II intron from pCE240 was re-targeted using the primers listed in **Table 2**, as previously described (28-30). To select for TargeTron insertional disruptions, transconjugants were exposed to 5 µg erythromycin ml^{-1} (Sigma-Aldrich) and

TABLE 1 Bacterial strains and plasmids

Strain or plasmid	Relevant genotype or features	Source, construction, or reference
Strains		
E. coli		
HB101	F⁻ *mcrB mrr hsdS20*(r_B^- m_B^-) *recA13 leuB6 ara-14 proA2 lacY1 galK2 xyl-5 mtl-1 rpsL20*	B. Dupuy
MC101	HB101 pRK24	B. Dupuy
MC277	HB101 pRK24 pMC211	33
MC314	HB101 pRK24 pMC235	This study
MC355	HB101 pRK24 pMC286	This study
MC373	HB101 pRK24 pMC316	This study
MC445	HB101 pRK24 pMC358	31
MC463	HB101 pRK24 pMC364	This study
MC464	HB101 pRK24 pMC362	This study
MC466	HB101 pRK24 pMC373	This study
MC468	HB101 pRK24 pMC375	31
MC469	HB101 pRK24 pMC376	This study
MC535	HB101 pRK24 pMC390	This study
MC580	HB101 pRK24 pMC455	This study
MC581	HB101 pRK24 pMC456	This study
MC616	HB101 pRK24 pMC467	This study
MC617	HB101 pRK24 pMC468	This study
MC628	HB101 pRK24 pMC470	This study
MC629	HB101 pRK24 pMC471	This study
MC630	HB101 pRK24 pMC472	This study
MC665	HB101 pRK24 pMC482	This study
MC667	HB101 pRK24 pMC483	This study
MC692	HB101 pRK24 pMC491	This study
MC693	HB101 pRK24 pMC492	This study
MC699	HB101 pRK24 pMC493	This study
MC700	HB101 pRK24 pMC495	This study
MC706	HB101 pRK24 pMC500	This study
MC707	HB101 pRK24 pMC501	This study
C. difficile		
630	Clinical isolate	69
630Δ*erm*	Erm^s derivative of strain 630	N. Minton (70)
JIR8094	Erm^s derivative of strain 630	C. Ellermeier (21, 71)
TCD20	JIR8094 *sigV*::*ermB*	C. Ellermeier (21)
R20291	Clinical isolate	72
MC282	630Δ*erm* pMC211	33
MC319	630Δ*erm dltD*::*ermB*	This study
MC361	630Δ*erm sigV*::*ermB*	This study
MC383	630Δ*erm sigT*::*ermB*	This study
MC448	630Δ*erm* pMC358	31
MC450	MC361 pMC360	This study
MC494	630Δ*erm* pMC364	This study
MC495	630Δ*erm* pMC362	This study
MC497	630Δ*erm* pMC373	This study
MC499	630Δ*erm* pMC375	31
MC500	630Δ*erm* pMC376	This study
MC510	MC361 pMC211	This study
MC512	MC361 pMC358	This study
MC513	MC361 pMC364	This study
MC514	MC361 pMC362	This study
MC515	MC361 pMC373	This study
MC519	MC361 pMC375	This study
MC520	MC361 pMC376	This study
MC551	630Δ*erm* pMC390	This study
MC552	MC361 pMC390	This study
RT1075	630Δ*erm sigD*::*ermB*	R. Tamayo (45)
MC582	630Δ*erm* pMC455	This study
MC583	630Δ*erm* pMC456	This study
MC584	MC361 pMC455	This study
MC585	MC361 pMC456	This study
MC619	630Δ*erm* pMC467	This study
MC620	630Δ*erm* pMC468	This study
MC632	630Δ*erm* pMC470	This study
MC633	630Δ*erm* pMC471	This study
MC634	630Δ*erm* pMC472	This study
MC635	MC361 pMC470	This study
MC636	MC361 pMC471	This study
MC637	MC361 pMC472	This study
MC668	630Δ*erm* pMC482	This study
MC669	MC361 pMC482	This study
MC682	630Δ*erm* pMC483	This study
MC683	MC361 pMC483	This study
MC695	630Δ*erm* pMC491	This study
MC696	630Δ*erm* pMC492	This study
MC697	MC361 pMC491	This study
MC698	MC361 pMC492	This study
MC701	MC361 pMC493	This study
MC702	MC361 pMC495	This study
MC703	630Δ*erm* pMC493	This study
MC704	630Δ*erm* pMC495	This study
MC714	630Δ*erm* pMC500	This study
MC710	630Δ*erm* pMC501	This study
MC711	MC361 pMC500	This study
MC712	MC361 pMC501	This study
MC744	630Δ*erm* pMC523	This study
MC745	MC361 pMC523	This study
MC746	630Δ*erm* pMC524	This study
MC747	MC361 pMC524	This study
Plasmids		
pRK24	Tra^+ Mob^+; *bla tet*	73
pCR2.1	*bla kan*	Invitrogen
pUC19	Cloning vector; *bla*	74
pCE240	*C. difficile* TargeTron construct based on pJIR750ai (group II intron, *ermB*::RAM *ltrA*); *catP*	C. Ellermeier (30)
pSMB47	Tn*916* integrational vector; Cm^r Erm^r	75
pMC123	*E. coli-C. difficile* shuttle vector; *bla catP*	36
pMC111	pCE240 with *dltD*-targeted intron	12
pMC211	pMC123 P*cprA*	33
pMC235	pMC123 with *dltD*-targeted intron (at nt 367), *ermB*::RAM *ltrA catP*	This study
pMC276	pCE240 with *sigV*-targeted intron	This study
pMC286	pMC123 with *sigV*-targeted intron (at nt 380), *ermB*::RAM *ltrA catP*	This study
pMC312	pCR2.1 with *sigT*-targeted intron	This study
pMC314	pCE240 with *sigT*-targeted intron	This study
pMC316	pMC123 with *sigT*-targeted intron (at nt 537), *ermB*::RAM *ltrA catP*	This study
pMC358	pMC123 *phoZ*	31
pMC360	pMC123 P*cprA*::*sigV*	This study
pMC362	pMC123 $PdltD_{200}$::*phoZ*	This study
pMC364	pMC123 $PdltD_{100}$::*phoZ*	This study
pMC373	pMC123 $PdltD_{300\ (630\Delta erm)}$::*phoZ*	This study
pMC375	pMC123 $PdltD_{600\ (630\Delta erm)}$::*phoZ*	31

(Continued on following page)

TABLE 1 (Continued)

Strain or plasmid	Relevant genotype or features	Source, construction, or reference
pMC376	pMC123 P$dltD_{600\ (R20291)}$::*phoZ*	This study
pMC390	pMC123 P$dltD_{112}$::*phoZ*	This study
pMC455	pMC123 P$dltD_{119}$::*phoZ*	This study
pMC456	pMC123 P$dltD_{170}$::*phoZ*	This study
pMC467	pMC123 P$dltD_{25}$::*phoZ*	This study
pMC468	pMC123 P$dltD_{50}$::*phoZ*	This study
pMC470	pMC123 P$dltD_{140}$::*phoZ*	This study
pMC471	pMC123 P$dltD_{150}$::*phoZ*	This study
pMC472	pMC123 P$dltD_{160}$::*phoZ*	This study
pMC482	pMC123 P$dltD_{130}$::*phoZ*	This study
pMC483	pMC123 P$dltD_{75}$::*phoZ*	This study
pMC491	pMC123 P$dltD_{T43C}$::*phoZ*	This study
pMC492	pMC123 P$dltD_{T51C}$::*phoZ*	This study
pMC493	pMC123 P$dltD_{130–75}$::*phoZ*	This study
pMC495	pMC123 P$dltD_{G95A}$::*phoZ*	This study
pMC500	pMC123 P$dltD_{C93A}$::*phoZ*	This study
pMC501	pMC123 P$dltD_{G92A}$::*phoZ*	This study
pMC523	pMC123 P$dltD_{A38C}$::*phoZ*	This study
pMC534	pMC123 P$dltD_{T48C}$::*phoZ*	This study

TABLE 2 Oligonucleotides

Primer	Sequence[a] (5′→3′)	Purpose, source, or reference[b]
oMC38	5′-AAAGACGGAGTCACAAGTCACC-3′	*dltD* qPCR (CD2154) (12)
oMC39	5′-CTGCTTTATACTCGTCACTTCCC-3′	*dltD* qPCR (CD2154) (12)
oMC44	5′-CTAGCTGCTCCTATGTCTCACATC-3′	*rpoC* qPCR (CD0067) (12)
oMC45	5′-CCAGTCTCTCCTGGATCAACTA-3′	*rpoC* qPCR (CD0067) (12)
oMC74	5′-AAAAGCTTTTGCAACCCACGTCGATCGTGAAAAAGTTGTCTTGGTGCGCCCAGATAGGGTG-3′	*dltD* intron retargeting (12)
oMC75	5′-CAGATTGTACAAATGTGGTGATAACAGATAAGTCGTCTTGTTTAACTTACCTTTCTTTGT-3′	*dltD* intron retargeting (12)
oMC76	5′-CGCAAGTTTCTAATTTCGGTTACTTTTCGATAGAGGAAAGTGTCT-3′	*dltD* intron retargeting (12)
oMC193	5′-TGTATAAGGCACTATACTCAGTGG-3′	*sigV* qPCR (CD1558)
oMC194	5′-ACTCTCCAGTCTCATCTATAAGGTC-3′	*sigV* qPCR (CD1558)
oMC447	5′-GGCGTAGTATTTTTATTTGGGTTAG-3′	*dltD*::TargeTron screening
oMC547	5′-TGGATAGGTGGAGAAGTCAGT-3′	*tcdA* qPCR (CD0663) (33)
oMC548	5′-GCTGTAATGCTTCAGTGGTAGA-3′	*tcdA* qPCR (CD0663) (33)
oMC703	5′-AAAAGCTTTTGCAACCCACGTCGATCGTGAAAGAGCTTTGGAAGTGCGCCCAGATAGGGTG-3′	*sigV* (CD1558) intron retargeting
oMC704	5′-CAGATTGTACAAATGTGGTGATAACAGATAAGTCTTGGAAGATAACTTACCTTTCTTTGT-3′	*sigV* (CD1558) intron retargeting
oMC705	5′-CGCAAGTTTCTAATTTCGGTTGCTCTTCGATAGAGGAAAGTGTCT-3′	*sigV* (CD1558) intron retargeting
oMC731	5′-GCTACTTCTTCAATCTTTAAATCTTC-3′	*sigV*::TargeTron screening
oMC800	5′-AAAAGCTTTTGCAACCCACGTCGATCGTGAATCTGTTCTGATTGTGCGCCCAGATAGGGTG-3′	*sigT* (CD0677) intron retargeting
oMC801	5′-CAGATTGTACAAATGTGGTGATAACAGATAAGTCCTGATTCATAACTTACCTTTCTTTGT-3′	*sigT* (CD0677) intron retargeting
oMC802	5′-CGCAAGTTTCTAATTTCGGTTACAGATCGATAGAGGAAAGTGTCT-3′	*sigT* (CD0677) intron retargeting
oMC815	5′-TGGATTCTCTTAAGGAAGAACAATACTTTA-3′	*sigT* qPCR (CD0677)
oMC816	5′-CCTTAACTTCATCTACTGAATAACCTTCA-3′	*sigT* qPCR (CD0677)
oMC817	5′-GCGCTACGATTTGCATAGAAGG-3′	*sigT*::TargeTron screening
oMC818	5′-GCTCATATGATTACCTCCGTGTTTTC-3′	*sigT*::TargeTron screening
oMC823	5′-GCCGGATCCATTTTCTCTCCTCTAAAAATATTCAAA-3′	P*dlt* cloning (31)
oMC826	5′-GCGGAATTCTGATAGTATATAGTTTATATTAGAAAATATAAG-3′	Pdlt_{300} cloning (630Δ*erm* specific)
oMC827	5′-GCGGAATTCGTTAAAATGTCAAATTATAAGTATGAAAAAG-3′	Pdlt_{200} cloning
oMC828	5′-GCGGAATTCGTTTTGACGATTTTATTACAATTTTG-3′	Pdlt_{100} cloning
oMC850	5′-GCGGAATTCTTCTTATATACCATCTGAAATACAGG-3′	Pdlt_{600} cloning (630Δ*erm* specific) (31)
oMC851	5′-CGCGGATCCGGAGGGAGATTTTACAGGAATG-3′	*sigV* + RBS cloning
oMC852	5′-GCCTGCAGGTCATTCTTTTTATCCCTACTCTTC-3′	*sigV* cloning
oMC853	5′-GCGGAATTCTTCTTATATACCATCTGAAATACAAG-3′	Pdlt_{600} cloning (R20291 specific)
oMC901	5′-CTGAAGCGAAGGCAACTGAA-3′	*phoZ* qPCR (31)
oMC902	5′-GCTTGCTGTCCGACCAAATA-3′	*phoZ* qPCR (31)
oMC977	5′-GCGGAATTCGTATCAAAAAAAGTTTTG-3′	Pdlt_{112} cloning
oMC1023	5′-TTGTTGAATTACTAAGTTCTGATGACCC-3′	P*dlt* 5′ RACE (SP1)
oMC1024	5′-TCTCCCTCAAAAGTTCATCAGTTTTAG-3′	P*dlt* 5′ RACE (SP2)
oMC1028	5′-GCGGAATTCTGTAACAGTATCAAAAAAAG-3′	Pdlt_{119} cloning
oMC1029	5′-GCGGAATTCGTGCTAAAAAGAAATTTATTTTTG-3′	Pdlt_{170} cloning
oMC1067	5′-AATTCTGAATATTTTTAGAGGAGAGAAAATG-3′	Pdlt_{25} cloning
oMC1068	5′-GATCCATTTTCTCTCCTCTAAAAATATTCAG-3′	Pdlt_{25} cloning
oMC1069	5′AATTCAATATGATTAATAATAACATAAATTTGAATATTTTTAGAGGAGAGAAAATG-3′	Pdlt_{50} cloning
oMC1070	5′GATCCATTTTCTCTCCTCTAAAAATATTCAAATTTATGTTATTATTAATCATATTG-3′	Pdlt_{50} cloning
oMC1071	5′-GCGGAATTCTTTTCTTTTTTTTTACAA-3′	Pdlt_{140} cloning
oMC1072	5′-GCGGAATTCTTTGGCGTTTTTTTC-3′	Pdlt_{150} cloning
oMC1073	5′-GCGGAATTCGAAATTTATTTTTGG-3′	Pdlt_{160} cloning
oMC1079	5′-GCGGAATTCGTAGTTGAATATAC-3′	Pdlt_{75} cloning
oMC1080	5′-GCGGAATTCTTTTACAATTTTGTAAC-3′	Pdlt_{130} cloning
oMC1107	5′-GCGGAATTCATTTTCTCTCCTCTAAAATTGTAATAAAATCGTC-3′	P$dlt_{130–75}$ cloning
oMC1108	5′-CAAAAAAAGTTTTAACGATTTTATTAC-3′	SDM of P*dlt* (G-95A)
oMC1109	5′-GTAATAAAATCGTTAAAACTTTTTTTG-3′	SDM of P*dlt* (G-95A)
oMC1110	5′-CAAAAAAAGTTTTGAAGATTTTATTAC-3′	SDM of P*dlt* (C-93A)
oMC1112	5′-CAAAAAAAGTTTTGACAATTTTATTAC-3′	SDM of P*dlt* (G-92A)
oMC1114	5′-ACATATCAAAACCAATATGATTAATAATAACA-3′	SDM of P*dlt* (T-51C)
oMC1115	5′-TGTTATTATTAATCATATTGGTTTTGATATGT-3′	SDM of P*dlt* (T-51C)
oMC1116	5′-CAAAACTAATATGACTAATAATAACATAAATTTG-3′	SDM of P*dlt* (T-43C)
oMC1117	5′-CAAATTTATGTTATTATTAGTCATATTAGTTTTG-3′	SDM of P*dlt* (T-43C)
oMC1124	5′-GTAATAAAATCTTCAAAACTTTTTTTG-3′	SDM of P*dlt* (C-93A)
oMC1125	5′-GTAATAAAATTGTCAAAACTTTTTTTG-3′	SDM of P*dlt* (G-92A)
oMC1147	5′-CATATCAAAACTAACATGATTAATAATAAC-3′	SDM of P*dlt* (T-48C)
oMC1148	5′-GTTATTATTAATCATGTTAGTTTTGATATG-3′	SDM of P*dlt* (T-48C)
oMC1149	5′-CTAATATGATTAATVATAAVATAAATTTG-3′	SDM of P*dlt* (A-38C)
oMC1150	5′-CAAATTTATGTTATGATTAATCATATTAG-3′	SDM of P*dlt* (A-38C)

[a] Underlined sequences denote restriction sites or intron retarget sites.

[b] Abbreviations: qPCR, quantitative PCR; RBS, ribosome binding site; SDM, site-directed mutagenesis.

50 µg kanamycin ml^{-1} (Sigma-Aldrich) to select against *E. coli*.

To generate alkaline phosphatase reporter gene promoter fusions, regions of various lengths upstream of *dltD* were PCR-amplified from either *C. difficile* strain 630Δ*erm* or R20291 genomic DNA, as noted for the primers listed in **Table 2**. For site-directed mutagenesis of the promoter region, mutations were generated via Splicing by Overlap Extension (SOEing) PCR using the primers listed in **Table 2**. These products were independently ligated into the *Eco*RI/*Bam*HI sites of pMC358 (31) to generate the plasmids listed in **Table 2**. Plasmids were confirmed by sequencing (Eurofins MWG Operon) and introduced into *E. coli* strain MC101 by transformation. The resulting *E. coli* strains were then conjugated to *C. difficile* strain 630Δ*erm* or MC361, selecting for thiamphenicol resistance, as previously described (12, 32).

To complement the *sigV* mutant, the *sigV* coding sequence was cloned into pMC211 to place expression of *sigV* under the control of the nisin-inducible *cpr* promoter, as previously described (33, 34). The resulting plasmid (pMC360) was conjugated with MC361 as described above. Strains 630Δ*erm* and MC361 containing the empty pMC211 vector served as controls.

Phase contrast microscopy. *C. difficile* strains were grown in BHIS alone or supplemented with 1 mg lysozyme ml^{-1} as described above. 1 ml of actively growing culture was removed from the anaerobic chamber, centrifuged at full speed for 1 min, and resuspended in 5 µl supernatant. 2 µl of resuspended pellet was placed on top of a thin layer of 0.7% agarose on a microscope slide. For comparison of the 630Δ*erm* and JIR8094 strains, 250 µl of actively growing *C. difficile* cultures in BHIS at an OD_{600} of 0.50 was plated on 70:30 agar (35). After 24 hours, growth was scrapped from these plates,

resuspended in BHIS, and 2 µl was placed on top of a thin layer of 0.7% agarose on a microscope slide. Phase contrast microscopy was performed using an X100 Ph3 oil-immersion objective on a Nikon Eclipse Ci-L microscope.

Quantitative Reverse Transcription PCR analysis (qRT-PCR). Actively growing *C. difficile* cultures were diluted to an OD_{600} of approximately 0.05 in BHIS alone or with 1.0 mg lysozyme ml^{-1} or 200 µg polymyxin B ml^{-1}. Cultures were grown to an OD_{600} of 0.5, harvested into cold 1:1 ethanol:acetone, and stored at -80˚C. Alternatively, for *in vitro* toxin expression experiments, 250 µl of actively growing *C. difficile* cultures in BHIS at an OD_{600} of 0.50 was plated on 70:30 agar. After 12 hours, growth from these plates was scraped into cold 1.5:1.5:3 ethanol:acetone:water, and stored at -80˚C. In addition, cecal contents from animals infected with *C. difficile* were collected post-mortem into cold 1:1 ethanol:acetone and stored at -80˚C. RNA was purified and treated with DNaseI before cDNA synthesis as previously described (36-38). 50 µg of RNA was used as template for cDNA generation from *in vitro* samples, and 200 µg of RNA was used as template for cDNA generation from cecal samples. The IDT PrimerQuest tool was used to design qRT-PCR primers (http://www.idtdna.com/Scitools/Applications/Primerquest). Each qRT-PCR reaction was performed in technical triplicate for at least three biological replicates. *rpoC* served as an internal control transcript to normalize expression for relative quantification. The means and standard error of the means for the transcriptional ratios of variable and control sets are presented and compared using either a one- or two-way analysis of variance with Dunnett's or Sidak's multiple comparisons tests, as indicated.

Alkaline phosphatase activity assay. *C. difficile* strains containing the promoter-reporter gene fusions listed in **Table 1** were grown to mid-logarthmic phase (OD_{600} ~0.5), 1 ml

samples were harvested in duplicate, and pelleted cells were stored at -20˚C. The samples were analyzed for alkaline phosphatase **(**AP) activity as previously described (31). Briefly, samples were washed in 0.5 ml wash buffer (10 mM Tris-HCl, pH 8.0, 10 mM $MgSO_4$) and resuspended in 800 µl of assay buffer (1 M Tris-HCl, pH 8.0, 0.1 M $ZnCl_2$). 50 µl 0.1% SDS and 50 µl chloroform were added to the samples, which were then vortexed for 15 sec. Samples were incubated for 5 min at 37˚C then for 5 min on ice. After rewarming to room temperature, 100 µl of 0.4% pNP (p-nitrophenyl phosphate in 1 M Tris-HCl, pH 8.0) was added to samples in 10 sec intervals. Samples were mixed by inversion and incubated at 37˚C until the development of yellow color. To stop the reaction, 100 µl of 1 M KH_2PO_4 was added in 10 sec intervals and the samples were placed on ice. Developed samples were then centrifuged at 4˚C for 5 minutes and the supernatant OD_{550} and OD_{420} values recorded. AP activity was calculated as follows: $((OD_{420} – (1.75*OD_{550}))*1000)/(OD_{600}*Vol*time)$. OD_{600} refers to the absorbance of the culture at 600 nm at the time of sample collection. Vol is the volume of sample analyzed (1 ml). Time is the total reaction time from addition of pNP to the addition of stop buffer. Results are represented as the means of calculated AP activity and standard errors of the means from at least three biological replicates, each performed as technical duplicates. Data were excluded from analysis if technical duplicates varied from each other by greater than 25%. Data were analyzed with a two-way analysis of variance with Dunnett’s multiple comparisons tests. Data from site-directed mutagenesis constructs were analyzed using the two-tailed Student’s *t* test with correction for multiple comparisons by the Holm-Sidak method.

Quantification of D-alanine ester content in teichoic acids. The amount of D-alanine esters incorporated into teichoic acids of cell walls was quantified as previously described, with minor modifications (12, 39, 40). Cultures were grown anaerobically at 37˚C in BHIS or in BHIS supplemented with 0.6 mg lysozyme ml^{-1} or 150 µg polymyxin B ml^{-1}. 50 ml was harvested by centrifugation at an OD_{600} of 0.5, and cell pellets were stored at -20˚C. Cell pellets were washed three times with 1 ml 0.1 M MES (Sigma Aldrich), pH 6.0 before boiling for 15 min in 0.5 ml 0.2% SDS, 0.1 M MES, pH 6.0 to partially purify cell walls. Pelleted cell walls were then washed four times with 1 ml 0.1 M MES, pH 6.0. The washed and pelleted cell walls were dried on a tabletop vacuum centrifuge heated to 55˚C. Total cell wall contents were determined by weighing the dried pellets. To release D-alanine residues, the pellets were resuspended in 0.5 ml 0.1 M sodium pyrophosphate (Sigma Aldrich), pH 8.3 and incubated at 60˚C for 3 h. The samples were then centrifuged and the supernatant was transferred to a fresh tube for use in the quantification assay, as described previously (12). Results are the means and standard errors of the means from at least three biological replicates, each performed as technical duplicates. Data were analyzed using a two-way analysis of variance with Dunnett's multiple comparisons tests.

5' Rapid Amplification of cDNA Ends (5' RACE). RNA was purified from cells collected as described above for qRT-PCR. After DNase I treatment, the RNA was used as a template to generate cDNA using the Roche 5'/3' RACE 2^{nd} generation kit, according to the manufacturer's protocol. Primer oMC1023 was used for first-strand synthesis, and oMC1024 and the Roche oligo-T primer were used for the subsequent PCR amplification step. The resulting cDNA products were purified and either sequenced directly (Eurofins

MWG Operon) or cloned into pCR2.1 (Invitrogen TOPO TA cloning kit) before sequencing.

Animal studies. All animal studies were approved in advance by the Emory University Institutional Animal Care and Use Committee (IUCAC). Female Syrian golden hamsters (*Mesocricetus auratus;* Charles River Laboratories) were housed individually in sterile cages in an animal biosafety level 2 facility within the Emory University Division of Animal Resources. Hamsters were provided sterile water and rodent feed pellets *ad libitum*. To induce susceptibility to infection with *C. difficile*, hamsters were orally gavaged once with clindamycin (30 mg/kg body weight) 7 days prior to inoculation with *C. difficile* (41, 42). Hamsters were inoculated by oral gavage with approximately 5000 *C. difficile* spores, which were prepared as described previously (33). After preparation, spores were diluted in PBS with 1% bovine serum albumin to prevent clumping of spores and stored at room temperature in glass vials to prevent adhesion to plastic. Prior to plating, aliquots of spores were heated for 20 minutes at 55˚C. Spores were enumerated by plating these heated aliquots on BHIS + 0.1% taurocholate to induce germination. Spore preparations were heated for 20 minutes at 55˚C prior to inoculating animals. Multiple cohorts of hamsters were tested for each strain of *C. difficile* (630Δ*erm*, MC319, MC361, JIR8094, TCD20, or a one-to-one mixture of 630Δ*erm* and MC319) for a total of at least 12 hamsters per strain. A hamster treated with clindamycin, but not inoculated with *C. difficile*, served as a negative control for each cohort. After inoculation, hamsters were weighed at least once per day and fecal samples were collected daily. Hamsters were monitored for disease symptoms and considered moribund if they either lost ≥ 15% of their highest body weight or developed symptoms of diarrhea, lethargy, and wet tail. To prevent unnecessary

suffering, hamsters meeting either of these criteria were euthanized. Cecal contents were collected at the time of morbidity (post-mortem). Colony forming units (CFU) were enumerated from daily fecal samples and from cecal samples by resuspension in 1x PBS, serial dilution, and plating onto TCCFA agar (43, 44). CFU were enumerated after 48 h incubation on TCCFA. For samples from animals co-infected with 630Δ*erm* and MC319, samples were plated on both TCCFA and TCCFA with 2 µg/ml erythromycin to distinguish between the strains. These CFU counts were then used to calculate the competitive index (CI) for MC319, using the formula CI = number of MC319 CFU/ml over number of 630Δ*erm* CFU/ml (in cecal contents) divided by number of MC319 spores/ml over number of 630Δ*erm* spores/ml (in original inoculum). Differences in CFU counts were analyzed using a one-way analysis of variance with Dunnett's multiple comparisons tests, and differences in survival were analyzed using log-rank regression.

Accession numbers. *C. difficile* strain 630 (GenBank accession NC_009089.1); *C. difficile* strain R20291 (NC_013316.1). The locus tags for individual genes mentioned in the text are listed in **Table 2**.

Statistical analysis. All statistical analysis was performed using GraphPad Prism version 6.00 for Mac OS X, GraphPad Software (La Jolla, CA, USA).

RESULTS

Impact of *sigD, sigT* and *sigV* disruption on CAMP resistance

In order to test our hypothesis that Dlt-mediated CAMP resistance is regulated by alternative sigma factors in *C. difficile*, insertion mutants were generated in *sigV*, *sigD* and *sigT* in strain 630Δ*erm* using group II intron targeting (28, 45). In previous work, we

generated a *C. difficile* mutant with a non-functional *dltDABC* operon (12), but this mutant was derived from the parent strain JIR8094, which is non-motile and has a virulence defect (46). Unlike JIR8094, 630Δ*erm* retains the virulence profile of the clinical parent strain, 630, and is therefore a more clinically relevant strain (47-49) The *dlt* mutation was regenerated in the strain 630Δ*erm* background for these studies. The growth phenotype of these mutants was then assessed in the presence of the antimicrobials, lysozyme and polymyxin B (**Fig. 1**). The strain R20291, a clinical isolate of the epidemic 027 ribotype, was also included in order to assess the antimicrobial sensitivities of this clinically relevant strain. All of the mutants had growth comparable to the parent strain in BHIS; however, the *dlt* and *sigV* mutants both had attenuated growth in BHIS supplemented with 1 mg/ml lysozyme (**Fig. 1A**). The lysozyme-deficient growth phenotype was more pronounced in the *dlt* mutant than in the *sigV* mutant. The R20291 strain, had a slight growth defect in lysozyme when compared to the 630Δ*erm* strain. Growth of the *dlt* mutant was also attenuated in BHIS supplemented with 200 μg/ml polymyxin B (**Fig. 1B**). These findings validate earlier studies that D-alanylation by the Dlt pathway is important for CAMP resistance (12) and suggest that σ^V is a candidate regulator of *dlt* in lysozyme. The attenuated growth of the *sigV* mutant in lysozyme was complemented by expression of *sigV* from a plasmid, similar to previous studies (**Fig. S1**, (21)). The *sigV* mutant did not, however, have a growth defect in polymyxin B (**Fig. 1B**), demonstrating that σ^V is not necessary for *dlt* regulation in polymyxin B. In contrast to the phenotype observed for *sigV*, neither a *sigT* nor a *sigD* mutant were attenuated for growth in lysozyme (**Fig. 1A**). The *sigT* and *sigD* mutants were slightly attenuated for growth in polymyxin B during log phase, but ultimately achieved the same cell density as the parent strain (**Fig. 1B**). These

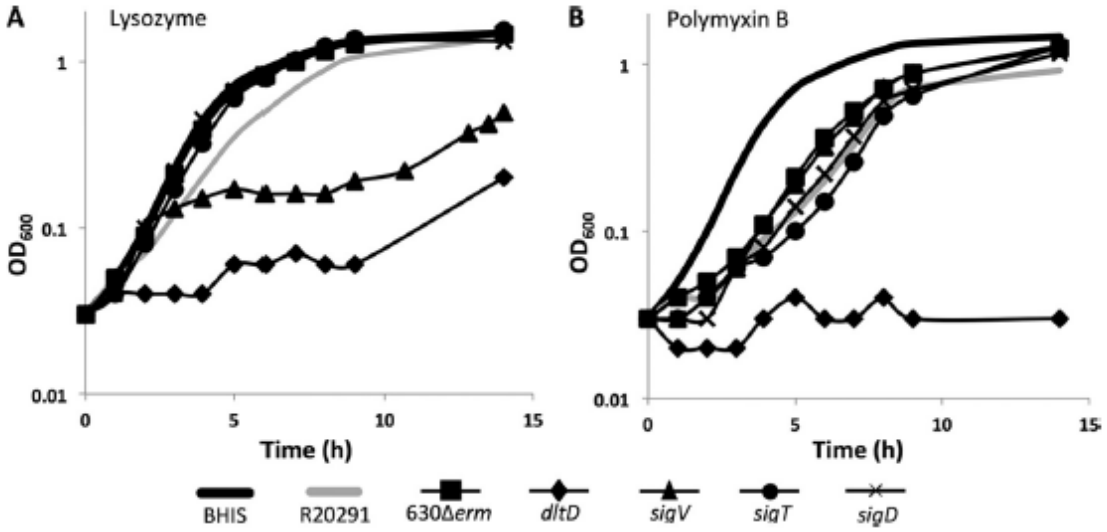

Figure 1. *dlt* and *sigV* mutants have attenuated growth in lysozyme, and a *dlt* mutant has attenuated growth in polymyxin B. Active cultures of strains 630Δ*erm*, R20291, *dltD* (MC319), *sigV* (MC361), *sigT* (MC383), and *sigD* (RT1074) were diluted an to OD_{600} of 0.05 in BHIS supplemented with (**A**) 1 mg/ml lysozyme, or (**B**) 200 µg/ml polymyxin B. All strains grew similarly in BHIS alone, as depicted with the solid black line on each graph. Graphs are representative growth curves from three biological replicates.

results indicate that σ^T and σ^D are not critical for regulation of the *dlt* operon in *C. difficile* in response to polymyxin B or lysozyme.

dlt and *sigV* expression are induced by CAMPs

Based on the similar phenotypes of the *dlt* and *sigV* mutants when grown in CAMPs, we further explored σ^V as a potential regulator of the Dlt pathway in response to antimicrobials. We hypothesized that if σ^V regulates *dlt* expression in response to CAMPs, then expression of *sigV* and the *dlt* operon would be simultaneously induced upon exposure to these compounds. Using qRT-PCR, we detected significantly higher *dltD* expression in 630Δ*erm* and R20291 cells grown in 1.0 mg lysozyme ml^{-1} or 200 μg polymyxin B ml^{-1}, compared to cells grown in BHIS alone. (**Fig. 2A**). The increase in *dltD* expression during growth in lysozyme or polymyxin B was more pronounced in the R20291 strain (~15-fold) than in 630Δ*erm* (~8-fold). The expression of *dltD* was greater during growth in lysozyme than in polymyxin B for both R20291 and 630Δ*erm*. But, there was no significant change in *dltD* expression for the *sigV* mutant during growth in lysozyme. This result strongly suggests that σ^V is necessary for increased *dlt* expression in response to lysozyme. Similar to *dltD* regulation, we found that *sigV* expression increases in both R20291 and 630Δ*erm* in response to lysozyme (**Fig. 2A**), with a larger fold-change in R20291 (~80-fold vs. 40-fold, respectively).

In contrast, the *sigV* mutant had a similar change in *dltD* expression during growth in polymyxin B as the parent strain, indicating that a mechanism(s) other than σ^V can regulate *dlt* in response to polymyxin B (**Fig. 2B**). In polymyxin B, *sigV* expression was only marginally higher in the 630Δ*erm* background compared to untreated 630Δ*erm*,

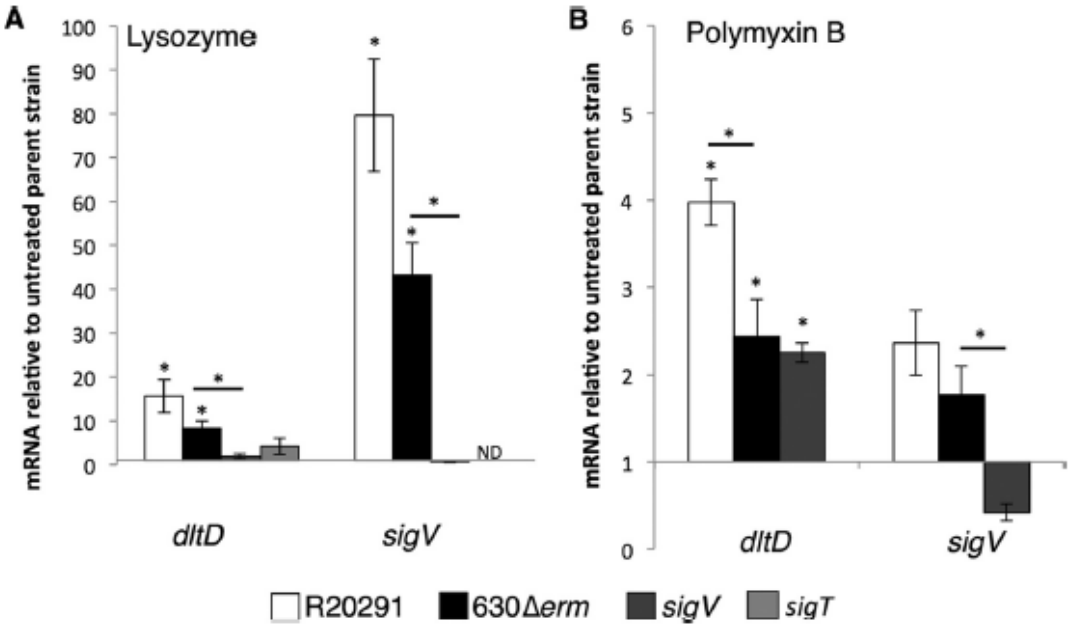

Figure 2. *dltD* and *sigV* expression are induced in lysozyme. qRT-PCR analysis of *dltD* and *sigV* expression in R20291, 630Δ*erm*, *sigV* (MC361), *sigT* (MC383), and *dltD* (MC319) grown in BHIS supplemented with 1 mg/ml lysozyme (**A**) or 200 µg/ml polymyxin B (**B**) as described in Methods. mRNA levels in 630Δ*erm* and the mutant derivatives of this strain (*sigV, sigT, dltD)* are normalized to 630Δ*erm* in BHIS alone. mRNA levels in R20291 are normalized to expression levels in R20291 in BHIS alone. ND indicates not determined. The *sigT* mutant was not assessed in polymyxin B. The means and SEM of three biological replicates are shown. Data were analyzed by a two-way analysis of variance with Sidak's multiple comparison tests. * indicates $p < 0.05$ compared to the untreated parent strain, unless otherwise noted by a bar between the compared strains.

suggesting that the adaptive response to polymyxin B is not σ^V-dependent in this strain (**Fig. 2B**). In contrast, R20291 induced *sigV* and *dlt* transcript more than strain 630Δ*erm* in polymyxin B. These data suggest that R20291 and 630Δ*erm* may have different mechanisms for regulating *dlt* gene expression during growth in polymyxin B, and that σ^V is not a significant regulator of the adaptive response to polymyxin B in the 630Δ*erm* strain. As expected, *sigV* was not expressed in the *sigV* mutant under any condition tested (**Fig. 2**).

dlt and *sigV* mutants have altered morphology in lysozyme

Because *dltD* and *sigV* expression was increased in lysozyme, and growth of these mutants was also affected by lysozyme, we hypothesized that lysozyme has a greater impact on the cell wall of these mutants than on the parent strain. To test this, we used phase contrast microscopy to assess the cellular morphology of the *dlt* and *sigV* mutants during growth in lysozyme (**Fig. 3**). Although the *sigV* and *dlt* mutants have normal morphology in BHIS medium (**Fig. 3A-C**), both mutants displayed altered phenotypes in lysozyme compared to the parent strain, 630Δ*erm*. In both mutant strains, some of the bacteria took on a curved morphology (**Fig 3F and G**). In addition, many of the *dlt* and *sigV* mutant cells lysed during growth in lysozyme, and some of the *dlt* mutant cells appeared elongated. Although more lytic cells were observed in the *sigV* mutant than the *dlt* mutant, the *dlt* mutant grew much more slowly in lysozyme than the *sigV* strain (**Fig. 1A**), suggesting that the *dlt* cells were dying more rapidly. Hence, lysozyme is more effective against *C. difficile* that lack σ^V or cannot incorporate D-alanine into the cell wall.

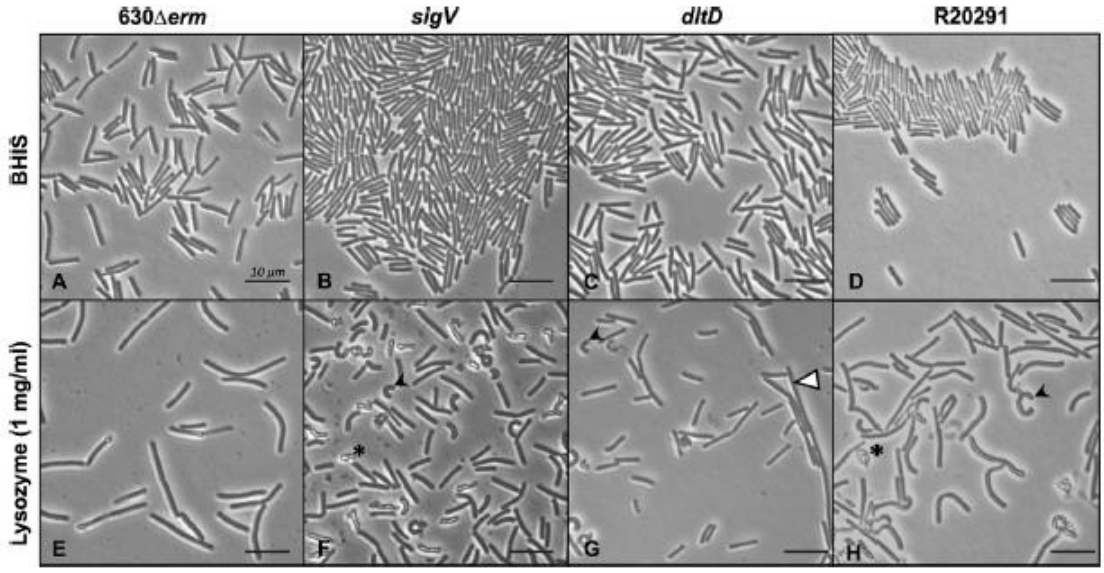

Figure 3. *dlt* and *sigV* mutants have altered cell morphology in lysozyme. Representative phase contrast micrographs of 630Δ*erm*, *sigV* mutant (MC361), *dltD* mutant (MC319), and R20291 were grown in BHIS alone (**A-D**) or BHIS supplemented with 1 mg/ml lysozyme to mid-log phase (**F-H**). Black arrowheads indicate examples of curved morphology, * indicates examples of lysed cells and the white arrowhead indicates an example of an elongated cell.

Similar to the *sigV* and *dlt* mutants, R20291 adopted altered morphologies and phenotypes in lysozyme, including curved cell shapes, elongated cells, and apparent cell lysis (**Fig. 3H**). The more dramatic effect of lysozyme on cell morphology in R20291 compared to 630Δ*erm* parallels the slight growth defect that we observed in R20291 in lysozyme (**Fig. 1A**). These findings indicate that strain R20291 is more affected by lysozyme than 630Δ*erm*.

D-alanylation of the cell wall increases upon exposure to CAMPs

The Dlt pathway is responsible for catalyzing the addition of D-alanine (D-ala) to teichoic acids in the cell wall of *C. difficile* (12, 13). To determine if the observed increases in *dlt* expression affect D-alanylation of the cell wall, we examined the D-ala content of R20291, 630Δ*erm*, and the *sigV* and *dlt* mutants, grown with and without polymyxin B or lysozyme. We calculated the amount of D-ala esters present in purified cell walls of 630Δ*erm*, R20291, the *sigV* mutant, and the *dlt* mutant grown in BHIS alone or in BHIS supplemented with 0.6 mg lysozyme ml^{-1} or 150 µg polymyxin B ml^{-1} as described in Materials and Methods (**Fig. 4**). As previously observed, the *dlt* mutant had undetectable D-ala content in the cell wall (12). As expected from *dlt* expression analyses, the relative D-ala content in 630Δ*erm* and R20291 was higher in cells exposed to lysozyme or polymyxin B than for cells grown in BHIS alone. D-ala content was higher in 630Δ*erm* than in R20291 in BHIS and with added lysozyme, suggesting that these strains inherently differ in their ability to D-alanylate teichoic acids. The D-ala content of the *sigV* mutant in BHIS alone was similar to that of 630Δ*erm*. The *sigV* mutant did not have a significantly altered amount of D-ala when exposed to lysozyme or polymyxin B. These data

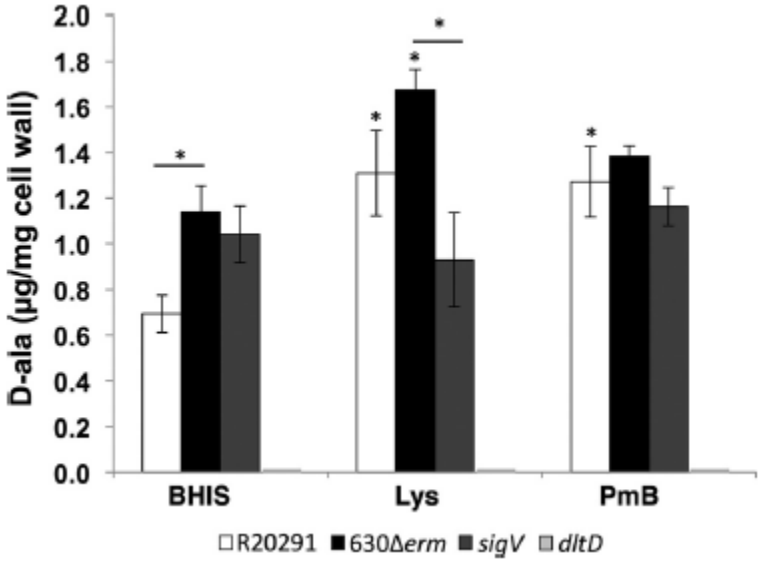

Figure 4. A *sigV* mutant does not increase D-alanine cell wall content in lysozyme. R20291, 630Δ*erm*, *sigV* (MC361), and *dltD* (MC319) were grown in BHIS alone or in BHIS supplemented with either 0.6 mg/ml lysozyme (Lys) or 150 µg/ml polymyxin B (PmB). Results are presented as the means and SEM from at least three biological replicates, each performed as technical duplicates. Data were analyzed by a two-way analysis of variance with Dunnett's multiple comparison tests. *indicates $p < 0.05$ compared to the untreated parent strain, except where indicated by a bar between the compared strains.

demonstrate that σ^V is not necessary for basal-level D-alanylation of the cell wall that occurs in the absence of CAMPs, but σ^V is required for increased D-alanylation in the presence of lysozyme.

Identification of *dlt* promoter elements

To evaluate the potential promoter elements necessary for σ^V-dependent and independent transcription of the *dlt* operon, we created a series of transcriptional fusions of the predicted *dltD* promoter to a *phoZ* (alkaline phosphatase) reporter (31). Segments upstream of the *dltD* translational start site (TSS) were amplified and ligated to the *phoZ* reporter gene within a plasmid vector (**Fig. 5A**). The resultant plasmids were conjugated independently into 630Δ*erm* and the *sigV* mutant. To assess potential promoter functions of this region, the resultant strains were grown with or without lysozyme and assayed for alkaline phosphatase (AP) activity (**Table 3**).

Initially, reporter fusions containing the 600 bp region upstream of the *dltD* start codon from strains 630Δ*erm* or R20291 were assessed for activity in both the 630Δ*erm* and *sigV* mutant strains (Pdlt_{600}*::phoZ* and Pdlt_{600}*::phoZ* (R20291); **Table 3**). As predicted, this region contains the necessary promoter elements to support transcription, as evidenced by AP activity. Despite multiple nucleotide differences between the P*dlt* sequences of the R20291 and 630Δ*erm* strains (**Fig. 5B**), the AP activity generated from the respective promoter fusions (expressed in the 630Δ*erm* background) were comparable, indicating that these sequence changes do not affect promoter activity. Importantly, these fusions demonstrated lysozyme-dependent induction of activity in 630Δ*erm*, but only lower,

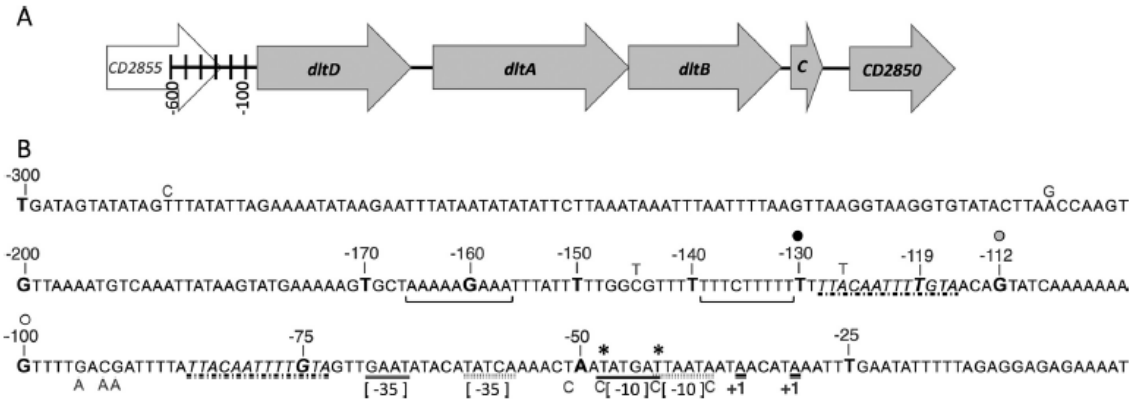

Figure 5. The *dlt* promoter region. (**A**) Schematic of the *dlt* operon and the upstream region used in promoter fusion constructs. The *dlt* operon consists of four genes, *dltDABC*. CD2850 encodes a putative DeoR-type regulator, is co-transcribed with the *dltDABC* operon, and is not required for expression or function of the Dlt pathway (12). CD2855 lies 288 bp upstream of *dltD* and is not part of the operon (12). Promoter fusion constructs were made with segments of the upstream region included. (**B**) DNA sequence from strain 630Δ*erm* from 300 bp upstream of the predicted *dltD* translational start site. Sequence differences in strain R20291 are shown above the sequence. Promoter fusions were created of the indicated sizes marked by bolded nucleotides. The transcriptional start sites identified by 5' RACE analysis are underlined and identified by +1. Identified tandem direct repeat sequences are denoted by italics with black dashed underline. Identified complementary regions are denoted by black brackets above the sequence. Possible spacing for the -10 and -35 of a putative weak σ^A promoter are marked with gray dashed underlines, and possible spacing for the -10 and -35 of a stronger σ^A promoter and overlapping σ^V-dependent promoter are marked with a solid black underline. Base pairs altered by site-directed mutagenesis are indicated below the sequence. * marks the

nucleotides that when mutated abolished promoter activity. White circle denotes minimum required for promoter activity, gray circle denotes region required for lysozyme-dependent activity, and black circle denotes region required for full level of activity.

TABLE 3 Alkaline phosphatase activity from P*dlt*::*phoZ* fusions

Reporter fusion	Activity for strain in medium[a]			
	630Δ*erm*		*sigV* mutant	
	BHIS alone	BHIS + Lys[b]	BHIS alone	BHIS + Lys[c]
phoZ	2 ± 0	2 ± 0	2 ± 0	2 ± 0
Pdlt_{75}::*phoZ*	2 ± 0	2 ± 0	2 ± 0	2 ± 0
Pdlt_{100}::*phoZ*	17 ± 4	23 ± 3	23 ± 7	19 ± 1
Pdlt_{112}::*phoZ*	9 ± 1	21 ± 2	8 ± 1	8 ± 2
Pdlt_{119}::*phoZ*	8 ± 1	26 ± 1	7 ± 0	8 ± 1
Pdlt_{130}::*phoZ*	30 ± 1	**124** ± 10	15 ± 3	**36** ± 4
Pdlt_{140}::*phoZ*	29 ± 7	**116** ± 20	22 ± 3	**30** ± 7
Pdlt_{150}::*phoZ*	31 ± 5	**122** ± 17	26 ± 5	**31** ± 5
Pdlt_{160}::*phoZ*	58 ± 15	**174** ± 31	26 ± 2	**36** ± 3
Pdlt_{170}::*phoZ*	79 ± 4	**197** ± 8	69 ± 0	**63** ± 15
Pdlt_{200}::*phoZ*	44 ± 8	**144** ± 18	49 ± 6	**46** ± 1
Pdlt_{300}::*phoZ*	32 ± 2	**135** ± 10	42 ± 7	**38** ± 3
Pdlt_{600}::*phoZ*	59 ± 6	**173** ± 9	49 ± 8	**32** ± 4
Pdlt_{600}::*phoZ* (R20291)	54 ± 8	**146** ± 23	48 ± 3	**42** ± 14

[a] 630Δ*erm* and *sigV* mutant (MC361) with *dlt* promoter::*phoZ* fusion plasmids were grown in BHIS alone or with 1 mg/ml lysozyme and assayed for AP activity as described in Materials and Methods. Results are the means of calculated AP units ± standard errors of the means for at least three biological replicates. All biological replicates were performed as technical duplicates.

[b] Data were analyzed by a two-way analysis of variance with Sidak's multiple-comparison test, comparing data to the same strain and fusion in BHIS. Bold text indicates $P < 0.05$.

[c] Data were analyzed by a two-way analysis of variance and Sidak's multiple-comparison test, comparing data to the same fusion in strain 630Δ*erm* grown in lysozyme. Bold text indicates $P < 0.05$.

constitutive-level activity was observed in the *sigV* mutant. These results demonstrate that σ^V is required for lysozyme-dependent expression from the *dlt* promoter.

To determine the minimal sequence required for transcription, we examined activity from increasingly larger portions of sequence, beginning at 25 nt upstream of the *dltD* TSS. Segments from 25-75 nt upstream of the *dltD* TSS (P*dlt*$_{25}$*::phoZ*, P*dlt*$_{50}$*::phoZ,* and P*dlt*$_{75}$*::phoZ* fusions) did not generate significant AP activity in the 630Δ*erm* or *sigV* backgrounds, indicating that the 75 bp upstream region is not sufficient for transcription. The P*dlt*$_{100}$*::phoZ* fusion had modest AP activity, demonstrating that the 100 bp region upstream of the *dltD* TSS is sufficient for transcription. The AP activity of the P*dlt*$_{100}$::*phoZ* fusion was not inducible in lysozyme, which suggests that this region does not contain sequence elements necessary for lysozyme-dependent induction of transcription. Additionally, there were no differences between AP activity of P*dlt*$_{100}$::*phoZ* in the parent strain or *sigV* mutant. Thus, the sequence between 75-100 bp upstream of the *dltD* start codon contains the minimal promoter elements for constitutive, low-level transcription of the operon, but is not sufficient for σ^V-dependent transcription.

Sequence analyses of the region revealed two direct repeat sequences spanning from nt -73 to -85 and nt -116 to -128, suggesting that these areas could be involved in regulation. We created constructs using additional nucleotides (P*dlt*$_{112}$::*phoZ*, P*dlt*$_{119}$::*phoZ* and P*dlt*$_{130}$::*phoZ*) to investigate the function of this region. Lysozyme-inducible AP activity was observed with all three constructs in the parent strain, with the highest constitutive and lysozyme-induced activity found for the P*dlt*$_{130}$*::phoZ* fusion (**Table 3**). Lower promoter activity was observed with the P*dlt*$_{112}$::*phoZ* and P*dlt*$_{119}$::*phoZ* in the parent and *sigV* strains, suggesting the direct repeat region may be involved in lysozyme-

independent (constitutive) expression of *dlt*. AP activity from Pdlt_{112}::*phoZ* and Pdlt_{119}::*phoZ* in the *sigV* mutant was not inducible in lysozyme. Therefore, the segment 112 bp upstream of the *dltD* TSS contains a sequence necessary for lysozyme-dependent and σ^V-dependent induction of transcription (**Fig. 5B**)

In addition to the direct repeat sequences mentioned above, two segments of complementary sequence were identified at nt -131 to -139 and nt -157 to -165. Additional reporter fusion constructs were generated to examine these larger segments of the P*dlt* upstream region for differences in regulation (Pdlt_{140}::*phoZ,* Pdlt_{150}::*phoZ,* Pdlt_{160}::*phoZ* and Pdlt_{170}::*phoZ*). The constructs containing promoter segments from -130 to -150 nt upstream of the *dltD* TSS in the 630Δ*erm* strain demonstrated similar levels of AP activity to each other. The *sigV* mutant had lower AP activity with all of these constructs when grown in BHIS, than in medium containing lysozyme. Higher AP activity was observed for 630Δ*erm* strains expressing the Pdlt_{160}::*phoZ* or Pdlt_{170}::*phoZ* fusions, than with the shorter promoter segments. In fact, the Pdlt_{170}::*phoZ* reporter fusion had higher AP activity with or without lysozyme than fusions containing more upstream sequence (Pdlt_{200}::*phoZ,* Pdlt_{300}::*phoZ,* or Pdlt_{600}::*phoZ*). These data suggest that the region 170-200 nt upstream of the *dltD* TSS may contain elements that negatively affect σ^V-independent promoter activity; however, the factors that contribute to this regulation are not known.

To further characterize the *dlt* operon promoter elements and identify potential sites of RNA polymerase binding, we performed 5' RACE analysis on mRNA extracted from 630Δ*erm* grown in the presence of 1 mg/ml lysozyme. This analysis revealed transcriptional start sites at 30 bp and 35 bp upstream of the predicted *dltD* translational start (**Fig. 5B**). The location of transcriptional start sites 5 nt apart suggests that two unique,

but perhaps overlapping, promoters are involved in *dlt* transcription. However, these transcriptional start sites and the anticipated -10 and -35 sites (**Fig. 5B**) are positioned in a segment that was insufficient for reporter expression (P*dlt*$_{75}$*::phoZ*, **Table 3**). Together, these results suggest that RNA polymerase initiates transcription from promoters within the 75 nt upstream of the *dltD* start codon, but additional upstream sequence is needed to facilitate transcription.

Based on the 5' RACE results, we predicted that σ^A and/or σ^V -10 promoter elements may be located either 49-42 bp or 51-45 bp upstream of the *dltD* TSS (**Fig. 5B**). We therefore performed site-directed mutagenesis on the nucleotides at positions -43, -51, -92, -93, and -95 bp upstream of the *dltD* TSS. The AP activity from P*dlt*$_{300}$G-95A::*phoZ,* P*dlt*$_{300}$C-93A::*phoZ,* P*dlt*$_{300}$G-92A::*phoZ,* P*dlt*$_{300}$T-51C::*phoZ* were all comparable to the activity observed from the native-sequence P*dlt*$_{300}$*::phoZ* construct in both the parent strain and *sigV* mutant carrying these constructs during growth in BHIS and lysozyme (**Table 4**). Therefore, we conclude that T-51, G-92, C-93, and G-95 are not essential for constitutive or lysozyme-dependent expression of *dlt*. However, the P*dlt*$_{300}$T-43C::*phoZ* fusion had negligible AP activity in the parent strain in either BHIS or lysozyme. Further, the *sigV* mutant containing the P*dlt*$_{300}$T-43C::*phoZ* construct also lacked expression in BHIS and lysozyme. Hence, nucleotide T-43 is critical for both constitutive and σ^V-dependent, lysozyme-induced transcription of *dlt.* These results strongly suggest that σ^A and σ^V-dependent promoters overlap at T-43. Alternatively, it is possible that σ^V-dependent expression in lysozyme is indirect. In that case, overlapping σ^A-dependent promoters would be used for both constitutive and lysozyme-induced expression with lysozyme-induction mediated by a regulatory factor controlled by σ^V.

TABLE 4 Alkaline phosphatase activity from P*dlt*::*phoZ* fusions with site-directed mutagenesis

Reporter fusion	Activity for strain in medium[a,b]			
	630Δ*erm*		*sigV* mutant	
	BHIS alone	BHIS + Lys	BHIS alone	BHIS + Lys
Pdlt_{300}::*phoZ*	32 ± 2	135 ± 10	42 ± 7	38 ± 3
Pdlt_{300}A-38C::*phoZ*	18 ± 1	102 ± 4	19 ± 3	24 ± 3
Pdlt_{300}T-43C::*phoZ*	**2** ± 0	**2** ± 0	2 ± 0	**3** ± 0
Pdlt_{300}T-48C::*phoZ*	**2** ± 0	**3** ± 0	2 ± 0	**3** ± 0
Pdlt_{300}T-51C::*phoZ*	42 ± 14	145 ± 18	33 ± 5	32 ± 4
Pdlt_{300}G-92A::*phoZ*	31 ± 3	126 ± 4	27 ± 3	43 ± 7
Pdlt_{300}C-93A::*phoZ*	31 ± 5	123 ± 9	48 ± 7	54 ± 7
Pdlt_{300}G-95A::*phoZ*	45 ± 13	149 ± 20	50 ± 7	61 ± 9
Pdlt_{130}::*phoZ*	30 ± 1	124 ± 10	15 ± 3	36 ± 4
P$dlt_{130–75}$::*phoZ*[c]	**2** ± 0	**2** ± 0	1 ± 0	**2** ± 0

[a] 630Δ*erm* and *sigV* mutant (MC361) with *dlt* promoter::*phoZ* fusion plasmids were grown in BHIS alone or with 1 mg/ml lysozyme and assayed for AP activity as described in Materials and Methods. Results are the means of calculated AP units ± standard errors of the means for at least three biological replicates. All biological replicates were performed as technical duplicates.

[b] The activities from site-directed mutagenesis constructs were compared to the native-sequence Pdlt_{300}::*phoZ* under the same conditions by Student's two-tailed *t* test with correction for multiple comparisons by the Holm-Sidak method. Bold text indicates $P \leq 0.05$.

[c] AP activity compared to activity from the full-length Pdlt_{130}::*phoZ* construct in the same strain and under the same conditions.

In order to test whether separate σ^A- and σ^V-dependent promoters overlap at T-43, we performed site-directed mutagenesis at the nucleotides -48 and -38 bp upstream of the *dlt* TSS (**Figure 5B**). If distinct -10 promoter elements overlap at T-43, the -48 and -38 nucleotides would be the initial and final nucleotides of these elements, respectively. The P*dlt*$_{300}$T-48C::*phoZ* fusion had negligible AP activity in both the parent strain and the *sigV* mutant in BHIS or in lysozyme, suggesting that the T-48 is a necessary for both constitutive and lysozyme-dependent transcription (**Table 4**). Compared to the native-sequence P*dlt*$_{300}$*::phoZ* construct, AP activity from P*dlt*$_{300}$A-38C::*phoZ* was lower in the parent strain and the *sigV* mutant in both BHIS and lysozyme. However, the mutation at A-38 did not abolish the induction of activity in lysozyme in the parent strain, indicating that σ^V-dependent transcription was retained. Therefore, A-38 may be important for basal *dlt* transcription, as well as σ^V-dependent transcription in lysozyme.

σ^V and the Dlt pathway impact *C. difficile* virulence *in vivo*

Because the *sigV* and *dlt* mutants are more sensitive to lysozyme (**Fig. 1A**), we hypothesized that these mutants would be less fit *in vivo*. In a previous study, Ho et al. demonstrated that a *sigV* mutant is significantly attenuated in a hamster model of infection (21). However, that study was performed in the JIR8094 strain, which is attenuated for virulence *in vivo* (46, 50). To determine the relative impacts of the *dlt* and *sigV* mutations on virulence, hamster infections were performed using the *dlt* and *sigV* isogenic mutants derived from the 630Δ*erm* strain.

Seven days after a single dose of clindamycin, hamsters were gavaged with approximately 5000 spores of 630Δ*erm*, *dltD* or *sigV*, as described in the Materials and Methods. Fecal samples were collected daily and cecal samples were collected at the point

of morbidity (post-mortem) to enumerate CFU. Hamsters infected with the *sigV* mutant reached morbidity significantly faster than those infected with 630Δ*erm* (46.2 h ± 17.9 h 630Δ*erm* v. 33.2 h ± 6.3 h *sigV*), demonstrating that σ^V affects virulence *in vivo* (**Fig. 6A**). At the point of morbidity, the ceca of hamsters infected with the *sigV* mutant contained significantly more CFU than those infected with 630Δ*erm*, indicating that this mutant has a growth advantage in the host (**Fig. 6B**). Hamsters infected with the *dlt* mutant also reached morbidity significantly earlier than those infected with 630Δ*erm* (46.2 h ± 17.9 h 630Δ*erm* v. 35.8 h ± 5.0 h *dlt*), but hamsters infected with the *dlt* mutant strain had similar CFU counts in cecal samples compared to the parent strain. These data suggest that the lack of D-ala in the cell wall contributes to increased virulence *in vivo*, but does not provide a growth advantage to the bacterium.

To determine if the increased virulence observed with *dlt* mutant infections could be due to an altered ability of the host to recognize the bacterium (*i.e.*, immune system response to the lipoteichoic acid antigen), we performed competitive infections with 1:1 mixtures of 630Δ*erm* and *dlt* mutant spores. Hamsters co-infected with the mixture of 630Δ*erm* and *dlt* mutant spores reached morbidity earlier than those infected with the 630Δ*erm* alone and at a rate comparable to those infected with the *dlt* mutant alone (35.4 h ± 5.1 h for co-infection v. 46.2 h ± 17.9 h for 630Δ*erm* and 35.8 h ± 5.0 h for *dlt*). The *dlt* mutant therefore remains more virulent than 630Δ*erm*, even when 630Δ*erm* is present. The total number of CFU recovered from the ceca of co-infected hamsters was comparable to the number of CFU recovered from the ceca of hamsters infected with either 630Δ*erm* or the *dlt* mutant alone. Similar numbers of 630Δ*erm* and *dlt* CFU were recovered from the ceca of co-infected hamsters (**Fig. 6B**), and the mean competitive index for the *dlt* mutant

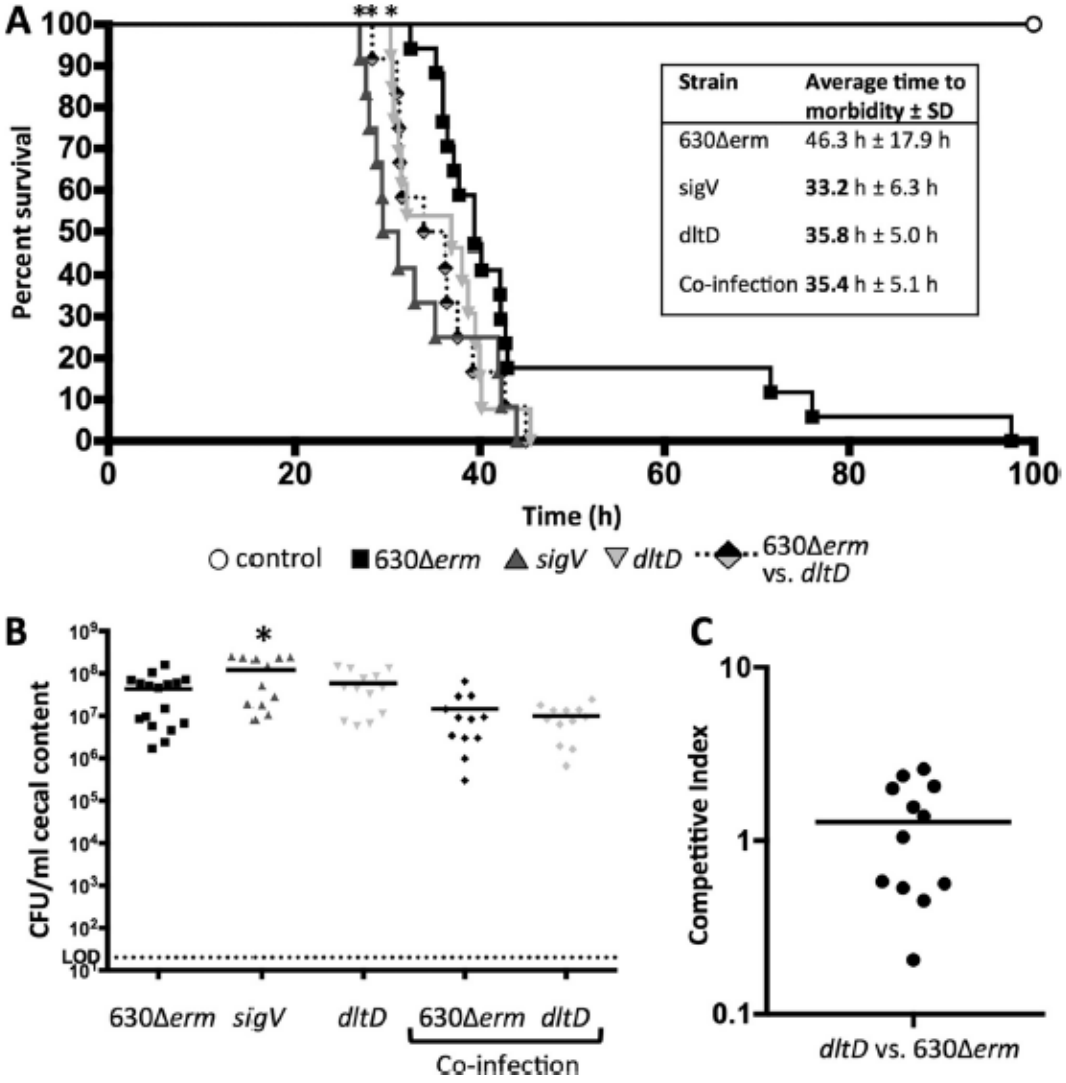

Figure 6. *dlt* and *sigV* mutants are more virulent than the parent strain in a hamster model of infection. Syrian golden hamsters were inoculated with approximately 5000 spores of 630Δ*erm* (n = 17), *dltD* (MC319; n = 13), *sigV* (MC361; n = 12), or a 1:1 mixture of 630Δ*erm* and MC319 (630Δ*erm* vs. *dltD;* n = 12). (**A**) Kaplan-Meier survival curve depicting time to morbidity. * indicates $p \leq 0.05$ by log-rank test. The inset table lists the average time to morbidity for each strain ± SD with bold text indicating $p \leq 0.05$ by log-

rank test. (**B**) Total number of *C. difficile* CFU recovered from cecal contents collected post-mortem. Dotted line demarcates limit of detection. Solid black line marks the mean. Numbers of CFU are compared to 630Δ*erm* by a one-way analysis of variance with Dunnett's multiple comparisons tests (* indicates $p < 0.05$). (**C**) Competive index (CI) of the *dlt* mutant for each hamster co-infected with 630Δ*erm* and the *dlt* mutant is shown. CI = 1 indicates no fitness advantage. CI < 1 indicates reduced fitness of the *dlt* mutant. CI > 1 indicates increased fitness of the *dlt* mutant.

was 1.2 (**Fig. 6C**), suggesting that neither strain had a significant competitive advantage *in vivo*.

Because our results for *sigV* mutant infections differed from results previously obtained in the JIR8094 background (21), we performed an additional experiment using JIR8094 and TCD20 strains (kindly provided by C. Ellermeier), to determine the basis for this variability (**Fig. S6**). In our hands, animals infected with JIR8094 strain succumbed to infection 3.7 days later on average than the 630Δ*erm* infected animals, similar to results obtained by other investigators (47, 51). The animals infected with strain TCD20 (JIR8094 *csfV/sigV* mutant) presented with symptoms of CDI and became moribund faster than those infected with the JIR8094 parent strain (133.2 ± 75.2 h v. 76.9 ± 12.9 h for TCD20). This is in contrast to the findings of Ho et al., which observed a much longer time to morbidity with the JIR8094 strain and low morbidity with the JIR8094 *sigV* mutant (TCD20). Thus, both *sigV* mutant strains caused animals to become moribund more quickly than the parental strain-infected animals.

DISCUSSION

Resistance to CAMPs can enable the survival of bacterial pathogens within the host (52, 53). As an intestinal pathogen, *C. difficile* encounters many CAMPs in the gut, including those produced by the host and indigenous microbiota (2, 4, 7-9, 54, 55). One mechanism that enables *C. difficile* to resist killing by CAMPs is the altering of cell surface charge via the Dlt pathway, which adds D-alanines to cell wall teichoic acids (12, 13). In this paper, we demonstrate that expression of the Dlt pathway is regulated by the extracytoplasmic function sigma factor, σ^V. Moreover, we show that regulation of *dlt* by

σ^V occurs in response to the host-produced CAMP, lysozyme, and that the incorporation of D-alanine into the cell wall is critical for lysozyme resistance.

The other alternative sigma factors examined, σ^T and σ^D, did not significantly contribute to *dlt* expression under the conditions tested. Similar to previous findings, we observed that *sigT* expression increased about 2-fold in the presence of lysozyme (data not shown, (30)), implying that σ^T could contribute to lysozyme resistance through a mechanism other than Dlt. The *sigT* mutant also demonstrated a modest growth delay in polymyxin B (**Fig. 1**), but σ^T did not appear to influence *dlt* transcription in polymyxin B (**Fig. S3**), suggesting that σ^T contributes to polymyxin B resistance through an alternate mechanism. The *sigV* mutant did not demonstrate a growth defect in polymyxin B (**Fig. 1**) and the *sigV* mutant induced *dlt* expression in polymyxin B similar to the parent strain (**Fig. 2B**). Thus, polymyxin B induces *dlt* expression through a σ^D-, σ^T- and σ^V-independent mechanism.

Because the ribotype 027 epidemic strains have proven very successful in colonizing and causing disease (56-58), we considered that these strains might have increased resistance to lysozyme. As evidenced by growth assays (**Fig. 1**), the R20291 strain (027 ribotype) was more sensitive to both lysozyme and polymyxin B than the 630Δ*erm* strain (012 ribotype). Examination of *dlt* expression in R20291 showed that this strain induced *dlt* transcription more robustly than 630Δ*erm* in polymyxin B and lysozyme (**Fig. 2**). But, analyses of D-alanine cell wall content revealed that R20291 incorporated less total D-alanine than 630Δ*erm* at baseline and in the tested CAMPs. Moreover, R20291 had greater morphological cell changes in lysozyme than strain 630Δ*erm* (**Fig. 3**). But, the R20291 strain had significantly more D-alanine incorporation when grown in polymyxin

B than in BHIS alone, while no significant change in D-alanine content was observed for 630Δ*erm* in polymyxin B (**Fig. 4**). The difference in *dlt* transcription by these strains was not explained by the nucleotide changes in their *dlt* promoter sequences, as demonstrated with reporter fusions to the R20291 and 630Δ*erm* promoters (**Fig. S2**). Based on these results, it is likely that R20291 encodes a regulatory factor that influences *dlt* transcription in response to polymyxin B, which is not present in the 630Δ*erm* strain.

Our results identified the *dlt* operon as part of the σ^V regulon of *C. difficile*. In a previous study, Ho *et al.* identified σ^V as important for lysozyme resistance in *C. difficile* (21), and identified several σ^V-dependent transcripts including a peptidoglycan deacetylase, putative exported proteins, an ABC transporter system and many genes of unknown function, but *dlt* was not detected. σ^V and other ECF sigma factors have been shown to regulate *dlt* expression in *Bacillus subtilis*. *C. difficile* strain 630 has three identified ECF sigma factors, σ^T, σ^V, and σ^W (30), but σ^W is encoded in only a few strains (59). The R20291 genome encodes multiple sigma factors and putative regulatory proteins that are not present in strain 630. It is possible that in R20291 these regulators, or σ^D, are involved in transcription of *dlt* in response to other CAMPs or host conditions.

Though likely, these results do not definitively prove that σ^V directly regulates *dlt* in response to lysozyme. 5' RACE identified multiple transcriptional start sites, which would be expected if σ^A and σ^V directly mediate RNA polymerase binding from distinct promoters. The transcriptional start sites that we identified are 5 bp apart, which is close enough that two distinct promoters would likely overlap at nt T-43 (**Fig. 5B**). Site-directed mutagenesis of nucleotides within the predicted -10 promoter elements revealed that a single nucleotide changes at -43 or -48 upstream of the *dlt* TSS was sufficient to abolish

lysozyme-dependent and independent *dlt* expression (**Table 4**). In addition, mutagenesis of A-38 decreased both lysozyme-dependent and independent *dlt* expression, without abolishing induction of *dlt* expression in lysozyme. These findings imply that the promoter region required for σ^A and σ^V-dependent transcription of *dlt* overlap. Moreover, a reporter fusion containing the putative -10 and -35 elements (P*dlt*$_{75}$*::phoZ*) was not sufficient for activity, and full σ^V-dependent transcription was achieved only when additional upstream sequence was included (P*dlt*$_{130}$*::phoZ*). We hypothesize that the tandem repeats contained within this 130 bp region may be important for binding of additional σ^V-dependent regulatory factors. The region that is necessary for a σ^V-dependent lysozyme response (130-75 bp upstream of the *dltD* TSS) is farther upstream than the predicted locations of the promoters, based on the transcriptional start sites identified (**Fig. 5**). A construct containing only the 130-75 bp region had no AP activity, with or without added lysozyme (**Table 4**). These results indicate that this region does not contain sufficient elements for transcription initiation. Moreover, AP activity peaked with the P*dlt*$_{170}$*::phoZ* construct, which suggests that the regions of complementarity that we identified within this 170 bp region could be involved in secondary structures that impact transcription. Further studies are needed to identify additional factors that bind this region and influence *dlt* transcription.

Despite the increased sensitivity of the *sigV* and *dlt* mutants to lysozyme *in vitro* (**Fig. 1B**), both of these mutants demonstrated increased virulence *in vivo* (**Fig. 6A**). It is unlikely that this increased virulence is due to increased toxin production, because we observed similar levels of *tcdA* expression in both mutants *in vitro* (**Fig. S4A**). Levels of toxin expression in the cecal contents of infected hamsters at the time of morbidity were also similar between strains, although the cecal contents of hamsters infected with the *sigV*

mutant trended towards higher toxin levels (**Fig. S4B**). Given the importance of σ^V and Dlt in lysozyme resistance *in vitro*, one might expect that the lack of cell wall modification in the *dlt* and *sigV* mutants would make the bacteria more susceptible to innate immune clearance. However, the presence of cell wall modifications, while protective against innate immune effectors, are also immunogenic and may increase the host response to the pathogen. Thus, it is possible that the increased virulence of the *dlt* mutant may be due to an altered host immune response to this mutant. D-alanylated lipoteichoic acid (LTA) is an epitope for the host receptor, toll-like receptor 2 (TLR2) (60, 61). In most pathogens investigated, the lack of a functional Dlt pathway results in decreased virulence (14, 62-64). But it is possible that D-alanylation of LTA may be a mechanism by which *C. difficile* can mask the immunogenic portions of LTA and evade an immune response. Such a mechanism would be similar to how D-alanylation of LTA in *Staphylococcus aureus* masks antigenic portions of peptidoglycan resulting in decreased virulence because the immune system can better respond to antigens that are unmasked in the mutant (65). But in CDI, a more robust immune response leads to greater intestinal injury (55, 66, 67). Because the *dlt* mutant lacks D-alanylated LTA (**Fig. 4**), this mutant may elicit a stronger immune response, which causes more severe disease symptoms than the parent strain. In co-infection experiments, hamsters reached morbidity at a rate comparable to those infected with the *dlt* mutant alone (**Fig. 6A**), which would be expected if an enhanced immune response to the mutant leads to increased virulence. However, the parent strain did not have a colonization advantage during co-infection (**Fig. 6B** and **C**), as might be expected if the *dlt* mutant is more readily recognized by the immune system.

σ^V has been established as an important factor for colonization and virulence in *E. faecalis*, though in *E. faecalis* a *sigV* mutant is less virulent than the parent strain and σ^V does not control *dlt* expression (68). In *C. difficile*, the *sigV* mutant retains a baseline level of D-alanylated LTA (**Fig. 4**), but is unable to induce other σ^V-dependent modifications to the cell surface. The immunogenicity of σ^V-dependent surface modifications is unknown, but our results suggest that σ^V plays a role in host colonization and may affect recognition of the pathogen by the host. Moreover, the increased virulence that we observed for the *sigV* mutant contradicts an earlier finding of attenuated virulence for a *C. difficile sigV* mutant (21). This previous study was performed with a *sigV* mutant in the strain JIR8094 background. JIR8094 colonizes the intestine more slowly than 630Δ*erm*, has lower toxin A and B production (**Fig. S5A**), is non-motile, has lower expression of flagellar genes and is overall less virulent (46-48, 50, 69). The virulence defects of this strain explain the shorter average time to morbidity with our parent strain compared to that of Ho, *et al.* Moreover, in our hands, this *sigV* mutant (TCD20) was more virulent than the parent strain (**Fig. S6**). Our results with JIR8094 are more similar to previously published experiments with this strain (47) than the results obtained by Ho, *et al.* Possible reasons for the discrepancies observed between our results and those of Ho, *et al.* may be due to differences in the spore preparation, timing of clindamycin administration, variations in hamster genetics or differences in the microbiome of the animals used in these studies.

A number of other questions remain to be answered about the regulation of *dlt* and the role of σ^V in *C. difficile*. Does σ^V directly regulate *dlt* expression? Are the tandem repeats upstream of *dlt* binding sites for a regulatory factor? What factors regulate *dlt* expression in response to other triggers, such as polymyxin B? Despite these remaining

questions, our finding that σ^V regulates the Dlt pathway in *C. difficile* in response to lysozyme represents an important insight into the mechanisms that enable *C. difficile* colonization. These results underscore the complex relationship between mechanisms of antimicrobial resistance and the effects of these modifications on virulence. Mutants in more virulent isolates, such as R20291, may allow for further study of these mechanisms in the mouse model of CDI, which would enable more detailed investigation of the immune response to cell wall modifications. Surviving the innate immune response is a critical step in the process of disease progression, and therefore represents a key window of opportunity for therapeutic intervention and prevention of pathogenesis. Identifying ways to increase *C. difficile* susceptibility to innate immune responses may help extend the utility and efficacy of our current antibiotic therapies.

FUNDING INFORMATION

This research was supported by the U.S. National Institutes of Health through research grants DK087763, DK101870, AI109526 and AI116933 to S.M.M., T32 GM008169 to E.C.W., and T32 AI106699 to K.L.N. The content of this manuscript is solely the responsibility of the authors and does not necessarily reflect the official views of the National Institutes of Health.

ACKNOWLEDGEMENTS

We give special thanks thank Rita Tamayo for providing us with the *sigD* mutant (RT1075) and Craig Ellermeier for strains JIR8094 and TCD20. We also give thanks to Bill Shafer, Charles Moran, Joanna Goldberg and members of the McBride lab for helpful suggestions

and discussions during the course of this work. We also thank Jeremy Boss for use of the Bio-Rad CFX96 real-time PCR detection system.

REFERENCES

1. **Lessa FC, Mu Y, Bamberg WM, Beldavs ZG, Dumyati GK, Dunn JR, Farley MM, Holzbauer SM, Meek JI, Phipps EC, Wilson LE, Winston LG, Cohen JA, Limbago BM, Fridkin SK, Gerding DN, McDonald LC.** 2015. Burden of *Clostridium difficile* Infection in the United States. N Engl J Med **372:**825-834.

2. **Eckmann L.** 2005. Defence molecules in intestinal innate immunity against bacterial infections. Curr Opin Gastroenterol **21:**147-151.

3. **Wah J, Wellek A, Frankenberger M, Unterberger P, Welsch U, Bals R.** 2006. Antimicrobial peptides are present in immune and host defense cells of the human respiratory and gastrointestinal tracts. Cell Tissue Res **324:**449-456.

4. **Tollin M, Bergman P, Svenberg T, Jornvall H, Gudmundsson GH, Agerberth B.** 2003. Antimicrobial peptides in the first line defence of human colon mucosa. Peptides **24:**523-530.

5. **Lakshminarayanan B, Guinane CM, O'Connor PM, Coakley M, Hill C, Stanton C, O'Toole PW, Ross RP.** 2013. Isolation and characterization of bacteriocin-producing bacteria from the intestinal microbiota of elderly Irish subjects. J Appl Microbiol **114:**886-898.

6. **Drissi F, Buffet S, Raoult D, Merhej V.** 2015. Common occurrence of antibacterial agents in human intestinal microbiota. Front Microbiol **6:**441.

7. **Muller CA, Autenrieth IB, Peschel A.** 2005. Innate defenses of the intestinal epithelial barrier. Cell Mol Life Sci **62:**1297-1307.

8. **Dommett R, Zilbauer M, George JT, Bajaj-Elliott M.** 2005. Innate immune defence in the human gastrointestinal tract. Mol Immunol **42:**903-912.

9. **Mason DY, Taylor CR.** 1975. The distribution of muramidase (lysozyme) in human tissues. J Clin Pathol **28:**124-132.

10. **Nizet V.** 2006. Antimicrobial peptide resistance mechanisms of human bacterial pathogens. Curr Issues Mol Biol **8:**11-26.

11. **Nawrocki KL, Crispell EK, McBride SM.** 2014. Antimicrobial Peptide Resistance Mechanisms of Gram-Positive Bacteria. Antibiotics (Basel) **3:**461-492.

12. **McBride SM, Sonenshein AL.** 2011. The *dlt* operon confers resistance to cationic antimicrobial peptides in *Clostridium difficile*. Microbiology **157:**1457-1465.

13. **Neuhaus FC, Baddiley J.** 2003. A continuum of anionic charge: structures and functions of D-alanyl-teichoic acids in gram-positive bacteria. Microbiol Mol Biol Rev **67:**686-723.

14. **Le Jeune A, Torelli R, Sanguinetti M, Giard JC, Hartke A, Auffray Y, Benachour A.** 2010. The extracytoplasmic function sigma factor SigV plays a key role in the original model of lysozyme resistance and virulence of *Enterococcus faecalis*. PLoS One **5:**e9658.

15. **Guariglia-Oropeza V, Helmann JD.** 2011. *Bacillus subtilis* sigma(V) confers lysozyme resistance by activation of two cell wall modification pathways, peptidoglycan O-acetylation and D-alanylation of teichoic acids. J Bacteriol **193:**6223-6232.

16. **Antunes A, Camiade E, Monot M, Courtois E, Barbut F, Sernova NV, Rodionov DA, Martin-Verstraete I, Dupuy B.** 2012. Global transcriptional control by glucose and carbon regulator CcpA in Clostridium difficile. Nucleic Acids Res **40:**10701-10718.

17. **Cao M, Helmann JD.** 2004. The *Bacillus subtilis* Extracytoplasmic-Function X Factor Regulates Modification of the Cell Envelope and Resistance to Cationic Antimicrobial Peptides. J Bacteriol **186:**1136-1146.

18. **Estacio W, Anna-Arriola SS, Adedipe M, Marquez-Magana LM.** 1998. Dual promoters are responsible for transcription initiation of the fla/che operon in Bacillus subtilis. J Bacteriol **180:**3548-3555.

19. **Perego M, Glaser P, Minutello A, Strauch MA, Leopold K, Fischer W.** 1995. Incorporation of D-alanine into lipoteichoic acid and wall teichoic acid in Bacillus subtilis. Identification of genes and regulation. J Biol Chem **270:**15598-15606.

20. **Helmann JD.** 2002. The extracytoplasmic function (ECF) sigma factors. Adv Microb Physiol **46:**47-110.

21. **Ho TD, Williams KB, Chen Y, Helm RF, Popham DL, Ellermeier CD.** 2014. *Clostridium difficile* extracytoplasmic function sigma factor sigmaV regulates lysozyme resistance and is necessary for pathogenesis in the hamster model of infection. Infect Immun **82:**2345-2355.

22. **Hastie JL, Williams KB, Sepulveda C, Houtman JC, Forest KT, Ellermeier CD.** 2014. Evidence of a bacterial receptor for lysozyme: binding of lysozyme to the anti-sigma factor RsiV controls activation of the ECF sigma factor sigmaV. PLoS Genetics **10:**e1004643.

23. **Luria SE, Burrous JW.** 1957. Hybridization between *Escherichia coli* and *Shigella*. J Bacteriol **74:**461-476.

24. **Smith CJ, Markowitz SM, Macrina FL.** 1981. Transferable tetracycline resistance in *Clostridium difficile*. Antimicrob Agents Chemother **19:**997-1003.

25. **Bouillaut L, McBride SM, Sorg JA.** 2011. Genetic manipulation of *Clostridium difficile*. Curr Protoc Microbiol **Chapter 9:**Unit 9A 2.

26. **Edwards AN, Suarez JM, McBride SM.** 2013. Culturing and maintaining *Clostridium difficile* in an anaerobic environment. J Vis Exp doi:10.3791/50787**:**e50787.

27. **Sorg JA, Dineen SS.** 2009. Laboratory maintenance of Clostridium difficile. Curr Protoc Microbiol **Chapter 9:**Unit9A 1.

28. **Heap JT, Pennington OJ, Cartman ST, Carter GP, Minton NP.** 2007. The ClosTron: a universal gene knock-out system for the genus *Clostridium*. J Microbiol Methods **70:**452-464.

29. **Karberg M, Guo H, Zhong J, Coon R, Perutka J, Lambowitz AM.** 2001. Group II introns as controllable gene targeting vectors for genetic manipulation of bacteria. Nat Biotechnol **19:**1162-1167.

30. **Ho TD, Ellermeier CD.** 2011. PrsW is required for colonization, resistance to antimicrobial peptides, and expression of extracytoplasmic function sigma factors in *Clostridium difficile*. Infect Immun **79:**3229-3238.

31. **Edwards AN, Pascual RA, Childress KO, Nawrocki KL, Woods EC, McBride SM.** 2015. An alkaline phosphatase reporter for use in *Clostridium difficile*. Anaerobe **32C:**98-104.

32. **Dineen SS, Villapakkam AC, Nordman JT, Sonenshein AL.** 2007. Repression of *Clostridium difficile* toxin gene expression by CodY. Mol Microbiol **66:**206-219.

33. **Edwards AN, Nawrocki KL, McBride SM.** 2014. Conserved oligopeptide permeases modulate sporulation initiation in *Clostridium difficile*. Infect Immun **82:**4276-4291.

34. **Purcell EB, McKee RW, McBride SM, Waters CM, Tamayo R.** 2012. Cyclic diguanylate inversely regulates motility and aggregation in Clostridium difficile. J Bacteriol **194:**3307-3316.

35. **Putnam EE, Nock AM, Lawley TD, Shen A.** 2013. SpoIVA and SipL are Clostridium difficile spore morphogenetic proteins. J Bacteriol **195:**1214-1225.

36. **McBride SM, Sonenshein AL.** 2011. Identification of a genetic locus responsible for antimicrobial peptide resistance in *Clostridium difficile*. Infect Immun **79:**167-176.

37. **Dineen SS, McBride SM, Sonenshein AL.** 2010. Integration of metabolism and virulence by *Clostridium difficile* CodY. J Bacteriol **192:**5350-5362.

38. **Suarez JM, Edwards AN, McBride SM.** 2013. The *Clostridium difficile cpr* locus is regulated by a noncontiguous two-component system in response to type A and B lantibiotics. J Bacteriol **195:**2621-2631.

39. **Hyyrylainen HL, Vitikainen M, Thwaite J, Wu H, Sarvas M, Harwood CR, Kontinen VP, Stephenson K.** 2000. D-Alanine substitution of teichoic acids as a modulator of protein folding and stability at the cytoplasmic membrane/cell wall interface of *Bacillus subtilis*. J Biol Chem **275:**26696-26703.

40. **Fisher N, Shetron-Rama L, Herring-Palmer A, Heffernan B, Bergman N, Hanna P.** 2006. The *dltABCD* operon of *Bacillus anthracis sterne* is required for virulence and resistance to peptide, enzymatic, and cellular mediators of innate immunity. J Bacteriol **188:**1301-1309.

41. **Bartlett JG, Onderdonk AB, Cisneros RL, Kasper DL.** 1977. Clindamycin-associated colitis due to a toxin-producing species of Clostridium in hamsters. J Infect Dis **136:**701-705.

42. **Chang TW, Bartlett JG, Gorbach SL, Onderdonk AB.** 1978. Clindamycin-induced enterocolitis in hamsters as a model of pseudomembranous colitis in patients. Infect Immun **20:**526-529.

43. **Wilson KH, Silva J, Fekety FR.** 1981. Suppression of Clostridium difficile by normal hamster cecal flora and prevention of antibiotic-associated cecitis. Infect Immun **34:**626-628.

44. **George WL, Sutter VL, Citron D, Finegold SM.** 1979. Selective and differential medium for isolation of Clostridium difficile. J Clin Microbiol **9:**214-219.

45. **Bordeleau E, Purcell EB, Lafontaine DA, Fortier LC, Tamayo R, Burrus V.** 2015. Cyclic di-GMP riboswitch-regulated type IV pili contribute to aggregation of Clostridium difficile. J Bacteriol **197:**819-832.

46. **McKee RW, Mangalea MR, Purcell EB, Borchardt EK, Tamayo R.** 2013. The second messenger cyclic Di-GMP regulates Clostridium difficile toxin production by controlling expression of sigD. J Bacteriol **195:**5174-5185.

47. **Lyras D, O'Connor JR, Howarth PM, Sambol SP, Carter GP, Phumoonna T, Poon R, Adams V, Vedantam G, Johnson S, Gerding DN, Rood JI.** 2009. Toxin B is essential for virulence of Clostridium difficile. Nature **458:**1176-1179.

48. **Kuehne SA, Cartman ST, Heap JT, Kelly ML, Cockayne A, Minton NP.** 2010. The role of toxin A and toxin B in Clostridium difficile infection. Nature **467:**711-713.

49. **Goulding D, Thompson H, Emerson J, Fairweather NF, Dougan G, Douce GR.** 2009. Distinctive profiles of infection and pathology in hamsters infected with Clostridium difficile strains 630 and B1. Infect Immun **77:**5478-5485.

50. **Viswanathan VK.** 2014. Memories of a virulent past. Gut Microbes **5:**143-145.

51. **Wu X, Hurdle JG.** 2014. The Clostridium difficile proline racemase is not essential for early logarithmic growth and infection. Can J Microbiol **60:**251-254.

52. **Hancock RE, Diamond G.** 2000. The role of cationic antimicrobial peptides in innate host defences. Trends Microbiol **8:**402-410.

53. **Peschel A.** 2002. How do bacteria resist human antimicrobial peptides? Trends Microbiol **10:**179-186.

54. **Kelly CP, Becker S, Linevsky JK, Joshi MA, O'Keane JC, Dickey BF, LaMont JT, Pothoulakis C.** 1994. Neutrophil recruitment in *Clostridium difficile* toxin A enteritis in the rabbit. J Clin Invest **93:**1257-1265.

55. **Kelly CP, Kyne L.** 2011. The host immune response to *Clostridium difficile*. J Med Microbiol **60:**1070-1079.

56. **Redelings MD, Sorvillo F, Mascola L.** 2007. Increase in *Clostridium difficile*-related mortality rates, United States, 1999-2004. Emerg Infect Dis **13:**1417-1419.

57. **McDonald LC, Killgore GE, Thompson A, Owens RC, Jr., Kazakova SV, Sambol SP, Johnson S, Gerding DN.** 2005. An epidemic, toxin gene-variant strain of *Clostridium difficile*. N Engl J Med **353:**2433-2441.

58. **Warny M, Pepin J, Fang A, Killgore G, Thompson A, Brazier J, Frost E, McDonald LC.** 2005. Toxin production by an emerging strain of *Clostridium difficile* associated with outbreaks of severe disease in North America and Europe. Lancet **366:**1079-1084.

59. **Sebaihia M, Wren BW, Mullany P, Fairweather NF, Minton N, Stabler R, Thomson NR, Roberts AP, Cerdeno-Tarraga AM, Wang H, Holden MT, Wright A, Churcher C, Quail MA, Baker S, Bason N, Brooks K, Chillingworth T, Cronin A, Davis P, Dowd L, Fraser A, Feltwell T, Hance Z, Holroyd S, Jagels K, Moule S, Mungall K, Price C, Rabbinowitsch E, Sharp S, Simmonds M, Stevens K, Unwin L, Whithead S, Dupuy B, Dougan G, Barrell B, Parkhill J.** 2006. The multidrug-resistant human pathogen Clostridium difficile has a highly mobile, mosaic genome. Nat Genet **38:**779-786.

60. **Opitz B, Schroder NW, Spreitzer I, Michelsen KS, Kirschning CJ, Hallatschek W, Zahringer U, Hartung T, Gobel UB, Schumann RR.** 2001. Toll-like receptor-2 mediates Treponema glycolipid and lipoteichoic acid-induced NF-kappaB translocation. J Biol Chem **276:**22041-22047.

61. **Schroder NW, Morath S, Alexander C, Hamann L, Hartung T, Zahringer U, Gobel UB, Weber JR, Schumann RR.** 2003. Lipoteichoic acid (LTA) of Streptococcus pneumoniae and Staphylococcus aureus activates immune cells via

Toll-like receptor (TLR)-2, lipopolysaccharide-binding protein (LBP), and CD14, whereas TLR-4 and MD-2 are not involved. J Biol Chem **278:**15587-15594.

62. **Cox KH, Ruiz-Bustos E, Courtney HS, Dale JB, Pence MA, Nizet V, Aziz RK, Gerling I, Price SM, Hasty DL.** 2009. Inactivation of DltA Modulates Virulence Factor Expression in Streptococcus pyogenes. PLoS ONE **4:**e5366.

63. **Morath S, Geyer A, Hartung T.** 2001. Structure–Function Relationship of Cytokine Induction by Lipoteichoic Acid fromStaphylococcus aureus. The Journal of Experimental Medicine **193:**393-398.

64. **Grangette C, Nutten S, Palumbo E, Morath S, Hermann C, Dewulf J, Pot B, Hartung T, Hols P, Mercenier A.** 2005. Enhanced antiinflammatory capacity of a Lactobacillus plantarum mutant synthesizing modified teichoic acids. Proc Natl Acad Sci U S A **102:**10321-10326.

65. **Tabuchi Y, Shiratsuchi A, Kurokawa K, Gong JH, Sekimizu K, Lee BL, Nakanishi Y.** 2010. Inhibitory role for D-alanylation of wall teichoic acid in activation of insect Toll pathway by peptidoglycan of Staphylococcus aureus. J Immunol **185:**2424-2431.

66. **Savidge TC, Pan WH, Newman P, O'Brien M, Anton PM, Pothoulakis C.** 2003. Clostridium difficile toxin B is an inflammatory enterotoxin in human intestine. Gastroenterology **125:**413-420.

67. **Kim H, Rhee SH, Kokkotou E, Na X, Savidge T, Moyer MP, Pothoulakis C, LaMont JT.** 2005. Clostridium difficile toxin A regulates inducible cyclooxygenase-2 and prostaglandin E2 synthesis in colonocytes via reactive oxygen species and activation of p38 MAPK. J Biol Chem **280:**21237-21245.

68. **Le Jeune A, Torelli R, Sanguinetti M, Giard J-C, Hartke A, Auffray Y, Benachour A.** 2010. The Extracytoplasmic Function Sigma Factor SigV Plays a Key Role in the Original Model of Lysozyme Resistance and Virulence of Enterococcus faecalis. PLoS ONE **5:**e9658.

69. **Stevenson E, Minton NP, Kuehne SA.** 2015. The role of flagella in Clostridium difficile pathogenicity. Trends Microbiol **23:**275-282.

70. **Wust J, Hardegger U.** 1983. Transferable resistance to clindamycin, erythromycin, and tetracycline in *Clostridium difficile*. Antimicrob Agents Chemother **23:**784-786.

71. **Hussain HA, Roberts AP, Mullany P.** 2005. Generation of an erythromycin-sensitive derivative of Clostridium difficile strain 630 (630Deltaerm) and demonstration that the conjugative transposon Tn916DeltaE enters the genome of this strain at multiple sites. J Med Microbiol **54:**137-141.

72. **O'Connor JR, Lyras D, Farrow KA, Adams V, Powell DR, Hinds J, Cheung JK, Rood JI.** 2006. Construction and analysis of chromosomal Clostridium difficile mutants. Mol Microbiol **61:**1335-1351.

73. **Stabler RA, He M, Dawson L, Martin M, Valiente E, Corton C, Lawley TD, Sebaihia M, Quail MA, Rose G, Gerding DN, Gibert M, Popoff MR, Parkhill J, Dougan G, Wren BW.** 2009. Comparative genome and phenotypic analysis of *Clostridium difficile* 027 strains provides insight into the evolution of a hypervirulent bacterium. Genome Biol **10:**R102.

74. **Thomas CM, Smith CA.** 1987. Incompatibility group P plasmids: genetics, evolution, and use in genetic manipulation. Annu Rev Microbiol **41:**77-101.

75. **Yanisch-Perron C, Vieira J, Messing J.** 1985. Improved M13 phage cloning vectors and host strains: nucleotide sequences of the M13mp18 and pUC19 vectors. Gene **33:**103-119.

76. **Manganelli R, Provvedi R, Berneri C, Oggioni MR, Pozzi G.** 1998. Insertion vectors for construction of recombinant conjugative transposons in *Bacillus subtilis* and *Enterococcus faecalis*. FEMS Microbiol Lett **168:**259-268.

CHAPTER 10

Appendix VI - The Phosphotransfer Protein CD1492 Represses Sporulation Initiation in *Clostridium difficile*

Kevin O. Childress*, Adrianne N. Edwards*, Kathryn L. Nawrocki, Emily C. Woods, Sarah E. Anderson and Shonna M. McBride

*Co-First Authors

This work was published in 2016 in *Infection and Immunity*.

K.L.N. performed experiments for Figure 4 and assisted with manuscript revision.

Article Citation:

Childress, K. O., Edwards, A. N., Nawrocki, K. L., Woods, E. C., Anderson, S. E., & McBride, S. M. (2016). The Phosphotransfer Protein CD1492 Represses Sporulation Initiation in Clostridium difficile. *Infection and Immunity*, IAI-00735. PMCID 27647869

ABSTRACT

The formation of spores is critical for survival of *Clostridium difficile* outside of the host gastrointestinal tract. Persistence of *C. difficile* spores greatly contributes to the spread of *C. difficile* infection (CDI), and the resistance of spores to antimicrobials facilitates the relapse of infection. Despite the importance of sporulation to *C. difficile* pathogenesis, the molecular mechanisms controlling spore formation are not well understood. The initiation of sporulation is known to be regulated through activation of the conserved transcription factor, Spo0A. Multiple regulators influence Spo0A activation in other species; however, many of these factors are not conserved in *C. difficile*, and few novel factors have been identified. Here, we investigate the function of a protein, CD1492, which is annotated as a kinase and originally proposed to promote sporulation by directly phosphorylating Spo0A. We found that deletion of *CD1492* results in increased sporulation, indicating that CD1492 is a negative regulator of sporulation. Accordingly, we observed increased transcription of Spo0A-dependent genes in the *CD1492* mutant. Deletion of CD1492 also resulted decreased toxin production *in vitro* and in decreased virulence in the hamster model of CDI. Further, the *CD1492* mutant demonstrated effects on gene expression that are not associated with Spo0A activation, including lower *sigD* and *rstA* transcription, suggesting that this protein interacts with factors other than Spo0A. Altogether, the data indicate that CD1492 negatively affects sporulation and positively influences motility and virulence. These results provide further evidence that *C. difficile* sporulation is regulated differently from that of other endospore forming species.

INTRODUCTION

Clostridium difficile causes severe diarrheal infections that are difficult to treat and easily transmitted. *C. difficile* enters the host as a dormant spore, which then germinates in the presence of bile salts to form a vegetative cell (1, 2). The vegetative form of *C. difficile* then grows and divides in the host gastrointestinal (GI) tract, producing toxins that cause the symptoms of disease (3, 4). During infection, a subset of *C. difficile* vegetative cells initiate the process of sporulation and morphologically transform into spores (5, 6). These spores are metabolically dormant and highly resistant to oxygen, heat and chemicals that would destroy the vegetative form of *C. difficile* (7-9).

Although the signals that activate sporulation of *C. difficile* have not been identified, it is expected that the master regulatory factor, Spo0A, must be phosphorylated for the sporulation gene expression program to begin (10-12). Once phosphorylated, active Spo0A binds DNA, promoting the expression of early sporulation-specific genes and initiating spore formation (10, 13). In the extensively studied spore-former, *Bacillus subtilis*, activation of Spo0A is accomplished through a phosphorelay that is composed of sensor histidine kinases and a series of phosphotransfer proteins that tightly control the phosphorylation state of Spo0A (14, 15). The *C. difficile* genome does not encode an apparent phosphorelay but does contain three putative sensor histidine kinase proteins that are anticipated to directly phosphorylate and activate Spo0A (11, 16). One of these histidine kinase proteins, CD2492, was shown to positively affect *C. difficile* sporulation and another, CD1579, was shown to directly interact with and transfer phosphate to Spo0A *in vitro* (11). The function of the third putative sporulation histidine kinase, CD1492, is not known.

In this study, we investigated the role of the putative sporulation kinase, CD1492, in *C. difficile* sporulation. We examined the sporulation-specific gene expression and resulting phenotypes of a *CD1492* deletion mutant and strains over-expressing wild-type or mutated *CD1492* alleles. Our results indicate that CD1492 is involved in the initiation of sporulation, but contrary to its proposed function, this protein plays a role in preventing spore formation. In addition, we found that the *CD1492* null mutant exhibited changes in gene expression that are not directly dependent on Spo0A activation or sporulation, including decreased production of TcdA and motility regulators. Furthermore, the *CD1492* mutant was significantly less virulent in a hamster model of infection.

MATERIALS AND METHODS

Cultivation of bacteria. *Clostridium difficile* cultures were grown in an anaerobic chamber (Coy Laboratory Products) containing an atmosphere of 85% nitrogen, 10% hydrogen and 5% CO_2 at 37°C as described previously (17). *C. difficile* strains were cultured in brain heart infusion medium supplemented with 2% yeast extract (BHIS) as broth or 1.5% agar medium (18). *Escherichia coli* were grown at 37°C in L broth (19) or agar plates, or BHIS medium supplemented with 20 μg/ml chloramphenicol or 100 μg/ml ampicillin as needed. Thiamphenicol (2-10 μg/ml) was used for selection of *C. difficile* plasmids and kanamycin (50 μg/ml) was utilized for counterselection against *E. coli*, as previously detailed (20-22). Taurocholate (Sigma-Aldrich) was added to cultures at 0.1% to induce spore germination (23).

Strain and plasmid construction. The plasmids and bacterial strains used in this study are listed in **Table 1,** and the details of vector constructions are outlined in **File S1** of the supplemental materials. Primer design was based on *C. difficile* strain 630 genomic sequence (GenBank accession NC_009089.1), and the 630Δ*erm* derivative was used for PCR amplification and cloning. Plasmid DNA isolation, PCR and cloning were performed using standard protocols. Plasmid sequences were verified prior to use (Eurofins MWG Operon). *C. difficile* genomic DNA was isolated as previously described (24, 25). *C. difficile-E. coli* conjugations and gene deletions were carried out as previously indicated (22, 23, 26).

Single Nucleotide Polymorphism (SNP) Analysis. *C. difficile* genomic DNA was prepared as previously described (24, 25). Genomic DNA was quantitated using a Nanodrop (Thermo Scientific), and 1 ng DNA was used for library preparation. Libraries were generated using the Nextera XT DNA Library Preparation kit (Illumina); dual barcoding and sequencing primers were added according to the manufacturer's protocol. Libraries were validated by microelectrophoresis quantified, pooled and clustered on an Illumina MiSeq instrument in 150 base paired-read reactions. Per sample reads were mapped to the *C. difficile* 630 reference genome (GenBank no. AM180355). All variant analysis was performed and annotated with CLC Genomics Workbench v9.0, using the "Fixed Ploidy Variant Detection" and "Annotate with Overlap Information" tools.

Sporulation efficiency assays and phase contrast microscopy. *C. difficile* cultures were started in BHIS supplemented with 0.1% taurocholate to allow for germination of spores

Table 1. Bacterial Strains and plasmids

Plasmid or Strain	Relevant genotype or features	Source, construction or reference
Strains		
E. coli		
HB101	F⁻ *mcrB mrr hsdS20*(r_B^- m_B^-) *recA13 leuB6 ara-14 proA2 lacY1 galK2 xyl-5 mtl-1 rpsL20*	B. Dupuy
MC277	HB101 containing pRK24 and pMC211	(28)
MC527	HB101 containing pRK24 and pMC381	This study
MC559	HB101 containing pRK24 and pMC386	This study
MC779	HB101 containing pRK24 and pMC539	This study
C. difficile		
630	Clinical isolate	(65)
630Δ*erm*	Erm^S derivative of strain 630	N. Minton (66)
MC282	630Δ*erm* pMC211	(28)
MC587	630Δ*erm* pMC386	This study
MC674	630Δ*erm* Δ*CD1492*	This study
MC729	630Δ*erm* Δ*CD1492* pMC211	This study
MC730	630Δ*erm* Δ*CD1492* pMC386	This study
MC771	630Δ*erm* Δ*CD1492* pMC539	This study
Plasmids		
pRK24	Tra^+, Mob^+; *bla*, *tet*	(67)
pUC19	Cloning vector; *bla*	(68)
pMTL-SC7315	For allelic exchange in non-epidemic *C. difficile* strains	N. Minton (26)
pMC123	*E. coli-C. difficile* shuttle vector, *bla catP*	(69)
pMC211	pMC123 P*cprA*	(28)
pMC381	pMTL7315 Δ*CD1492* cassette	This study
pMC386	pMC211 with *CD1492*	This study
pMC538	pUC19 *CD1492* H668A	This study
pMC539	pMC211 with *CD1492* H668A	This study

Table 2. Oligonucleotides

Primer	Sequence (5'→3')	Use/location
oMC44	5'- CTAGCTGCTCCTATGTCTCACATC -3'	(69)
oMC45	5'- CCAGTCTCTCCTGGATCAACTA -3'	(69)
oMC112	5'- GGCAAATGTAAGATTTCGTACTCA -3'	*tcdB* (*CD0660*) qPCR (28)
oMC113	5'- TCGACTACAGTATTCTCTGAC -3'	*tcdB* (*CD0660*) qPCR (28)
oMC189	5'- TGCCTCTTGTAAAGAGTATAGCA -3'	*sigD* (*CD0266*) qPCR (24)
oMC190	5'- GCATCAATCAATCCAATGACTCCAC -3'	*sigD* (*CD0266*) qPCR (24)
oMC331	5'- CTCAAAGCGCAATAAATCTAGGAGC -3'	*spo0A* (*CD1214*) qPCR (28)
oMC332	5'- TTGAGTCTCTTGAACTGGTCTAGG -3'	*spo0A* (*CD1214*) qPCR (28)
oMC333	5'- AGTAAGGGTATGGGCAAAGTATTACA -3'	*CD1579* qPCR (24)
oMC334	5'- CCACTTCATTTGAGAACAACTCTTTG -3'	*CD1579* qPCR (24)
oMC335	5'- ACTTGTAAGAAGTGCTGAAGGTGGTA -3'	*CD1492* qPCR (24)
oMC336	5'- GTCATATCGACCAAATCACTTGAAACAC -3'	*CD1492* qPCR (24)
oMC337	5'- CAGGAATTTGTGACTATCTGGGAAATGG -3'	*CD2492* qPCR (24)
oMC338	5'- TCCCATTTGCCTTTATTTGAACTTGA -3'	*CD2492* qPCR (24)
oMC339	5'- GGGCAAATATACTTCCTCCTCCAT -3'	*sigE* (*CD2643*) qPCR (28)
oMC340	5'- TGACTTTACACTTTCATCTGTTTCTAGC -3'	*sigE* (*CD2643*) qPCR (28)
oMC355	5'- CTGTTGGAATATCTAGGCGATAAGC -3'	*rstA* (*CD3668*) qPCR (24)
oMC356	5'- TGGTCCTCAGCCTTGTTTAATTC -3'	*rstA* (*CD3668*) qPCR (24)
oMC365	5'- GGAAGTAACTGTTGCCAGAGAAGA -3'	*sigF* (*CD0772*) qPCR (28)
oMC366	5'- CGCTCCTAACTAGACCTAAATTGC -3'	*sigF* (*CD0772*) qPCR (28)
oMC547	5'- TGGATAGGTGGAGAAGTCAGT -3'	*tcdA* qPCR (*CD0663*) (28)
oMC548	5'- GCTGTAATGCTTCAGTGGTAGA -3'	*tcdA* qPCR (*CD0663*) (28)
oMC569/ tcdRqF	5'- AGCAAGAAATAACTCAGTAGATGATT -3'	*tcdR* qPCR (*CD0659*) (40)
oMC570/ tcdRqR	5'- TTATTAAATCTGTTTCTCCCTCTTCA -3'	*tcdR* qPCR (*CD0659*) (40)
oMC897	5'- GCCATGGATCCTTGGAAGAATTGTGGTAACATA TTTATAG -3'	*CD1492* cloning
oMC898	5'- GATGCCTGCAGACGCATCAAATACAACTAAAGTA ATAAA -3'	*CD1492* cloning
oMC911	5'- GCGCGGCCGCGAGTAGGAAATCTGGCTTAT -3'	*CD1492* deletion construct
oMC912	5'- ACAACTAAAGCACTTCTTCATTTTTATATAGTTTTA CC -3'	*CD1492* deletion construct
oMC913	5'- TGAAGAAGTGCTTTAGTTGTATTTGATGCGTTTT A -3'	*CD1492* deletion construct
oMC914	5'- GCGCGGCCGCCAGCCTTGTCATTTTTTAGATT G -3'	*CD1492* deletion construct
fliCqF	5'- TACAAGTTGGAGCAAGTTATGGAAC -3'	(40)
fliCqR	5'- GTTGTTATACCAGCTGAAGCCATTA -3'	(40)

within the starting inoculum and 0.2% fructose to prevent sporulation. When cultures reached an OD_{600} of 0.5, 250 µl was applied evenly to 70:30 agar medium and incubated anaerobically at 37°C (27). Samples were scraped from the plates at the timepoints indicated for each experiment and evaluated for sporulation frequency by both phase-contrast counting and enumeration of ethanol resistant spores. Samples for phase-contrast microscopy were resuspended in BHIS broth and applied to slides as previously described (28). Phase-contrast microscopy was performed using a Nikon Eclipse Ci-L microscope with a X100 Ph3 oil-immersion objective and images were acquired with a DS-Fi2 camera. Two or more fields of view were captured for each strain, and a minimum of 1000 cells were assessed and enumerated per experiment. The percentage of spores present was calculated as the number of spores divided by the total number of cells. The mean percent spores and standard error of the mean were calculated from at least three independent experiments (24).

To determine the number of viable spores in the total viable population, *C. difficile* cultures were grown on 70:30 sporulation agar as described above and ethanol resistance assays were performed. After 24 h growth, cells were resuspended in BHIS to an OD_{600} of 1.0, serially diluted in BHIS and plated onto BHIS agar medium to enumerate vegetative cells. A 0.5 ml aliquot of culture was then mixed with 95% ethanol and water to a final concentration of 28.5%. Ethanol-treated cells were vortexed and incubated at room temperature for 15 minutes, then serially diluted in 1X PBS containing 0.1% taurocholate and plated onto BHIS plates containing 0.1% taurocholate to enumerate spore outgrowth. Plates were incubated for a minimum of 24 h and CFU calculated per ml of starting culture. The sporulation frequency was calculated as the number of ethanol-resistant spores divided

by the total number of cells (combined counts of spores and vegetative cells/ml). A *spo0A* mutant (MC310) was used as a control to ensure vegetative cell death in ethanol.

Quantitative reverse transcription PCR analysis (qRT-PCR). *C. difficile* cultures were harvested from 70:30 sporulation agar and resuspended into a cold solution of 1.5:1.5:3 ethanol-acetone-dH_2O and stored immediately at -80°C. RNA was purified from the cell cultures and cDNA synthesized as described previously (28, 29). 50 ng or 200 ng of cDNA was used per reaction for standard or cecal quantitative PCR analysis, respectively. qRT-PCR was performed using the Bioline SensiFAST SYBR and Fluorescein kit, and a Roche Lightcycler 96 instrument. Reactions without reverse transcriptase were included for each primer set to detect genomic DNA contamination. qPCR primers were designed using the IDT PrimerQuest program. qPCR was performed in technical triplicate for each cDNA sample and primer pair combination. Primer efficiencies were calculated for each primer set prior to assays. Results were calculated using the comparative cycle threshold method, normalized to the internal control transcript, *rpoC* (30). A minimum of four biological replicates were assessed. Relative expression results are presented as the means and standard errors of the means. The two-tailed Student's *t* test was performed to assess statistical significance in expression ratios between the control and test groups.

Animal studies. Spores were prepared and enumerated for animal experiments as previously described (28). Female Syrian golden hamsters (*Mesocricetus auratus*) weighing 70-110 g were obtained from Charles River Laboratories and maintained in an animal biosafety level 2 room within the Division of Animal Resources at Emory

University. Animals were housed individually and provided standard rodent chow and water *ad libitum*. Hamsters were administered a single dose of clindamycin (Day -7; 30 mg/kg body weight) by oral gavage seven days prior to infection. At day 0, hamsters were administered approximately 5000 spores of a single *C. difficile* strain and monitored several times per day for display of disease symptoms (weight loss, lethargy, diarrhea or wet tail). All animals were weighed at least once per day and fecal samples were collected daily for enumeration of total cells throughout the experiment. Experiments were performed two times using cohorts of five to six animals per *C. difficile* strain tested. Additional animals that received clindamycin but were not administered *C. difficile* served as negative controls in each experiment. Animals were considered moribund and euthanized if (i) they lost 15% or more of their body weight or (ii) if they presented with diarrhea and lethargy. Hamsters were euthanized by CO_2 asphyxiation followed by a thoracotomy. Following euthanasia, animals were necropsied and cecal contents were collected for enumeration of *C. difficile* and RNA isolation. Cecal samples used for RNA isolation were stored in 1:1 ethanol-acetone at -80°C. Strain-specific differences in *C. difficile* CFU recovered from feces and cecal contents were determined by single factor analysis of variance (GraphPad Prism 6) and by a two-tailed Student's *t* test (Excel; Microsoft). Differences in hamster survival for animals infected with MC674 (*CD1492)* or 630Δ*erm* were assessed using the log rank test (GraphPad Prism 6).

SDS-PAGE and Western blot analysis. *C. difficile* strains 630Δ*erm*, MC674 (*CD1492*), MC282 (630Δ*erm* P*cpr*), MC729 (*CD1492* P*cpr*), MC730 (*CD1492* P*cpr::CD1492*) and MC771 (*CD1492* P*cpr::CD1492* H668A) were grown in TY medium for 24 h at 37°C as

previously described (24), except strains were cultivated in BHIS overnight. Total protein was quantitated using the Pierce Micro BCA Protein Assay Kit (Thermo Scientific), and 8 µg total protein was loaded onto pre-cast TGX 4-15% gradient gels (Bio-Rad), separated by electrophoresis and subsequently transferred to 0.45 µm nitrocellulose membranes (Bio-Rad). Western blot analysis was conducted using mouse anti-TcdA antibodies (Novus Biologicals) followed by goat anti-mouse AlexaFluor 488 secondary antibody (Life Technologies). Imaging and densitometry were performed using a ChemiDoc and Image Lab Software (Bio-Rad), and three biological replicates were analyzed for each strain. The Student's two-tailed *t* test and an one-way ANOVA followed by Dunnett's multiple comparisons test were performed to assess statistical differences in TcdA protein levels between the mutant and parent strain, and the complemented strains, respectively (GraphPad Prism 6). A representative Western blot image is shown.

Motility studies. Strains were grown in BHIS medium to an OD_{600} of 0.5, and 5 µl of culture was spotted into the center of one-half concentration BHI plates containing 0.3% agar. Swimming diameters were measured every 24 h for a total of 168 h. Results represent the means and standard error of the means for a minimum of three independent experiments. A two-tailed Student's *t* test was performed to determine statistical differences in outcomes for the mutant and parent strains.

RESULTS

Deletion of the Predicted Orphan Kinase *CD1492* Results in Increased Spore Formation. The genome of *C. difficile* strain 630 encodes three putative orphan histidine

kinases that have been implicated as sporulation sensor kinases: CD1492, CD1579 and CD2492 (11). Previous investigations found that disruption of the CD2492 kinase results in a significant decrease in spore formation, while the CD1579 kinase was shown to affect Spo0A phosphorylation *in vitro* (11). CD1492, the third suspected sporulation sensor kinase, has not been directly linked to a sporulation phenotype or phosphorylation of Spo0A *in vitro.* As outlined in **Fig. 1**, CD1492 and CD2492 both have multiple predicted transmembrane segments, while CD1579 is an apparent cytosolic protein. All three proteins have predicted histidine kinase catalytic domains of typical sensor histidine kinases.

To investigate the potential influence of CD1492 on sporulation, we deleted the coding sequence by double cross-over using markerless allelic exchange (**Fig. S2**) (26). Expression of *CD1492* in the *CD1492* null mutant, MC674, was ablated, as expected, and no growth defect was observed in any medium tested (not shown). Whole genome single nucleotide polymorphism (SNP) analysis using Illumina next-generation sequencing revealed no additional nucleotide changes in the *CD1492* mutant (see Methods). The *CD1492* mutant was tested for the ability to sporulate on 70:30 sporulation agar (27). As demonstrated in **Fig. 2A**, the *CD1492* mutant produced significantly more spores than the parent strain, having a sporulation frequency approximately 2.4-fold higher than the parent strain as determined by phase-contrast microscopy (630Δ*erm*, 23.4 ± 5.1%; MC674, 56.4 ± 6.8%). Similarly, the production of ethanol-resistant spores was 3.4-fold higher for the

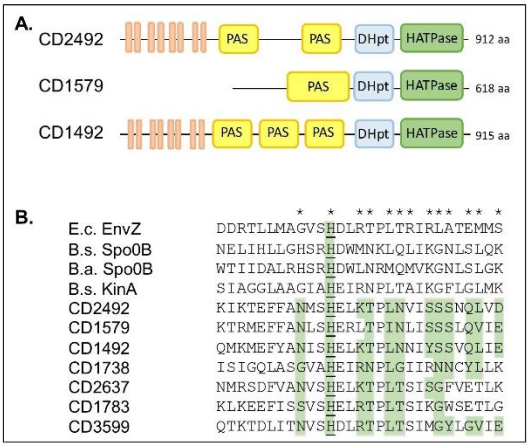

Figure 1. *In silico* analysis of sporulation-associated histidine kinases. A) Domain alignments of the *B. subtilis* and *C. difficile* sporulation kinases and *E. coli* EnvZ. Tan boxes represent predicted transmembrane domains; the HATPase region includes the kinase catalytic domain (56, 57). **B**) Alignment of the dimerization and histidine phosphotransfer sub-domains of *C. difficile* and *B. subtilis* histidine kinases. The known or suspected conserved histidine is underlined. Asterisks represent the residues involved in direct interactions with the cognate response regulators (11, 61, 62), and shaded residues are highly conserved within *C. difficile.*

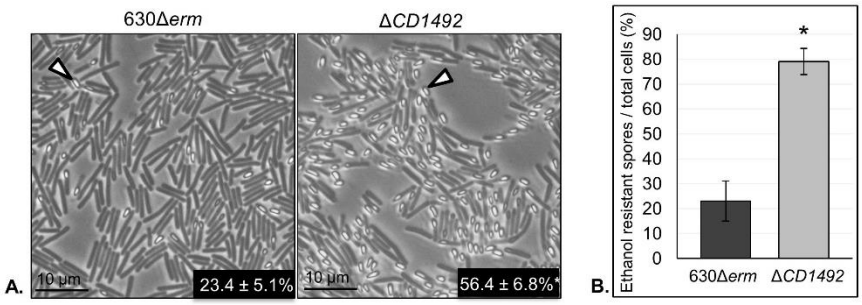

Figure 2. **The Δ*CD1492* mutant has a hypersporulation phenotype.** A) Representative phase-contrast micrographs of the parent strain (630Δ*erm*) and the Δ*CD1492* mutant (MC674) grown on 70:30 sporulation agar for 24 h. Open arrowheads indicate phase-bright spores. B) Ethanol-resistant spore formation frequency per total viable cells of the 630Δ*erm* and Δ*CD1492* mutant strains collected from 70:30 sporulation agar after 24 h. Sporulation frequencies were calculated as described for each assay in the Methods. The means and standard error of the means are shown. * $P \leq 0.05$ by a two-tailed Student's *t* test.

Table 3. The *CD1492* mutant forms more ethanol resistant *C. difficile* spores on 70:30 sporulation agar.

Strain	Vegetative Cells[a] (CFU/ml)	Spores[b] (CFU/ml)	Total cells[c] (CFU/ml)	Sporulation frequency[d]	Percent sporulation (%)
630Δ*erm*	$1.49 \times 10^8 \pm 2.13 \times 10^7$	$3.60 \times 10^7 \pm 6.18 \times 10^6$	$1.85 \times 10^8 \pm 1.61 \times 10^7$	$2.23 \times 10^{-1} \pm 7.28 \times 10^{-2}$	22.3 ± 7.28
ΔCD1492	$1.64 \times 10^7 \pm 3.88 \times 10^6$	$5.33 \times 10^7 \pm 5.98 \times 10^6$	$6.97 \times 10^7 \pm 8.03 \times 10^6$	$7.76 \times 10^{-1} \pm 5.18 \times 10^{-2}$	77.6 ± 5.18

[a] Vegetative cells are the number of CFU recovered on BHIS plates.
[b] Spores refers to the total number of CFU that survived ethanol treatment, as described in the Methods and Materials, and recovered on BHIS plates supplemented with 0.1% taurocholate.
[c] Total cells include both vegetative cells and spores.
[d] Sporulation frequency is calculated as the number of ethanol resistant spores divided by the total cells.

CD1492 mutant, compared to the parent strain (**Fig. 2B**; 630Δ*erm*, 23.0 ± 8.0%; MC674, 79.1 ± 5.3%), demonstrating that the spores produced by the mutant are fully formed and viable. The high spore-forming phenotype of the *CD1492* mutant suggests that unlike many other sporulation histidine kinases, CD1492 is a negative regulator of sporulation initiation. Based on the mutant phenotype, CD1492 is unlikely to function solely as a sporulation sensor kinase that activates Spo0A by phosphorylation, as was predicted through *in silico* analyses. Alternatively, CD1492 may act as a phosphatase that inactivates Spo0A to prevent sporulation, or it may activate a sporulation-repressing function.

The *CD1492* mutant has elevated sporulation-specific gene expression. To determine the effect of the *CD1492* mutation on sporulation initiation, the abundance of key early sporulation transcripts were measured during growth on sporulation medium, relative to the parent strain. Transcription of the master sporulation regulator, *spo0A*, was slightly higher in the *CD1492* mutant after 12 h on sporulation medium, but this difference did not reach statistical significance (**Fig. 3A**). Further, the transcription of the Spo0A-dependent sigma factors, *sigF* and *sigE*, were more than 2-fold higher in the *CD1492* mutant strain ($P \leq 0.05$). SigF and SigE are required for forespore and mother cell-specific sporulation gene expression, respectively (31). The greater sporulation frequencies and higher early sporulation gene expression for the *CD1492* mutant suggests that a greater proportion of these cells enter the sporulation pathway.

As mentioned previously, CD1492 is one of three orphan kinases that are proposed to function as sporulation sensor kinases. We found that expression of one of the suspected

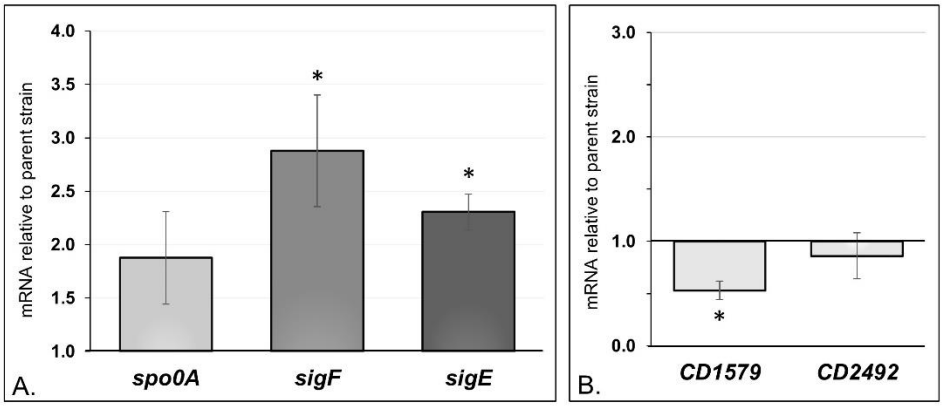

Figure 3. Expression of key early sporulation regulators and putative sporulation kinases in the Δ*CD1492* mutant. Transcriptional analysis of **A**) *spo0A*, *sigF* and *sigE*, and **B**) predicted sporulation kinases *CD1579* and *CD2492* expression in the Δ*CD1492* mutant (MC674) relative to the parent strain, 630Δ*erm*. Cultures were grown on 70:30 sporulation agar for 12 h, RNA harvested, cDNA prepared and qRT-PCR performed using gene specific primers, as outlined in Methods. The means and standard error of the means for at least three biological replicates are shown. *$P \leq 0.05$ by a two-tailed Student's *t* test.

sporulation kinases, *CD1579*, was 2-fold lower in the *CD1492* mutant, while expression of *CD2492* was similar to the parent strain (**Fig. 3B**). Thus, CD1492 has a modest effect on the expression of one of the other suspected kinases.

In the model spore-former *B. subtilis*, the sporulation sensor kinases facilitate sporulation initiation through the sporulation phosphorelay, which consists of the intermediate proteins Spo0F and Spo0B that enable phosphotransfer to Spo0A (32). As initiators of sporulation, the *B. subtilis* kinases are expressed prior to the onset of sporulation, and their expression wanes in a sporulating population as sporulation progresses (32). We investigated the expression of *CD1492* during growth on sporulation medium to determine how the timing of its transcription relates to sporulation initiation. Samples of the parent strain were taken during growth on 70:30 medium and assessed for *CD1492* and *sigE* expression over time (**Fig. S3**). Relative to transcription at 6 h after transfer to sporulation medium (H_6, logarithmic phase), the transcription of *CD1492* increased about 5-fold at 8 h post-inoculation (H_8). *CD1492* transcripts declined at later time points, even as levels of the early mother cell sigma factor, *sigE*, remained elevated. The decline in *CD1492* expression during early sporulation implies that CD1492 is involved prior to the initiation of sporulation. The hypersporulation phenotype of the *CD1492* mutant and the timing of *CD1492* expression suggests that CD1492 acts as a negative regulator of sporulation before initiation.

A conserved catalytic histidine residue is required for CD1492 function. To confirm that the *CD1492* deletion was responsible for the mutant phenotypes, complementation was performed using a wild-type *CD1492* allele under the control of the nisin-inducible

cprA promoter (20, 28). Illustrated in **Figure 4**, complementation of the *CD1492* mutant with an inducible *CD1492* allele (*CD1492* p*cprA::CD1492*, MC730) resulted in reduced spore formation. The restoration of the parental sporulation phenotype in the complemented strain demonstrates that the *CD1492* mutation is responsible for the increased sporulation frequency of the mutant and suggests that the timing of CD1492 expression is not critical to its function as a negative sporulation regulator (**Fig. 4, Fig. S3** and **Fig. S4**). In addition, expression of exogenous *CD1492* in the parent strain (630Δ*erm* p*PcprA::CD1492*, MC587, **Fig. 4**) decreased the number of ethanol-resistant spore formed, suggesting that overexpression of CD1492 can reduce sporulation in an otherwise wild-type strain. This is similar to the sporulation sensor kinases of *Bacillus* and *Clostridium* species that can affect sporulation when overexpressed (33-35). To determine if CD1492 functions as a predicted sensor histidine kinase, we created a site-directed mutation at the conserved histidine residue, substituting an alanine (H668A). Histidine to alanine substitutions in the conserved histidine catalytic residues of sensor kinases result in an inability of the protein to transfer phosphate signals, thereby rendering them non-functional (15, 36). When the *CD1492* H668A mutated allele was used to complement the *CD1492* mutant (*CD1492* p*cprA::CD1492*-H668A, MC771), sporulation frequency did not decrease relative to the mutant (**Fig. 4**). The inability of the *CD1492* H668A allele to restore the mutant phenotype strongly suggests that the phosphotransfer capability of CD1492 is essential to its function as an inhibitor of sporulation.

Deletion of *CD1492* results in decreased virulence in an animal model of infection. Although the *CD1492* mutant exhibits higher sporulation frequency *in vitro*, the function

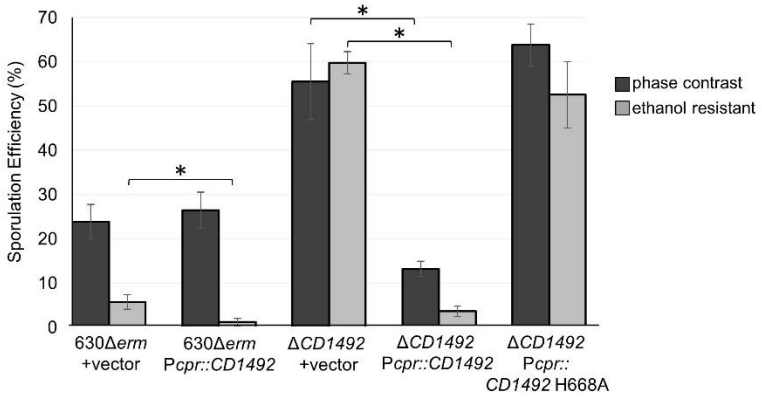

Figure 4. Complementation of Δ*CD1492* and site-directed mutagenesis of conserved sensor kinase residues. Sporulation frequencies calculated from the ratios of spores to vegetative cells by phase contrast micrographs obtained at H_{24} (black bars) or from cells before and after treatment with ethanol (grey bars). Strains 630Δ*erm* p*Pcpr* (MC282, vector control), 630Δ*erm* p*PcprA::CD1492* (MC587), Δ*CD1492* p*Pcpr* (MC729, vector control), Δ*CD1492* p*PcprA::CD1492* (MC730) and Δ*CD1492* p*PcprA::CD1492*-H668A (MC771) were grown on 70:30 sporulation agar plates supplemented with 2 µg ml^{-1} thiamphenicol and 1 µg ml^{-1} nisin and sporulation frequency assays were performed as described in Methods. The means and standard error of the means for at least four biological replicates are shown. *$P \leq 0.05$ by a two-tailed Student's *t* test.

of CD1492 in sporulation in the intestine and the effect of CD1492 on pathogenesis are not known. To this end, we examined the *CD1492* mutant in a hamster model of *C. difficile* infection. Female Syrian golden hamsters were infected by oral gavage with approximately 5000 spores from either the *CD1492* mutant or the parent strain, 630Δ*erm*. Following inoculation, animals were monitored for disease symptoms, and fecal samples were acquired every 24 h post-infection for enumeration of *C. difficile*. As shown in **Figure 5A**, hamsters infected with *CD1492* mutant spores became moribund much more slowly than animals infected with the parent strain (mean times to morbidity: 630Δ*erm*, 45.5 ± 3.5 h; Δ*CD1492*, 107.9 ± 52.5 h; $P < 0.01$, Log rank test). Enumeration of total *C. difficile* shed from the feces of infected animals revealed no significant differences in CFU between the *CD1492* mutant or parent strain infections, indicating that the mutant strain does not have an observable growth defect *in vivo* (**Fig. 5B**). Likewise, *C. difficile* CFU were similar in the cecal contents of *CD1492* and parent strain-infected animals, post-mortem (**Fig. 5C**). These data indicate that the decreased virulence observed in *CD1492* mutant infections are not caused by *in vivo* defects in the outgrowth of spores or vegetative cells.

The *CD1492* mutant produces less TcdA and has lower expression of toxin-associated regulators and motility genes. Based on the decreased virulence and lack of growth defect for the *CD1492* strain *in vivo*, we hypothesized that this mutant may have lower expression of the two major virulence factors, toxins TcdA and TcdB (3). To investigate the impact of CD1492 on toxin production, we analyzed the expression of toxin *in vitro* and *in vivo.* The expression of *tcdA* was two-fold lower in the *CD1492* mutant for cultures grown on sporulation agar (**Fig. 6A**), but no change in *tcdB* expression was observed. Supporting

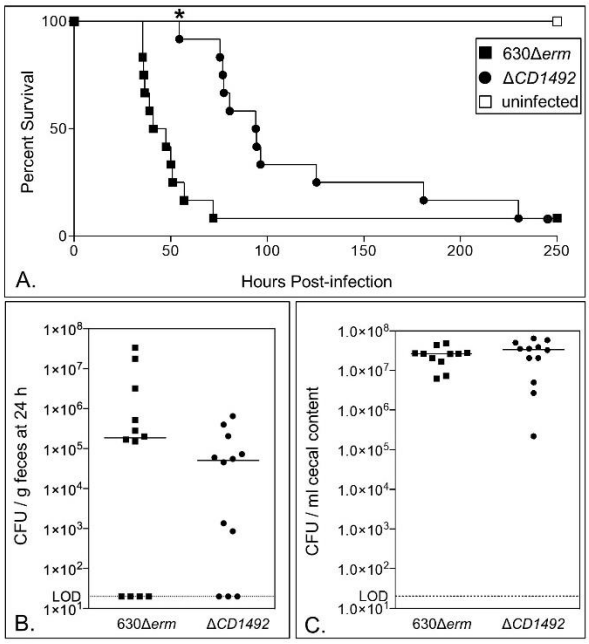

Figure 5. Deletion of *CD1492* results in decreased virulence in the hamster model of infection. **A**) Kaplan-Meier survival plot of the survival times for Syrian golden hamsters infected with 5000 spores of *C. difficile* strains 630Δ*erm* (n = 12) or MC674 (Δ*CD1492*; n = 12). The mean times to morbidity were: 630Δ*erm*, 45.5 ± 3.5 h; Δ*CD1492*, 107.9 ± 52.5 h. ($P < 0.01$, Log rank test). Total colony forming units (CFU) of *C. difficile* recovered from **B**) feces at 24 h post-infection or **C**) per ml of cecal content recovered post-mortem. Solid lines in B and C panels represent the median CFU for each strain and dotted lines denote the limit of detection (2 x 10^1 CFU/g or CFU/ml); Statistical significance was assessed by one-way ANOVA. Animals infected with 630Δ*erm* served as positive infection controls that were shown in a parallel study (22).

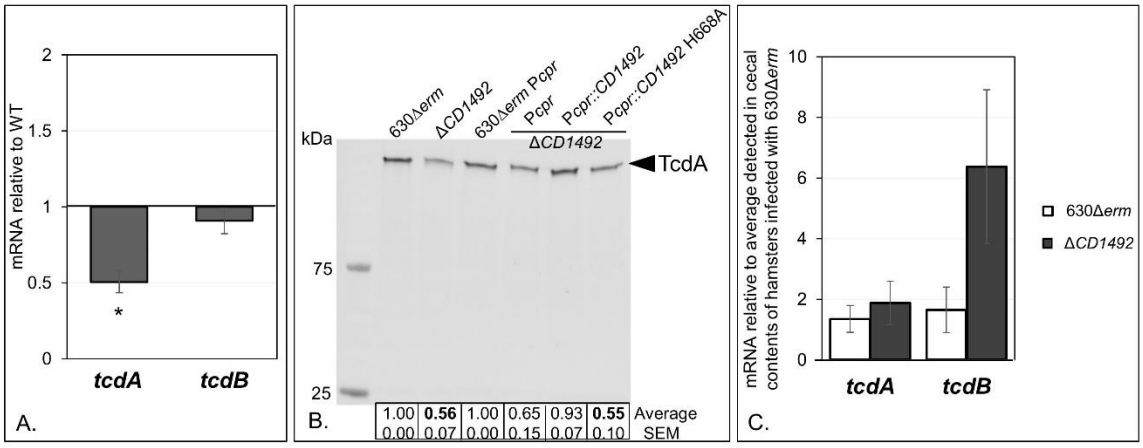

Figure 6. Toxin production in the Δ*CD1492* mutant. A) Transcriptional analysis of the primary toxins, *tcdA* and *tcdB* in the Δ*CD1492* mutant (MC674) relative to the parent strain, 630Δ*erm*. Cultures were grown on 70:30 agar medium for 12 h, RNA harvested, cDNA prepared and qRT-PCR performed using gene specific primers, as outlined in Methods. **B**) A representative Western blot analysis of TcdA in 630Δ*erm*, Δ*CD1492* (MC674), 630Δ*erm* p*Pcpr* (MC282, vector control), Δ*CD1492* p*Pcpr* (MC729, vector control), Δ*CD1492* pP*cprA::CD1492* (MC730) and Δ*CD1492* pP*cprA::CD1492*-H668A (MC771) grown in TY medium 24 h. The means ± SEM are shown below for three independent experiments; bold text indicates statistical significance compared to the parent strain by a two-tailed student's *t* test or by an one-way ANOVA followed by Dunnett's multiple comparisons test, as described in the Methods. **C**) qRT-PCR analysis of *tcdA* and *tcdB* transcript levels in cecal contents of hamsters infected with 630Δ*erm* (n = 5) or MC674 (Δ*CD1492;* n = 5). The means ± SEM are shown (*, $P \leq 0.05$ by a two-tailed Student's *t* test).

these results, a similar decrease in TcdA production was detected in strains that did not encode a functional *CD1492* gene by Western blot of *in vitro* cultures using anti-TcdA antibody (**Fig. 6B**). Examination of toxin transcripts from the cecal contents of animals that succumbed to infection revealed considerable variability in *tcdB* transcript production in *CD1492* mutant-infected animals, but differences in toxin expression did not achieve statistical significance (**Fig. 6C**).

Although the *CD1492* mutant produces less *tcdA* transcript *in vitro*, it is unlikely that CD1492 is a direct regulator of toxin transcription. Toxin expression in *C. difficile* is affected by multiple regulatory factors that integrate complex cellular nutritional signals to control nutrient acquisition and motility (37). TcdA and TcdB are directly transcribed by the toxin-specific sigma factor, TcdR, which in turn is transcribed by the motility sigma factor, SigD (FliA) (38-40). Multiple negative regulators can also repress *tcdR* transcription, thereby preventing toxin production (41, 42). We investigated the expression of the positive regulator of toxin transcription, *sigD*, to determine if its transcription was affected in the *CD1492* mutant. As shown in **Figure 7A**, *sigD* expression is over six-fold lower in the *CD1492* mutant grown on sporulation agar. A corresponding decrease in *fliC* transcription, which is SigD-dependent, was also observed for the *CD1492* mutant, indicating that SigD activity is also reduced. Decreased SigD activity is known to dramatically lower *tcdA* and *tcdB* expression, as well as flagellum production and motility (20, 39, 40). Accordingly, we examined the swimming motility of the *CD1492* mutant compared to the parent strain on soft agar medium (**Fig. 7B**), but observed no significant difference in motility *in vitro*. However, examination of *C. difficile fliC* transcription from

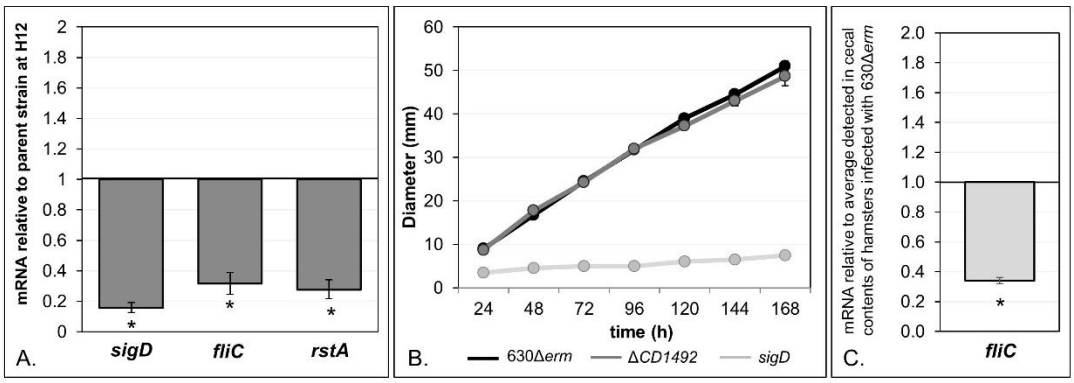

Figure 7. The Δ*CD1492* mutant has decreased expression of toxin, motility and sporulation regulators. A) qRT-PCR analysis of the motility and toxin-associated sigma factor, *sigD*, the *sigD*-dependent gene, *fliC*, and the sporulation and *sigD* regulator, *rstA*, in the Δ*CD1492* mutant relative to the parent strain, 630Δ*erm.* Cultures were grown on 70:30 agar medium for 12 h, RNA harvested, cDNA prepared and qPCR performed using gene specific primers, as outlined in the Methods. **B**) Motility of 630Δ*erm*, Δ*CD1492* (MC674) and *sigD* (RT1075, negative control) in one-half concentration BHI with 0.3% agar. Swimming diameters were measured every 24 h for a total of 168 h. **C**) qRT-PCR analysis of *fliC* transcript levels in cecal contents of hamsters infected with 630Δ*erm* (n = 5) or MC674 (Δ*CD1492;* n = 5). The means ± SEM are shown (*, $P \leq 0.05$ by a two-tailed Student's *t* test).

the cecum of infected animals revealed lower *fliC* expression in hamsters infected with the *CD1492* mutant, demonstrating that SigD activity is decreased *in vivo* (**Fig. 7C**). The timing and expression of *sigD* and flagellar genes during infection affects colonization and virulence in *C. difficile* and other motile pathogens, and thus, is likely contributing to the decreased virulence of the *CD1492* mutant in the animal model (43-47).

The specific factors that control *sigD* transcription and activity have not been fully elucidated for *C. difficile in vitro*, and even less is known about the regulation of SigD *in vivo*. A few negative regulators of SigD have been identified, including the early sporulation effector, RstA, the stationary phase sigma factor, SigH, and the anti-sigma factor, FlgM (24, 39, 48, 49). We examined transcription of *rstA* on sporulation medium and found that its expression was more than three-fold lower in the *CD1492* mutant than for the parent strain (**Fig. 7A**). This finding is intriguing, as an *rstA* null mutant has higher *sigD* expression, and accordingly, RstA negatively affects *sigD* transcription (24). Further investigation of the expression profiles for the *CD1492* and *rstA* mutants revealed that the gene expression and sporulation profiles of these mutants are reversed (**Table 4**). The inverse correlation of gene expression and phenotypes between the *rstA* and *CD1492* mutants strongly suggests that the activity of these factors are linked within a regulatory pathway, likely with CD1492 functioning "upstream" of RstA. Although it is possible that CD1492 acts directly on Spo0A as a phosphatase, the effects of CD1492 on *sigD* and *rstA* expression suggest that CD1492 functions at least partially independent of Spo0A (10).

DISCUSSION

The formation of endospores is critical for the survival of *C. difficile* outside of the host and for the dissemination of the bacterium to new hosts (50). The basic morphological

Table 4. Comparison of gene expression and phenotypes of *rstA* and *CD1492* null mutants.

Phenotype[b]		Fold-change vs. parent *CD1492*	Fold-change vs. parent *rstA*[a]
Sporulation frequency[c]		**↑2.4**	**↓20.1**
Virulence[d]		**↓2.4**	**↑1.3**
Gene Expression[b]	**Proposed Function**		
CD2492	sporulation sensor kinase	↓1.2	**↑2.4**
CD1579	sporulation sensor kinase	**↓1.9**	**↑4.9**
CD1492	sporulation sensor kinase	—[e]	**↑2.4**
rstA	sporulation/*sigD* regulator	**↓3.6**	—[e]
spo0A	sporulation master regulator	↑1.9	↓1.4
sigF	sporulation sigma factor	**↑2.9**	**↓2.2**
sigE	sporulation sigma factor	**↑2.3**	**↓6.4**
sigD	motility sigma factor	**↓6.3**	**↑2.5**
fliC	flagellar component	**↓3.1**	**↑3.5**
tcdR	toxin sigma factor	0.0	**↑2.9**
tcdA	toxin A	**↓2.0**	**↑4.0**
tcdB	toxin B	↓1.1	**↑3.5**

[a] *rstA* values obtained under the same experimental conditions, previously reported (24)
[b] All mean fold-change values reported relative to parent strain, 630Δ*erm*; bold indicates $P \leq 0.05$ by two-tailed Student's *t* test
[c] As determined by phase-contrast microscopy
[d] Defined here as fold-change in time to morbidity in hamsters
[e] No significant transcript levels detected in null mutants

programs for producing a dormant spore are similar between *C. difficile* and well-characterized spore formers, such as *Bacillus subtilis*, but the specific factors that regulate the entry into sporulation are not well conserved (5, 10, 16, 31, 51, 52). The specific signals that activate sporulation are not known, but it is anticipated that like other sporulating Firmicutes, the sporulation initiation and inhibiting signals for *C. difficile* are transmitted through predicted sporulation sensor histidine kinases, including CD1492. Our investigation found that the predicted sporulation kinase, CD1492, inhibits sporulation initiation. Moreover, CD1492 affects the function of factors other than its anticipated target, Spo0A, including the expression of the sporulation regulator, RstA, and the motility and toxin regulator, SigD. As a result, CD1492 impacts both sporulation and motility during infection of a host.

In the spore-forming Firmicutes, the master regulator of sporulation, Spo0A, is activated by phosphorylation and inactivated by dephosphorylation (16, 53). In the sporulating anaerobes that have been studied, most of the predicted orphan kinases that affect sporulation initiation function as Spo0A activators (34, 35). Mutation of the catalytic histidine residue in CD1492 resulted in a loss of activity and failure to restore the mutant phenotype (*CD1492* p*PcprA::CD1492*-H668A, MC771). Therefore, CD1492 may function as a kinase on a target other than Spo0A, but more likely acts as a phosphatase on Spo0A. In addition to CD1492 of *C. difficile,* other predicted sensor kinases were found to negatively impact sporulation in two anaerobic species: *Clostridium acetobutylicum and Ruminiclostridium thermocellum* (formerly *Clostridium*). In *C. acetobutylicum*, the predicted kinase, Ca_C0437, represses sporulation and can catalyze ATP-dependent dephosphorylation of Spo0A~P *in vitro* (35)(**Fig. S5**). *In vitro* phosphotransfer data

suggests that Ca_C0437 acts as a phosphatase, playing a similar role to the Spo0E and Rap proteins that inactivate Spo0A in *B. subtilis* (54, 55). A similar sporulation histidine kinase-like protein, Clo1313_1973, was identified in *R. thermocellum* (34)(**Fig. S5**). The role of these histidine kinase-like phosphatases in preventing initiation is further evidence that the anaerobic spore formers evolved strategies that are distinct from the *Bacillus* model, but still achieve the same goal of Spo0A inactivation.

In *C. acetobutylicum*, three positive and one negative-acting sporulation kinase-like proteins have been identified, while in *R. thermocellum*, four positive and one negative regulator were found (34, 35)(**Fig. S5**). Analysis of these sporulation sensor mutants uncovered the existence of two genetic pathways that can lead to activation of sporulation in each of these species (34, 35). *C. difficile* has three putative sporulation histidine kinase-like proteins: CD1492 and CD2492, which are predicted membrane proteins, and CD1579, which is likely cytosolic (11)(**Fig. 1**). Comparing the sporulation sensors of *C. difficile*, *R. thermocellum* and *C. acetobuylicum* (smart.embl-heidelberg.de; (56, 57), there is tremendous variability in sensor architecture, and there are no known or apparent structural features that are predictive of the role these factors play in the initiation cascade (**Fig. 1** and **Fig. S5**). BLAST analysis also revealed that orthologs of CD1492 are encoded in closely related species, such as *C. sordellii, C. dakarense* and *C. mangenotii*, but these factors have not been characterized. Based on the protein structures and what is known about the initiation pathways, it appears that each species evolved independent means for processing the signals that stimulate or inhibit sporulation, which is expected since these distant relatives inhabit very different ecological niches.

The phosphatase functions of sensor kinases are known to contribute to the activation state of their cognate response regulators (58-60). The roles of Ca_C0437, Clo1313_1973 and CD1492 as phosphatases are supported by the hypersporulation phenotypes observed in the respective null mutants, though the mechanisms of phosphatase activity have not been characterized. Traditionally, the specific functions of sporulation phosphotransfer proteins have been examined through *in vitro* phosphotransfer assays, which demonstrate the ability of potential interacting partners to give or receive phosphate (11, 14, 35, 61, 62). While *in vitro* phosphotransfer assays can demonstrate interactions between individual sporulation initiation factors, phosphotransfer between these proteins often occurs in both directions *in vitro*, whereas *in vivo*, one direction of transfer is favored (14, 32). Consequently, the results of these assays are often not reliable indicators of the direction of transfer or the order of pathway components. However, a combination of phosphotransfer assays, genetic analyses, overexpression phenotypes and characterization of multiple null mutants in pathway components can help unravel the roles of individual factors, which we plan to perform in future studies (32, 34).

In addition to defining the specific role of CD1492 in Spo0A activation, determining how CD1492 affects RstA and SigD will help to reveal how these factors interact to control both sporulation and pathogenesis. Previous studies of sporulation-defective *spo0A* and *rstA* mutants have observed different effects on virulence and have revealed indirect links between sporulation and pathogenesis (12, 24, 63, 64). Although the spore-forming anaerobes are currently thought to have a simplified mechanism for initiating sporulation, the discovery of interactions between regulators of initiation, toxin production and motility indicates that the initiation process in these species is far from

simple. The data suggest that there are multiple layers of transcriptional and post-translational regulation, as well as protein-protein interactions that control these processes. Further defining the complex genetic pathways, the protein interactions and the signals that activate sporulation in *C. difficile* could provide clues to manipulate this process and prevent the spread of disease.

ACKNOWLEDGEMENTS

We give special thanks to Charles Moran and members of the McBride lab for helpful suggestions and discussions during the course of this work. In addition, the authors would like to thank Gregory Tharp, Nirav Patel and Steven Bosinger of the Yerkes Genomics Core Laboratory for assistance with the next-generation sequencing experiments and data analysis. The Genomics Core receives financial support from P51 OD011132 "Support of the Yerkes National Primate Research Center". This research was supported by the U.S. National Institutes of Health through research grants DK087763, DK101870, AI109526 and AI116933 to S.M.M., T32 GM008169 to E.C.W. and T32 AI106699 to K.L.N. The content of this manuscript is solely the responsibility of the authors and does not necessarily reflect the official views of the National Institutes of Health.

REFERENCES

1. **Wilson KH, Kennedy MJ, Fekety FR.** 1982. Use of sodium taurocholate to enhance spore recovery on a medium selective for *Clostridium difficile*. *J Clin Microbiol* **15:**443-446.
2. **Sorg JA, Sonenshein AL.** 2008. Bile salts and glycine as cogerminants for *Clostridium difficile* spores. *J Bacteriol* **190:**2505-2512.

3. **Voth DE, Ballard JD.** 2005. *Clostridium difficile* toxins: mechanism of action and role in disease. *Clin Microbiol Rev* **18:**247-263.

4. **Theriot CM, Young VB.** 2015. Interactions between the gastrointestinal microbiome and *Clostridium difficile*. *Annu Rev Microbiol* **69:**445-461.

5. **McBride SM.** 2014. More Than One Way to Make a Spore. *Microbe* **9:**153-157.

6. **Koenigsknecht MJ, Theriot CM, Bergin IL, Schumacher CA, Schloss PD, Young VB.** 2015. Dynamics and establishment of *Clostridium difficile* infection in the murine gastrointestinal tract. *Infect Immun* **83:**934-941.

7. **Dubberke E.** 2012. Strategies for prevention of *Clostridium difficile* infection. *J Hosp Med* **7 Suppl 3:**S14-17.

8. **Vohra P, Poxton IR.** 2011. Efficacy of decontaminants and disinfectants against *Clostridium difficile*. *J Med Microbiol* **60:**1218-1224.

9. **Ali S, Moore G, Wilson AP.** 2011. Spread and persistence of *Clostridium difficile* spores during and after cleaning with sporicidal disinfectants. *J Hosp Infect* **79:**97-98.

10. **Fimlaid KA, Bond JP, Schutz KC, Putnam EE, Leung JM, Lawley TD, Shen A.** 2013. Global analysis of the sporulation pathway of *Clostridium difficile*. *PLoS Genet* **9:**e1003660.

11. **Underwood S, Guan S, Vijayasubhash V, Baines SD, Graham L, Lewis RJ, Wilcox MH, Stephenson K.** 2009. Characterization of the sporulation initiation pathway of *Clostridium difficile* and its role in toxin production. *J Bacteriol* **191:**7296-7305.

12. **Pettit LJ, Browne HP, Yu L, Smits WK, Fagan RP, Barquist L, Martin MJ, Goulding D, Duncan SH, Flint HJ, Dougan G, Choudhary JS, Lawley TD.** 2014. Functional genomics reveals that *Clostridium difficile* Spo0A coordinates sporulation, virulence and metabolism. *BMC Genomics* **15:**160.

13. **Sonenshein AL.** 2000. Control of sporulation initiation in *Bacillus subtilis*. Curr *Opin Microbiol* **3:**561-566.

14. **Burbulys D, Trach KA, Hoch JA.** 1991. Initiation of sporulation in *B. subtilis* is controlled by a multicomponent phosphorelay. *Cell* **64:**545-552.

15. **Hoch JA.** 2000. Two-component and phosphorelay signal transduction. *Curr Opin Microbiol* **3:**165-170.

16. **Paredes CJ, Alsaker KV, Papoutsakis ET.** 2005. A comparative genomic view of clostridial sporulation and physiology. *Nat Rev Microbiol* **3:**969-978.

17. **Edwards AN, Suarez JM, McBride SM.** 2013. Culturing and maintaining *Clostridium difficile* in an anaerobic environment. *J Vis Exp* doi:10.3791/50787**:**e50787.

18. **Smith CJ, Markowitz SM, Macrina FL.** 1981. Transferable tetracycline resistance in *Clostridium difficile*. *Antimicrob Agents Chemother* **19:**997-1003.

19. **Luria SE, Burrous JW.** 1957. Hybridization between *Escherichia coli* and *Shigella. J Bacteriol* **74:**461-476.

20. **Purcell EB, McKee RW, McBride SM, Waters CM, Tamayo R.** 2012. Cyclic diguanylate inversely regulates motility and aggregation in *Clostridium difficile*. *J Bacteriol* ***194*:**3307-3316.

21. **Sorg JA, Dineen SS.** 2009. Laboratory maintenance of *Clostridium difficile*. *Curr Protoc Microbiol* **Chapter 9:**Unit9A 1.

22. **McBride SM, Sonenshein AL.** 2011. The dlt operon confers resistance to cationic antimicrobial peptides in *Clostridium difficile*. *Microbiology* **157:**1457-1465.

23. **Bouillaut L, McBride SM, Sorg JA.** 2011. Genetic manipulation of *Clostridium difficile*. *Curr Protoc Microbiol* **Chapter 9:**Unit 9A 2.

24. **Edwards AN, Tamayo R, McBride SM.** 2016. A novel regulator controls *Clostridium difficile* sporulation, motility and toxin production. *Mol Microbiol* **100:**954-971.

25. **Harju S, Fedosyuk H, Peterson KR.** 2004. Rapid isolation of yeast genomic DNA: Bust n' Grab. *BMC Biotechnol* **4:**8.

26. **Cartman ST, Kelly ML, Heeg D, Heap JT, Minton NP.** 2012. Precise manipulation of the *Clostridium difficile* chromosome reveals a lack of association between the tcdC genotype and toxin production. *Appl Environ Microbiol* **78:**4683-4690.

27. **Putnam EE, Nock AM, Lawley TD, Shen A.** 2013. SpoIVA and SipL are *Clostridium difficile* spore morphogenetic proteins. *J Bacteriol* **195:**1214-1225.

28. **Edwards AN, Nawrocki KL, McBride SM.** 2014. Conserved oligopeptide permeases modulate sporulation initiation in *Clostridium difficile*. *Infect Immun* **82:**4276-4291.

29. **Dineen SS, McBride SM, Sonenshein AL.** 2010. Integration of metabolism and virulence by *Clostridium difficile* CodY. *J Bacteriol* **192:**5350-5362.

30. **Schmittgen TD, Livak KJ.** 2008. Analyzing real-time PCR data by the comparative C(T) method. *Nat Protoc* **3:**1101-1108.

31. **Pereira FC, Saujet L, Tome AR, Serrano M, Monot M, Couture-Tosi E, Martin-Verstraete I, Dupuy B, Henriques AO.** 2013. The spore differentiation pathway in the enteric pathogen *Clostridium difficile*. *PLoS Genet* **9:**e1003782.

32. **Jiang M, Shao W, Perego M, Hoch JA.** 2000. Multiple histidine kinases regulate entry into stationary phase and sporulation in *Bacillus subtilis*. *Mol Microbiol* **38:**535-542.

33. **Perego M, Cole SP, Burbulys D, Trach K, Hoch JA.** 1989. Characterization of the gene for a protein kinase which phosphorylates the sporulation-regulatory proteins Spo0A and Spo0F of *Bacillus subtilis*. *J Bacteriol* **171:**6187-6196.

34. **Mearls EB, Lynd LR.** 2014. The identification of four histidine kinases that influence sporulation in *Clostridium thermocellum*. *Anaerobe* **28:**109-119.

35. **Steiner E, Dago AE, Young DI, Heap JT, Minton NP, Hoch JA, Young M.** 2011. Multiple orphan histidine kinases interact directly with Spo0A to control the initiation of endospore formation in *Clostridium acetobutylicum*. *Mol Microbiol* **80:**641-654.

36. **Suarez JM, Edwards AN, McBride SM.** 2013. The *Clostridium difficile cpr* locus is regulated by a noncontiguous two-component system in response to type A and B lantibiotics. *J Bacteriol* **195:**2621-2631.

37. **Bouillaut L, Dubois T, Sonenshein AL, Dupuy B.** 2015. Integration of metabolism and virulence in *Clostridium difficile*. *Res Microbiol* **166:**375-383.

38. **Mani N, Dupuy B.** 2001. Regulation of toxin synthesis in *Clostridium difficile* by an alternative RNA polymerase sigma factor. *Proc Natl Acad Sci* U S A **98:**5844-5849.

39. **El Meouche I, Peltier J, Monot M, Soutourina O, Pestel-Caron M, Dupuy B, Pons JL.** 2013. Characterization of the SigD regulon of *C. difficile* and its positive control of toxin production through the regulation of *tcdR*. *PLoS One* **8:**e83748.

40. **McKee RW, Mangalea MR, Purcell EB, Borchardt EK, Tamayo R.** 2013. The second messenger cyclic Di-GMP regulates *Clostridium difficile* toxin production by controlling expression of *sigD*. *J Bacteriol* **195:**5174-5185.

41. **Antunes A, Martin-Verstraete I, Dupuy B.** 2011. CcpA-mediated repression of *Clostridium difficile* toxin gene expression. *Mol Microbiol* **79:**882-899.

42. **Dineen SS, Villapakkam AC, Nordman JT, Sonenshein AL.** 2007. Repression of *Clostridium difficile* toxin gene expression by CodY. *Mol Microbiol* **66:**206-219.

43. **Aubry A, Hussack G, Chen W, KuoLee R, Twine SM, Fulton KM, Foote S, Carrillo CD, Tanha J, Logan SM.** 2012. Modulation of toxin production by the flagellar regulon in *Clostridium difficile*. *Infect Immun* **80:**3521-3532.

44. **Scaria J, Janvilisri T, Fubini S, Gleed RD, McDonough SP, Chang YF.** 2011. *Clostridium difficile* transcriptome analysis using pig ligated loop model reveals modulation of pathways not modulated in vitro. *J Infect Dis* **203:**1613-1620.

45. **Dingle TC, Mulvey GL, Armstrong GD.** 2011. Mutagenic analysis of the *Clostridium difficile* flagellar proteins, FliC and FliD, and their contribution to virulence in hamsters. *Infect Immun* **79:**4061-4067.

46. **Baban ST, Kuehne SA, Barketi-Klai A, Cartman ST, Kelly ML, Hardie KR, Kansau I, Collignon A, Minton NP.** 2013. The role of flagella in *Clostridium difficile* pathogenesis: comparison between a non-epidemic and an epidemic strain. *PLoS One* **8:**e73026.

47. **Janoir C.** 2016. Virulence factors of *Clostridium difficile* and their role during infection. *Anaerobe* **37:**13-24.

48. **Janoir C, Deneve C, Bouttier S, Barbut F, Hoys S, Caleechum L, Chapeton-Montes D, Pereira FC, Henriques AO, Collignon A, Monot M, Dupuy B.** 2013. Adaptive strategies and pathogenesis of *Clostridium difficile* from in vivo transcriptomics. *Infect Immun* **81:**3757-3769.

49. **Saujet L, Monot M, Dupuy B, Soutourina O, Martin-Verstraete I.** 2011. The key sigma factor of transition phase, SigH, controls sporulation, metabolism, and virulence factor expression in *Clostridium difficile*. *J Bacteriol* **193:**3186-3196.

50. **Deakin LJ, Clare S, Fagan RP, Dawson LF, Pickard DJ, West MR, Wren BW, Fairweather NF, Dougan G, Lawley TD.** 2012. The *Clostridium difficile spo0A* gene is a persistence and transmission factor. *Infect Immun* **80:**2704-2711.

51. **Saujet L, Pereira FC, Serrano M, Soutourina O, Monot M, Shelyakin PV, Gelfand MS, Dupuy B, Henriques AO, Martin-Verstraete I.** 2013. Genome-wide analysis of cell type-specific gene transcription during spore formation in *Clostridium difficile*. *PLoS Genet* **9:**e1003756.

52. **Edwards AN, McBride SM.** 2014. Initiation of sporulation in *Clostridium difficile*: a twist on the classic model. *FEMS Microbiol Lett* **358:**110-118.

53. **Brown DP, Ganova-Raeva L, Green BD, Wilkinson SR, Young M, Youngman P.** 1994. Characterization of *spo0A* homologues in diverse *Bacillus* and *Clostridium* species identifies a probable DNA-binding domain. *Mol Microbiol* **14:**411-426.

54. **Perego M, Hoch JA.** 1991. Negative regulation of *Bacillus subtilis* sporulation by the *spo0E* gene product. *J Bacteriol* **173:**2514-2520.

55. **Perego M.** 2001. A new family of aspartyl phosphate phosphatases targeting the sporulation transcription factor Spo0A of Bacillus subtilis. *Mol Microbiol* **42:**133-143.

56. **Schultz J, Milpetz F, Bork P, Ponting CP.** 1998. SMART, a simple modular architecture research tool: identification of signaling domains. *Proc Natl Acad Sci* U S A **95:**5857-5864.

57. **Letunic I, Doerks T, Bork P.** 2015. SMART: recent updates, new developments and status in 2015. *Nucleic Acids Res* **43:**D257-260.

58. **Kenney LJ.** 2010. How important is the phosphatase activity of sensor kinases? *Curr Opin Microbiol* **13:**168-176.

59. **Raivio TL, Silhavy TJ.** 1997. Transduction of envelope stress in *Escherichia coli* by the Cpx two-component system. *J Bacteriol* **179:**7724-7733.

60. **De Wulf P, Lin EC.** 2000. Cpx two-component signal transduction in *Escherichia coli*: excessive CpxR-P levels underlie CpxA* phenotypes. *J Bacteriol* **182:**1423-1426.

61. **Stephenson K, Hoch JA.** 2002. Evolution of signalling in the sporulation phosphorelay. *Mol Microbiol* **46:**297-304.

62. **Skerker JM, Perchuk BS, Siryaporn A, Lubin EA, Ashenberg O, Goulian M, Laub MT.** 2008. Rewiring the specificity of two-component signal transduction systems. *Cell* **133:**1043-1054.

63. **Mackin KE, Carter GP, Howarth P, Rood JI, Lyras D.** 2013. Spo0A differentially regulates toxin production in evolutionarily diverse strains of *Clostridium difficile*. *PLoS One* **8:**e79666.

64. **Rosenbusch KE, Bakker D, Kuijper EJ, Smits WK.** 2012. *C. difficile* 630Delta*erm* Spo0A regulates sporulation, but does not contribute to toxin production, by direct high-affinity binding to target DNA. *PLoS One* **7:**e48608.

65. **Wust J, Hardegger U.** 1983. Transferable resistance to clindamycin, erythromycin, and tetracycline in *Clostridium difficile*. *Antimicrob Agents Chemother* **23:**784-786.

66. **Hussain HA, Roberts AP, Mullany P.** 2005. Generation of an erythromycin-sensitive derivative of *Clostridium difficile* strain 630 (630Deltaerm) and demonstration that the conjugative transposon Tn916DeltaE enters the genome of this strain at multiple sites. *J Med Microbiol* **54:**137-141.

67. **Thomas CM, Smith CA.** 1987. Incompatibility group P plasmids: genetics, evolution, and use in genetic manipulation. *Annu Rev Microbiol* **41:**77-101.

68. **Yanisch-Perron C, Vieira J, Messing J.** 1985. Improved M13 phage cloning vectors and host strains: nucleotide sequences of the M13mp18 and pUC19 vectors. *Gene* **33:**103-119.

69. **McBride SM, Sonenshein AL.** 2011. Identification of a genetic locus responsible for antimicrobial peptide resistance in *Clostridium difficile*. *Infect Immun* **79:**167-176.

CHAPTER 11

Appendix VII - Antimicrobial Peptide Resistance Mechanisms of Gram-Positive Bacteria

Kathryn L. Nawrocki, Emily K. Crispell, and Shonna M. McBride

This work was published in 2014 in *Antibiotics.*

K.L.N. wrote the majority of the manuscript.

Article Citation:

Nawrocki, K. L., Crispell, E. K., & McBride, S. M. (2014). Antimicrobial peptide resistance mechanisms of gram-positive bacteria. *Antibiotics*, *3*(4), 461-492. doi: 10.3390/antibiotics3040461 PMCID 4239024

ABSTRACT

Antimicrobial peptides, or AMPs, play a significant role in many environments as a tool to remove competing organisms. In response, many bacteria have evolved mechanisms to resist these peptides and prevent AMP-mediated killing. The development of AMP resistance mechanisms is driven by direct competition between bacterial species, as well as host and pathogen interactions. Akin to the number of different AMPs found in nature, resistance mechanisms that have evolved are just as varied and may confer broad-range resistance or specific resistance to AMPs. Specific mechanisms of AMP resistance prevent AMP-mediated killing against a single type of AMP, while broad resistance mechanisms often lead to a global change in the bacterial cell surface and protect the bacterium from a large group of AMPs that have similar characteristics. AMP resistance mechanisms can be found in many species of bacteria and can provide a competitive edge against other bacterial species or a host immune response. Gram-positive bacteria are one of the largest AMP producing groups, but characterization of Gram-positive AMP resistance mechanisms lags behind that of Gram-negative species. In this review we present a summary of the AMP resistance mechanisms that have been identified and characterized in Gram-positive bacteria. Understanding the mechanisms of AMP resistance in Gram-positive species can provide guidelines in developing and applying AMPs as therapeutics, and offer insight into the role of resistance in bacterial pathogenesis.

1. INTRODUCTION

Antimicrobial peptides (AMPs) and the bacterial resistance mechanisms against them have been co-evolving for eons. A diverse array of life forms can produce AMPs, which can be used to promote immune defenses, nutrient acquisition or elimination of rival

organisms from the environment. As a result, AMPs are found in a multitude of environments, ranging from mammalian tissues to soil and aquatic environments. This ubiquitous presence of AMPs in the environment provides strong selective pressure to drive the development of bacterial resistance against these peptides.

AMPs are typically small, charged, amphipathic molecules that can be produced in a variety of structures. Though structurally diverse, most AMPs work by interacting with the bacterial cell surface, followed by disruption of cellular integrity. Accordingly, the majority of bacterial resistance mechanisms function by limiting the interaction of AMPs with the bacterial cell surface. Mechanisms of AMP resistance include trapping or sequestering of peptides, outright destruction of AMPs by proteolysis, removal of AMPs from the cell via active transport, and structural modification of the cell surface to avoid interaction with AMPs. Many of these resistance mechanisms are upregulated in response to AMPs, allowing the bacteria to adaptively counter the effects of AMPs. Loss of these resistance mechanisms can impair the ability of bacteria to colonize plant or animal hosts and can attenuate virulence for many pathogens. Mechanisms of resistance may evolve specifically within a bacterial lineage or be genetically transferred from other AMP-resistant organisms.

In this review, we evaluate the available literature on Gram-positive bacterial resistance mechanisms to antimicrobial peptides. This review highlights methods of AMP resistance based on mode of action and location within the Gram-positive bacterial cell. We begin with an overview of resistance mechanisms that act on AMPs extracellularly, and then discuss bacterial cell surface alterations. Finally, we consider removal of AMPs from the bacterial cell via transport.

2. EXTRACELLULAR MECHANISMS OF RESISTANCE: ENZYMATIC DEGRADATION AND AMP BLOCKING

The initial site of AMP interaction is at the bacterial cell surface. As a result, extracellular mechanisms of AMP inactivation have evolved as a first line of defense to minimize damage to the bacterial cell. Extracellular AMP resistance mechanisms have arisen in two main forms: enzymatic inactivation and sequestration (see Table 1 and Figure 1). The majority of these direct targeting mechanisms have evolved to recognize cationic AMPs. Cationic AMPs are positively charged peptides that may differentially target negatively charged moieties on the outer cell envelope, including teichoic acids, lipid II, and phosphatidylglycerol [1–3].

2.1 Extracellular Proteases

The degradation of AMPs by proteases is a mechanism of resistance found in many Gram-positive species, including *Enterococcus faecalis*, *Staphylococcus aureus*, and *Staphylococcus epidermidis* [4–6]. AMP-degrading proteases generally have broad substrate specificity, are typically found in mammalian pathogens, and include both metallopeptidases and cysteine proteases [7,8]. This section will present several examples of AMP-degrading proteases produced by Gram-positive bacteria and detail their effects on resistance.

AMP-degrading proteases are often secreted by bacteria into their surrounding extracellular environments. Gelatinase, an extracellular metallopeptidase produced by some strains of the opportunistic pathogen *E. faecalis*, cleaves the human cathelicidin, LL-37, resulting in the loss of antimicrobial activity *in vitro* [4]. The production of gelatinase by *E. faecalis* is associated with bacterial dissemination in animal models of disease and

with increased incidence of dental caries in humans [9,10]. One example of a secreted protease made by *S. aureus* that confers AMP resistance is the aureolysin enzyme [5]. Aureolysin can hydrolyze the C-terminal bactericidal domain of LL-37, rendering the AMP inactive [11]. An infection model using human macrophages revealed that aureolysin contributes to Staphylococcal persistence within the phagosomal compartment [12], an environment that contains high levels of the antimicrobial peptide, LL-37 [13]. Additionally, some species of Staphylococci possess proteases that combat anionic AMPs such as dermcidin, a negatively charged peptide secreted by human sweat glands [14]. SepA (or SepP1) made by *S. epidermidis*, is a secreted metalloprotease that can cleave and inactivate dermcidin [6,15]. The SepA protease appears to specifically target dermcidin *in vitro* [6,16].

Gram-positive proteases are also capable of targeting AMPs at the bacterial surface. SpeB is a cysteine proteinase secreted by the pathogenic bacterium *Streptococcus pyogenes* [17]. SpeB has broad substrate specificity and cleaves AMPs, such as LL-37, and other host proteins such as fibrin, immunoglobulins, and other immune modulators [4,18–21]. In an example of adaptive resistance, SpeB was found to complex with the host α_2-macroglobulin (α_2M) proteinase inhibitor during infection [22]. The catalytically active SpeB-α_2M complexes are retained on the bacterial cell surface by association with the *S. pyogenes* G-related α_2M-binding protein (GRAB) [22,23]. The SpeB-α_2M complex has higher proteinase activity against LL-37, relative to free SpeB, and reduces killing of *S. pyogenes in vitro* [22].

Table 1. Summary of Gram-positive Antimicrobial Peptides (AMP) Resistance Mechanisms.

Name	Mechanism of Action	Antimicrobial Resistance	Organisms	Reference
AMP Degradation				
Aureolysin	Protease	LL-37	*S. aureus*	[5,11]
Gelatinase	Protease	LL-37	*E. faecalis*	[4,10]
SepA	Protease	dermcidin	*S. epidermidis*	[6,16]
SpeB	Protease	LL-37	*S. pyogenes*	[4,21,22]
Sequestration/Competition for AMP target				
M Protein	Binding at surface	LL-37	*S. pyogenes*	[24]
PilB	Binding at surface	cathelicidins	*S. agalactiae*	[25]
SIC	Extracellular binding	α-defensins, LL-37, lysozyme	*S. pyogenes*	[26,27]
Staphylokinase	Extracellular binding	Cathelicidin, defensins	*S. aureus*	[28,29]
LciA	Binding at surface	Lactococcin A	*L. lactis*	[30,31]
Capsule	Binding/shielding	Polymyxin B, HNP-1	*S. pneumoniae*	[32]
Exopolysaccharide	Shielding/ Sequestration	LL-37, hBD-3, dermcidin	*S. epidermidis*	[33–35]
LanI lipoproteins	Binding or competition	lantibiotics	*L. lactis*, *B. subtilis*, other lantibiotic producers	[36–38]
Cell Surface Modifications				
DltABCD	D-alanylation of teichoic acids	daptomycin, vancomycin, nisin, defensins, protegrins	*S. aureus*, *L. monocytogenes*, *B. cereus*, *C. difficile*, *S. pyogenes*, *S. agalactiae*, *B. anthracis*, *S. suis*	[2,39–45]
MprF	Lysylation of phoshatidylglycerol	defensins, thrombin-induced platelet microbicidal protein	*S. aureus*, *L. monocytogenes*, *B. anthracis*, *M. tuberculosis*	[46–50]
OatA	Peptidoglycan O-acetylase	lysozyme	*S. aureus*, *S. epidermidis*, *S. lugdunensis*, *E. faecalis*, *L. monocytogenes*	[51–54]
PdgA	Peptidoglycan *N*-acetylglucosamine deacetylase A	lysozyme	*S. pneumoniae*, *E. faecalis*, *S. suis*, *L. monocytogenes*, *B. anthracis*	[55–58]
NamH	*N*-acetylmuramic acid hydroxylase	lysozyme	*M. smegmatis*	[59]

Table 1. *Cont.*

Name	Mechanism of Action	Antimicrobial Resistance	Organisms	Reference
AMP Efflux				
One-component transporter				
LmrB	ABC transporter	LsbA/LsbB	*L. lactis*	[60]
QacA	ABC transporter/ alteration of membrane structure	thrombin-induced platelet microbicidal protein (tPMP)	*S. aureus*	[61]
BceAB type				
AnrAB	ABC transporter	nisin, gallidermin, bacitracin, β-lactams	*L. monocytogenes*	[62,63]
BceAB	ABC transporter	Bacitracin [a], actagardine, mersacidin, plectasin	*B. subtilis* [a], *S. mutans*	[64–68]
BraAB	ABC transporter	nisin, nukacin ISK-1, bacitracin	*S. aureus*	[69]
PsdAB	ABC transporter	nisin, enduracidin, gallidermin, subtilin	*B. subtilis*	[66]
MbrAB	ABC transporter	bacitracin	*S. mutans*	[35]
SP0812-SP0813	ABC transporter	bacitracin, vancoresmycin	*S. pneumoniae*	[70]
SP0912-SP0913	ABC transporter	bacitracin, lincomycin, nisin	*S. pneumoniae*	[71]
VraDE	ABC transporter	bacitracin, nisin, nukacin ISK-1	*S. aureus*	[69,72–76]
VraFG	ABC transporter	nisin, colistin, bacitracin, vancomycin, indolicidin, LL-37, hBD3	*S. aureus*, *S. epidermidis*	[69,72,75, 77–79]
YsaCB	ABC transporter	nisin	*L. lactis*	[80]
BcrAB type				
BcrAB(C)	ABC transporter	bacitracin	*B. licheniformis*	[81]
BcrAB(D)	ABC transporter	bacitracin	*E. faecalis*	[82,83]
LanFEG type				
As-48EFG(H)	ABC transporter	AS-48	*E. faecalis*	[84]
CprABC	ABC transporter	nisin, galidermin, other lantibiotics	*C. difficile*	[85,86]
EpiFEG(H)	ABC transporter	epidermin, gallidermin	*S. epidermidis*	[87]
LtnFE(I)	ABC transporter	lacticin 3147	*L. lactis*	[88,89]
McdFEG	ABC transporter	macedocin	*S. macedonicus*	[90]
MrsFGE	ABC transporter	mersacidin	*Bacillus sp. HIL Y-84, 54728*	[91,92]
MutFEG	ABC transporter	mutacin II	*S. mutans*	[93]
NisFEG(I)	ABC transporter	nisin	*L. lactis*	[37,94]
NukFEG(H)	ABC transporter	nukacin	*S. warneri*	[95,96]
SboFEG	ABC transporter	salivaricin B	*S. salivarius*	[97]
ScnFEG	ABC transporter	streptococcin A-FF22	*S. pyogenes*	[98]
SmbFT	ABC transporter	Smb, haloduracin	*S. mutans*	[99]
SpaFEG	ABC transporter	subtilin	*B. subtilis*	[36,100]

[a] Confers only bacitracin resistance in *B. subtilis*.

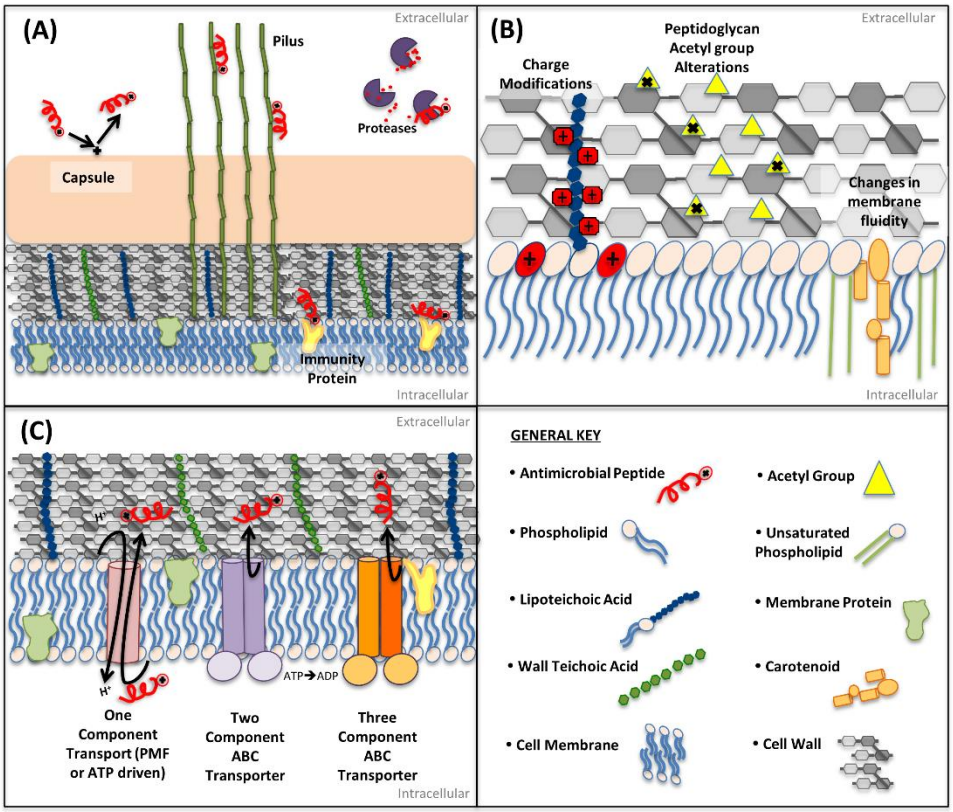

Figure 1. Overview of Antimicrobial Peptide Resistance Mechanisms in Gram-Positive Bacteria. (**A**) Extracellular mechanisms of AMP resistance include peptide degradation by secreted proteases, AMP sequestration by secreted or membrane associated protein (e.g., pili, immunity proteins, M proteins), or blocking by capsule polysaccharides; (**B**) Cell wall and membrane modifications include: Alteration of charge by lysination of the phospholipid head groups or D-alanylation of the lipoteichoic backbone, modification of the cell wall by deacetylation of N-acetylglucosamine or O-acetylation of N-acetylmuramyl residues, and alterations in membrane fluidity by phospholipid tail saturation or carotenoid additions; (**C**) Transport mechanisms of antimicrobial efflux from the cell include: ATP-driven ABC transporters composed of a single, double, or triple protein pump and involve a supplementary immunity protein, or single protein transporters driven by proton motive force.

2.2. Protein-Mediated Sequestration

Sequestration is another extracellular mechanism of AMP resistance [24–29,101]. Some Gram-positive bacteria produce extracellular or surface-linked proteins that directly bind to AMPs and block access to the cell membrane. Mechanisms of protein-mediated AMP sequestration vary between species and strains. We have highlighted specific examples of AMP sequestration mechanisms identified amongst strains of *S. pyogenes*, *S. aureus*, *Streptococcus agalactiae*, and *Lactococcus lactis*.

Proteins that inhibit AMP activity through binding can be secreted into the extracellular environment to inhibit contact of bactericidal peptides with the cellular surface. For example, the Streptococcal inhibitor of complement (SIC) produced by *S. pyogenes* is a hydrophilic, secreted protein that sequesters many AMPs, thereby preventing them from reaching cell-surface targets [102]. SIC binds to α-defensins, LL-37, and lysozyme, neutralizing the AMPs and inhibiting their bactericidal activity against *S. pyogenes* [27,102,103]. SIC production promotes bacterial survival *in vitro* and increases the virulence of *S. pyogenes* in animal models of disease [26,104]. Staphylokinase secretion by *S. aureus* is another example of an extracellular AMP resistance mechanism. Production of the staphylokinase protein by *S. aureus* occurs through the lysogenic conversion of the hlb β-hemolysin toxin gene by a bacteriophage harboring the *sak* gene [105–107]. Staphylokinase binds the murine cathelicidin mCRAMP *in vivo* and also complexes with human defensins HNP-1 and HNP-2 to reduce their bactericidal effects [28,29]. Studies of staphylokinase binding suggest that the staphylokinase-cathelicidin complex promotes host tissue invasion by activating the conversion of plasminogen to the host extracellular

matrix-degrading enzyme, plasmin, although the role this conversion plays in Staphylococcal virulence remains unclear [29,101,108].

Proteins attached to the cellular surface can also bind AMPs to prevent contact with cell-associated targets. Examples of such proteins include the M1 protein of *S. pyogenes* and the pilus subunit, PilB of *S. agalactiae*. M1 of *S. pyogenes* can be found on the surface of most clinical isolates and has been linked to both host tissue adherence and invasive disease [109]. A hyper-variable extracellular portion of the M1 protein was shown to bind LL-37 and prevent the AMP from reaching the cell membrane [24]. The sequestration of LL-37 by M1 also promotes Streptococcal survival in neutrophil extracellular traps (NETs) by reducing LL-37 activity [24]. Like the M proteins of *S. pyogenes*, pili are also associated with invasive disease and promotion of host cell adherence by *S. agalactiae* [110,111]. Pili are large, filamentous, multimeric protein complexes expressed on the cell surface of *S. agalactiae* and other bacteria. Expression of the Streptococcal pilin subunit, PilB, promotes association of LL-37 with the bacterial cell surface and correlates with increased resistance to the murine cathelicidin mCRAMP *in vitro* [25]. In addition, pilB mutants of *S. agalactiae* (GBS) exhibit reduced fitness relative to wild-type strains in murine infection models [25]. These data suggest that in addition to the adhesin properties of pili, pilus-mediated binding of AMPs also contributes to *S. agalactiae* virulence within the host.

Another family of membrane-associated AMP resistance proteins encompasses the LanI immunity proteins of some bacteriocin producer strains. LanI proteins are typically encoded near a bacteriocin biosynthetic operon and provide protection against the bacteriocin made by the producer bacterium [112,113]. LanI-type immunity proteins are lipoproteins that anchor to the bacterial cell surface and confer resistance by either binding directly to

AMPs or outcompeting AMPs by binding directly to the cellular target [114–117]. The LanI lipoproteins often work in concert with LanFEG transporters, possibly acting as substrate-binding partners for specific lantibiotics. The best characterized of the transporter-associated LanI proteins are the NisI and SpaI lipoproteins found in strains of *L. lactis* and *Bacillus subtilis*, respectively [36,37,118] (described in transporter section). But, several lantibiotic producers encode only a LanI immunity protein and do not encode an apparent LanFEG transporter (e.g., PepI of *S. epidermidis* [119], lactocin S [120] of *L. sakei* and epicidin 280 of *S. epidermidis* [121]). In these systems, the LanI lipoprotein confers full immunity to the associated lantibiotic. Though some LanI structures have been characterized, LanI lipoproteins generally have low, if any, homology to one another [116,122]. Thus, it is unclear if mechanism of action for LanI-mediated immunity is conserved between different LanI lipoproteins.

2.3. Inhibition of AMP Activity by Surface-Associated Polysaccharides

Extracellular polysaccharide production has long been recognized as a factor that promotes both virulence and host colonization by many bacteria [123–125]. Extracellular polysaccharides are composed of structurally diverse polymers that are enzymatically produced by some Gram-positive species [126,127]. Extracellular polysaccharides that are attached to the cellular surface through covalent linkages with the cell wall are known as capsules (capsular polysaccharide, or CPS), while loosely attached polymers are referred to as exopolysaccharides, or EPS [128–130]. Polysaccharide-mediated AMP resistance is thought to occur by shielding the bacterial membrane via binding or electrostatic repulsion of AMPs [34,131].

The production of capsular polysaccharides provides resistance to a variety of AMPs and other antimicrobials and can allow some bacteria to evade host detection. Capsule-AMP binding can be mediated by the electrostatic interaction of positively charged AMPs with the negatively charged polysaccharide capsule [32]. For example, free capsular extracts from *Streptococcus pneumoniae* bind both polymyxin B and the α-defensin HNP-1, preventing these AMPs from reaching the cell membrane and promoting bacterial survival *in vitro*. Additionally, both polymyxin B and HNP-1 promote release of the capsule from *S. pneumoniae* without loss of cell viability, suggesting that capsule release may be a mechanism of AMP resistance by sequestering AMPs away from the bacterial cell surface [32]. In another example, production of the exopolysaccharide intercellular adhesion, PIA, by *S. epidermidis* reduces killing by human defensin hBD-3, cathelicidin (LL-37), and the anionic AMP dermcidin. PIA is hypothesized to shield the bacterial membrane from the effects of AMPs [33,34]. Predictably, PIA production is associated with *S. epidermidis* virulence in multiple animal infection models [132,133]. However, while many exopolysaccharide capsules can provide resistance to AMPs, this protection is not universal to all capsule-producing Gram-positive bacteria [134–136].

3. MEMBRANE AND CELL WALL MODIFICATIONS

The bacterial cell wall and membrane comprise a major target for the bactericidal activity of AMPs [137–139]. Bacteria frequently modify cell surface components to counter the effects of AMPs by reducing the net negative charge of the cell, altering membrane fluidity, or directly modifying AMP targets [140–142].

3.1. Repulsion of AMPs

Many AMPs target bacterial cells through electrostatic interactions with the cell surface [137–139]. The net charge of the bacterial cell surface is generated by anionic components of the cell membrane and cell wall, such as phospholipids and teichoic acids [143–145]. In turn, positively charged AMPs are attracted to the negatively charged bacterial cell surface [144,145]. Hence, a broad strategy of resistance to positively charged AMPs is to alter the components on the cell surface to decrease the net negative charge of the cell, thereby limiting the electrostatic interaction of AMPs with the bacterial cell surface.

One component of the bacterial cell membrane that carries a negative charge is phosphatidylglycerol [144,145]. But in many Gram-positive bacteria, the negative charge on phosphatidylglycerol can be masked via the addition of a positively charged amino acid by the multipeptide resistance factor protein, MprF [146,147]. MprF is an intergral lysyl-phosphatidylglycerol synthetase that synthesizes and translocates aminoacylated-phosphatidylglycerol to the external membrane layer of the bacterial cell. MprF synthases were initially found to incorporate a positively charged lysine into phosphatidylglycerol (Lys-PG), decreasing the net negative charge on the bacterial membrane. In *S. aureus*, *Listeria monocytogenes*, *E. faecalis*, *Enterococcus faecium*, *B. subtilis*, and *Bacillus anthracis*, the aminoacylation of phosphatidylglycerol by MprF confers resistance to positively charged AMPs [47–49,148–150]. Additionally, an MprF homolog is present in *Mycobacterium tuberculosis*, which also confers resistance to positively charged AMPs. This MprF homolog, LysX, carries out the same functions as MprF, with the addition of a lysyl-tRNA synthetase activity [46,151]. Lysinylation of phosphatidylglycerol confers resistance to a broad spectrum of AMPs, including human defensins, gallidermin, nisin,

lysozyme, daptomycin, polymyxin B, and vancomycin (Table 1) [46,150–159]. In addition to lysine modifications, some MprF orthologs can modify membrane phosphatidylglycerol with multiple amino acids, including alanine and arginine [149,160]. The enhanced antimicrobial resistance provided by aminoacylation of phosphatidylglycerol is also associated with increased virulence for several Gram-positive pathogens [46,48,49,161,162].

The Dlt pathway is another enzymatic mediator of AMP resistance that has been identified and studied in many Gram-positive genera including *Staphylococcus*, *Listeria*, *Enterococcus*, *Bacillus*, *Clostridium*, *Streptococcus*, and *Lactobacillus* [2,40–45,163–168]. The enzymatic functions of the DltABCD proteins lead to the D-alanylation of teichoic acids and lipoteichoic acids of the cell wall [169]. The addition of D-alanine to the backbone of teichoic acids can mask the negative charge present along these glycopolymers, thereby leading to increased surface charge and lower attraction of positively charged antimicrobials [169]. Similar to MprF, D-alanylation of teichoic acids by the Dlt pathway leads to a global change in charge distribution across the cell surface, allowing resistance to a broad range of cationic AMPs including vancomycin, nisin, gallidermin daptomycin, polymyxin B, lysozyme, and cathelicidins [2,39,141,163,166,170–172].

In addition to charge modification of teichoic acids, high-resolution microscopy of Group B *Streptococcus* revealed that D-alanylation could increase cell wall density, leading to increased surface rigidity [173]. Accordingly, D-alanylation may confer resistance to AMPs both by reducing the electrostatic interactions between AMPs and the cell surface and by decreasing the permeability of the cell wall [173]. As AMPs are

ubiquitous within animals, D-alanylation of the cell wall can affect host colonization for pathogens and non-pathogenic species [41,152,164,174,175].

3.2. Target Modification

The cell wall is a common antimicrobial target for Gram-positive organisms. As a result, bacteria have evolved multiple modifications that limit antimicrobial targeting of the cell wall. Lysozyme, or *N*-acetylmuramide glycanhydrolase, an antimicrobial enzyme, is an important component of the host innate immune defense. Lysozyme is cationic at physiological pH, which facilitates its interaction with negatively charged bacterial surfaces. The cationic and muramidase activities of lysozyme directly target the bacterial peptidoglycan, the primary constituent of the cell wall [176]. The muramidase domain of lysozyme hydrolyzes the β-1,4 linkages between *N*-acetylglucosamine and *N*-acetylmuramic acid of peptidoglycan, leading to the breakdown of the peptidoglycan macromolecular structure and eventual lysis of the cell [177–179]. As a result, bacterial resistance mechanisms have evolved to counter both the muramidase and cationic activities of lysozyme. In this section, we detail the mechanisms by which peptidoglycan is modified to limit lysozyme activity.

Two peptidoglycan modifiers that contribute to AMP resistance in some Gram-positive bacteria are the enzymes PgdA and OatA. It is proposed that the modifications made by both of these enzymes lead to steric hindrance between AMPs and the cell surface, thereby limiting the contact between lysozyme and its target [180]. PgdA deacetylates *N*-acetylglucosamine residues of peptidoglycan, generating a less favorable substrate for lysozyme [181–184]. PgdA was first implicated as a peptidoglycan deacetylase in the respiratory pathogen *S. pneumoniae*. PdgA and other peptidoglycan deacetylase orthologs

have been shown to contribute to AMP resistance in many bacteria, including *Enterococcus*, *Streptococcus*, *Listeria* and *Bacillus* species [55–58,180,183,185]. Moreover, deacetylation of peptidoglycan enhances colonization and virulence in several pathogens, including *E. faecalis*, *L. monocytogenes* and *S. pneumoniae* [185–187]. As *N*-acetylglucosamine deacetylases are encoded within the genomes of most Gram-positive bacteria, these enzymes likely contribute to lysozyme and host colonization in many more species.

OatA (also known as Adr in *S. pneumoniae*) is another type of peptidoglycan modifying enzyme found in Gram-positive bacteria that confers resistance to lysozyme [188–190]. OatA performs *O*-acetylation at the C6-OH group of *N*-acetylmuramyl residues in peptidoglycan [188–190]. *O*-acetylation of *N*-acetylmuramyl residues is thought to prevent lysozyme from interacting with the β-1,4 linkages of peptidoglycan by steric hindrance [180]. OatA and orthologous proteins have been characterized in *Staphylococcus*, *Enterococcus*, *Lactococcus*, *Bacillus*, *Streptococcus* and *Listeria* species [51,52,54,58,180,187,191]. Like deacetylation mechanisms, *O*-acetylation of peptidoglycan is likely to be widespread among Firmicutes and has been noted to contribute to virulence in animal models of infection [52,54,187,190,192].

A peptidoglycan modifier unique to *Mycobacterium* is the enzyme NamH (*N*-acetylmuramic acid hydroxylase). NamH hydroxylates *N*-acetylmuramic acid residues leading to the production *N*-glycolylmuramic acid. The modification of peptidoglycan by NamH was determined to confer lysozyme resistance in *Mycobacterium smegmatis* [59]. It is likely that NamH confers lysozyme resistance to Mycobacterial species through the generation of *N*-glycolylmuramic acid, as NamH is well conserved in Mycobacterial

genomes. It is hypothesized that *N*-glycolylmuramic acid residues may stabilize the cell wall; however, the mechanism of resistance is not fully understood [193]. However, recent work suggests that the presence of an *N*-glycolyl group blocks lysozyme from accessing the β-1,4 peptidoglycan bonds, preventing the muramidase activity of lysozyme and leaving the cell wall intact [59].

3.3. Alterations to Membrane Order

Apart from AMP repulsion and AMP target modifications as mechanisms of resistance, other changes in membrane composition can also reduce the susceptibility of bacteria to AMP-mediated killing. Alterations in Gram-positive membrane composition appear to contribute to AMP resistance by affecting the peptide interactions with the cell membrane. In particular, the degree of membrane fluidity appears to be an important determinant of AMP susceptibility.

One example of a membrane alteration that confers AMP resistance is the saturation of membrane fatty acids. Investigations into the cell membrane components of nisin-resistant *L. monocytogenes* showed that some resistant strains contained a higher proportion of saturated (straight chain) fatty acids versus unsaturated (branched chain) fatty acids [194,195]. Additionally, a nisin resistant strain of *L. monocytogenes* produced lower concentrations of the lipid head group phosphatidylglycerol and less diphosphatidylglycerol than a nisin-susceptible strain [194–196]. This nisin-resistant strain also contained higher concentrations of the lipid head group, phosphatidylethanolamine, while the anionic membrane component, cardiolipin, was decreased [197]. These studies suggest that higher concentrations of saturated fatty acids, a decrease in phophatidylglycerol and an increase in phophatidylethanolamine head groups in the

Listeria membrane lead to a decrease in cell membrane fluidity [194–197]. It is proposed that the decrease in membrane fluidity increases nisin resistance by hindering nisin insertion into the membrane [197].

The addition of other membrane components can also increase rigidity and lead to resistance to host AMPs and daptomycin in *S. aureus* [198]. Increased membrane rigidity in some Gram-positive organisms can result from carotenoid overproduction [199,200]. Carotenoids are organic pigments made of repeating isoprene units that are produced by plants, bacteria, and fungi [201]. Carotenoids, such as staphyloxanthin made by *S. aureus*, can stabilize the leaflets of the cell membrane by increasing order in the fatty acid tails of membrane lipids and lead to decreased susceptibility to AMPs [199,202,203]. This stabilization of fatty acid tails leads to an increase in cell membrane rigidity, which is suggested to limit insertion of AMPs into the membrane [204,205].

Though a higher concentration of saturated fatty acids in the membrane confers AMP resistance in some bacteria, other bacteria increase unsaturated fatty acid concentrations to increase resistance. In *S. aureus*, increased levels of unsaturated membrane lipids increase the resistance to the host AMP, tPMP (thrombin-induced platelet microbicidal proteins) [206]. Unsaturated fatty acids contain double bonds along the length of their carbon chain, which causes lipid disorder, thereby increasing membrane fluidity and impacting resistance to antimicrobials [206,207]. Other studies in AMP resistance found that methicillin-resistant *S.aureus* isolates that developed resistance to daptomycin also had increased resistance to host tPMPs and the human neutrophil peptide, hNP-1. These co-resistant strains have a phenotype defined by increased cell wall thickness and

increased membrane fluidity [198]. It is hypothesized that these altered membrane arrangements may prevent efficient AMP insertion into the membrane [198,206,207].

At present, there is no clear explanation as to how alterations in membrane fluidity or rigidity lead to AMPs resistance. From the examples discussed above, it could be argued that the degree of fluidity required for resistance to a particular AMP may be as varied as the structures of the AMPs themselves, or perhaps is constrained to groups with similar mechanisms of action.

4. AMP EFFLUX MECHANISMS

Transport, or efflux, is a common mechanism used by Gram-positive bacteria for the removal of toxic compounds and antimicrobials from cells. The majority of antimicrobial peptide efflux mechanisms consist of multi-protein ABC (ATP-binding cassette) transporter systems, which use ATP to drive the transport of substrates across or out of the cell membrane [208]. There are three primary types of ABC transporter systems implicated in Gram-positive AMP resistance: three-component ABC-transporters, two-component ABC-transporters, and single protein multi-drug resistance transporters, or MDR pumps [209]. All ABC-transporters are composed of two distinct domains: the transmembrane domain (permease) and the nucleotide-binding domain (NBD), which facilitates ATP-binding [209]. A less common efflux mechanism that has been identified is the Major Facilitator (MFS) Transporter module, which facilitates small solute transport via a chemiosmotic ion gradient [210]. This section will present the key types of AMP transporters found in Gram-positive bacteria and highlight the AMP resistance characteristics of these systems.

4.1. Three-Component (LanFEG) Transporter Systems

Three-component ABC transporters, or LanFEG systems, are best characterized in AMP-producing bacteria. LanFEG systems are members of the ABC-type 2 sub-family of transporters, and consist of one protein with a nucleotide-binding domain (LanF) and two distinct transmembrane permeases (LanE and LanG) [211]. The majority of the characterized LanFEG systems are self-immunity mechanisms that provide protection against bacteriocins (typically lantibiotics) made by bacteriocin producer strains [38,112] (Table 1). The LanFEG transporters are often found in conjunction with LanI membrane-associated lipoproteins that can function in tandem with the transporter to provide greater resistance to AMPs [112,212,213].

The best-characterized LanFEG transporters are the NisFEG and SpaFEG systems found in strains of *L. lactis* and *B. subtilis* that produce the lantibiotic AMPs nisin and subtilin, respectively. Both NisFEG and SpaFEG provide resistance to their cognate substrates, but full resistance is achieved in concert with their associated substrate-binding lipoproteins, NisI and SpaI [100,213–215]. Immunity to the lantibiotic nukacin ISK from *Streptococcus warneri* does not involve a LanI protein, but instead contains a distinct membrane-associated protein termed NukH [96,216]. In contrast to the LanI proteins, NukH is not a lipoprotein; however, NukH does appear to function as a substrate-binding partner to the NukFEG transporter. Similar to LanI, NukH confers partial immunity to nukacin ISK, but full immunity requires the complete NukFEGH system [216,217].

Most characterized LanFEG systems confer resistance only to the AMP made by a producer strain, although examples have been identified that provide resistance to multiple AMP substrates in non-producer bacteria. In *Clostridium difficile*, the CprABC transporter (a LanFEG ortholog) confers resistance to nisin, gallidermin, and likely other structurally

dissimilar lantibiotic peptides [85,86]. The regulation of immunity and AMP biosynthetic genes are typically coupled in bacteriocin producer strains [112]. The ability of the CprABC system to confer resistance to multiple unrelated peptides may result from the uncoupling of the immunity mechanism from bacteriocin synthesis. But non-producers that have immunity genes in the absence of AMP biosynthetic operons can have relaxed substrate specificity that allows for recognition of multiple bacteriocins. Thus, Lan transporter cross-immunity to multiple AMPs could provide a significant competitive advantage to non-producer bacteria. Indeed, a homology search for LanFEG proteins reveals that the genomes of many other Firmicutes encode predicted bacteriocin transporters that are not coupled with apparent bacteriocin synthesis genes. Hence, like other antibacterial resistance mechanisms, the LanFEG systems have found their way into non-producing species [85,86].

4.2. Two-Component ABC-Transporter Systems

Two-component ABC-transporters make up the majority of transporter-mediated AMP resistance characterized in non-AMP producing bacteria. The canonical two-component ABC-transporter consists of one nucleotide-binding protein and a separate membrane-spanning permease [218,219]. Unlike most LanFEG systems, two-component transporters often provide resistance to multiple AMPs and are common among Gram-positive bacteria. As outlined in Table 1, numerous examples of these transporters have been identified that can provide resistance to AMPs produced by humans and bacteria, including cyclic peptides and some non-peptide antibiotics [218,220].

There are two main types of two-component ABC-transporter systems that confer resistance to AMPs among Gram-positive bacteria. The first and most common type is

often referred to as the BceAB group [218,221]. BceAB transporter systems contain an archetypal ATP-binding protein of about 225–300 amino acids and a larger permease component that ranges in size from 620–670 amino acids. The prototype of this transporter group, BceAB, was first identified as a bacitracin resistance mechanism in *B. subtilis* [67,68]. Since the identification of BceAB, dozens of similar transporters have been discovered in pathogenic and non-pathogenic Gram-positive species, including *S. aureus*, *L. monocytogenes*, *S. pneumoniae*, and *L. lactis* (see Table 1 for examples) [62,71,77,80]. Members of the BceAB group have demonstrated resistance to a wide-range of bacteriocins, mammalian and fungal defensins, peptide antibiotics, and other antimicrobial compounds (Table 1). Although many of the BceAB transporters confer resistance to AMPs *in vitro*, the roles of these transporters in the virulence of pathogenic species are not known.

Another common type of a Gram-positive ABC-transporter that confers AMP resistance is the BcrAB(C) system. The BcrAB(C) transporter confers resistance to bacitracin and was originally identified in a bacitracin producer strain of *Bacillus licheniformis* [81]. BcrAB transporters can be distinguished from the BceAB systems by size and topology: BcrA is an ATP-binding cassette that ranges from about 280–320 amino acids, while the BcrB permease modules are smaller, at approximately 200–250 amino acids. BcrAB is often encoded with a third protein, BcrC (or BcrD), which allows for higher resistance to bacitracin than the BcrAB transporter alone [81,222,223]. Initially it was hypothesized that BcrC functioned as part of the BcrAB ABC-transporter, however it was later demonstrated that BcrC acts as an undecaprenyl pyrophosphate (UPP) phosphatase that competes with bacitracin for UPP [222]. The BcrAB transporters are predicted to be

structurally similar to the LanFEG transporters, though the Lan systems function through two dissimilar permease components, while Bcr systems operate with only one permease subunit (BcrB) [38,82,218]. Aside from the bacitracin producer strains, BcrAB and orthologous transporters have been shown to confer resistance to bacitracin in many strains of *E. faecalis*, as well as some *Streptococcus* and *Clostridium* species [35,82,83,224].

4.3. Single Membrane Protein Antimicrobial Transporters

Multi-drug resistance (MDR) ABC-transporters are common bacterial mechanisms of resistance to peptide and non-peptide antibiotics [225]. Though these transporters are most common among characterized mechanisms for non-peptide antimicrobial resistance in Gram-positive bacteria, there are examples of MDR transporters that confer resistance to AMPs. One notable MDR AMP resistance mechanism consists of the LmrA/B proteins encoded by some *L. lactis* strains [60,226]. A LmrA MDR efflux pump was first described in a non-producer strain of *L. lactis* [226]. LmrB is an ortholog of LmrA found in *L. lactis* strains that produce the bacteriocins LsbA and LsbB [60]. LmrA/LmrB are membrane proteins with six predicted transmembrane segments and a C-terminal, nucleotide-binding domain [60]. LmrA provides broad resistance against a long list of peptide antibiotics and cytotoxic compounds, while LmrB confers resistance to the two bacteriocins LsbA and LsbB [60,226]. A BLASTp homology search revealed the presence of additional orthologs of LmrA/B encoded within the genomes of hundreds of Gram-positive Firmicutes, though the function and significance of these remains unknown.

A less common type of single-protein transporter involved in antimicrobial peptide resistance is exemplified by the QacA transporter of *S. aureus* [61]. QacA is a member of the major facilitator superfamily (MFS) of membrane transport proteins, which use proton

motive force, rather than ATP, to drive the efflux of substrates [227]. QacA confers resistance to a variety of toxic dyes, antiseptics and disinfectants [228,229]. In addition to cationic toxins, QacA provides resistance to thrombin-induced platelet microbicidal protein (tPMP), a host-derived antimicrobial peptide [61]. QacA-dependent tPMP resistance was found to confer a survival advantage in an animal model of infection, and increased resistance to tPMP in *S. aureus* also correlates with endocarditis in humans [61,230]. QacA orthologs have also been identified in other staphylococci, as well as in *Enterococcus* and *Bacillus* species, though the ability of these orthologs to transport AMPs is not understood [231,232].

5. CONCLUSIONS

Antimicrobial peptides are diverse in both structure and function and are produced by all forms of life. As such, AMPs are an ancient defense mechanism, and resistance mechanisms to AMPs have been selected for as long as AMPs have existed. Gram-positive bacteria are ancient producers of AMPs and as a consequence, these organisms likely developed some of the first AMP resistance mechanisms.

Herein we have detailed a wide variety of AMP resistance mechanisms found in Gram-positive bacteria (summarized in Figure 1). AMPs resistance mechanisms can be broad spectrum, such as MprF and the Dlt pathway which function by decreasing the net negative charge of the bacterial cell surface, thereby reducing the attraction for positively charged AMPs from the cell. Conversely, AMP resistance mechanisms can be highly specific and only confer resistance to a single peptide. AMP resistance mechanisms can be confined to a particular species or genus, such as NamH in *Mycobacterium*, or can be distributed among multiple species, such as the LanFEG systems. AMPs resistance

mechanisms are dynamic; they can be passed from species to species via bacteriophages or horizontal gene transfer, and can change specificity and function over time through evolution [85,86,105,233]. Under selective pressure, AMP resistance mechanisms can evolve to suit the needs of a particular species in its own niche [234].

At present, many AMPs are being investigated as potential antimicrobial therapies [235–240]. AMP drug development should be carefully vetted because like any naturally-produced antimicrobial, cognate resistance mechanisms for AMPs are already present in the producer bacterium. While these resistance mechanisms may be found more frequently in producer strains, each has the propensity to be passed on to other genera or species within a shared environmental niche. Because the presence of AMPs provides high selective pressure for the acquisition of resistance, it is important to consider the potential for resistance mechanism transfer between bacteria when developing AMPs for clinical use [241,242]. Additionally, depending on the AMP resistance mechanism that is selected for, a multitude of issues may arise if the mechanism of resistance is broad-spectrum. A broad-spectrum AMP resistance mechanism could restrict the already limited clinical treatment options for use against some Gram-positive pathogens and may undermine our own immune response by conferring resistance to our own innate immune system peptides [243].

Antimicrobial peptide resistance is not as well characterized for Gram-positive bacteria as it is for Gram-negative bacteria. Thus, it is likely that many more mechanisms of antimicrobial resistance remain to be discovered in Gram-positive species. As more AMPs are found, new Gram-positive AMP resistance mechanisms will undoubtedly be revealed.

ACKNOWLEDGMENTS

We give special thanks to Rita Tamayo and Adrianne Edwards for helpful criticism of this manuscript. We sincerely apologize to any colleagues whose work was not cited due to the large volume of manuscripts on this topic. This work was supported by the U.S. National Institutes of Health through research grants DK087763 and DK101870 to SMM and training grant AI106699 to KLN. The content of this manuscript is solely the responsibility of the authors and does not necessarily reflect the official views of the National Institutes of Health.

Author Contributions

K.L.N., E.K.C. and S.M.M. wrote the manuscript.

Conflicts of Interest

The authors declare no conflict of interest.

REFERENCES

1. **Koprivnjak, T.; Peschel, A.** Bacterial resistance mechanisms against host defense peptides. *Cell. Mol. Life Sci*. 2011, *68*, 2243–2254.
2. **Peschel, A.; Otto, M.; Jack, R.W.; Kalbacher, H.; Jung, G.; Gotz, F.** Inactivation of the dlt operon in *Staphylococcus aureus* confers sensitivity to defensins, protegrins, and other antimicrobial peptides. *J. Biol. Chem.* 1999, *274*, 8405–8410.

3. **Staubitz, P.; Neumann, H.; Schneider, T.; Wiedemann, I.; Peschel, A.** MprF-mediated biosynthesis of lysylphosphatidylglycerol, an important determinant in staphylococcal defensin resistance. *FEMS Microbiol. Lett.* 2004, *231*, 67–71.

4. **Schmidtchen, A.; Frick, I.M.; Andersson, E.; Tapper, H.; Bjorck, L.** Proteinases of common pathogenic bacteria degrade and inactivate the antibacterial peptide LL-37. *Mol. Microbiol.* 2002, *46*, 157–168.

5. **Sabat, A.; Kosowska, K.; Poulsen, K.; Kasprowicz, A.; Sekowska, A.; van Den Burg, B.; Travis, J.; Potempa, J.** Two allelic forms of the aureolysin gene (*aur*) within *Staphylococcus aureus*. *Infect. Immun.* 2000, *68*, 973–976.

6. **Lai, Y.; Villaruz, A.E.; Li, M.; Cha, D.J.; Sturdevant, D.E.; Otto, M.** The human anionic antimicrobial peptide dermcidin induces proteolytic defence mechanisms in staphylococci. *Mol. Microbiol.* 2007, *63*, 497–506.

7. **Hase, C.C.; Finkelstein, R.A.** Bacterial extracellular zinc-containing metalloproteases. *Microbiol. Rev.* 1993, *57*, 823–837.

8. **Del Papa, M.F.; Hancock, L.E.; Thomas, V.C.; Perego, M.** Full activation of *Enterococcus faecalis* gelatinase by a C-terminal proteolytic cleavage. *J. Bacteriol.* 2007, *189*, 8835–8843.

9. **Engelbert, M.; Mylonakis, E.; Ausubel, F.M.; Calderwood, S.B.; Gilmore, M.S.** Contribution of gelatinase, serine protease, and fsr to the pathogenesis of *Enterococcus faecalis* endophthalmitis. *Infect. Immun.* 2004, *72*, 3628–3633.

10. **Thurlow, L.R.; Thomas, V.C.; Narayanan, S.; Olson, S.; Fleming, S.D.; Hancock, L.E.** Gelatinase contributes to the pathogenesis of endocarditis caused by *Enterococcus faecalis*. *Infect. Immun.* 2010, *78*, 4936–4943.

11. **Sieprawska-Lupa, M.; Mydel, P.; Krawczyk, K.; Wojcik, K.; Puklo, M.; Lupa, B.; Suder, P.; Silberring, J.; Reed, M.; Pohl, J.; *et al*.** Degradation of human antimicrobial peptide LL-37 by *Staphylococcus aureus*-derived proteinases. *Antimicrob. Agents Chemother*. 2004, *48*, 4673–4679.

12. **Kubica, M.; Guzik, K.; Koziel, J.; Zarebski, M.; Richter, W.; Gajkowska, B.; Golda, A.; Maciag-Gudowska, A.; Brix, K.; Shaw, L.** A potential new pathway for *Staphylococcus aureus* dissemination: The silent survival of *S. aureus* phagocytosed by human monocyte-derived macrophages. *PLoS One* 2008, *3*, e1409.

13. **Rivas-Santiago, B.; Hernandez-Pando, R.; Carranza, C.; Juarez, E.; Contreras, J.L.; Aguilar-Leon, D.; Torres, M.; Sada, E.** Expression of cathelicidin LL-37 during *Mycobacterium tuberculosis* infection in human alveolar macrophages, monocytes, neutrophils, and epithelial cells. *Infect. Immun.* 2008, *76*, 935–941.

14. **Schittek, B.; Hipfel, R.; Sauer, B.; Bauer, J.; Kalbacher, H.; Stevanovic, S.; Schirle, M.; Schroeder, K.; Blin, N.; Meier, F.; *et al*.** Dermcidin: A novel human antibiotic peptide secreted by sweat glands. *Nat. Immunol.* 2001, *2*, 1133–1137.

15. **Teufel, P.; Gotz, F.** Characterization of an extracellular metalloprotease with elastase activity from *Staphylococcus epidermidis*. *J. Bacteriol.* 1993, *175*, 4218–4224.

16. **Cheung, G.Y.; Rigby, K.; Wang, R.; Queck, S.Y.; Braughton, K.R.; Whitney, A.R.; Teintze, M.; DeLeo, F.R.; Otto, M.** *Staphylococcus epidermidis* strategies to avoid killing by human neutrophils. *PLoS Pathog*. 2010, *6*, e1001133.

17. **Hauser, A.R.; Stevens, D.L.; Kaplan, E.L.; Schlievert, P.M.** Molecular analysis of pyrogenic exotoxins from *Streptococcus pyogenes* isolates associated with toxic shock-like syndrome. *J. Clin. Microbiol*. 1991, *29*, 1562–1567.

18. **Elliott, S.D.** A proteolytic enzyme produced by group A Streptococci with special reference to its effect on the type-specific M antigen. *J. Exp. Med.* 1945, *81*, 573–592.

19. **Kapur, V.; Majesky, M.W.; Li, L.L.; Black, R.A; Musser, J.M.** Cleavage of interleukin 1 beta (IL-1 beta) precursor to produce active IL-1 beta by a conserved extracellular cysteine protease from *Streptococcus pyogenes*. *Proc. Natl. Acad. Sci. USA* 1993, *90*, 7676–7680.

20. **Kapur, V.; Topouzis, S.; Majesky, M.W, Li, L.L.; Hamrick, M.R.; Hamill, R.J.; Patti, J.M.; Musser, J.M.** A conserved *Streptococcus pyogenes* extracellular cysteine protease cleaves human fibronectin and degrades vitronectin. *Microb. Pathog.* 1993, *15*, 327–346.

21. **Rasmussen, M.; Bjorck, L.** Proteolysis and its regulation at the surface of *Streptococcus pyogenes*. *Mol. Microbiol.* 2002, *43*, 537–544.

22. **Nyberg, P.; Rasmussen, M.; Bjorck, L.** Alpha2-Macroglobulin-proteinase complexes protect *Streptococcus pyogenes* from killing by the antimicrobial peptide LL-37. *J. Biol. Chem.* 2004, *279*, 52820–52823.

23. **Rasmussen, M.; Muller, H.P.; Bjorck, L.** Protein GRAB of *Streptococcus pyogenes* regulates proteolysis at the bacterial surface by binding alpha2-macroglobulin. *J. Biol. Chem.* 1999, *274*, 15336–15344.

24. **Lauth, X.; von Kockritz-Blickwede, M.; McNamara, C.W.; Myskowski, S.; Zinkernagel, A.S.; Beall, B.; Ghosh, P.; Gallo, R.L.; Nizet, V.** M1 protein allows Group A streptococcal survival in phagocyte extracellular traps through cathelicidin inhibition. *J. Innate. Immun.* 2009, *1*, 202–214.

25. **Maisey, H.C.; Quach, D.; Hensler, M.E.; Liu, G.Y.; Gallo, R.L.; Nizet, V.; Doran, K.S.** A group B streptococcal pilus protein promotes phagocyte resistance and systemic virulence. *FASEB J.* 2008, *22*, 1715–1724.

26. **Frick, I.M.; Akesson, P.; Rasmussen, M.; Schmidtchen, A.; Bjorck, L.** SIC, a secreted protein of *Streptococcus pyogenes* that inactivates antibacterial peptides. *J. Biol. Chem.* 2003, *278*, 16561–16566.

27. **Fernie-King, B.A.; Seilly, D.J.; Davies, A.; Lachmann, P.J.** Streptococcal inhibitor of complement inhibits two additional components of the mucosal innate immune system: Secretory leukocyte proteinase inhibitor and lysozyme. *Infect. Immun.* 2002, *70*, 4908–4916.

28. **Jin, T.; Bokarewa, M.; Foster, T.; Mitchell, J.; Higgins, J.; Tarkowski, A.** *Staphylococcus aureus* resists human defensins by production of staphylokinase, a novel bacterial evasion mechanism. *J. Immunol.* 2004, *172*, 1169–1176.

29. **Braff, M.H.; Jones, A.L.; Skerrett, S.J.; Rubens, C.E.** *Staphylococcus aureus* exploits cathelicidin antimicrobial peptides produced during early pneumonia to promote staphylokinase-dependent fibrinolysis. *J. Infect. Dis*. 2007, *195*, 1365–1372.

30. **Diep, D.B.; Havarstein, L.S.; Nes, I.F.** Characterization of the locus responsible for the bacteriocin production in *Lactobacillus plantarum* C11. *J. Bacteriol.* 1996,*178*, 4472–4483.

31. **Diep, D.B.; Skaugen, M.; Salehian, Z.; Holo, H.; Nes, I.F.** Common mechanisms of target cell recognition and immunity for class II bacteriocins. *Proc. Natl. Acad. Sci. USA* 2007, *104*, 2384–2389.

32. **Llobet, E.; Tomas, J.M.; Bengoechea, J.A.** Capsule polysaccharide is a bacterial decoy for antimicrobial peptides. *Microbiology* 2008, *154*, 3877–3886.

33. **Vuong, C.; Kocianova, S.; Voyich, J.M.; Yao, Y.; Fischer, E.R.; DeLeo, F.R.; Otto, M.** A crucial role for exopolysaccharide modification in bacterial biofilm formation, immune evasion, and virulence. *J. Biol. Chem.* 2004, *279*, 54881–54886.

34. **Vuong, C.; Voyich, J.M.; Fischer, E.R.; Braughton, K.R.; Whitney, A.R.; DeLeo, F.R.; Otto, M.** Polysaccharide intercellular adhesin (PIA) protects *Staphylococcus epidermidis* against major components of the human innate immune system. *Cell. Microbiol.* 2004, *6*, 269–275.

35. **Tsuda, H.; Yamashita, Y.; Shibata, Y.; Nakano, Y.; Koga, T.** Genes involved in bacitracin resistance in *Streptococcus mutans*. *Antimicrob. Agents Chemother*. 2002, *46*, 3756–3764.

36. **Klein, C.; Entian, K.D.** Genes involved in self-protection against the lantibiotic subtilin produced by *Bacillus subtilis* ATCC 6633. *Appl. Environ. Microbiol.* 1994, *60*, 2793–2801.

37. **Kuipers, O.P.; Beerthuyzen, M.M.; Siezen, R.J.; de Vos, W.M.** Characterization of the nisin gene cluster nisABTCIPR of *Lactococcus lactis*. Requirement of expression of the *nisA* and *nisI* genes for development of immunity. *Eur. J. Biochem.* 1993, *216*, 281–291.

38. **Saris, P.E.; Immonen, T.; Reis, M.; Sahl, H.G.** Immunity to lantibiotics. *Antonie Van Leeuwenhoek* 1996, *69*, 151–159.

39. **Peschel, A.; Vuong, C.; Otto, M.; Gotz, F.** The D-alanine residues of *Staphylococcus aureus* teichoic acids alter the susceptibility to vancomycin and the activity of autolytic enzymes. *Antimicrob. Agents Chemother.* 2000, *44*, 2845–2847.

40. **Abachin, E.; Poyart, C.; Pellegrini, E.; Milohanic, E.; Fiedler, F.; Berche, P.; Trieu-Cuot, P.** Formation of D-alanyl-lipoteichoic acid is required for adhesion and virulence of *Listeria monocytogenes*. *Mol. Microbiol.* 2002, *43*, 1–14.

41. **Abi Khattar, Z.; Rejasse, A.; Destoumieux-Garzon, D.; Escoubas, J.M.; Sanchis, V.; Lereclus, D.; Givaudan, A.; Kallassy, M.; Nielsen-Leroux, C.; Gaudriault, S.** The dlt operon of *Bacillus cereus* is required for resistance to cationic antimicrobial peptides and for virulence in insects. *J. Bacteriol.* 2009, *191*, 7063–7073.

42. **Cox, K.H.; Ruiz-Bustos, E.; Courtney, H.S.; Dale, J.B.; Pence, M.A.; Nizet, V.; Aziz, R.K. Gerling, I; Price, S.M.; Hasty, D.L.** Inactivation of DltA modulates virulence factor expression in *Streptococcus pyogenes*. *PLoS One* 2009, *4*, e5366.

43. **Fisher, N.; Shetron-Rama, L.; Herring-Palmer, A.; Heffernan, B.; Bergman, N.; Hanna, P.** The dltABCD operon of *Bacillus anthracis* sterne is required for

virulence and resistance to peptide, enzymatic, and cellular mediators of innate immunity. *J. Bacteriol.* 2006, *188*, 1301–1309.

44. **Fittipaldi, N.; Sekizaki, T.; Takamatsu, D.; Harel, J.; Dominguez-Punaro Mde, L.; von Aulock, S.; Draing, C.; Marois, C.; Kobisch, M.; Gottschalk, M.** D-Alanylation of lipoteichoic acid contributes to the virulence of *Streptococcus suis*. *Infect. Immun.* 2008, *76*, 3587–3594.

45. **Poyart, C.; Pellegrini, E.; Marceau, M.; Baptista, M.; Jaubert, F.; Lamy, M.C.; Trieu-Cuot, P.** Attenuated virulence of *Streptococcus agalactiae* deficient in D-alanyl-lipoteichoic acid is due to an increased susceptibility to defensins and phagocytic cells. *Mol. Microbiol.* 2003, *49*, 1615–1625.

46. **Maloney, E.; Stankowska, D.; Zhang, J.; Fol, M.; Cheng, Q.J.; Lun, S.; Bishai, W.R.; Rajagopalan, M.; Chatterjee, D.; Madiraju, M.V.** The two-domain LysX protein of *Mycobacterium tuberculosis* is required for production of lysinylated phosphatidylglycerol and resistance to cationic antimicrobial peptides. *PLoS Pathog.* 2009, *5*, e1000534.

47. **Samant, S.; Hsu, F.F.; Neyfakh, A.A.; Lee, H.** The *Bacillus anthracis* protein MprF is required for synthesis of lysylphosphatidylglycerols and for resistance to cationic antimicrobial peptides. *J. Bacteriol.* 2009, *191*, 1311–1319.

48. **Thedieck, K.; Hain, T.; Mohamed, W.; Tindall, B.J.; Nimtz, M.; Chakraborty, T.; Wehland, J.; Jansch, L.** The MprF protein is required for lysinylation of phospholipids in listerial membranes and confers resistance to cationic antimicrobial peptides (CAMPs) on *Listeria monocytogenes*. *Mol. Microbiol.* 2006, *62*, 1325–1339.

49. **Peschel, A.; Jack, R.W.; Otto, M.**; Collins, L.V.; Staubitz, P.; Nicholson, G.; Kalbacher, H.; Nieuwenhuizen, W.F.; Jung, G.; Tarkowski, A.; *et al*. *Staphylococcus aureus* resistance to human defensins and evasion of neutrophil killing via the novel virulence factor MprF is based on modification of membrane lipids with l-lysine. *J. Exp. Med.* 2001, *193*, 1067–1076.

50. **Oku, Y.; Kurokawa, K.; Ichihashi, N.; Sekimizu, K.** Characterization of the *Staphylococcus aureus mprF* gene, involved in lysinylation of phosphatidylglycerol. *Microbiology* 2004, *150*, 45–51.

51. **Bera, A.; Herbert, S.; Jakob, A.; Vollmer, W.; Gotz, F.** Why are pathogenic staphylococci so lysozyme resistant? The peptidoglycan O-acetyltransferase OatA is the major determinant for lysozyme resistance of *Staphylococcus aureus*. *Mol. Microbiol.* 2005, *55*, 778–787.

52. **Bera, A.; Biswas, R.; Herbert, S.; Gotz, F.** The presence of peptidoglycan O-acetyltransferase in various staphylococcal species correlates with lysozyme resistance and pathogenicity. *Infect. Immun.* 2006, *74*, 4598–4604.

53. **Herbert, S.; Bera, A.; Nerz, C.; Kraus, D.; Peschel, A.; Goerke, C.; Meehl, M.; Cheung, A.; Gotz, F.** Molecular basis of resistance to muramidase and cationic antimicrobial peptide activity of lysozyme in staphylococci. *PLoS Pathog.* 2007, *3*, e102.

54. **Aubry, C.; Goulard, C.; Nahori, M.A.; Cayet, N.; Decalf, J.; Sachse, M.; Boneca, I.G.; Cossart, P.; Dussurget, O.** OatA, a peptidoglycan O-acetyltransferase involved in *Listeria monocytogenes* immune escape, is critical for virulence. *J. Infect. Dis.* 2011, *204*, 731–740.

55. **Vollmer, W.; Tomasz, A.** The pgdA gene encodes for a peptidoglycan N-acetylglucosamine deacetylase in *Streptococcus pneumoniae*. *J. Biol. Chem.* 2000, *275*, 20496–20501.

56. **Fittipaldi, N.; Sekizaki, T.; Takamatsu, D.; de la Cruz Dominguez-Punaro, M.; Harel, J.; Bui, N.K.; Vollmer, W.; Gottschalk, M.** Significant contribution of the pgdA gene to the virulence of *Streptococcus suis*. *Mol. Microbiol.* 2008, *70*, 1120–1135.

57. **Boneca, I.G.; Dussurget, O.; Cabanes, D.; Nahori, M.A.; Sousa, S.; Lecuit, M.; Psylinakis, E.; Bouriotis, V.; Hugot, J.P.; Giovannini, M.; *et al.*** A critical role for peptidoglycan N-deacetylation in *Listeria* evasion from the host innate immune system. *Proc. Natl. Acad. Sci. USA* 2007, *104*, 997–1002.

58. **Laaberki, M.H.; Pfeffer, J.; Clarke, A.J.; Dworkin, J.** O-Acetylation of peptidoglycan is required for proper cell separation and S-layer anchoring in *Bacillus anthracis*. *J. Biol. Chem.* 2011, *286*, 5278–5288.

59. **Raymond, J.B.; Mahapatra, S.; Crick, D.C.; Pavelka, M.S., Jr.** Identification of the namH gene, encoding the hydroxylase responsible for the N-glycolylation of the mycobacterial peptidoglycan. *J. Biol. Chem.* 2005, *280*, 326–333.

60. **Gajic, O.; Buist, G.; Kojic, M.; Topisirovic, L.; Kuipers, O.P.; Kok, J.** Novel mechanism of bacteriocin secretion and immunity carried out by lactococcal multidrug resistance proteins. *J. Biol. Chem.* 2003, *278*, 34291–34298.

61. **Kupferwasser, L.I.; Skurray, R.A.; Brown, M.H.; Firth, N.; Yeaman, M.R.; Bayer, A.S.** Plasmid-mediated resistance to thrombin-induced platelet microbicidal

protein in staphylococci: role of the qacA locus. *Antimicrob. Agents Chemother.* 1999, *43*, 2395–2399.

62. **Mandin, P.; Fsihi, H.; Dussurget, O.; Vergassola, M.; Milohanic, E.; Toledo-Arana, A.; Lasa, I.; Johansson, J.; Cossart, P.** VirR, a response regulator critical for *Listeria monocytogenes* virulence. *Mol. Microbiol.* 2005, *57*, 1367–1380.

63. **Collins, B.; Curtis, N.; Cotter, P.D.; Hill, C.; Ross, R.P.** The ABC transporter AnrAB contributes to the innate resistance of *Listeria monocytogenes* to nisin, bacitracin, and various beta-lactam antibiotics. *Antimicrob. Agents Chemother.* 2010, *54*, 4416–4423.

64. **Rietkotter, E.; Hoyer, D.; Mascher, T.** Bacitracin sensing in *Bacillus subtilis*. *Mol. Microbiol.* 2008, *68*, 768–85.

65. **Schneider, T.; Kruse, T.; Wimmer, R.; Wiedemann, I.; Sass, V.; Pag, U.; Jansen, A.; Nielsen, A.K.; Mygind, P.H.; Raventos, D.S.; *et al.*** Plectasin, a fungal defensin, targets the bacterial cell wall precursor Lipid II. *Science* 2010, *328*, 1168–1172.

66. **Staron, A.; Finkeisen, D.E.; Mascher, T.** Peptide antibiotic sensing and detoxification modules of *Bacillus subtilis*. *Antimicrob. Agents Chemother.* 2011, *55*, 515–525.

67. **Mascher, T.; Margulis, N.G.; Wang, T.; Ye, R.W.; Helmann, J.D.** Cell wall stress responses in *Bacillus subtilis*: The regulatory network of the bacitracin stimulon. *Mol. Microbiol.* 2003, *50*, 1591–604.

68. **Ohki, R.; Giyanto; Tateno, K.; Masuyama, W.; Moriya, S.; Kobayashi, K.; Ogasawara, N**. The BceRS two-component regulatory system induces expression

of the bacitracin transporter, BceAB, in *Bacillus subtilis*. *Mol. Microbiol.* 2003, *49*, 1135–1144.

69. **Kawada-Matsuo, M.; Yoshida, Y.; Zendo, T.; Nagao, J.; Oogai, Y.; Nakamura, Y.; Sonomoto, K.; Nakamura, N.; Komatsuzawa, H.** Three distinct two-component systems are involved in resistance to the class I bacteriocins, Nukacin ISK-1 and nisin A, in *Staphylococcus aureus*. *PLoS One* 2013, *8*, e69455.

70. **Becker, P.; Hakenbeck, R.; Henrich, B.** An ABC transporter of *Streptococcus pneumoniae* involved in susceptibility to vancoresmycin and bacitracin. *Antimicrob. Agents Chemother.* 2009, *53*, 2034–2041.

71. **Majchrzykiewicz, J.A.; Kuipers, O.P.; Bijlsma, J.J.** Generic and specific adaptive responses of *Streptococcus pneumoniae* to challenge with three distinct antimicrobial peptides, bacitracin, LL-37, and nisin. *Antimicrob. Agents Chemother.* 2010, *54*, 440–451.

72. **Li, M.; Cha, D.J.; Lai, Y.; Villaruz, A.E.; Sturdevant, D.E.; Otto, M.** The antimicrobial peptide-sensing system aps of *Staphylococcus aureus*. *Mol. Microbiol.* 2007, *66*, 136–147.

73. **Sass, P.; Jansen, A.; Szekat, C.; Sass, V.; Sahl, H.G.; Bierbaum, G.** The lantibiotic mersacidin is a strong inducer of the cell wall stress response of *Staphylococcus aureus*. *BMC Microbiol*. 2008, *8*, e186.

74. **Yoshida, Y.; Matsuo, M.; Oogai, Y.; Kato, F.; Nakamura, N.; Sugai, M.; Komatsuzawa, H.** Bacitracin sensing and resistance in *Staphylococcus aureus*. *FEMS Microbiol. Lett.* 2011, *320*, 33–39.

75. **Hiron, A.; Falord, M.; Valle, J.; Debarbouille, M.; Msadek, T.** Bacitracin and nisin resistance in *Staphylococcus aureus*: a novel pathway involving the BraS/BraR two-component system (SA2417/SA2418) and both the BraD/BraE and VraD/VraE ABC transporters. *Mol. Microbiol.* 2011, *81*, 602–622.

76. **Pietiainen, M.; Francois, P.; Hyyrylainen, H.L.; Tangomo, M.; Sass, V.; Sahl, H.G.; Schrenzel, J.; Kontinen, V.P.** Transcriptome analysis of the responses of *Staphylococcus aureus* to antimicrobial peptides and characterization of the roles of vraDE and vraSR in antimicrobial resistance. *BMC Genomics* 2009, *10*, 429.

77. **Meehl, M.; Herbert, S.; Gotz, F.; Cheung, A.** Interaction of the GraRS two-component system with the VraFG ABC transporter to support vancomycin-intermediate resistance in *Staphylococcus aureus*. *Antimicrob. Agents Chemother.* 2007, *51*, 2679–2689.

78. **Falord, M.; Karimova, G.; Hiron, A.; Msadek, T.** GraXSR proteins interact with the VraFG ABC transporter to form a five-component system required for cationic antimicrobial peptide sensing and resistance in *Staphylococcus aureus*. *Antimicrob. Agents Chemother.* 2012, *56*, 1047–1058.

79. **Li, M.; Lai, Y.; Villaruz, A.E.; Cha, D.J.; Sturdevant, D.E.; Otto, M.** Gram-positive three-component antimicrobial peptide-sensing system. *Proc. Natl. Acad. Sci. USA* 2007, *104*, 9469–9474.

80. **Kramer, N.E.; van Hijum, S.A.; Knol, J.; Kok, J.; Kuipers, O.P.** Transcriptome analysis reveals mechanisms by which *Lactococcus lactis* acquires nisin resistance. *Antimicrob. Agents Chemother.* 2006, *50*, 1753–1761.

81. **Podlesek, Z.; Comino, A.; Herzog-Velikonja, B.; Zgur-Bertok, D.; Komel, R.; Grabnar, M.** *Bacillus licheniformis* bacitracin-resistance ABC transporter: Relationship to mammalian multidrug resistance. *Mol. Microbiol.* 1995, *16*, 969–976.

82. **Manson, J.M.; Keis, S.; Smith, J.M.; Cook, G.M.** Acquired bacitracin resistance in *Enterococcus faecalis* is mediated by an ABC transporter and a novel regulatory protein, BcrR. *Antimicrob. Agents Chemother.* 2004, *48*, 3743–3748.

83. **Matos, R.; Pinto, V.V.; Ruivo, M.; Lopes Mde, F.** Study on the dissemination of the bcrABDR cluster in *Enterococcus* spp. reveals that the BcrAB transporter is sufficient to confer high-level bacitracin resistance. *Int. J. Antimicrob. Agents* 2009, *34*, 142–147.

84. **Diaz, M.; Valdivia, E.; Martinez-Bueno, M.; Fernandez, M.; Soler-Gonzalez, A.S.; Ramirez-Rodrigo, H.; Maqueda, M.** Characterization of a new operon, as-48EFGH, from the as-48 gene cluster involved in immunity to enterocin AS-48. *Appl. Environ. Microbiol.* 2003, *69*, 1229–1236.

85. **McBride, S.M.; Sonenshein, A.L.** Identification of a genetic locus responsible for antimicrobial peptide resistance in *Clostridium difficile*. *Infect. Immun.* 2011, *79*, 167–176.

86. **Suarez, J.M.; Edwards, A.N.; McBride, S.M.** The *Clostridium difficile* cpr locus is regulated by a non-contiguous two-component system in response to type A and B lantibiotics. *J. Bacteriol.* 2013, *195*, 2621–2631.

87. **Otto, M.; Peschel, A.; Gotz, F.** Producer self-protection against the lantibiotic epidermin by the ABC transporter EpiFEG of *Staphylococcus epidermidis* Tu3298. *FEMS Microbiol. Lett.* 1998, *166*, 203–211.

88. **Draper, L.A.; Grainger, K.; Deegan, L.H.; Cotter, P.D.; Hill, C.; Ross, R.P.** Cross-immunity and immune mimicry as mechanisms of resistance to the lantibiotic lacticin 3147. *Mol. Microbiol.* 2009, *71*, 1043–1054.

89. **McAuliffe, O.; O'Keeffe, T.; Hill, C.; Ross, R.P.** Regulation of immunity to the two-component lantibiotic, lacticin 3147, by the transcriptional repressor LtnR. *Mol. Microbiol.* 2001, *39*, 982–993.

90. **Papadelli, M.; Karsioti, A.; Anastasiou, R.; Georgalaki, M.; Tsakalidou, E.** Characterization of the gene cluster involved in the biosynthesis of macedocin, the lantibiotic produced by *Streptococcus macedonicus*. *FEMS Microbiol. Lett.* 2007, *272*, 75–82.

91. **Altena, K.; Guder, A.; Cramer, C.; Bierbaum, G.** Biosynthesis of the lantibiotic mersacidin: Organization of a type B lantibiotic gene cluster. *Appl. Environ. Microbiol.* 2000, *66*, 2565–2571.

92. **Guder, A.; Schmitter, T.; Wiedemann, I.; Sahl, H.G.; Bierbaum, G.** Role of the single regulator MrsR1 and the two-component system MrsR2/K2 in the regulation of mersacidin production and immunity. *Appl. Environ. Microbiol.* 2002, *68*, 106–113.

93. **Chen, P.; Qi, F.; Novak, J.; Caufield, P.W.** The specific genes for lantibiotic mutacin II biosynthesis in *Streptococcus mutans* T8 are clustered and can be transferred en bloc. *Appl. Environ. Microbiol.* 1999, *65*, 1356–1360.

94. **Siegers, K.; Entian, K.D.** Genes involved in immunity to the lantibiotic nisin produced by *Lactococcus lactis* 6F3. *Appl. Environ. Microbiol.* 1995, *61*, 1082–1089.

95. **Aso, Y.; Nagao, J.; Koga, H.; Okuda, K.; Kanemasa, Y.; Sashihara, T.; Nakayama, J.; Sonomoto, K.** Heterologous expression and functional analysis of the gene cluster for the biosynthesis of and immunity to the lantibiotic, nukacin ISK-1. *J. Biosci. Bioeng.* 2004, *98*, 429–436.

96. **Aso, Y.; Sashihara, T.; Nagao, J.; Kanemasa, Y.; Koga, H.; Hashimoto, T.; Higuchi, T.; Adachi, A.; Nomiyama, H.; Ishizaki, A.; *et al.*** Characterization of a gene cluster of *Staphylococcus warneri* ISK-1 encoding the biosynthesis of and immunity to the lantibiotic, nukacin ISK-1. *Biosci. Biotechnol. Biochem.* 2004, *68*, 1663–1671.

97. **Hyink, O.; Wescombe, P.A.; Upton, M.; Ragland, N.; Burton, J.P.; Tagg, J.R.** Salivaricin A2 and the novel lantibiotic salivaricin B are encoded at adjacent loci on a 190-kilobase transmissible megaplasmid in the oral probiotic strain *Streptococcus salivarius* K12. *Appl. Environ. Microbiol.* 2007, *73*, 1107–1113.

98. **McLaughlin, R.E.; Ferretti, J.J.; Hynes, W.L.** Nucleotide sequence of the streptococcin A-FF22 lantibiotic regulon: model for production of the lantibiotic SA-FF22 by strains of *Streptococcus pyogenes*. *FEMS Microbiol. Lett.* 1999, *175*, 171–177.

99. **Biswas, S.; Biswas, I.** SmbFT, a putative ABC transporter complex, confers protection against the lantibiotic Smb in Streptococci. *J. Bacteriol.* 2013, *195*, 5592–5601.

100. **Stein, T.; Heinzmann, S.; Dusterhus, S.; Borchert, S.; Entian, K.D.** Expression and functional analysis of the subtilin immunity genes spaIFEG in the subtilin-sensitive host *Bacillus subtilis* MO1099. *J. Bacteriol.* 2005, *187*, 822–828.

101. **Rabijns, A.; de Bondt, H.L.; de Ranter, C.** Three-dimensional structure of staphylokinase, a plasminogen activator with therapeutic potential. *Nat. Struct. Biol.* 1997, *4*, 357–360.

102. **Akesson, P.; Sjoholm, A.G.; Bjorck, L.** Protein SIC, a novel extracellular protein *of Streptococcus pyogenes* interfering with complement function. *J. Biol. Chem.* 1996, *271*, 1081–1088.

103. **Pence, M.A.; Rooijakkers, S.H.; Cogen, A.L.; Cole, J.N.; Hollands, A.; Gallo, R.L.; Nizet, V.** Streptococcal inhibitor of complement promotes innate immune resistance phenotypes of invasive M1T1 group A *Streptococcus*. *J. Innate Immun.* 2010, *2*, 587–595.

104. **Buckley, A.M.; Spencer, J.; Candlish, D.; Irvine, J.J.; Douce, G.R.** Infection of hamsters with the UK *Clostridium difficile* ribotype 027 outbreak strain R20291. *J. Med. Microbiol.* 2011, *60*, 1174–1180.

105. **Xia, G.; Wolz, C.** Phages of *Staphylococcus aureus* and their impact on host evolution. *Infect. Genet. Evol.* 2014, *21*, 593–601.

106. **Van Wamel, W.J.; Rooijakkers, S.H.; Ruyken, M.; van Kessel, K.P.; van Strijp, J.A.** The innate immune modulators staphylococcal complement inhibitor and chemotaxis inhibitory protein of *Staphylococcus aureus* are located on beta-hemolysin-converting bacteriophages. *J. Bacteriol*. 2006, *188*:1310–1315.

107. **Coleman, D.C.; Sullivan, D.J.; Russell, R.J.; Arbuthnott, J.P.; Carey, B.F.; Pomeroy, H.M.** *Staphylococcus aureus* bacteriophages mediating the simultaneous lysogenic conversion of beta-lysin, staphylokinase and enterotoxin A: Molecular mechanism of triple conversion. *J. Gen. Microbiol.* 1989, *135*, 1679–1697.

108. **Jin, T.; Bokarewa, M.; McIntyre, L.;Tarkowski, A.; Corey, G.R.; Reller, L.B.; Fowler, V.G., Jr.** Fatal outcome of bacteraemic patients caused by infection with staphylokinase-deficient *Staphylococcus aureus* strains. *J. Med. Microbiol.* 2003, *52*, 919–923.

109. **Bisno, A.L.; Brito, M.O.; Collins, C.M.** Molecular basis of group A streptococcal virulence. *Lancet Infect. Dis.* 2003, *3*, 191–200.

110. **Madzivhandila, M.; Adrian, P.V.; Cutland, C.L.; Kuwanda, L.; Madhi, S.A.** Distribution of pilus islands of group B *streptococcus* associated with maternal colonization and invasive disease in South Africa. *J. Med. Microbiol.* 2013, *62*, 249–253.

111. **Maisey, H.C.; Hensler, M.; Nizet, V.; Doran, K.S.** Group B streptococcal pilus proteins contribute to adherence to and invasion of brain microvascular endothelial cells. *J. Bacteriol*. 2007, *189*, 1464–1467.

112. **Chatterjee, C.; Paul, M.; Xie, L.; van der Donk, W.A.** Biosynthesis and mode of action of lantibiotics. *Chem. Rev.* 2005, *105*, 633–684.

113. **Alkhatib, Z.; Abts, A.; Mavaro, A.; Schmitt, L.; Smits, S.H.** Lantibiotics: How do producers become self-protected? *J. Biotechnol.* 2012, *159*, 145–154.

114. **Halami, P.M.; Stein, T.; Chandrashekar, A.; Entian, K.D.** Maturation and processing of SpaI, the lipoprotein involved in subtilin immunity in *Bacillus subtilis* ATCC 6633. *Microbiol. Res.* 2010, *165*, 183–189.

115. **Hoffmann, A.; Schneider, T.; Pag, U.; Sahl, H.G.** Localization and functional analysis of PepI, the immunity peptide of Pep5-producing *Staphylococcus epidermidis* strain 5. *Appl. Environ. Microbiol.* 2004, *70*, 3263–3271.

116. **Christ, N.A.; Bochmann, S.; Gottstein, D.; Duchardt-Ferner, E.; Hellmich, U.A.; Dusterhus, S.; Kotter, P.; Guntert, P.; Entian, K.D. Wohnert, J.** The First structure of a lantibiotic immunity protein, SpaI from *Bacillus subtilis*, reveals a novel fold. *J. Biol. Chem.* 2012, *287*, 35286–35298.

117. **Qiao, M.; Immonen, T.; Koponen, O.; Saris, P.E.** The cellular location and effect on nisin immunity of the NisI protein from *Lactococcus lactis* N8 expressed in *Escherichia coli* and *L. lactis*. *FEMS Microbiol. Lett.* 1995, *131*, 75–80.

118. **Takala, T.M.; Saris, P.E.** C terminus of NisI provides specificity to nisin. *Microbiology* 2006, *152*, 3543–3549.

119. **Reis, M.; Eschbach-Bludau, M.; Iglesias-Wind, M.I.; Kupke, T.; Sahl, H.G.** Producer immunity towards the lantibiotic Pep5: Identification of the immunity gene pepI and localization and functional analysis of its gene product. *Appl. Environ. Microbiol.* 1994, *60*, 2876–2883.

120. **Skaugen, M.; Abildgaard, C.I.; Nes, I.F.** Organization and expression of a gene cluster involved in the biosynthesis of the lantibiotic lactocin S. *Mol. Gen. Genet.* 1997, *253*, 674–686.

121. **Heidrich, C.; Pag, U.; Josten, M.; Metzger, J.; Jack, R.W.; Bierbaum, G.; Jung, G.; Sahl, H.G.** Isolation, characterization, and heterologous expression of the novel lantibiotic epicidin 280 and analysis of its biosynthetic gene cluster. *Appl. Environ. Microbiol.* 1998, *64*, 3140–3146.

122. **Twomey, D.; Ross, R.P.; Ryan, M.; Meaney, B.; Hill, C.** Lantibiotics produced by lactic acid bacteria: structure, function and applications. *Antonie Van Leeuwenhoek* 2002, *82*, 165–185.

123. **Peterson, P.K.; Wilkinson, B.J.; Kim, Y.; Schmeling, D.; Quie, P.G.** Influence of encapsulation on staphylococcal opsonization and phagocytosis by human polymorphonuclear leukocytes. *Infect. Immun.* 1978, *19*, 943–949.

124. **Nelson, A.L.; Roche, A.M.; Gould, J.M.; Chim, K.; Ratner, A.J.; Weiser, J.N.** Capsule enhances pneumococcal colonization by limiting mucus-mediated clearance. *Infect. Immun.* 2007, *75*, 83–90.

125. **Ashbaugh, C.D.; Warren, H.B.; Carey, V.J.; Wessels, M.R.** Molecular analysis of the role of the group A streptococcal cysteine protease, hyaluronic acid capsule, and M protein in a murine model of human invasive soft-tissue infection. *J. Clin. Invest.* 1998, *102*, 550–560.

126. **Kogan, G.; Uhrin, D.; Brisson, J.R.; Paoletti, L.C.; Blodgett, A.E.; Kasper, D.L.; Jennings, H.J.** Structural and immunochemical characterization of the type VIII group B *Streptococcus* capsular polysaccharide. *J. Biol. Chem.* 1996, *271*, 8786–8790.

127. **Bentley, S.D.; Aanensen, D.M.; Mavroidi, A.; Saunders, D.; Rabbinowitsch, E.; Collins, M.; Donohoe, K.; Harris, D.; Murphy, L.; Quail, M.A.; *et al.***

Genetic analysis of the capsular biosynthetic locus from all 90 pneumococcal serotypes. *PLoS Genet.* 2006, *2*, e31.

128. **Candela, T.; Fouet, A.** *Bacillus anthracis* CapD, belonging to the gamma-glutamyltranspeptidase family, is required for the covalent anchoring of capsule to peptidoglycan. *Mol. Microbiol.* 2005, *57*, 717–726.

129. **Deng, L; Kasper, D.L.; Krick, T.P.; Wessels, M.R.** Characterization of the linkage between the type III capsular polysaccharide and the bacterial cell wall of group B *Streptococcus*. *J. Biol. Chem.* 2000, *275*, 7497–7504.

130. **Mack, D.; Fischer, W.; Krokotsch, A.; Leopold, K.; Hartmann, R.; Egge, H.; Laufs, R.** The intercellular adhesin involved in biofilm accumulation of *Staphylococcus epidermidis* is a linear beta-1,6-linked glucosaminoglycan: purification and structural analysis. *J. Bacteriol.* 1996, *178*, 175–83.

131. **Campos, M.A.; Vargas, M.A.; Regueiro, V.; Llompart, C.M.; Alberti, S.; Bengoechea, J.A.** Capsule polysaccharide mediates bacterial resistance to antimicrobial peptides. *Infect. Immun.* 2004, *72*, 7107–7114.

132. **Rupp, M.E.; Fey, P.D.; Heilmann, C.; Gotz, F.** Characterization of the importance of *Staphylococcus epidermidis* autolysin and polysaccharide intercellular adhesin in the pathogenesis of intravascular catheter-associated infection in a rat model. *J. Infect. Dis.* 2001, *183*, 1038–1042.

133. **Rupp, M.E.; Ulphani, J.S.; Fey, P.D.; Bartscht, K.; Mack, D.** Characterization of the importance of polysaccharide intercellular adhesin/hemagglutinin of *Staphylococcus epidermidis* in the pathogenesis of biomaterial-based infection in a mouse foreign body infection model. *Infect. Immun.* 1999, *67*, 2627–2632.

134. **Beiter, K.; Wartha, F.; Hurwitz, R.; Normark, S.; Zychlinsky, A.; Henriques-Normark, B.** The capsule sensitizes *Streptococcus pneumoniae* to alpha-defensins human neutrophil proteins 1 to 3. *Infect. Immun.* 2008, *76*, 3710–3716.

135. **Wartha, F.; Beiter, K.; Albiger, B.; Fernebro, J.; Zychlinsky, A.; Normark, S.; Henriques-Normark, B.** Capsule and D-alanylated lipoteichoic acids protect *Streptococcus pneumoniae* against neutrophil extracellular traps. *Cell. Microbiol.* 2007, *9*, 1162–1171.

136. **Jansen, A.; Szekat, C.; Schroder, W.; Wolz, C.; Goerke, C.; Lee, J.C.; Turck, M.; Bierbaum, G.** Production of capsular polysaccharide does not influence *Staphylococcus aureus* vancomycin susceptibility. *BMC Microbiol*. 2013, *13*, e65.

137. **Boman, H.G.** Peptide antibiotics and their role in innate immunity. *Annu. Rev. Immunol.* 1995, *13*, 61–92.

138. **Powers, J.P.; Hancock, R.E.** The relationship between peptide structure and antibacterial activity. *Peptides* 2003, *24*, 1681–1691.

139. **Zasloff, M.** Antimicrobial peptides of multicellular organisms. *Nature* 2002, *415*, 389–395.

140. **Nizet, V.** Antimicrobial peptide resistance mechanisms of human bacterial pathogens. *Curr. Issues. Mol. Biol.* 2006, *8*, 11–26.

141. **Peschel, A.** How do bacteria resist human antimicrobial peptides? *Trends Microbiol.* 2002, *10*, 179–186.

142. **Hancock, R.E.; Rozek, A.** Role of membranes in the activities of antimicrobial cationic peptides. *FEMS Microbiol. Lett.* 2002, *206*, 143–149.

143. **Weidenmaier, C.; Peschel, A.** Teichoic acids and related cell-wall glycopolymers in Gram-positive physiology and host interactions. *Nat. Rev. Microbiol.* 2008, *6*, 276–287.

144. **Goldfine, H.** Bacterial membranes and lipid packing theory. *J. Lipid. Res.* 1984, *25*, 1501–1507.

145. **Wiese, A.; Munstermann, M.; Gutsmann, T.; Lindner, B.; Kawahara, K.; Zahringer, U.; Seydel, U.** Molecular mechanisms of polymyxin B-membrane interactions: direct correlation between surface charge density and self-promoted transport. *J. Membr. Biol.* 1998, *162*, 127–138.

146. **Ernst, C.M.; Peschel, A.** Broad-spectrum antimicrobial peptide resistance by MprF-mediated aminoacylation and flipping of phospholipids. *Mol. Microbiol.* 2011, *80*, 290–299.

147. **Ernst, C.M.; Staubitz, P.; Mishra, N.N.; Yang, S.J.; Hornig, G.; Kalbacher, H.; Bayer, A.S.; Kraus, D.; Peschel, A.** The bacterial defensin resistance protein MprF consists of separable domains for lipid lysinylation and antimicrobial peptide repulsion. *PLoS Pathog.* 2009, *5*, e1000660.

148. **Kristian, S.A.; Durr, M.; van Strijp, J.A.; Neumeister, B.; Peschel, A.** MprF-mediated lysinylation of phospholipids in *Staphylococcus aureus* leads to protection against oxygen-independent neutrophil killing. *Infect. Immun.* 2003, *71*, 546–549.

149. **Bao, Y.; Sakinc, T.; Laverde, D.; Wobser, D.; Benachour, A.; Theilacker, C.; Hartke, A.; Huebner, J.** Role of mprF1 and mprF2 in the pathogenicity of *Enterococcus faecalis*. *PLoS One* 2012, *7*, e38458.

150. **Hachmann, A.B.; Angert, E.R.; Helmann, J.D.** Genetic analysis of factors affecting susceptibility of *Bacillus subtilis* to daptomycin. *Antimicrob. Agents Chemother*. 2009, *53*, 1598–1609.

151. **Maloney, E.; Lun, S.; Stankowska, D.; Guo, H.; Rajagoapalan, M.; Bishai, W.R.; Madiraju, M.V.** Alterations in phospholipid catabolism in *Mycobacterium tuberculosis* lysX mutant. *Front. Microbiol.* 2011, *2*, e19.

152. **Weidenmaier, C.; Peschel, A.; Kempf, V.A.; Lucindo, N.; Yeaman, M.R.; Bayer, A.S.** DltABCD- and MprF-mediated cell envelope modifications of *Staphylococcus aureus* confer resistance to platelet microbicidal proteins and contribute to virulence in a rabbit endocarditis model. *Infect. Immun.* 2005, *73*, 80338038.

153. **Mukhopadhyay, K.; Whitmire, W.; Xiong, Y.Q.; Molden, J.; Jones, T.; Peschel, A.; Staubitz, P.; Adler-Moore, J.; McNamara, P.J.; Proctor, R.A.; *et al*.** *In vitro* susceptibility of *Staphylococcus aureus* to thrombin-induced platelet microbicidal protein-1 (tPMP-1) is influenced by cell membrane phospholipid composition and asymmetry. *Microbiology* 2007, *153*, 1187–1197.

154. **Ruzin, A.; Severin, A.; Moghazeh, S.L.; Etienne, J.; Bradford, P.A.; Projan, S.J.; Shlaes, D.M.** Inactivation of mprF affects vancomycin susceptibility in *Staphylococcus aureus*. *Biochim. Biophys. Acta* 2003, *1621*, 117–121.

155. **Nishi, H.; Komatsuzawa, H.; Fujiwara, T.; McCallum, N.; Sugai, M.** Reduced content of lysyl-phosphatidylglycerol in the cytoplasmic membrane affects susceptibility to moenomycin, as well as vancomycin, gentamicin, and

antimicrobial peptides, in *Staphylococcus aureus*. *Antimicrob. Agents Chemother.* 2004, *48*, 4800–4807.

156. **Jones, T.; Yeaman, M.R.; Sakoulas, G.; Yang, S.J.; Proctor, R.A.; Sahl, H.G.; Schrenzel, J.; Xiong, Y.Q.; Bayer, A.S.** Failures in clinical treatment of *Staphylococcus aureus* infection with daptomycin are associated with alterations in surface charge, membrane phospholipid asymmetry, and drug binding. *Antimicrob. Agents Chemother.* 2008, *52*, 269–278.

157. **Friedman, L.; Alder, J.D.; Silverman, J.A.** Genetic changes that correlate with reduced susceptibility to daptomycin in *Staphylococcus aureus*. *Antimicrob. Agents Chemother.* 2006, *50*, 2137–2145.

158. **Yang, S.J.; Mishra, N.N.; Rubio, A.; Bayer, A.S.** Causal role of single nucleotide polymorphisms within the mprF gene of *Staphylococcus aureus* in daptomycin resistance. *Antimicrob. Agents Chemother.* 2013, *57*, 5658–5664.

159. **Salzberg, L.I.; Helmann, J.D.** Phenotypic and transcriptomic characterization of *Bacillus subtilis* mutants with grossly altered membrane composition. *J. Bacteriol.* 2008, *190*, 7797–7807.

160. **Roy, H.; Ibba, M.** Broad range amino acid specificity of RNA-dependent lipid remodeling by multiple peptide resistance factors. *J. Biol. Chem.* 2009, *284*, 29677–29683.

161. **Mishra, N.N.; Yang, S.J.; Chen, L.; Muller, C.; Saleh-Mghir, A.; Kuhn, S.; Peschel, A.; Yeaman, M.R.; Nast, C.C.; Kreiswirth, B.N.; *et al.*** Emergence of daptomycin resistance in daptomycin-naive rabbits with methicillin-resistant *Staphylococcus aureus* prosthetic joint infection is associated with resistance to

host defense cationic peptides and mprF polymorphisms. *PLoS One* 2013, *8*, e71151.

162. **Slavetinsky, C.J.; Peschel, A.; Ernst, C.M.** Alanyl-phosphatidylglycerol and lysyl-phosphatidylglycerol are translocated by the same MprF flippases and have similar capacities to protect against the antibiotic daptomycin in *Staphylococcus aureus*. *Antimicrob. Agents Chemother.* 2012, *56*, 3492–3497.

163. **McBride, S.M.; Sonenshein, A.L.** The dlt operon confers resistance to cationic antimicrobial peptides in *Clostridium difficile*. *Microbiology* 2011, *157*, 1457–1465.

164. **Walter, J.; Loach, D.M.; Alqumber, M.; Rockel, C.; Hermann, C.; Pfitzenmaier, M.; Tannock, G.W.** D-alanyl ester depletion of teichoic acids in *Lactobacillus reuteri* 100-23 results in impaired colonization of the mouse gastrointestinal tract. *Environ. Microbiol.* 2007, *9*, 1750–1760.

165. **Koprivnjak, T.; Mlakar, V.; Swanson, L.; Fournier, B.; Peschel, A.; Weiss, J.P.** Cation-induced transcriptional regulation of the dlt operon of *Staphylococcus aureus*. *J. Bacteriol.* 2006, *188*, 3622–3630.

166. **Le Jeune, A.; Torelli, R.; Sanguinetti, M.; Giard, J.C.; Hartke, A.; Auffray, Y.; Benachour, A.** The extracytoplasmic function sigma factor SigV plays a key role in the original model of lysozyme resistance and virulence of *Enterococcus faecalis*. *PLoS One* 2010, *5*, e9658.

167. **Neuhaus, F.C.; Heaton, M.P.; Debabov, D.V.; Zhang, Q.** The dlt operon in the biosynthesis of D-alanyl-lipoteichoic acid in *Lactobacillus casei*. *Microb. Drug Resist.* 1996, *2*, 77–84.

168. **Perego, M.; Glaser, P.; Minutello, A.; Strauch, M.A.; Leopold, K.; Fischer, W.** Incorporation of D-alanine into lipoteichoic acid and wall teichoic acid in *Bacillus subtilis*. Identification of genes and regulation. *J. Biol. Chem.* 1995, *270*, 15598–15606.

169. **Neuhaus, F.C.; Baddiley, J.** A continuum of anionic charge: Structures and functions of D-alanyl-teichoic acids in gram-positive bacteria. *Microbiol. Mol. Biol. Rev.* 2003, *67*, 686–723.

170. **Yang, S.J.; Kreiswirth, B.N.; Sakoulas, G.; Yeaman, M.R.; Xiong, Y.Q.; Sawa, A.; Bayer, A.S.** Enhanced expression of dltABCD is associated with the development of daptomycin nonsusceptibility in a clinical endocarditis isolate of *Staphylococcus aureus*. *J. Infect. Dis.* 2009, *200*, 1916–1920.

171. **Guariglia-Oropeza, V.; Helmann, J.D.** *Bacillus subtilis* sigma(V) confers lysozyme resistance by activation of two cell wall modification pathways, peptidoglycan O-acetylation and D-alanylation of teichoic acids. *J. Bacteriol*. 2011, *193*, 6223–6232.

172. **Jann, N.J.; Schmaler, M.; Kristian, S.A.; Radek, K.A.; Gallo, R.L.; Nizet, V.; Peschelm A.; Landmann, R.** Neutrophil antimicrobial defense against *Staphylococcus aureus* is mediated by phagolysosomal but not extracellular trap-associated cathelicidin. *J. Leukoc. Biol.* 2009, *86*, 1159–1169.

173. **Saar-Dover, R.; Bitler, A.; Nezer, R.; Shmuel-Galia, L.; Firon, A.; Shimoni, E.; Trieu-Cuot, P.; Shai, Y.** D-Alanylation of lipoteichoic acids confers resistance to cationic peptides in group B *streptococcus* by increasing the cell wall density. *PLoS Pathog*. 2012, *8*, e1002891.

174. **Kristian, S.A.; Lauth, X.; Nizet, V.; Goetz, F.; Neumeister, B.; Peschel, A.; Landmann, R.** Alanylation of teichoic acids protects *Staphylococcus aureus* against Toll-like receptor 2-dependent host defense in a mouse tissue cage infection model. *J. Infect. Dis.* 2003, *188*, 414–423.

175. **Collins, L.V.; Kristian, S.A.; Weidenmaier, C.; Faigle, M.; van Kessel, K.P.; van Strijp, J.A.; Gotz, F.; Neumeister, B.; Peschel, A.** *Staphylococcus aureus* strains lacking D-alanine modifications of teichoic acids are highly susceptible to human neutrophil killing and are virulence attenuated in mice. *J. Infect. Dis.* 2002, *186*, 214–219.

176. **Meyer, K.; Thompson, R.; Palmer, J.W.; Khorazo, D.** The nature of lysozyme action. *Science* 1934, *79*, 61.

177. **Meyer, K.; Palmer, J.W.; Thompson, R.; Khorazo, D.** On the mechanism of lysozyme action. *J. Biol. Chem.* 1936, *113*, 479–486.

178. **Chipman, D.M.; Sharon, N.** Mechanism of lysozyme action. *Science* 1969, *165*, 454–65.

179. **Nash, J.A.; Ballard, T.N.; Weaver, T.E.; Akinbi, H.T.** The peptidoglycan-degrading property of lysozyme is not required for bactericidal activity *in vivo*. *J. Immunol.* 2006, *177*, 519–526.

180. **Hebert, L.; Courtin, P.; Torelli, R.; Sanguinetti, M.; Chapot-Chartier, M.P.; Auffray, Y.; Benachour, A.** *Enterococcus faecalis* constitutes an unusual bacterial model in lysozyme resistance. *Infect. Immun.* 2007, *75*, 5390–5398.

181. **Amano, K.; Araki, Y.; Ito, E.** Effect of N-acyl substitution at glucosamine residues on lysozyme-catalyzed hydrolysis of cell-wall peptidoglycan and its oligosaccharides. *Eur. J. Biochem.* 1980, *107*, 547–553.

182. **Amano, K.; Hayashi, H.; Araki, Y.; Ito, E.** The action of lysozyme on peptidoglycan with N-unsubstituted glucosamine residues. Isolation of glycan fragments and their susceptibility to lysozyme. *Eur. J. Biochem.* 1977, *76*, 299–307.

183. **Psylinakis, E.; Boneca, I.G.; Mavromatis, K.; Deli, A.; Hayhurst, E.; Foster, S.J.; Varum, K.M.; Bouriotis, V.** Peptidoglycan N-acetylglucosamine deacetylases from *Bacillus cereus*, highly conserved proteins in *Bacillus anthracis*. *J. Biol. Chem.* 2005, *280*, 30856–30863.

184. **Blair, D.E.; Schuttelkopf, A.W.; MacRae, J.I.; van Aalten, D.M.** Structure and metal-dependent mechanism of peptidoglycan deacetylase, a streptococcal virulence factor. *Proc. Natl. Acad. Sci. USA* 2005, *102*, 15429–15434.

185. **Vollmer, W.; Tomasz, A.** Peptidoglycan N-acetylglucosamine deacetylase, a putative virulence factor in *Streptococcus pneumoniae*. *Infect. Immun.* 2002, *70*, 7176–7178.

186. **Benachour, A.; Ladjouzi, R.; le Jeune, A.; Hebert, L.; Thorpe, S.; Courtin, P.; Chapot-Chartier, M.P.; Prajsnar, T.K.; Foster, S.J.; Mesnage, S.** The lysozyme-induced peptidoglycan N-acetylglucosamine deacetylase PgdA (EF1843) is required for *Enterococcus faecalis* virulence. *J. Bacteriol.* 2012, *194*, 6066–6073.

187. **Rae, C.S.; Geissler, A.; Adamson, P.C.; Portnoy, D.A.** Mutations of the *Listeria monocytogenes* peptidoglycan N-deacetylase and O-acetylase result in enhanced

lysozyme sensitivity, bacteriolysis, and hyperinduction of innate immune pathways. *Infect. Immun.* 2011, *79*, 3596–3606.

188. **Crisostomo, M.I.; Vollmer, W.; Kharat, A.S.; Inhulsen, S.; Gehre, F.; Buckenmaier, S.; Tomasz, A.** Attenuation of penicillin resistance in a peptidoglycan O-acetyl transferase mutant of *Streptococcus pneumoniae*. *Mol. Microbiol.* 2006, *61*, 1497–1509.

189. **Bera, A.; Biswas, R.; Herbert, S.; Kulauzovic, E.; Weidenmaier, C.; Peschel, A.; Gotz, F.** Influence of wall teichoic acid on lysozyme resistance in *Staphylococcus aureus*. *J. Bacteriol.* 2007, *189*, 280–283.

190. **Davis, K.M.; Akinbi, H.T.; Standish, A.J.; Weiser, J.N.** Resistance to mucosal lysozyme compensates for the fitness deficit of peptidoglycan modifications by *Streptococcus pneumoniae*. *PLoS Pathog.* 2008, *4*, e1000241.

191. **Veiga, P.; Bulbarela-Sampieri, C.; Furlan, S.; Maisons, A.; Chapot-Chartier, M.P.; Erkelenz, M.; Mervelet, P.; Noirot, P.; Frees, D.; Kuipers, O.P.; *et al*.** SpxB regulates O-acetylation-dependent resistance of *Lactococcus lactis* peptidoglycan to hydrolysis. *J. Biol. Chem.* 2007, *282*, 19342–19354.

192. **Shimada, T.; Park, B.G.; Wolf, A.J.; Brikos, C.; Goodridge, H.S.; Becker, C.A.; Reyes, C.N.; Miao, E.A.; Aderem, A.; Gotz, F.; *et al*.** *Staphylococcus aureus* evades lysozyme-based peptidoglycan digestion that links phagocytosis, inflammasome activation, and IL-1beta secretion. *Cell Host Microbe* 2010, *7*, 38–49.

193. **Brennan, P.J.; Nikaido, H.** The envelope of mycobacteria. *Annu. Rev. Biochem.* 1995, *64*, 29–63.

194. **Mazzotta, A.S.; Montville, T.J.** Nisin induces changes in membrane fatty acid composition of *Listeria monocytogenes* nisin-resistant strains at 10 degrees C and 30 degrees C. *J. Appl. Microbiol.* 1997, *82*, 32–38.

195. **Verheul, A.; Russell, N.J.; van't Hof, R.; Rombouts, F.M.; Abee, T.** Modifications of membrane phospholipid composition in nisin-resistant *Listeria monocytogenes* Scott A. *Appl. Environ. Microbiol.* 1997, *63*, 3451–3457.

196. **Ming, X.T.; Daeschel, M.A.** Nisin resistance of foodborne bacteria and the specific resistance responses of *Listeria monocytogenes* Scott A. *J. Food Protect.* 1993, *56*, 944–948

197. **Crandall, A.D.; Montville, T.J.** Nisin resistance in *Listeria monocytogenes* ATCC 700302 is a complex phenotype. *Appl. Environ. Microbiol.* 1998, *64*, 231–237.

198. **Mishra, N.N.; McKinnell, J.; Yeaman, M.R.; Rubio, A.; Nast, C.C.; Chen, L.; Kreiswirth, B.N.; Bayer, A.S.** *In vitro* cross-resistance to daptomycin and host defense cationic antimicrobial peptides in clinical methicillin-resistant *Staphylococcus aureus* isolates. *Antimicrob. Agents Chemother.* 2011, *55*, 4012–4018.

199. **Mishra, N.N.; Liu, G.Y.; Yeaman, M.R.; Nast, C.C.; Proctor, R.A.; McKinnell, J.; Bayer, A.S.** Carotenoid-related alteration of cell membrane fluidity impacts *Staphylococcus aureus* susceptibility to host defense peptides. *Antimicrob. Agents Chemother*. 2011, *55*, 526–531.

200. **Mishra, N.N.; Rubio, A.; Nast, C.C.; Bayer, A.S.** Differential adaptations of methicillin-resistant *Staphylococcus aureus* to serial *in vitro* passage in daptomycin:

Evolution of daptomycin resistance and role of membrane carotenoid content and fluidity. *Int. J. Microbiol.* 2012, *2012*, e683450.

201. **Britton, G.** Structure and properties of carotenoids in relation to function. *FASEB J.* 1995, *9*, 1551–1558.

202. **Pelz, A.; Wieland, K.P.; Putzbach, K.; Hentschel, P.; Albert, K.; Gotz, F.** Structure and biosynthesis of staphyloxanthin from *Staphylococcus aureus*. *J. Biol. Chem.* 2005, *280*, 32493–32498.

203. **Katzif, S.; Lee, E.H.; Law, A.B.; Tzeng, Y.L.; Shafer, W.M.** CspA regulates pigment production in *Staphylococcus aureus* through a SigB-dependent mechanism. *J. Bacteriol.* 2005, *187*, 8181–8184.

204. **Subczynski, W.K.; Wisniewska, A.** Physical properties of lipid bilayer membranes: Relevance to membrane biological functions. *Acta Biochim. Pol.* 2000, 47, 613–625.

205. **Wisniewska, A.; Subczynski, W.K.** Effects of polar carotenoids on the shape of the hydrophobic barrier of phospholipid bilayers. *Biochim. Biophys. Acta* 1998, *1368*, 235–246.

206. **Bayer, A.S.; Prasad, R.; Chandra, J.; Koul, A.; Smriti, M.; Varma, A.; Skurray, R.A.; Firth, N.; Brown, M.H.; Koo, S.P.; *et al.*** *In vitro* resistance of *Staphylococcus aureus* to thrombin-induced platelet microbicidal protein is associated with alterations in cytoplasmic membrane fluidity. *Infect. Immun.* 2000, *68*, 35483553.

207. **Van Blitterswijk, W.J.; van der Meer, B.W.; Hilkmann, H**. Quantitative contributions of cholesterol and the individual classes of phospholipids and their

degree of fatty acyl (un)saturation to membrane fluidity measured by fluorescence polarization. *Biochemistry* 1987, *26*, 1746–1756.

208. **Davidson, A.L.; Chen, J.** ATP-binding cassette transporters in bacteria. *Annu. Rev. Biochem.* 2004, *73*, 241–268.

209. **Davidson, A.L.; Dassa, E.; Orelle, C.; Chen, J.** Structure, function, and evolution of bacterial ATP-binding cassette systems. *Microbiol. Mol. Biol. Rev.* 2008, *72*, 317–364.

210. **Pao, S.S.; Paulsen, I.T.; Saierk M.H. Jr.** Major facilitator superfamily. *Microbiol. Mol. Biol. Rev.* 1998, *62*, 1–34.

211. **Reizer, J.; Reizer, A.; Saier, M.H., Jr.** A new subfamily of bacterial ABC-type transport systems catalyzing export of drugs and carbohydrates. *Protein Sci.* 1992, *1*, 1326–1332.

212. **Stein, T.; Heinzmann, S.; Kiesau, P.; Himmel, B.; Entian, K.D.** The spa-box for transcriptional activation of subtilin biosynthesis and immunity in *Bacillus subtilis*. *Mol. Microbiol.* 2003, *47*, 1627–1636.

213. **Stein, T.; Heinzmann, S.; Solovieva, I.; Entian, K.D.** Function of *Lactococcus lactis* nisin immunity genes *nisI* and *nisFEG* after coordinated expression in the surrogate host *Bacillus subtilis*. *J. Biol. Chem.* 2003, *278*, 89–94.

214. **Immonen, T.; Saris, P.E.** Characterization of the *nisFEG* operon of the nisin Z producing *Lactococcus lactis* subsp. *lactis* N8 strain. *DNA Seq.* 1998, *9*, 263–274.

215. **Ra, S.R.; Qiao, M.; Immonen, T.; Pujana, I.; Saris, E.J.** Genes responsible for nisin synthesis, regulation and immunity form a regulon of two operons and are induced by nisin in *Lactoccocus lactis* N8. *Microbiology* 1996, *142*, 1281–1288.

216. **Aso, Y.; Okuda, K.; Nagao, J.; Kanemasa, Y.; Thi Bich Phuong, N.; Koga, H.; Shioya, K.; Sashihara, T.; Nakayama, J.; Sonomoto, K.** A novel type of immunity protein, NukH, for the lantibiotic nukacin ISK-1 produced by *Staphylococcus warneri* ISK-1. *Biosci. Biotechnol. Biochem.* 2005, *69*, 1403–1410.

217. **Okuda, K.; Yanagihara, S.; Shioya, K.; Harada, Y.; Nagao, J.; Aso, Y.; Zendo, T.; Nakayama, J.; Sonomoto, K**. Binding specificity of the lantibiotic-binding immunity protein NukH. *Appl. Environ. Microbiol.* 2008, *74*, 7613–7619.

218. **Gebhard, S.** ABC transporters of antimicrobial peptides in Firmicutes bacteria—Phylogeny, function and regulation. *Mol. Microbiol.* 2012, *86*, 1295–1317.

219. **Higgins, C.F.** ABC transporters: Physiology, structure and mechanism—An overview. *Res. Microbiol.* 2001, *152*, 205–210.

220. **Dintner, S.; Staron, A.; Berchtold, E.; Petri, T.; Mascher, T.; Gebhard, S.** Coevolution of ABC transporters and two-component regulatory systems as resistance modules against antimicrobial peptides in Firmicutes bacteria. *J. Bacteriol.* 2011, *193*, 3851–3862.

221. **Revilla-Guarinos, A.; Gebhard, S.; Mascher, T.; Zuniga, M.** Defence against antimicrobial peptides: Different strategies in Firmicutes. *Environ. Microbiol.* 2014, *16*, 1225–1237.

222. **Bernard, R.; El Ghachi, M.; Mengin-Lecreulx, D.; Chippaux, M.; Denizot, F.** BcrC from *Bacillus subtilis* acts as an undecaprenyl pyrophosphate phosphatase in bacitracin resistance. *J. Biol. Chem.* 2005, *280*, 28852–28857.

223. **Shaaly, A.; Kalamorz, F.; Gebhard, S.; Cook, G.M**. Undecaprenyl pyrophosphate phosphatase confers low-level resistance to bacitracin in *Enterococcus faecalis*. *J. Antimicrob. Chemother.* 2013, *68*, 1583–1593.

224. **Charlebois, A.; Jalbert, L.A.; Harel, J.; Masson, L.; Archambault, M**. Characterization of genes encoding for acquired bacitracin resistance in *Clostridium perfringens*. *PLoS One* 2012, *7*, e44449.

225. **Butaye, P.; Cloeckaert, A.; Schwarz, S.** Mobile genes coding for efflux-mediated antimicrobial resistance in Gram-positive and Gram-negative bacteria. *Int. J. Antimicrob. Agents* 2003, *22*, 205–210.

226. **Van Veen, H.W.; Venema, K.; Bolhuis, H.; Oussenko, I.; Kok, J.; Poolman, B.; Driessen, A.J.; Konings, W.N.** Multidrug resistance mediated by a bacterial homolog of the human multidrug transporter MDR1. *Proc. Natl. Acad. Sci. USA* 1996, *93*, 10668–10672.

227. **Saidijam, M.; Benedetti, G.; Ren, Q.; Xu, Z.; Hoyle, C.J.; Palmer, S.L.; Ward, A.; Bettaney, K.E.; Szakonyi, G.; Meuller, J.**; *et al*. Microbial drug efflux proteins of the major facilitator superfamily. *Curr. Drug Targets* 2006, *7*, 793–811.

228. **Littlejohn, T.G.; Paulsen, I.T.; Gillespie, M.T.; Tennent, J.M.; Midgley, M.; Jones, I.G.; Purewal, A.S.; Skurray, R.A.** Substrate specificity and energetics of antiseptic and disinfectant resistance in *Staphylococcus aureus*. *FEMS Microbiol. Lett.* 1992, *74*, 259–265.

229. **Leelaporn, A.; Paulsen, I.T.; Tennent, J.M.; Littlejohn, T.G.; Skurray, R.A.** Multidrug resistance to antiseptics and disinfectants in coagulase-negative staphylococci. *J. Med. Microbiol.* 1994, *40*, 214–220.

230. **Bayer, A.S.; Cheng, D.; Yeaman, M.R.; Corey, G.R.; McClelland, R.S.; Harrel, L.J.; Fowler, V.G., Jr.** *In vitro* resistance to thrombin-induced platelet microbicidal protein among clinical bacteremic isolates of *Staphylococcus aureus* correlates with an endovascular infectious source. *Antimicrob. Agents Chemother.* 1998, *42*, 3169–3172.

231. **Solheim, M.; Aakra, A.; Vebo, H.; Snipen, L.; Nes, I.F**. Transcriptional responses of *Enterococcus faecalis* V583 to bovine bile and sodium dodecyl sulfate. *Appl. Environ. Microbiol.* 2007, *73*, 5767–5774.

232. **Fernandez-Fuentes, M.A.; Abriouel, H.; Ortega Morente, E.; Perez Pulido, R.; Galvez, A.** Genetic determinants of antimicrobial resistance in Gram positive bacteria from organic foods. *Int. J. Food Microbiol.* 2014, *172*, 49–56.

233. **Gay, K.; Stephens, D.S.** Structure and dissemination of a chromosomal insertion element encoding macrolide efflux in *Streptococcus pneumoniae*. *J. Infect. Dis.* 2001, *184*, 56–65.

234. **Peschel, A.; Sahl, H.G.** The co-evolution of host cationic antimicrobial peptides and microbial resistance. *Nat. Rev. Microbiol.* 2006, *4*, 529–536.

235. **Eckert, R.** Road to clinical efficacy: Challenges and novel strategies for antimicrobial peptide development. *Future Microbiol.* 2011, *6*, 635–651.

236. **Marr, A.K.; Gooderham, W.J.; Hancock, R.E.** Antibacterial peptides for therapeutic use: Obstacles and realistic outlook. *Curr. Opin. Pharmacol.* 2006, *6*, 468–472.

237. **Hancock, R.E.; Sahl, H.G.** Antimicrobial and host-defense peptides as new anti-infective therapeutic strategies. *Nat. Biotechnol.* 2006, *24*, 1551–1557.

238. **Van Heel, A.J.; Mu, D.; Montalban-Lopez, M.; Hendriks, D.; Kuipers, O.P.** Designing and producing modified, new-to-nature peptides with antimicrobial activity by use of a combination of various lantibiotic modification enzymes. *ACS Synth. Biol.* 2013, *2*, 397–404.

239. **Jung, W.J.; Mabood, F.; Souleimanov, A.; Zhou, X.; Jaoua, S.; Kamoun, F.; Smith, D.L.** Stability and antibacterial activity of bacteriocins produced by *Bacillus thuringiensis* and *Bacillus thuringiensis* ssp. *kurstaki*. *J. Microbiol. Biotechnol.* 2008, *18*, 1836–1840.

240. **Chehimi, S.; Delalande, F.; Sable, S.; Hajlaoui, M.R.; van Dorsselaer, A.; Limam, F.; Pons, A.M.** Purification and partial amino acid sequence of thuricin S, a new anti-Listeria bacteriocin from *Bacillus thuringiensis*. *Can. J. Microbiol.* 2007, *53*, 284–290.

241. **Weigel, L.M.; Clewell, D.B.; Gill, S.R.; Clark, N.C.; McDougal, L.K.; Flannagan, S.E.; Kolonay, J.F.; Shetty, J.; Killgore, G.E. Tenover, F.C.** Genetic analysis of a high-level vancomycin-resistant isolate of *Staphylococcus aureus*. *Science* 2003, *302*, 1569–1571.

242. **Huddleston, J.R.** Horizontal gene transfer in the human gastrointestinal tract: Potential spread of antibiotic resistance genes. *Infect. Drug. Resist.* 2014, *7*, 167–176.

243. **Napier, B.A.; Band, V.; Burd, E.M.; Weiss, D.S.** Colistin heteroresistance in *Enterobacter cloacae* is associated with cross-resistance to the host antimicrobial lysozyme. *Antimicrob. Agents Chemother.* 2014, *58*, 5594–5597.